IOWA STATE UNIVERSITY
Digital Repository

Retrospective Theses and Dissertations

Iowa State University Capstones, Theses and Dissertations

2004

Enantiomeric separations using macrocyclic glycopeptide based chiral stationary phases, an application and mechanism study

Ling (Tom) Shi Xiao
Iowa State University

Follow this and additional works at: https://lib.dr.iastate.edu/rtd

 Part of the Analytical Chemistry Commons

Recommended Citation
Xiao, Ling (Tom) Shi, "Enantiomeric separations using macrocyclic glycopeptide based chiral stationary phases, an application and mechanism study " (2004). *Retrospective Theses and Dissertations*. 826.
https://lib.dr.iastate.edu/rtd/826

This Dissertation is brought to you for free and open access by the Iowa State University Capstones, Theses and Dissertations at Iowa State University Digital Repository. It has been accepted for inclusion in Retrospective Theses and Dissertations by an authorized administrator of Iowa State University Digital Repository. For more information, please contact digirep@iastate.edu.

www.manaraa.com

Enantiomeric separations using macrocyclic glycopeptide based chiral stationary phases, an application and mechanism study

by

Ling (Tom) Shi Xiao

A dissertation submitted to the graduate faculty
in partial fulfillment of the requirements for the degree of
DOCTOR OF PHILOSOPHY

Major: Analytical Chemistry

Program of Study Committee:
Daniel W. Armstrong, Major Professor
Robert S. Houk
Patricia A. Thiel
QiJing Zhang
Yan Zhao

Iowa State University
Ames, Iowa
2004

Copyright © Ling (Tom) Shi Xiao, 2004. All rights reserved.

UMI Number: 3136359

INFORMATION TO USERS

The quality of this reproduction is dependent upon the quality of the copy submitted. Broken or indistinct print, colored or poor quality illustrations and photographs, print bleed-through, substandard margins, and improper alignment can adversely affect reproduction.

In the unlikely event that the author did not send a complete manuscript and there are missing pages, these will be noted. Also, if unauthorized copyright material had to be removed, a note will indicate the deletion.

UMI®

UMI Microform 3136359

Copyright 2004 by ProQuest Information and Learning Company.

All rights reserved. This microform edition is protected against unauthorized copying under Title 17, United States Code.

ProQuest Information and Learning Company
300 North Zeeb Road
P.O. Box 1346
Ann Arbor, MI 48106-1346

Graduate College

Iowa State University

This is to certify that the doctoral dissertation of

Ling (Tom) Shi Xiao

has met the dissertation requirements of Iowa State University

Signature was redacted for privacy.

Major Professor

Signature was redacted for privacy.

For the Major Program

This dissertation is dedicated to

My parents, who raised me and encouraged me,

My teachers, who educated me and enabled me,

My wife and my kids, who supported and completed me.

TABLE OF CONTENTS

ABSTRACT

The purpose of my research was to further investigate the mechanism by which macrocyclic glycopeptides are able to separate enantiomers and to try to develop and expand their application in high performance liquid chromatography (HPLC) and other related separation techniques.

We first demonstrated a unique application of enantiomeric separations for chiral sulfoxides using macrocyclic glycopeptide chiral stationary phases (CSPs). A set of 42 chiral compounds containing stereogenic sulfur was prepared. There were 31 chiral sulfoxide compounds, three tosylated sulfilimines and eight sulfinate esters. The separations were done using five different macrocyclic glycopeptide chiral stationary phases (CSPs), namely ristocetin A, teicoplanin, teicoplanin aglycone (TAG), vancomycin and vancomycin aglycone (VAG) and seven eluents, three normal-phase mobile phases, two reversed phases and two polar organic mobile phases. Altogether the macrocyclic glycopeptide CSPs were able to separate the whole set of the 34 sulfoxide enantiomers and tosylated derivatives. Five of the eight sulfinate esters were also separated. The teicoplanin and TAG CSPs were the most effective CSPs able to resolve 35 and 33 of the 42 compounds respectively. The three other CSPs each were able to resolve more than 27 compounds. The normal-phase mode was the most effective followed by the reversed-phase mode with methanol–water mobile phases. Few of these compounds could be separated in the polar organic mode with 100% methanol mobile phases. Acetonitrile was also not a good solvent for the resolution of enantiomers of sulfur-containing compounds, neither in the reversed-phase nor in the polar organic mode. The structure of the chiral molecules was compared to the enantioselectivity factors obtained with the teicoplanin and TAG CSP. It is shown that the polarity, volume and shape of the

sulfoxide substituents influence the solute enantioselectivity factor. Changing the oxidation state of the sulfur atom from sulfoxides to sulfinate esters is detrimental to the compound's enantioselectivity. The enantiomeric retention order on the teicoplanin and TAG CSPs was very consistent: the (*S*)-(1)-sulfoxide enantiomer was always the less retained enantiomer. In contrast, the (*R*)-(2)-enantiomer was less retained by the ristocetin A, vancomycin and vancomycin aglycon columns, showing the complementarity nature of these CSPs. The macrocyclic glycopeptide CSPs provided broad selectivity and effective separations of chiral sulfoxides.

We further demonstrated another successful enantiomeric separation of a series of biologically active racemic analogues of dihydrofurocoumarin using this class of CSPs. The macrocyclic glycopeptides proved to be exceptionally selective for this class of compounds. All of the 28 chiral analogues were baseline separated on at least one of the macrocyclic glycopeptide CSPs. The teicoplanin CSP showed the broadest enantioselectivity with 24 of the compounds baseline separated. The TAG and the R CSPs produced 23 and 14 baseline separations respectively. All three mobile phase modes, i.e., normal phase (NP), reversed phase (RP), and new polar organic modes (PO), were evaluated. The NP mode proved to be most effective for the separation of chiral dihydrofurocoumarins on all CSPs tested. In the reversed phase (RP) mode, all three CSPs separated a similar number of compounds. It was observed that the structural characteristics of the analytes and steric effects are very important factors leading to chiral recognition. Hydrogen bonding was found to play a secondary role in chiral discrimination in the normal phase and polar organic modes. Hydrophobic interactions are important for chiral separation in the reversed phase mode. When coupled with circular dichroism, using the exciton coupling chirality method, the

enantiomeric elution order and the absolute configuration of some chiral dihydrofurocoumarins were successfully determined.

We also presented a systematic elution order reversal study using these naturally occurring chiral molecules as HPLC CSPs. Since these chiral selectors are structurally related, they tend to have similar, but not identical, enantioselectivities for most compounds. CSPs, of this type, with opposite enantioselectivities are rare. Two exceptions have been found to this. The oxazolidiones (starting materials for asymmetric synthesis) and dansyl amino acids all show a reversal in enantioselective retention on one of these three related CSPs. By using the HPLC assays developed for these compounds, the levels of enantiomeric impurities can be measured down to $\approx 0.01\%$. The enantiomeric purity of commercial oxazolidiones was determined.

The last part of this dissertation presented an absolute configuration determination approach using exciton coupling chirality method. First of all, a phenyl-substituted chiral dihydrofuroangelicin, 4-methyl-8-(2-*E*-phenylethenyl)-8,9-dihydro-2*H*-furo[2,3-*h*]-1-benzopyran-2-one, synthesized in racemic form, has been resolved by HPLC chiral separation, and its absolute configuration determined by the non-empirical exciton chirality method. The solution conformation has been investigated through NMR and molecular modeling methods: two minima found by molecular mechanics and DFT methods are in keeping with observed ^{1}H–^{1}H ^{3}J coupling constants and NOE effects. The experimental CD spectrum for the second eluted enantiomer shows a positive couplet between 230 and 350 nm (amplitude $A = +15.7$); by application of the exciton chirality method, the absolute configuration of this enantiomer at C8 is determined as (*S*). The experimental spectrum is in

very good agreement with the one evaluated by means of DeVoe coupled-oscillator calculations, using the DFT calculated geometries.

Secondly, we extended this method as a general method for dermination of the absolute configuration of dihydrofuroangelicins bearing a variety of C-8 substituted double bonds, synthesized in the racemic form and resolved through enantioselective chromatography. A combined chemical/chiroptical protocol has been developed in which the C=C double bonds are replaced with a styrenoid chromophore through either (i) cross metathesis, (ii) Heck reaction, or (iii) a combined method of cross metathesis and Heck reaction with about 1 mg sample under mild conditions. The coupling between the styrenoid and coumarin chromophores gives rise to clear-cut exciton coupled CD curves, suitable for assignments of absolute configurations. The solution conformation of the styrenoid derivatives is determined by NMR and DFT molecular modeling; the electronic structure of the 7-hydroxy coumarin chromophore is also clarified by semi-empirical and TDDFT methods. The conformation thus derived, in conjunction with quantitative DeVoe's coupled-oscillator CD calculation, establishes the absolute configurations of the coumarins. The theoretical study described herein justifies the straightforward approach of the current chemical/exciton chirality protocol to this type of dihydrofuroangelicins.

CHAPTER 1
GENERAL INTRODUCTION AND LITERATURE REVIEW

1.1. General Introduction

Enantiomeric separations and analysis have become increasingly important in many areas of science and technology. In the pharmaceutical industry and medicinal science, for example, it is well known that different enantiomers will have different physiological effects and biological dispositions. The demand for optically pure enantiomers has grown tremendously in recent years. It was reported that the overall sales for enantiomeric pure drugs in the year of 2001 exceeded 150 billion dollars. Especially after the announcement of the guidelines regarding the development of chiral pharmaceutical products by the US Food and Drug Administration in 1992, it has become a routine practice to assess the biological activity of each enantiomer of a chiral molecule. Since asymmetric synthesis methods for providing desired pure enantiomers is sometimes limited. Enantiomeric separations for these chiral compounds are desperately needed in both preparative and analytical scales.

Macrocyclic Glycopeptides are the fastest growing and newest class of chiral selectors in the enantiomeric separation arena. Since they were first introduced by Dr. Armstrong in 1994[1], they have made a tremendous impact on separation science. Hundreds of related application and mechanistic studies using this class of chiral selectors have been published in a relatively short period of time. Although certain binding sites or functional groups have been identified as being crucial for the enantomeric separations of particular compounds, the chiral recognition mechanism for this class of chiral selectors is not

completely understood. This is largely because of the fact that they are the newest class of chiral selectors and consequently there have been fewer opportunities for their examination.

The goal of my research is to investigate further the mechanism by which macrocyclic glycopeptides are able to separate enantiomers and try to develop and expand their application in high performance liquid chromatography (HPLC), super/subcritical fluid chromatography (SFC) and other related separation techniques.

This dissertation is presented with a general introduction and literature review plus two independent parts. The first part includes four complete scientific papers while the second part has two. Finally there is a general conclusion which summarizes the work and describes prospects for future research. The focus of the first part is on methods development and mechanistic studies for chiral separations of unusual analytes using macrocyclic glycopeptide chiral stationary phases (CSPs). This part includes an investigation of elution order reversal in HPLC chiral separation using this class of chiral stationary phases (CSPs), separation of a unique series of chiral compounds, sulfoxides, where sulfur is the stereogenic center, and the separation of dihydrofurocoumarin derivatives. All of these applications were successful and possible mechanisms of enantiomeric separations using this class of CSPs were examined. The second part of this research examines the successful application of the exciton coupling chirality protocol for determing the absolute configuration of dihydrofuroangelicin enantiomers.

1.2. LITERATURE REVIEW

A book chapter published in Methods in Molecular Biology (Chiral Separations)[1]

Tom Ling Xiao, Daniel W. Armstrong

1. Introduction

The development of effective, high efficiency enantiomeric separations is a tremendous success story(2). The separation of enantiomers is now accomplished by chiral chromatographic and electrophoretic methods, which includes gas chromatography (GC), high performance liquid chromatography (HPLC), thin layer chromatography (TLC), supercritical fluid chromatography (SFC), capillary electrochromatography (CEC), and capillary electrophoresis (CE). Enantioselective HPLC is the most widely used chromatographic method, both for analytical and preparative purposes, in most branches of science and technology including the pharmaceutical and environmental fields. The search for more effective and universal chiral stationary phases (CSPs) for HPLC is an ongoing and challenging topic for separation scientists.

The most useful and widely used chiral stationary phases (CSPs) are capable of separating a great variety of enantiomeric compounds while providing good efficiency, good loadability, and long term stability. The macrocyclic glycopeptides (a.k.a. macrocyclic antibiotics) may be the most promising chiral selectors in this respect. They are the newest class of chiral selectors, first introduced by Armstrong in 1994(1). They are the fastest growing and one of the most useful classes of chiral selectors in the world today. High efficiency enantiomeric separations of a wide variety of biological(1-41), pharmacological(2-39,42-50), agrochemical (51,52), and nutritional compounds(53), have been achieved using this class of chiral selectors.

---

[1] Reprinted with permission from Methods in Molecular Biology,(2004), 243(Chiral Separations), 113-171. Humana Press, Totowa.
Copyright © 2004 Humana Press, All rights reserved.

Prior to 1994, the use of macrocyclic glycopeptides was essentially unknown in separation science and technology. Vancomycin has been used as an antibiotic to treat severe staphylococcal infections, especially when bacterial resistance to other antibiotics has developed(4). The vancomycin-related antibiotics bind to the D-alanyl-D-alanine terminal group in the bacteria cell wall, thereby stopping bacterial development(23,54-56). Since the target of these antibiotics is the D-alanyl-D-alanine group, it was thought that they could be used in the separation of amino acid enantiomers(23). Interestingly, CSPs based on these macrocyclic glycopeptides effectively separated a wide variety of different enantiomeric compounds. CSPs based on macrocyclic glycopeptides have many of the enantioselectivity properties of more complex proteins and other polymeric selectors, with the advantages of a smaller size, good stability and good sample capacity(2,7).

There are literally hundreds of documented macrocyclic antibiotics. However, only a few appear to be broadly effective as chiral selectors. Three classes of macrocyclic antibiotics have been used successfully as chiral selectors. The first type is made up of *ansa* compounds, which consists of a chromophore spanned by an aliphatic bridge. These have been used mainly in capillary electrophoresis (CE) applications (15,57-59). The second type consists of macrocyclic peptides such as thiostrepton. These have had limited use in LC(2,60,61). The third and most important type is the macrocyclic glycopeptides, which have 3 or 4 fused macrocyclic rings. Various saccharide moieties are attached to the fused macrocyclic system.

The unique structure of the macrocyclic glycopeptides and their abundance of functionality (e.g. aromatic, hydroxyl, amine, and carboxylic acid moieties, amide linkages, hydrophobic pockets, etc.) give them broad selectivity for a wide variety of anionic, neutral, and cationic compounds. All of the defined molecular interactions that are necessary for chiral recognition are found within these relatively compact structures. These include possibilities for ionic interactions, hydrogen bonding, steric, dipole-dipole and π-π interactions as well as hydrophobic interactions. This allows for a wide variety of chiral separations in all known mobile phase modes (which includes the normal-phase mode (NP), reversed-phase mode (RP), and polar-organic mode (PO)). Each separation mode provides simultaneous but

different interactions for chiral recognition. This accounts for the large number of chiral separations and the variety of types of chiral compounds that are successfully separated with this class of CSP.

The first macrocyclic glycopeptide antibiotic introduced as a commercial CSP was vancomycin (Chirobiotic V)(2), followed by teicoplanin (Chirobiotic T)(7). In 1998, after having been successfully used in CE chiral separations, ristocetin A (Chirobiotic R) joined this group as the third CSP of this family(17). Over 230 chiral separations achieved on Chirobiotic R column in three different modes were reported in a single paper by Ekborg-Ott et.al.(17). Complementary selectivity to the other two Glycopeptide CSPs was found and the column showed excellent stability. However, a drawback for the Chirobiotic R is the high cost and scarcity of the ristocetin A chiral selector. The last commercialized member of this family of CSPs is teicoplanin aglycon (Chirobiotic TAG)(23), which was produced by simply removing the carbohydrate moieties from teicoplanin. The original motive in removing the pendant carbohydrate groups was to investigate the role of the sugar units in chiral recognition(23). Surprisingly, the new CSP had much improved selectivity for certain analytes. Recently, separations using the vancomycin aglycon CSP (VAG, i.e., vancomycin with its carbohydrate moieties removed) were achieved in our lab(43). Some improved separations were observed on VAG versus V(43). This CSP has not yet been commercialized. Avoparcin is another glycopeptide macrocyclic antibiotic evaluated as a CSP in HPLC by Armstrong's group in 1998 (19). This CSP will not be discussed in detail since it is not widely available. However, information on this CSP can be obtained from the original reference(19).

Although the macrocyclic glycopeptides have analogous structures, they have somewhat different enantioselectivities. In fact, one of the more useful features of this class of chiral selectors is their "principle of complementary separations". This means that if a partial enantiomeric separation is obtained with one glycopeptide, there is a strong probability that a baseline or better separation can be obtained with a related Chirobiotic CSP using the same or a similar mobile phase. The reason for this phenomenon is the sometimes subtle differences in the stereoselective binding sites between these related chiral stationary phases.

A fast screening approach for chiral HPLC method development, based on this complementary feature, was proposed by Wang et al(62). This is discussed in detail in section 4.4.

In a relatively short period of time after their introduction, the macrocyclic glycopeptide chiral selectors were used successfully in most chromatographic and electrophoretic methods including HPLC(1,2,7,9,11-14,16-27,29,31-43,45-52,62-84), HPLC-MS(44,85-89) TLC(3), CE(4,5,8,10,15,52,61,69,81,90-101), CEC(28,30,91,102,103), SFC(104-107), and in enhanced-fluidity liquid chromatography (EFLC)(108). Over one thousand enantiomeric separations have been reported using this class of chiral selectors, including both derivatized and underivatized amino acids, peptides, β-blockers, hydroxy-acids, amino esters, imides, hydantoins, and oxazolidinones, numerous non-steroidal anti-inflammatory compounds, lactic acids, and other pharmaceuticals and agrochemicals etc. Both analytical and preparative scale applications are reported(71). As was reported in the 2002 Analytical Chemistry review on Chiral Separations, " The number of publications in the field of chiral separations in high performance liquid chromatography has remained relatively steady, with the exception being a 50% increase in publications using macrocyclic glycopeptide-based chiral stationary phases"(92).

2. Materials

2.1. Structures and properties of macrocyclic glycopeptide antibiotics

All macrocyclic glycopeptide chiral selectors are naturally occurring compounds. Their molecular masses are between 1000 and 2100. The original macrocyclic antibiotics were discovered by scientists at the Eli Lilly Company in the 1950s(4). Vancomycin, ristocetin A, and teicoplanin are all active against Gram-positive bacteria(7). They are produced as fermentation products of *Streptomyces orientalis*, *Nocardia lurida*, and *Actinoplanes teichomyceticus*, respectively (56,109-112). Macrocyclic glycopeptide antibiotics are soluble in water, and acidic aqueous solutions, but are less soluble at neutral pH (113). They are moderately soluble in polar aprotic solvents (e.g., DMSO, DMF) but insoluble in most other organic solvents(113).

The three dimensional molecular structures of three of the commercialized macrocyclic glycopeptides that are used for CSPs have been reported(10). Figure 1 shows both the molecular "space-filling" model (Figure 1A) and the corresponding "stick" model (Figure 1B) for all four macrocycles. They all possess a characteristic "basket-shape" aglycon, which consists of a peptide core of complex amino acids and linked phenolic moieties. They are positioned to show a profile view of the "C-shaped" aglycon "basket". The colored regions in Figure 1A are hydrophilic groups as specified in the captions. The black area denotes the more hydrophobic regions, including amido linkages, aromatic rings, and apolar connecting carbons. The aglycon basket of all these molecules consists of either 3 or 4 fused macrocyclic rings. They differ in their size and shape, as well as the geometric arrangement of their numerous stereogenic centers and functional groups, which are responsible for their enantioselective properties. The macrocycles contain both ether and peptide linkages. They make the "aglycon" semi-rigid, but with some flexibility. Two important characteristics of the aglycon basket are (1) the openness of the C-shaped aglycon basket and (2) its degree of helical twist. Both of these features are illustrated in Figure 3. When the glycopeptides are observed in profile (as seen in Figures 1 and 3), "openness" is related to the distance between opposite ends of the aglycon. Clearly, vancomycin has the most open aglycon, with their shortest end-to-end distance being ~9.3 Å(10). Teicoplanin and TAG appear to have the most closed aglycon (almost cyclic) with the end-to-end distances varying from ~4.5 to 5.5 Å(10). Ristocetin A is intermediate, with end-to-end distances varying from ~5.2 to 8.8 Å(10). These variations in the end-to-end distances also are affected by the helical twist of the aglycon, as shown in Figure 3B. They also affects the shape and morphology of the individual macrocyclic rings, which form the aglycon "basket"(10). An unstrained macrocyclic ring can be nearly circular. Strained or deformed rings may be more elongated or oval-shaped(10).

Various numbers and types of small carbohydrates are attached to the aglycon via ether linkages. Three of these compounds also have aminosaccharide moieties. These sugar moieties, attached to the aglycon basket, are free to rotate and can assume a variety of orientations (Figure 1). The glycopeptides are amphoteric, containing both ionizable acidic

and basic groups. Thus, they can be positively charged, negatively charged or neutral depending on the pH of the mobile phase.

2.1.1 Vancomycin

In addition to the common features shared with other macrocyclic glycopeptides, vancomycin has a number of unique structural features. It has molecular weight of 1449, which makes it the smallest of the three macrocyclic glycopeptides (i.e. vancomycin, teicoplanin and ristocetin A). It has 18 stereogenic centers, as well as a pendant, freely rotating, disaccharide moiety consisting of D-glucose and vancosamine, and an N-methyl amino acid side chain around three fused macrocyclic rings bridged by five aromatic rings linked by ether and peptide bonds. Vancomycin has nine hydroxyl groups around the "basket-shaped" aglycon and on the attached disaccharide moiety, two amine groups (one primary and one secondary), and one carboxylic acid group. All these polar and ionizable groups are proximate to the ring structure and are able to offer strong hydrogen bonding and electrostatic interactions respectively with solute molecules. The pK's for vancomycin are 2.9, 7.2, 8.6, 9.6, 10.4, and 11.7 (61,114). Its pI value (isoelectric point, i.e., where vancomycin has a net zero charge) is 7.2(10). Below the pI value (which is the normal HPLC operational pH range pH=3.5 to 7.5), the ionizable groups should be positively charged. The aglycon of vancomycin also contains two chloro-substituted aromatic rings, together with seven amido groups and three phenolic groups. The aromatic rings and peptide linkages provide some rigidity to the aglycon and provide the opportunity for π-π interactions and dipolar interactions, respectively, with small molecules.

2.1.2 Teicoplanin

Teicoplanin has many unique characteristics, which make it complementary to vancomycin. One of the unusual structural characteristics of teicoplanin is that it has a hydrophobic acyl side chain ("hydrophobic tail") attached to a 2-amino-2-deoxy-β-D-glucopyranosyl moiety (Figure 1, Table 1). Consequently, teicoplanin is surface active and aggregates to form micelles(10,115). None of other glycopeptides has shown this type of behavior (Table 1).

Teicoplanin's critical micelle concentration in unbuffered aqueous solutions is ~0.18 mM(10). As a consequence of this molecular structure, teicoplanin shows a slightly lower solubility in water than the other macrocyclic glycopeptides(10).

Another unique character of teicoplanin is that it has a pI of approximately 3.5. From Table 1 and Figure 2, we can see that the mobility vs. pH curve is nearly flat between pH 3 and pH 7, which means that under normal operational conditions (pH=3.5~7.5), teicoplanin shows a slightly anionic character while vancomycin and ristocetin A both show cationic behavior. This difference makes teicoplanin somewhat unique among the macrocyclic glycopeptide antibiotics.

Teicoplanin has a single primary amine group and a single carboxylic acid group. The respective pKa values are around 9.2 and 2.5(9). Furthermore, teicoplanin is unique in that it has two amino saccharides, both of which are N-acylated (Figure 1), while both vancomycin and ristocetin A have an additional free amine group in an attached aminosaccharide moiety. Obviously, this additional amine affects the charge and overall ionization behavior of vancomycin and ristocetin A. There is a carboxylic acid moiety on the aglycon of both vancomycin and teicoplanin, while the equivalent group on ristocetin A is esterified (Figure1).

In addition to its ionizable groups, teicoplanin has 10 primary and secondary hydroxyl groups and four phenolic groups, which provide additional hydrogen bonding sites for chiral analytes. The less polar character of the interior of the aglycon "basket" and the ten carbon side chain will provide hydrophobic interaction sites. Teicoplanin has three attached monosaccharides moieties, two of which are D-glucosamine and one of which is D-mannose.

There are five closely related teicoplanin glycopeptides that have been identified, namely, teicoplanin A_2-1, A_2-2, A_2-3, A_2-4, and A_2-5(116). The five forms of teicoplanin have different fatty acid chains attached to the amine group of glucosamine, i.e., A_2-1 with (z)-4-decanoic acid, A_2-2 with 8-methynonoic acid, A_2-3 with n-decanoic acid, A_2-4 with 8-

methyldecanoic acid, and A_2-5 with 9-methyldecanoic acid, respectively. The most common teicoplanin glycopeptide is A_2-2, which has a molecular weight of 1879.7(116).

2.1.3 Teicoplanin Aglycon

The Chirobiotic TAG column is made by covalently bonding the aglycon part of teicoplanin to silica gel via a linkage chain. The sugar moieties are removed by the following method(23). First, teicoplanin is dissolved in 30:1/DMSO:80%H_2SO_4 (v:v) at concentration around 0.1M. Then the mixture is heated to 65°C for 1.5 hours. The phenoxy linkage of the nonylglucosamine is then hydrolyzed. To remove the mannose unit, addition of 80%H_2SO_4 is needed (at the same concentration as the starting solution) and the mixture kept at 65°C for 3 hours. To remove the last N-acetyl-β-D-glucosamine unit, the temperature is raised to 80°C for 24 hours(23). The aglycon of teicoplanin becomes water insoluble after the removal of the sugar units from teicoplanin. It consists of the four fused macrocyclic rings, which form "a semi-rigid basket." It still contains seven aromatic rings of which two are chloro-substituted, and five of which are ionizable phenolic moieties (Figure 1). Because it is just the aglycon portion of teicoplanin, the molecular weight drops to 1197. It has only 8 stereogenic centers, in the meantime, the number of hydroxyl groups also decreases to eight. However, the chiral selectivity is not necessarily decreased by the loss of the sugar moieties. The single primary amine, carboxylic acid group, and the phenolic moieties control the overall charge of the aglycon. These structural features and their effect on enantioselectivity will be discussed later in this chapter.

2.1.4 Ristocetin A

Ristocetin A is the third macrocyclic glycopeptide antibiotic used and commercialized as a CSP for HPLC. It is also the largest member of this class, with a MW of 2066. It has the greatest number of stereogenic centers (i.e., 37). It contains seven aromatic rings, six amide linkages, 21 hydroxyl groups, two primary amine groups and one methyl ester. It has four, rather than three, fused macrocyclic rings (one twelve-membered, one fourteen membered, and two sixteen membered rings) and a greater number and different types of attached sugar

moieties. Ristocetin A has a pendant tetrasaccharide and two monosaccharide moieties, composed of D-arabinose, D-mannose, D-glucose, and D-rhamnose. As mentioned before, the carboxylic acid group on ristocetin A is esterified (Figure 1). The pI value for Ristocetin A is 7.5, which means that under normal operational conditions (pH=3.5~7.5) it will show cationic behavior. The only other ionizable groups on ristocetin A are the phenolic moieties. Thus at operational pH value, these are generally protonated and probably serve mainly as hydrogen bonding sites.

2.2 Commercially available Glycopeptide Antibiotic Chiral Stationary Phases

2.2.1 Preparation of Glycopeptide Antibiotic CSPs

As mentioned before, the designations for commercialized macrocyclic glycopeptide CSPs for HPLC are Chirobiotic V, Chirobiotic R, Chirobiotic T, and Chirobiotic TAG based on the first letter of the corresponding glycopeptide chiral selectors attached to a 5μm spherical silica gel. The bonding reagents or linkage chains may be organosilanes that are terminated by carboxylic groups, amine groups, epoxy groups and isocyanate groups. Examples of such reagents are 2-(carbomethoxy)-ethyltrichlorosilane, 3-aminopropyldimethylethoxysilane, and (3-glycidoxypropyl) trimethoxysilane etc. Therefore, the linkage that covalently attaches the macrocycle to the tethers attached to silica may be an ether, thioether, amine, amide, carbamate or urea(61,114). Below are examples showing the attachment of Glycopeptide to silica employing 3-isocyanatopropyltriethoxylsilane (A and B).

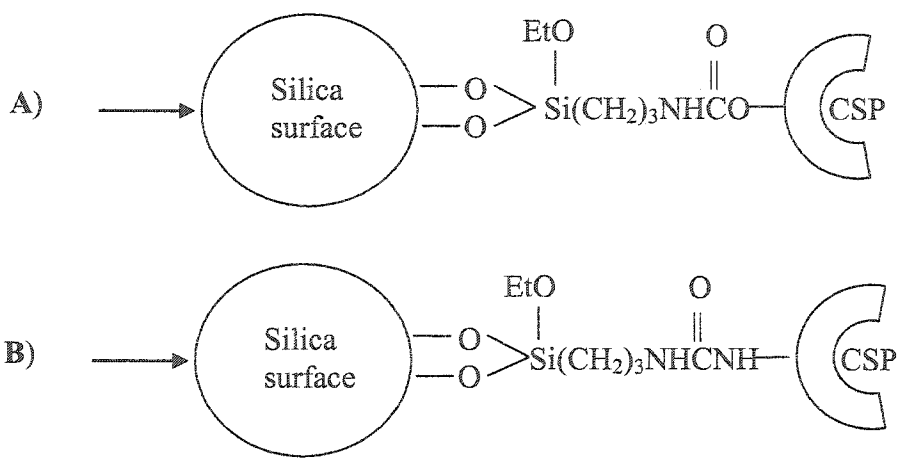

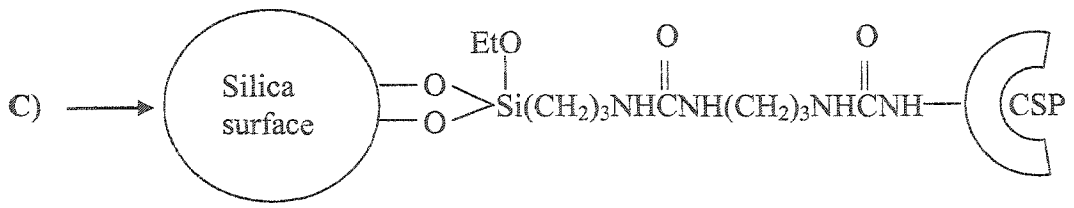

In the above diagrams, the "CSP" stands for the macrocyclic glycopeptide CSPs. Diagram A) and B) represent the CSPs react with 3-isocyanatopropyltriethoxylsilane through a hydroxyl group or an amino group forming a carbamate or a urea linkage respectively. Diagram C) also shows the chiral selector linked to γ-aminopropylsilanized silica gel via an alkyl diisocyanate moiety(61,114). On average, there are four linkage chains to every chiral selector(2).

Overall, these macrocyclic glycopeptide CSP are much more stable than traditional protein CSPs and have much higher loading capacities. In comparison to the cellulose and amylose phases, the Glycopeptides CSPs can tolerate a much wider range of solvents and consequently have greater versatility, stability, and longevity (71).

2.2.2 Chiral selector coverage

In HPLC, chiral selectors can be used as mobile phase additives or as part of the CSPs. In the case of as CSPs, the column loading (a.k.a. coverage of the chiral selectors) can affect retention, selectivity, efficiency, and enantioresolution. A systematic study of the effect of the surface coverage of these chiral selectors on column efficiency and enantiomeric selectivity was done(7,22). Surface coverage can be controlled by altering the initial reaction ratio (of selector to silica gel), the selector concentration, the reaction time, reaction temperature, and the other relevant reaction conditions. Separations were compared based on their capacity factors (k'), selectivity values (α), efficiencies (N) and resolution (Rs) for different coverage columns (high, medium and low) in all three mobile phase modes. It is reasonable that the retention is longer on the higher coverage CSP, which provides a greater number of chiral selector adsorption sites. However, the increase in selectivity factor (α) is relatively smaller. For most of the compounds, both shorter retention times and comparable

efficiencies and selectivities were achieved on medium coverage CSP for ristocetin A CSP (22). As can be seen from Figure 4, it is the more retained (i.e., the second eluting) enantiomer of each analyte that is most affected by changes in the loading of the chiral selectors on the CSP.

2.2.3 Chirobiotic Column care and stability

In order to get the best results and extend the column lifetime, the following column care steps should be followed:

1. Both new column and used columns that may display decreased resolution should be conditioned first with 50/50:CH_3CN/50mM NH_4OAc for 20 column volumes (sometimes, a buffer at an opposite range of the pH is good if the column has been used at one specific pH for a while), followed by 10 column volumes of HPLC grade water. Finally wash with 10 column volumes of organic solvent, i.e., acetonitrile or ethanol. This procedure will eliminate removable contaminants and adsorbed components that could block important binding sites on the CSP.
2. A test compound for a specific mobile phase should be selected to evaluate the performance of a specific Chirobiotic column (this is also referred to as the selectivity control test). The following table lists suggested test conditions for different Chirobiotic columns. The test compounds and the corresponding test conditions are chosen in order to achieve barely baseline separations so that decreased column performance (i.e., resolution and retention times) can be easily detected.

Table 2. Recommended Selectivity Test Compounds and Conditions for Chirobiotic Columns

CSPs	Test compound	Mobile phase	Retention times (min)
Chirobiotic V	Nefopam	100/0.1%:MeOH/NH_4TFA	13.4, 14.4
Chirobiotic T	Phenylalanine	30/70: EtOH/H_2O	5.2, 6.1
Chirobiotic TAG	Ornithine	20/80:MeOH/0.1M NaH_2PO4	7.2, 8.3
Chirobiotic R	Ketoprofen	100/0.01%:MeOH/NH_4OAc	6.9, 7.4

3. Because different mobile phase modes can be employed when using Chirobiotic columns, care should always be exercised in switching from one mobile phase to another. Normally Chirobiotic columns are best stored in isopropanol due to its weaker polarity, solubility properties, and good compatibility to any kind of mobile phase solvent. When switching from the polar organic mode, methanol should be first employed to remove acids and bases especially when trifluoroacetic acid was used. The column should be washed while it is connected to the system in order to purge all system lines and the detector cell. In switching from the normal phase mode, the column should be washed with ethanol first to get rid of hexane or other organic nonpolar solvents. When switching from the reversed phase mode, wash the column with water first and then follow with neat ethanol.
4. It is necessary to be aware of the pH stability range of silica gel based Chirobiotic columns, which is usually from 3.5 to 7.5. Strong acids (pH<2.0) or bases (pH>8) will cause column damage. Running with a pure water mobile phase should be avoided or at least reduced. A short presaturation column of 40 μm silica gel prior to the injector is useful for the Chirobiotic columns to extend their lifetime when using aqueous or reversed phase mobile phases. The function of this column is to saturate any water-containing mobile phase with silicic acid. It has an added benefit of filtering the mobile phase.
5. Never store columns, even for a short period of time, in buffer. This may cause the columns to clog or become damaged if the buffered solvent evaporates and precipitation occurs. Wash the column with water after using buffer solvents. Then flush the column with ethanol, methanol, isopropanol or acetonitrile.

3. Methods

Chiral Recognition Mechanism and Method development

3.1 Chiral Recognition Mechanism

Chiral recognition refers to the ability of the CSP to interact differently with two enantiomers. In most cases, this also leads their separation. Chromatographic separation depends on the ability of the CSP to preferentially interact with one of the analyte enantiomers when forming somewhat different, relatively short-lived, transient diastereomeric complexes. Separation is achieved based on the difference in retention times.

The interaction of two enantiomers with a CSP, can be expressed as the difference in free energy $-\Delta_{1,2}\ \Delta G^{\circ}$ (i.e., the free energy difference for the transfer of the enantiomers between the mobile phase and the stationary phase). It can be calculated from the separation factor, α, according to the following equations:

$$-\Delta_{1,2}\ \Delta G^{\circ} = \Delta_2 G^{\circ} - \Delta_1 G^{\circ}$$

$$-\Delta_{1,2}\ \Delta G^{\circ} = RT \ln k_2 / k_1 = RT \ln \alpha$$

Here, k_2 and k_1 are the retention factors of the two enantiomers. Thus, chiral discrimination can be expressed in thermodynamic terms. It usually turns out that only small energy differences are needed for the chromatographic resolution of enantiomers.

Understanding the chiral discrimination mechanism is useful when developing an optimum separation method for HPLC using macrocyclic glycopeptide CSPs. Although there is some debate about its simplistic nature, most chiral recognition models are still based on the three-point interaction rule, where a minimum of three simultaneous interactions between at least one enantiomer and the chiral stationary phase are required. However, the complex structures of macrocyclic glycopeptide CSPs can make it difficult to understand the exact interactions that lead to chiral recognition. Almost all possible intermolecular interactions leading to chiral recognition are available with macrocyclic glycopeptide CSPs. This is one thing that contributes to their wide applicability as chiral selectors. Another factor that increases the applicability of these CSPs, but also makes their mechanism of action harder to define, is that there can be different interactions in different chromatographic modes.

3.1.1 Reversed Phase Mode

In the reversed phase mode, as with achiral HPLC stationary phases, the glycopeptide CSP acts as a relatively nonpolar media compared to the polar hydroorganic mobile phase. Hydrophobic interactions between glycopeptide CSPs and chiral analytes were proposed by Armstrong et al(2) for the reversed phase mode and confirmed by other researchers(82). Thus, hydrophobic interactions between the nonpolar part of an analyte and the interior of the glycopeptide basket, is a dominant factor in retention and may also be one of the important factors contributing to chiral recognition. The possible hydrophobic interaction sites are shown as the black areas in Figure 1. Additional interactions that can lead to chiral recognition include electrostatic interactions, hydrogen bonding, dipole-dipole interactions, and steric repulsive interactions. Which interactions are most important for a specific compound, depends on the nature of that analyte (i.e., its size, geometry, number and type of functional groups, flexibility, etc) as well as the nature of the mobile phase used.

Electrostatic interactions can affect both retention and enantioselectivity. Figure 5 and Figure 6 show the pH effects on the retention factor, k, for dansyl-amino acids(82). An inflection point was observed for all the k versus pH plots as well as the selectivity factor versus pH plot. This point is very close to the pKa value of the solute amino group, which is 4.5. Below this point, the amine group of the analyte is protonated and retention is significantly increased. This could be attributed to the ionic interaction between protonated amine group of the analyte and the carboxylate group of the CSP. However, the selectivity factor, α, decreased somewhat (Figure 6). This reveals that the electrostatic interaction between the carboxylate group on the CSPs and the amine group on the analyte is effective only for increasing retention but not for enhancing chiral recognition of dansyl-amino acid enantiomers. After a comprehensive study, Peyrin, et al.(82) verified both thermodynamically and experimentally that the interaction between the amine moiety of teicoplanin CSP and the carboxylate group of dansyl-amino acids plays a crucial role in chiral recognition mechanism, which was consistent with previous results (7,9,11-13,23,42,66,74). Nair et al. reached a similar conclusion in 1996 using vancomycin as the chiral selector in a CE study(13). This was done by forming a copper complex that blocked the secondary amine group on the aglycon portion of vancomycin(13).

Additional evidence also was provided by the huge difference in selectivity when separating enantiomers of the dipeptide Ala-Gly and Gly-Ala (9). The selectivity factor (α) was significantly increased from 1.15 for DL-Ala-Gly to 10 for Gly-DL-Ala, while the only difference between these two peptides is the proximity of the terminal carboxylate group to the stereogenic center. In Gly-DL-Ala, the carboxylate group is directly connected to the stereogenic center while that of the DL-Ala-Gly is five atoms away from the stereogenic center. This result clearly showed the essential role of the teicoplanin amine group as well as the analyte carboxylate group (and its proximity to the chiral center) in the chiral recognition mechanism(9). In addition, the fact that chiral compounds with acidic groups (i.e., carboxylate, sulfinate, phosphate, etc.) are most easily resolved further support this as one of the important chiral interaction sites for acidic or anionic compounds.

3.1.2 Normal Phase Mode

In the normal phase mode, (where the mobile phase is nonpolar), the CSP behaves as a polar stationary phase. The strongly polar functional groups and aromatic rings of the CSP provide the interactions needed for both retention and chiral recognition. Therefore, hydrogen bonding, π-π interactions, dipole stacking, steric repulsion, and in some cases electrostatic interactions are the dominant interactions that occur between the CSP and the analytes in the normal phase mode. Note that the absence of water, by definition, precludes the possibility of hydrophobic interactions contributing to either retention or selectivity. However, in the presence of nonpolar solvents (as in the normal phase mode), the enhanced π-π and dipolar interactions often make up for the lost hydrophobic interactions that were important in the reversed phase mode.

3.1.3 New Polar Organic Mode

In the new polar organic mode, no nonpolar solvents (like hexane) are used. Generally, the main component in the polar organic mobile phase is an alcohol (e.g., methanol, ethanol, or isopropanol). The dominant interactions between the analyte and CSP usually involve hydrogen bonding, electrostatic, dipolar, and steric interactions (or some combination

thereof)(34). Chiral analytes suitable for this kind of mobile phase have some special requirements (*see* Note 1).

It should be noted that, the dominance of different types of interactions in the reversed phase mode versus the normal phase mode means that the chiral recognition mechanism can be very different in these modes. Consequently very different types of chiral molecules often can be separated in one mode vs. the other.

3.1.4 Role of Carbohydrate Moieties

The role of the pendant carbohydrate moieties in chiral recognition was studied by comparing separations performed on the Chirobiotic TAG and T columns(23). A significant selectivity increase was observed for separation of amphoteric molecules like the alpha, beta, gamma and cyclic amino acids as well as some other kinds of acids. This indicated the importance of the aglycon portion in chiral recognition. In this case, the carbohydrate moieties of the native teicoplanin molecule may intervene in the chiral recognition process in at least three possible ways: (i) steric hindrance, where the sugar units occupy room on the aglycon, which limits the access of other molecules to binding sites; (ii) blocking a possible interaction sites on the aglycon, where two sugars are linked to the aglycon through phenol hydroxyl groups and the third sugar is linked through an alcohol moiety (Figure 1); (iii) offering competing interaction sites, since the carbohydrates are themselves chiral and have hydroxyl, ether, and amido functional groups available for interaction(23).

Conversely, the resolution of some analytes, such as amino alcohols, which were excellent on Chirobiotic T, decreased on the Chirobiotic TAG column. This indicates the importance of the sugar units for enhancing chiral recognition for specific types of analytes.

As with the TAG CSP, removal of the sugar units from native vancomycin improved the selectivity of some neutral sulfoxides molecules(43). However, it completely destroyed chiral recognition in a series of racemic esters(117). This means that the carbohydrate moieties enhanced the enantioselective separation of some molecules, but decreases it for others.

Steric effects were also found to be very important for chiral recognition in all mobile phase modes. Bulky groups such as phenyl groups or methyl groups attached on or next to the stereogenic center can effect chiral separation when using macrocyclic glycopeptide CSPs(14,43).

3.2. Method Development

Before using a glycopeptide CSP, one should first examine the analyte structure. Macrocyclic glycopeptide CSPs are able to separate many kinds of molecules. However, molecules with the following characteristics are very likely to achieve baseline separation on these CSPs, if they have 1) ionizable groups to provide electrostatic interactions, 2) hydrogen bonding groups, 3) hydrophobic groups, 4) Bulky substituents next to or close to the chiral center, 5) One relatively polar functional group attach to or close to (α or β) the stereogenic center, and 6) aromatic groups capable of π-π interactions.

3.2.1 Optimizing Chiral Separations

Given the variety of the functionality that exists within the macrocyclic glycopeptides, Chirobiotic columns can work well in reverse phase, normal phase and polar organic modes. Most of the time, higher efficiencies are observed in the polar organic mode and normal phase mode. The ability to operate in different modes can be advantageous since different compounds separate best in different modes. If the polar organic mode is applicable (*see* Note 1), it is usually the best choice to start with. The solubility of the analytes in different solvents also affects the choice of the mobile phase modes, please refer to Note 2.

3.2.1.1 Reversed-phase Mode

Chirobiotic columns separate many compounds in the reversed-phase mode. Optimization of reversed-phase separations are done in much the same way as optimizing achiral separations on C18 columns. It is done by controlling the type and the percentage of organic modifier and other additives, the type and pH of the buffer, ionic strength, flow rate, and the temperature. These factors will be discussed below.

3.2.1.1.1 Organic modifier

The effect of organic modifier concentration on the retention of 5-methyl-5-phenylhydantoin in the reversed phase mode is shown in Figure 7(2). A typical U-shaped curve was obtained when plotting retention and resolution versus composition of organic modifier/aqueous solution (as was previously noted with cyclodextrin-based CSPs)(2). Longer retention and better resolution were usually observed in both the high and low concentration regions of organic modifier. This retention behavior clearly indicated that the importance of hydrophobic interactions between the analyte and the macrocycle at higher concentrations of aqueous buffer(2). When using higher concentration of organic modifier, hydrophobic interactions no longer contribute to retention. However, other interactions become increasingly dominant (e.g., hydrogen bonding, dipolar interactions, etc.).

The type of organic modifier can affect both selectivity and efficiency. If no separation is observed with the first solvent choice, switching to a different organic modifier is highly recommended. Figure 8 shows effects of different types of organic modifiers in the RP mode using vancomycin as the CSP selector. A variety of organic modifiers can be used to affect selectivity including methanol, ethanol, and isopropanol, acetonitrile (ACN), tetrahydrofuran (THF), etc. As shown in Figure 8, different macrocyclic glycopeptide CSPs have a different optimum type of organic modifier. For detail about choice of types of organic modifiers, please refer to Note 3. A typical starting composition ratio is 10/90:ACN/Buffer, pH 3.5-7.0, while the composition of 20/80 is recommended when using alcohol as modifier.

Figure 9 shows that the retention behavior of amino acids in the reversed phase mode is different from that of most other analytes. Amino acids often have smaller retention factors with water-rich mobile phases. This phenomenon may be due to the higher solubility of amino acids in water than in almost all other solvents. In addition, it was shown that the electrostatic interaction between the amino acid and the CSP is so strong that organic modifier concentration does not affect the retention and selectivity factor as much as it does other analytes(7). The resolution factor (Rs) does change with the mobile phase composition. This is because the Rs value depends on both the selectivity and the efficiency.

3.2.1.1.2 Buffers

Buffers are widely used in the mobile phase for Chirobiotic columns to control the ionization of both the analyte and the CSP. In addition, the buffer has ionic strength effects, and affects the selectivity for certain compounds via secondary interactions between the buffer and CSP and/or buffer and analyte. The use of buffer can increase the efficiency of the separation significantly(118). To obtain efficient and reproducible separations in the reverse phase mode, some buffers are essential for separations even for neutral compounds. For most commonly used buffers, please refer to Note 4.

Macrocyclic glycopeptides have ionizable groups as proteins do, therefore, their charge and perhaps their conformation can vary with the pH of the mobile phase. As mentioned previously in section 2.1, pH will have different effects with different Chirobiotic columns due to variations in their ionizable functional groups and their PI values.

Within the operating pH range (3.5 to 7.5), the strength of the short-lived complex formed by the CSP and the analyte can depend on the charge of the analyte. The charge of the analyte will in turn be affected by the pH of the mobile phase. Vancomycin and ristocetin A are both in cationic form, while teicoplanin and most amino acid analytes exist in the zwitterionic form (i.e. with an anionic $-COO^-$ group and a cationic $-NH_3^+$ group). Changes in the pH of the mobile phase can change the ionization of both the analyte and the CSP. Therefore, pH can affect the interaction mechanism even if the analyte is a neutral molecule. As a general rule, the starting pH should close to the pI value of glycopeptide antibiotics. Alternatively, test runs can be made at pH 4 and 7. After finding which pH extreme produces the optimum separation, adjust the pH to 0.5 pH unit above or below the pK of the analyte.

3.2.1.2 Normal-phase Mode

Macrocyclic glycopeptide CSPs effectively separate a variety of compounds in the normal-phase mode. There is no solvent induced denaturation or any irreversible change in these CSPs(2,43). One advantage of using Chirobiotic columns in the normal phase mode is the higher efficiency of most separations. Complementary selectivity to the reverse-phase mode

also is found in the normal-phase mode (i.e., even if no separation was observed in the RP mode, it may be obtained by switching to the NP mode, or vice versa). In normal phase HPLC, hydrogen bonding, π-π interactions, dipole-dipole stacking, and steric interactions are more important. Obviously, hydrophobic interactions are not relevant.

In normal phase HPLC, retention is controlled by adjusting the percentage of a polar organic modifier such as ethanol or propanol. Figure 10 shows the effect of added organic modifier on the retention of two pairs of enantiomers in the normal phase mode. For all enantiomers, retention is decreased as the percentage of organic modifier is increased. However, the exact effect of the mobile phase composition varies somewhat from compound to compound. Also it was observed that resolution can be dramatically changed by using different modifiers. Usually this results from a change in the efficiency of a separation. For example, the separation efficiencies with hexane/ethanol mobile phase mixtures are usually higher than that with hexane/isopropanol mixture on macrocyclic glycopeptide CSPs.

Different combinations of polar and non-polar solvents can affect the selectivity of a separation as well. The most commonly used non-polar solvents for Chirobiotic CSPs are hexane or heptane. Methyl *tert*-butyl ether (MtBE) was also found to be a useful non-polar solvent in some cases, when combined with alcohol or acetonitrile modifiers(43). Recently this unusual solvent combination was used with Chirobiotic V and VAG columns to separate racemic sulfoxide compounds(43). A significant increase in the number of separations was achieved when switching the mobile phase of Hex/EtOH to MtBE/EtOH, while the opposite effect was observed on Chirobiotic T and Chirobiotic TAG column.

The most common organic modifiers are alcohols (i.e., ethanol and isopropanol). Most of the time, the ethanol is the better organic modifier in terms of efficiency and resolution. However, it is worthwhile to mention that methanol is slightly soluble in hexane (about 1% v/v). Thus, in normal phase separations that require very little polar organic modifier, this may be an option. It was also reported that halogenated solvents as well as DMF and dioxane are sometimes useful on Chirobiotic CSPs in the normal phase mode(71).

Once a separation is achieved, adjusting other parameters to gain better resolution is necessary. These parameters include percentage and type of modifier, as well as small amounts of other additives, including some acids or bases.

3.2.1.3 New Polar-Organic Mode

The new polar-organic mode is a modification of the polar organic mode used with cyclodextrin bonded phases(119,120). Subsequently, this approach was found to be highly effective with macrocyclic glycopeptide CSPs (22,34,121).

This mode is more closely related to the normal phase mode than to the reverse-phase mode. Generally, the main component in the polar-organic mobile phase is an alcohol (e.g., methanol, ethanol, or isopropanol) with a very small amount of acid/base added to effect retention and selectivity. This mobile phase can be considered as an "extreme" case of the normal phase mode, or an "extreme" case of the reverse-phase mode. Methanol and ethanol are usually the best polar organic solvents when using the ristocetin A, teicoplanin and teicoplanin aglycon columns. If not enough retention is obtained, acetonitrile is added to the alcoholic mobile phase at varies ratios to gain an appropriate retention time.

There are usually two different factors that need to be adjusted to optimize a separation using polar organic mobile phases. The first one is the absolute amount of acid and base added, which is essential for optimization of retention and the second one is the relative ratio of acid to base, which controls selectivity (*see* Note 5). Figure 11 shows the effect of added acid and base on resolution in the polar organic mode.

One advantage of the polar organic mobile phase is that it can dissolve many analyte salts (i.e., amine hydrochlorides and sodium carboxylates etc.) that can not be dissolved with traditional normal phase solvents(119). Prior to the development of the polar organic mode, these more polar analytes and salts could only be separated in the reversed phase mode. Another advantage is that polar organic mobile phases are compatible with reverse phase solvents when these two formats are used in achiral-chiral column switching procedures(45,122-124).

The polar-organic mode should be considered first when doing methods development for analytes that meet the previously mentioned structural criteria (*see* Note 1). This mobile phase system offers several advantages such as simplicity, versatility and high efficiency. In addition, it uses methanol, which is a relatively inexpensive, less toxic solvent.

3.2.2 Miscellaneous Approaches for Improving Selectivity and Resolution

3.2.2.1 Temperature Effects

Temperature can effect the retention and resolution of chiral analytes on Chirobiotic columns (14,20,44,92,125,126). The reason for this can be attributed to a change in the binding constant of a solute to the CSP with temperature. Studies on the effect of temperature on separations using Chirobiotic V, Chirobiotic T, and Chirobiotic R columns in both normal-phase and reverse-phases have been reported(2,20,44,125). A systematic study of temperature effects on the resolution of 4-benzyl-2-oxazolidinone on vancomycin was done by Scott et al (75). It was observed that the temperature effect on the retention factor (k), separation factor (α), peak-to-peak separation distance, and efficiency (i.e. peak width) are all affected by temperature. Temperature and solvent composition are independent in terms of their effects toward the above factors. Usually an increased resolution can be achieved by lowering the separation temperature.

Figure 12 shows the effect of temperature for enantioselectivity of beta-methylphenylalanine separated on a Chirobiotic T column(14). This figure shows that poor resolution was observed at ambient temperature but improved resolution was observed at both higher and lower temperatures(14). There are two different temperature related effects on enantiomeric resolution(20). One is the thermodynamic effect, which is responsible for the observed decrease in the selectivity factor (α) when temperature is increased. This is due to the partition coefficients and therefore the Gibbs free energy change (ΔG^{o}) of transfer of the analyte between the mobile phase and the stationary phase with temperature(125). The other kinetic effect produces an increase in efficiency with an increase in temperature. This results from the decrease in viscosity and the increase in the analytes diffusion coefficients. In the

case of Figure 12, the latter kinetic effect dominates at higher temperature and the thermodynamic effect is dominant at lower temperature. There are two different mass transfer effects here. One is mobile phase mass transfer, where a reduced mobile phase viscosity occurs as temperature increases. However, an increase of temperature also increases the diffusion coefficient of the solute in both the mobile phase and the stationary phase, and it decreases the viscosity of the stationary phase (increasing stationary phase mass transfer). Therefore, a temperature increase usually provides a trade-off in terms of resolution. The increased efficiency is good for resolution, while the lessening of the peak-to-peak separation is bad for resolution.

It has been observed that changing the temperature has a greater effect on the retention of solutes in normal-phase chromatography than reverse-phase(20). Higher temperatures (>40 °C) can racemize some chiral compounds. Lower temperatures improve the separation for most compounds(44). However, the temperature effect must be determined on a case-by-case basis. The normal starting temperature is ambient temperature. Variations in temperature can be controlled by using a thermostated column temperature control device.

3.2.2.2 Flow Rates

The effect of flow rate on resolution is less pronounced with Chirobiotic columns than other factors. However, a general phenomenon observed with chiral stationary phases that have inclusion pockets is that there is an increase in resolution with a decrease in flow rate(71).

This effect was also observed for cyclodextrin-based columns particularly in the reverse-phase mode. Decreasing the flow rate increases the retention time, but in return, better resolution is obtained. Usually flow rate does not affect the enantioselectivity factor (α), but does affect the separation efficiency. This is reflected by the inverse relationship between resolution (Rs) and flow rate. Flow rates <0.5 ml/min are not very common since it will not produce further significant increases in resolution.

In the polar-organic mode, smaller effects have been observed. While in normal phase mode, no observable effects were shown on selectivity by increasing the flow rate up to three times

faster than the original condition(71). However, the resolution is affected slightly due to the change in efficiency. Consequently, higher flow rates are often used for normal phase separations as long as the back pressure is not excessive. Normal phase flow rates ran as high as 5 ml/min have been used in our lab. High efficiency normal phase separations are especially appealing to industry. For reverse phase LC, flow rates around 0.5 to 1.5 ml/min are recommended.

3.2.3 Supercritical Fluid Separations

It is worthwhile to mention that super/subcritical fluid chromatography (SFC), is a high speed chiral separation approach which can substitute for normal phase HPLC separations. It can be advantageous for industrial and preparative-scale chiral separations (107,127,128). SFC separations offer rapid column equilibration times, simple eluent compositions (i.e., CO_2 and an organic modifier such as methanol and/or organic acids and bases), and less waste solvent generation. Due to the very low viscosity of the SFC eluent, faster flow rates (greater than 4 mL/min) are frequently utilized. Normally, chiral separations using SFC can be achieved in less than 15 minutes(107). One drawback of this technique is that the observed peak shapes are not as smooth and symmetrical as those obtained in HPLC normal phase separations(107). This effect may result from the variation in the density and viscosity of the super/subcritical fluid due to the SFC operating conditions (i.e., temperature and pressure etc.). The solubility of the analyte in the eluent may be inhomogeneous over the length of the column, which in turn, will affect the signal response.

3.2.4 Complementary Separations

As mentioned previously, complementary selectivity is a very useful feature of the Chirobiotic series of columns. Figure 13 shows the principle of complementary separations using the Chirobiotic V and Chirobiotic T columns for the separation of warfarin and N-CBZ-Norvaline. It can be seen that a partial separation was significantly improved when switching from one to another related column in this family using the same mobile phase conditions. This phenomenon also exists between all other Chirobiotic columns.

3.3 Method Development with Individual Chirobiotic Columns

3.3.1 Vancomycin CSP (Chirobiotic V)

Vancomycin shows considerable enantioselectivity for neutral molecules, amides, acids, esters and cyclic amines etc. A wide variety of secondary and tertiary amines have been separated on the Chirobiotic V column in the polar organic (PO) mode. As discussed before, if a molecule meets the structural criteria in Note 1, the PO mode is the mobile phase of choice, followed by the normal phase (NP) mode and the revered phase (RP) mode, depending on solubility issues (*see* Note 2), etc. The following table and protocol flow chart provide a generic approach to a chiral separation using a Chirobiotic V column. Optimization is necessary following the starting mobile phase based on the criteria outlined in the previous sections.

Table 3. Starting Mobile Phase Compositions for Chirobiotic V(71)

Mode	Mobile phase composition	Solvent/additive ratios	Types of chiral analytes
PO	MeOH/HOAC/TEA	100/0.1/0.1	Amino alcohols and (cyclic) amines.
RP	THF/20mM NH_4NO_3, pH 5.5	10/90	Amines, imides, acids, profens.
NP	Hex/EtOH	80/20	Hydantoins, barbiturates, imides, and oxazolidinones.

Figure 14 shows the Method Development Protocol- Chirobiotic V

3.3.2 Teicoplanin CSP (Chirobiotic T)

The Chirobiotic T column seems to be particularly adept at resolving the following general classes of compounds: native amino acids (most ordinary alpha and beta amino acids are separated on Chirobiotic T)(7,9), N-blocked amino acids (including FMOC, CBZ, *t*-Boc etc), α-hydroxycarboxylic acids, acidic compounds (including carboxylic acids, phenols, etc.), small peptides(9), cyclic amides, sulfoxides(43), neural aromatic analytes(129), and other neutral cyclic amines containing aromatic moieties. Separations

normally obtained on a chiral crown ether or ligand exchange type CSP are also possible on the Chirobiotic T column. In general, there is no better chiral stationary phase for the separation of native amino acid enantiomers than that based on teicoplanin(61,114). In addition, beta-blockers (amino alcohols) have been resolved. It also shows the "complementary stereoselectivity" to Chirobiotic V, Chirobiotic R, and Chirobiotic TAG columns.

In methods development, the polar organic mode is the first utilized mode if the analyte meets the structural criteria (*see* Note 1). In the RP phase mode, the Chirobiotic T appears to achieve the best separations when an alcohol type mobile phase modifier is used (*see* Note 3). The order of priority for organic modifiers is MeOH > EtOH > THF > IPA. The exceptions are amino acids where EtOH modifier produced higher selectivities. The pH can be adjusted to optimize the RP mode separation. Lower pHs, to 3.8, produces a significant increase in retention for analytes with free carboxyl groups. In all cases, both selectivity and resolution varies with pH. Nonionizable analytes typically show less variation or a decrease in retention with the decrease in pH. The pH resulting in optimum selectivity (α) for nonionizable analytes, i.e. pH 7, rarely corresponds to the pH of optimum resolution, i.e. pH 4. Chirobiotic T is very sensitive to acidic conditions, therefore, the safest and most stable pH range is 3.8 to 7.0(71).

Chirobiotic T can be used in any NP mode, however, the preference of polar organic modifier for Chirobiotic T is EtOH. There are a few cases where IPA works better. The following Table 4. gives a summary of starting mobile phases for the Chirobiotic T column in all three mobile phase modes.

Table 4. Recommended Starting Mobile Phase Compositions for Chirobiotic T.

Mode	Mobile phase composition	Solvent/additive ratios	Types of chiral analytes
PO	MeOH/HOAC/TEA	100/0.1/0.1	Amino alcohols and N-blocked amino acids

RP	MeOH/0.1% TEAA, pH 4.1	20/80	α-hydroxy acids, oxazolidinones,
RP for amino acids	EtOH/H_2O	50/50	underivatized and N-blocked amino acids and peptides
NP	Hex/EtOH	80/20	Hydantoins and imides

Figure 15 shows the Method Development Protocol-Chirobiotic T

3.3.3 Teicoplanin Aglycon CSP (Chirobiotic TAG)

The Chirobiotic TAG is a variation of the Chirobiotic T and has shown excellent complementary selectivity to the Chirobiotic T. Much better resolution was observed for separation of amphoteric molecules, including many alpha, beta, gamma and cyclic amino acids, including carnitine, as well as other kind acids(23). It also showed remarkable selectivity for neutral molecules such as oxazolidinones, hydantoins, diazepines, coumarine derivatives and chiral sulfur containing compounds(7,36,43,129).

The mobile phase selection criteria are similar to that for Chirobiotic T. All of the points made under the Chirobiotic T are applicable to Chirobiotic TAG. The flow chart for method development protocol-Chirobiotic TAG is shown in Figure 16. We can see in Figure 16 that the single solvent (i.e., methanol, ethanol and acetonitrile) was used for Chirobiotic TAG as the mobile phase and it showed excellent resolution on some neutral molecules.

3.3.4 Ristocetin A (Chirobiotic R)

Chirobiotic R also is complementary to Chirobiotic V and Chirobiotic T with high selectivity for anionic chiral molecules and many amino acids(17). The mobile phase selection and separation optimization criteria are also similar to those for Chirobiotic T. It also appears to favor alcohol type mobile phase by a large margin. The following tables and flow chart will be very useful to start a separation using Chirobiotic R as a CSP.

Table 5. Recommended starting mobile phases for Chirobiotic R

Mode	Mobile phase composition	Solvent/additive ratios	Types of chiral analytes
PO	MeOH/HOAC/TEA	100/0.1/0.1	Alpha-hydroxy acids, profens, N-blocked amino acids
RP	MeOH/0.1% TEAA, pH 6.8	20/80	Alpha-hydroxyl/halogenated acids, substituted aliphatic acids, profens, N-blocked amino acids, hydantoins, peptides
RP	EtOH/H_2O	50/50	Amino acids
NP	Hex/EtOH	40/60	Imides, hydantoins, N-blocked amino acids

Fig 17 shows the Method Development Protocol-Chirobiotic R

3.4 Column Coupling for Rapid Screening Chiral Selectivity

"Column coupling" is a very useful application of the "complementary feature" of Chirobiotic columns. Since each of the Chirobiotic columns (i.e. Chirobiotic V, T, and R) has its unique selectivity in all three mobile phase modes towards different chiral racemates, it should be a very efficient way to put them together and make a combined column to do a fast screening for selectivity. This "coupling column" was made by ASTEC by combining three 10 cm Chirobiotic columns in the direction of increasing polarity regardless of the mobile phase type, i.e., Chirobiotic R→ V→ T. This technique is very useful. It allows for the evaluation of this entire class of chiral selectors with a single coupled column for the ability to separate a molecule. Even if a partial separation or a shoulder is obtained on the coupled column, a baseline separation is guaranteed with one of the columns in this class.

However, the enantiomeric elution order for an analyte on different columns may reverse(9,14,36,43), which may cause cancellation of the overall separation. Therefore, consideration of the elution order on different CHITOBIOTIC columns before screening is necessary. But it is very unlikely that the separation will be completely diminished by elution order reversal on different columns. Eventually some resolution should be able to be observed even like a partial split, or a shoulder peak. It has been observed that if a partial resolution of 0.6 or greater is obtained in the column coupling screening, a resolution of >1.5 baseline separation can be optimized on a 25 cm column for the

selected stationary phases(62). This fast screening method is very straightforward and requires minimum amount of time in searching for an optimum CSP.

Practically, in order to determine whether a chiral separation is achievable on Glycopeptide antibiotics CSP, three runs using this coupling column in the following order will be able to tell.

1. R + V + T in the new polar organic mode: MeOH/HOAC/TEA=100/0.02/0.01
2. R + V + T in reversed phase mode: MeOH/TEAA (0.1%, pH 6.0)= 25/75
3. V + T in normal phase mode: EtOH/Hexane=60/40

Once a partial or complete separation is done on the coupling column, the following optimization steps in specific mobile phase modes should be followed to get a better resolution on a single CSP(71).

Table 6. Recommended optimization steps following the coupling column screening

Optimize in PO Mode	Optimize in RP Mode	Optimize in NP Mode
1. choose a single analytical column (25cm R, T, or V) 2. choose proper acid/base (HOAC, TEA, TFA, NH4OH or salts etc.) 3. adjust acid/base ratio (4/1 to 1/4) or salt concentration 0.01% to 1%. Higher concentration of salts results in lower retention 4. change flow rate, lower flow rate often results in higher resolution. 5. decrease temperature can increase resolution	1. Choose a single analytical column (25 cm R, T, or V) 2. Choose proper organic modifier (THF for V, MeOH for R and T) 3. Change the concentration of organic modifier. Higher concentration results lower retention. 4. Choose proper buffer (TEAA, NH4OAC, NH4NO3, Na citrate) 5. Change the concentration of aqueous buffer range: 0.05% to 1% 6. Change pH of aqueous buffer. 7. Change flow rate. 8. Decrease temperature	1. Choose a single analytical column (25 cm R, T, or V) 2. Choose proper polar solvent (EtOH, IPA) 3. Change the concentration of polar solvent. Higher concentration results lower retention. 4. Add small amounts of acid + base as modifiers. 5. Change temperature (T); selectivity and elution order may change with T. Lower T, increase Rs, higher T may lead to co-elution and finally reversal of elution order. Maximum operation temperature is 65°C.

3.5 Applications using Glycopeptide Antibiotic CSPs

The use of Glycopeptide Antibiotic CSPs has resulted in the successful separation of most types of neutral, acidic, and basic compounds. Table 7 summarizes the separations achieved on the Chirobiotic V, T, R, and TAG columns. They are classified as amino acids and peptides, N-blocked amino acid, alcohols, acids, sulfoxides, neutral molecules etc. The name of the compound separated, the column type, mobile phase conditions, separation parameters, and reference are all listed in Table 7. This is not intended to be a complete database for these columns, but rather an attempt to give example of the variety of compounds that have been separated using Chirobiotic columns. This may provide a useful starting point, as well as provide pertinent references for scientists interested in LC enantiomeric separation.

Some general trends concerning types of chiral compounds separated on these columns can be noted from the information listed in Table 7.

1) First of all, almost all amino acids and N-blocked amino acids are easily separated on these columns. The Chirobiotic TAG provided the best selectivity for native amino acids, followed by the Chirobiotic T column (which usually produces higher efficiency separations). N-blocked amino acids usually are best separated by the Chirobiotic T and Chirobiotic V columns. Chirobiotic V column works best for esters compared to other Chirobiotic columns.

2) Neutral aromatic molecules are best separated in the normal phase mode, and sometimes in the polar organic mode (if they have at least two polar functional groups). The separation efficiency in these modes is usually good. Reversed phase separations are also possible.

3) Acidic or anionic molecules, including many non-steroidal anti-inflammatory compounds, are best separated in the polar organic mode or reversed phase mode. The Chirobiotic V column separates the most amine-containing compounds (particularly, 2°, 3° and cyclic amines) as does the Chirobiotic T column. None of the Chirobiotic columns separate

primary amine compounds well unless they also have other polar functional groups (e.g. amino acids, amino alcohols, etc.).

4) When compounds are separated by both the Chirobiotic T and TAG columns, usually the TAG column has greater selectivity, and the T-column shows greater efficiency.

Given the wide applicability of these columns, it is clear that use will expand in the future.

4. Notes

1. Chiral analytes suitable for the new polar organic mobile phase mode should have at least two polar functional groups. These functional groups include alcohols, halogens (F, Cl, Br, I), nitrogen in any form (primary, secondary, and tertiary amines), carbonyl, carboxyl, oxidized forms of sulfur and phosphorus, for example. At least one of the analyte's polar functional groups must be on or near the stereogenic center. The other polar group can be located anywhere in the molecule. It is also beneficial if the analyte has some steric bulk or aromatic rings close to the stereogenic center.

2. To choose the best mobile phase mode for a separation, the solubility of the sample in the mobile phase is a key issue, particularly for preparative scale separations. If the analyte is soluble only in organic solvents, either the normal phase or polar organic mode can be used (depending on the number and locations of functional groups on the chiral molecule, see Note 1). When the solute is water soluble only, the reverse-phase mode is required. There are some solutes that can be separated in both reversed-phase and polar organic modes. This gives the analyst a choice of conditions. Likewise some other analytes can be separated in both polar-organic and normal phase modes. Usually one mode is superior to the other in terms of separation speed, resolution, sample loadability, and compatibility to prior sample work-up procedures.

3. In the reversed phase mode, different macrocyclic glycopeptide CSPs prefer different type of organic modifiers. For example, THF and ACN work best on Chirobiotic V and VAG,

while Chirobiotic T, TAG and R produce better selectivity and efficiencies with alcohol-type modifiers. The elutropic strength for ACN and THF is about twice that of alcohols on Chirobiotic columns.

4. Recommended buffers in the reversed phase mode in the order of their usefulness are as follows: triethylammonium acetate (TEAA), ammonium acetate, ammonium nitrate, and sodium citrate. The percentage of the buffer salts can be varied from 0.01% to 1% depending on the retention factor of specific analytes. Normally, the higher the buffer concentration, the shorter is the observed retention. Buffer solutions with 0.1% TEAA are most frequently used. They are prepared by titrating a 0.1% solution of triethylamine with glacial acetic acid, to the appropriate pH.

5. The absolute amount of added acid and base in the polar organic mode is essential for optimization of the retention time. If the analyte elutes too fast, the concentration of the acid/base pair is reduced, or acetonitrile can be added to the mobile phase. On the other hand, if the analyte is strongly retained, the acid/base concentration is increased. The range of concentrations for the acid/base pair are between 1% and 0.001%. If an acid/base concentration >1% is needed, this indicates that the analyte is too polar and that a reverse-phase separation may be preferred. Concentration below 0.001% indicates a normal-phase system may be preferred.

The ratio of acid to base controls the degree to which the ionizable solutes are protonated or deprotonated(119). It is a key factor that affects the selectivity. By adjusting the ratio of acid to base and the overall percentage of both acid and base, retention and resolution both can be affected. The typical starting ratio is 1:1 (mole/mole), and then a 1:2 or 2:1 ratio are used to find the most improved resolution. The ratio of acid to base can be as high as 5:1. Acids and bases that can be used with Chirobiotic columns include triethylamine, ammonia, acetic acid, TFA, etc. TFA is usually used in 50% of the amount of acetic acid due to its greater acidity. Ammonium acetate, ammonium trifluoroacetate and ammonium formate are very popular mobile phase additives in both HPLC and LC-MS.

Table 7 Chiral Separations Achieved on Chirobiotic Columns (cont'd on next page)

Chiral Compound	Chirobiotic Column	Mobile Phase	Reference	Note
Amino acids, derivatives and peptides				
Native amino acid (Including 20 naturally occurring and amino acids not found in proteins)	T, TAG, R	RP	(9,17,23,29,35,74,78,88,130,131)	More than 70 compounds
Dopa (DL-3-(3,4-Dihydroxyphenyl) alanine)	T,TAG,R	RP	(9,17,23,29)	Antiparkisonian
Folinic acid (5-formyl-5,6,7,8-tetrahydrofolate)	T,TAG	RP	(23,29)	Antianemic
Carnitine and Acetyl carnitine	T, TAG	RP, PO	(23,29,35)	fat fighter
N-blocked amino acids				
Dansyl (5-dimethylamino-1-naphthalenesulfonyl) amino acids	T, R, V	RP,PO,NP	(2,7,17,19,22,36,82,132)	
N-2,4-Dinitrophenyl-amino acids	R,T	RP,PO,NP	(7,17)	
N-2,4-Dinitrophenyl-α-amino-carboxylic acid	R,T	RP,PO	(7,17)	
N-3,5-Dinitro-2-pyridyl-aminoacids	T,R	PO,NP,RP	(7,17,19,22)	
N-3,5-Dinitrobenzoyl-amino acids	V, T, R	RP,PO,NP	(2,7,17,19,22)	
N-Acetyl-amino acids	R, T	RP,PO	(7,17,29,35,133)	
N-Acetyl-n-fluro-phenylalanine	R,T	RP,PO	(7,17,29)	
N-fluoro-amino acids	R	RP	(17)	
N-methyl-amino acids	R	RP	(17)	
N-Benzoyl-amino acids	V, T, R	RP,PO,NP	(2,7,17,19,22)	
N-blocked tryptophan analogues	R	RP	(125)	7 compounds
N-Carbamyl-amino acids	R,T, V	RP,PO	(2,7,17)	
N-CBZ (carbobenzyloxy) amino acids	V, T, R	RP,PO,NP	(2,7,17,19,22)	
N-FMOC (9-Fluorenylmethyl chloroformate) Amino acids	T, R	RP,NP	(17,19)	
N-Formyl-amino acids	R,T	RP,PO	(7,17)	
N-Phthaloyl-amino acids	R	PO,NP	(17)	
N-Phthaloyl-glycyl-amino acids	R,T	RP,PO,NP	(7,17)	
N-t-BOC (tert-Butoxycarbonyl) Amino acids	T,V,R	RP	(2,7,17,74,118)	
Other amino acids				
Synthetic amino acid analogues containing 1,2,3,4-tetrahydroisoquinoline, tetraline or 1,2,3,4-tetrahydro-2-carboline skeletons	R	RP, PO	(31)	28 compounds
Unusual amino acid analogs (Tyrosine, phenylalanine, tetrahydroisoquinoline, aminotetralin, tryptophan analogs etc)	R	PO,RP	(134)	25 compounds
Unusual ring- and α-methyl-substituted phenylalanine analogs	T	RP	(38)	6 compounds
Secondary amino acids possessing 1,2,3,4-tetrahydroisoquinoline and related analogues	T	RP	(26)	9 compounds
Unusual secondary aromatic amino acids	T	RP	(18)	
Unusual β-methyl-substituted amino acids	T	RP	(25)	4 compounds
β-amino acids	T	RP	(135)	13 compounds
Unusual cyclic β-substituted α-amino acids	T	RP	(80,92,126)	5 compounds
Unusual amino acids (phenylalanine, tyrosine analogues and analogues containing 1,2,3,4-tetrahydroisoquinoline, tetraline, 1,2,3,4-tetrahydro-2-carboline, cyclopentane, cyclohexane, bicycle[2.2.1]heptane or heptene skeletons)	T	RP	(14)	31 compounds

Table 7. continued

β-substituted –β-alanines	T, R	RP, PO	(33)	8 compounds
β-substituted –tryptophan analogues	T	RP	(27)	5 compounds
β-methyl-amino acids (tyrosine, phenylalanine, tryptophan, and 1,2,3,4-tetrahydroisoquinoline-3-carboxylic acid)	T	RP	(14,20)	4 compounds
2-pyrrolidone-5-carboxylic acid	T,TAG	RP	(23,29)	
3-(n-naphthyl) alanine	V,R	NP,RP	(2,17)	
4-bromo-phenylalanine	R	RP	(17)	
4-chloro- phenylalanine	R	RP	(17)	
5 or 7-benzyloxy-tryptophan	R	RP,PO	(17)	
Baclofen	T	RP	(7)	
Carnitine and *O*-acylcarnitine derivatives	T	RP	(40)	13 compounds
Carnitine and *O*-acylcarnitine derivatives	T	RP	(136)	13 compounds
Penicillamine	R	RP	(17)	
selenomethionine	T	RP	(89)	HPLC-ICP-MS
Dopa and 3-*O*-methyl-dopa	T	RP	(49)	Antiparkisonian
Theanine	R	RP	(17)	
Both N and Carboxy-Protected amino acids (PAAs)				
Fmoc-Ser-OH, Fmoc-Asp-OH, Fmoc-Arg-(Pmc)-OH, Fmoc-Asp-(OtBu)-OH, Fmoc-Glu-(OtBu)-OH, etc.	T	RP	(46)	21 compounds
Di- and tripeptides	R,T	RP	(7,9,17)	60 compounds
Amino alcohols, (β-blockers, β-adrenoreceptor blocking drugs)				
(R)- and (S)-atenolol (elution order determined)	T	PO	(45)	anticardiovascular
Alprenolol	T, V, R	PO	(2,137,138)	antihypertensive
Arotinolol	T, V	PO		antihypertensive
Atenolol	T, V, TAG	PO	(23,29)	antiarhytmic
Labeltalol	V	PO	(28)	achieved in CEC
Metoprolol	T, R	PO	(7,17)	antihypertensive
Oxprenolol	T, V	PO	(2,7)	antihypertensive
Pindolol	T, TAG, V	PO	(23,29,71,87)	antihypertensive
Practolol	T	PO	(139)	antihypertensive
propranolol	T, V, R	PO	(2,137)	antihypertensive
Propranolol, metoprolol	V, T	PO	(71,87)	antihypertensive
Sotalol	V	PO	(28)	achieved in CEC
Calcium Channel Blockers (modulators)				antihypertensive
4-aryldihydropyrimidine derivatives (DHPMs)	V, T	RP	(47)	27 compounds
Nicardipine	V, T	PO	(87)	
Other cardiovascular drugs				
albuterol (a.k.a. salbutamol)	V, T	PO	(71,72)	β_2 adrenoreceptor agonist

Table 7. continued

Alkylamino derivatives of aryloxypropanols	V, T	PO	(34)	62 compounds anti-cardiovascular disorder
Clenbuterol	T	PO	(139)	β_2 adrenoreceptor
denopamine				Cardiotonic
flosequinan				vasodilator
formoterol				β_2 adrenoreceptor agonist
pinacidil				antihypertensive
simendan				intotropic drug
Terfenadine	T	RP, PO		antihistaminic
Valsartan,				angiotensin II
Verapamil	T	RP, PO	(29)	antianginal
Warfarin	T, TAG,R, V	RP	(2,7,17,23, 29)	anticoagulant
Non-steroidal anti-inflammatory				
Benoxaprofen	V	RP	(71)	
Carprofen	T	RP	(7)	
Fenoprofen	V	RP	(71)	
Fenoprofen Methyl Ester	V	RP	(71)	
Flurbiprofen	T,V	RP	(7,19,71)	
Ibuprofen	T, V,R	RP	(7,19,22)	
Indoprofen	T, R, V	RP	(2,7,17,19)	
ketoprofen	T, V, R	RP	(7,17,19,22 ,71)	
Surfrofen	T	RP	(7,19)	
Chiral acids				
1,1-binaphthyl-2,2'-diyl hydrogen phosphate	V	RP	(2)	
2-(2,4-dichlorophenoxy)propionic acid	T	RP	(7,140)	
2-(2-chlorophenoxy)propionic acid	T	RP,NP	(7)	
2-(3-chlorophenoxy)propionic acid	T	RP	(7)	
2-(4-chloro-2-methylphenoxy)propionic acid	T	RP	(140)	
2-(4-chlorophenoxy)propionic acid	T	NP,RP	(7,19)	
2-(4-Hydroxyphenoxy)propionic acid	T	RP	(7)	
2-(4-Nitrophenyl)propionic acid	T	RP	(7)	
2-Imidazolidone-4-carboxylic acid	T	PO	(7,19)	
2-Phenoxypropionic acid	T	RP	(7)	
2-Phenylpropionic acid	T,R	RP,PO	(19)	
2-Phenylpropionic acid	T	RP	(7)	
3-(4-Hydroxyphenyl) lactic acid	T	RP	(7)	
3-(Benzyloxycarbonyl)-4-oxazolidine carboxylic acid	T	RP	(21)	
3-amino-3-phenylpropionic acid	R	PO	(19)	
3-Hydroxy-4-methoxymandelic acid	T,R	RP,PO	(7,17)	
3-Indolelacedtic acid	T,R	RP,PO	(7,17)	
4-Hydroxy mandelic acid	T, TAG,R	RP, PO	(7,17,22,23 ,29,35)	urinary antiseptic
6-Methoxy-1,2,3,4-tetrahydro-9*H*-pyrido[3,4-*b*]indole-1-carboxylic acid	R	RP	(19)	

Table 7. continued

Alkoxy-Substituted Esters of Phenylcarbamic Acid	V, T	PO	(32,42)	30 compounds Local anaesthetics
Aryloxyphenoxypropanoic acid	T	RP	(48)	Antitumor agent
Atrolactic acid	R,T	PO,RP	(7,22)	
Benzocyclobutenecarboxylic acid	T	RP	(7)	
Cis-2-amino cyclohexane carboxylic acid	T, TAG	RP, PO	(23,29)	
Iopanic acid	T	RP	(7)	
Mandelic acid	T,R	RP,PO	(7,17,21,22 ,35)	
Neproxen	R	RP	(19)	
p-Chloromandelic acid	T	RP	(7)	
Ritalinic acid (RA)	V, T	PO	(87)	
trans-4-Cartinine-carboxylic acid	T	RP	(7)	
Tropic acid	T	RP, PO	(7,29)	
α-amino-2-thiopheneacetic acid	R	RP	(19)	
α-Methoxyphenylacetic acid	T	RP	(7)	
β-Phenyllactic acid	R,T	PO,RP	(7,22)	
Mecoprop, mecoprop-methyl	T, TAG	RP,PO	(23,29)	herbicide
Chiral Amines				
N-Benzyl-α-methyl-benzylamine	V	PO	(21)	
N-Benzyl-1-(1-naphthyl)-ethylamine hydrochloride	V	PO	(21)	
Phenyl propanolamine (Norephedrine)	T	RP, PO	(29)	
Idazoxan	V	RP	(2)	
α-(1-aminoethyl)-hydroxybenzyl alcohol	V	RP	(2)	
Bupivacaine	V,T	RP	(2,7)	
N-(3,5-dinitrobenzoyl)-α-methylbenzylamine	V	RP	(2)	
β-Hydroxyphenethylamine	R	RP,NP	(17,19)	
Penicillamine	R	RP	(19)	
Nα-Benzoylarginine-β-naphthylamine	T	PO	(7)	
Plant growth regulators and related indole compounds				
3-(3-indolyl)-butyric acid, abscisic acid and structural related compounds including a variety of substituted tryptophan etc.	T, R	RP	(52)	18 compounds
Organometallic complexes				
Tris-diimine ruthenium(II) complexes	T, TAG	RP	(141)	9 compounds
Ferrocenylalkyl polyfluoroalkyl benzimidazoles	V, T	RP, NP	(41)	3 compounds
Other heterocyclic compounds				
Polyfluoroalkyl benzimidazoles	V, T	RP,NP	(41)	
4-Benzyl-2-oxazolidinone	T, V	RP,NP	(16,19,75)	
4-, or 5- substituted racemic pyridones (Substituted 2-methoxy-6-oxo-1,4,5,6-tetrahydropyridine-3-carbonitriles)	V, T	RP	(68)	9 compounds
dl-threo-Methylphenidate	V	RP	(86)	antihyperactive
Oxazepam	V, T	PO	(87)	
Temazepam	V	RP	(2)	
cyclic imidic compds (barbiturates, piperidine-2,6-diones, and mephenytoin) including mephobarbital and thalidomide, hexobarbital etc)	V	RP, NP	(142)	11 compounds

Table 7. continued

Citalopram and its 2 N-demethylated metabolites demethylcitalopram and didemethylcitalopram	V	RP	(138)	
RS - 4- phenyl - 2- oxazolidinone	V, R, T	RP,NP, PO	(36)	
RS- 4- benzyl- 2- oxazolidinone	V, R, T	RP,NP, PO	(2,7,19,36)	
RS- 4- benzyl- 3-propionyl- oxazolidinone	V, R, T	RP,NP, PO	(36)	
RS- 5,5,dimethyl-4-phenyl-2-oxazolidionone	V, R, T	RP,NP, PO	(36)	
RS-3-benzyloxy carbonyl-4-oxazolidine carboxylic acid	V, R, T	RP,NP, PO	(36)	
4S,5R(+) - cis- 4,5- diphenyl-2-oxazolidinone	V, R, T	RP,NP, PO	(36)	
Coumachlor	T, TAG, V	RP,PO	(2,7,19,23, 35)	rodenticide
Coumafuryl	V,T	RP, NP.PO	(2,7)	
5-Methyl-5-phenyl hydantoin	T, TAG, V,R	RP,PO,NP	(2,7,17,19, 22,23,29,3 5)	anticonvulsant
Styrene oxide	T, TAG	RP,PO	(23)	
Thioridazine	T, TAG	RP,PO	(23)	antipsychotic
Tetrakis[1-[(4-tert-butyl-phenyl)sulfonyl]-pyrro-lidine-carboxylate] dirhodium(II)	V	PO	(21)	synthesis intermediate
2-methyl-4-phenyl indanone	T	RP	(35)	
phenylphthalide	T	RP	(35)	
γ-(2-naphthyl)-butyrolactone	T	RP	(35)	
γ-Phenyl- γ-butyrolactone	T	NP	(7)	
Althiazide	T, V	RP, NP	(2,29)	diuretic
3-methyl-5-cano-6-methoxy-3,4-dihydro-2-pyridone	V	RP	(2)	
Thioridazine	V	RP	(2)	
5-(4-hydroxyphenyl)-5-phenylhydandoin	V,R,T	RP,NP	(2,7,17,22)	
5-(3-hydroxyphenyl)-5-phenylhydandoin	R	NP	(17)	
3-benzoylphthalide	V	RP	(2)	
3-phenylphthalide	T	RP	(7)	
2,2,2-trifluoro-1-(9-anthryl)ethanol	V	RP	(2)	
Mephobarbital	V	NP	(2)	
Hexobarbital	V	RP	(2)	
3a,4,5,6-tetrahydrosuccinimide[3,4-b]acenaphthen-10-one	V, T,R	RP,NP	(2,7,17,19, 22)	
1-benzoyl-2-tert-butyl-3-methyl-4-imideazolidinone	V,T	RP,NP	(2,7)	
3-[2-(2-bromoacetamido)acetamido] PROXYL	V	RP	(2)	
Ethyl-2-pyrrolidone-5-carboxylate	V	RP,NP	(2,19)	
α-carbethoxy-γ-phenyl-γ-butyrolactone	V	RP,NP	(2,19)	
CGA-40919	V	RP	(2)	
Ftorafur	V	RP,NP	(2,19)	
5-(4-methylphenyl)-5-phenylhydantoin	V,T	RP,NP	(2,7,19)	
1,1'-bi-2-naphthol	V	RP	(2)	
γ-phenyl-γ-butyrolactone	V,R	RP,PO	(2,17)	
Ethyl-2-pyrrolidone-5-carboxylate	V	RP	(2)	
Chlorthalidone	R	NP	(22)	
5-Phenyl-2-(2-propynylamino)2-oxazolin-4-one	R,T	NP	(7,22)	
Althiazide	T,R	RP,NP	(7,17)	
4-Benzyl-2-methoxy-6-oxo-1,4,5,6-tetrahydrophyridine-3-carbonitrile	T	RP	(7)	
4-Phenyl-2-methoxy-6-oxo-1,4,5,6-tetrahydrophyridine-3-carbonitrile	T	NP	(7)	
4-Cyclohexyl-2-methoxy-6-oxo-1,4,5,6-tetrahydrophyridine-3-carbonitrile	T	RP,NP	(7)	

Table 7. continued

4-Methyl-2-methoxy-6-oxo-1,4,5,6-tetrahydrophyridine-3-carbonitrile	T	NP	(7)	
Devrinol	T	RP	(7)	
Tetrahydropapaveroline hydrochloride	T	PO	(7)	
Mephentoin	T	NP	(7)	
TAPA	R	NP	(17)	
Tetrantoin	R	NP,PO	(17)	
Chlorthalidone	R	NP	(17)	
1-Benzocyclobutenecarbonitrile	R	NP	(17)	
1-Acetoxy-8-hydroxy-1,4,4a,9a-tetra-hydroanthraquinone	R	NP	(17)	
Fluoxetine, Terbutaline	V,T	PO	(87)	
Bromacil	T, TAG, V	RP, PO	(2,7,19,23,29)	herbicide
Mephenytoin	V,T	RP,NP	(2,19)	
devrinol	V	RP	(2)	
norverapamil	V	RP	(2)	
Verapamil	V	RP	(2,19)	
Semisynthetic ergot alkaloids Nicergoline (α-adrenergic blocking agent), lisuride (serotonin antagonist), terguride (mixed D_2 agonist/antagonist of the pituitary) meluol.	V, T	RP	(76)	
Other neutral compounds				
Aminoglutethimide	V,R	RP,NP	(2,17)	
Bendroflumethiazide	V,T	RP	(2,7)	
Benzoin methyl ester	V	RP	(2)	
Captopril diastereoisomers	T	RP	(44)	antihypertensive
Furo-Coumarine derivatives	T,R,V,TAG ,VAG	RP,PO,NP	(129)	27 compounds
Indapamide	V	RP,NP	(2)	
Mandelamide	V,T	RP,NP	(2,7)	
Methsuximide	V,T	RP	(2,7)	
N-(1-Phenylethyl)maleimide	V	RP	(21)	
N-(α-Methylbenzyl)phthlic acid monoamide	T	RP	(7)	
N,N'-bis(α-methylbenzyl)sulfamide	V	RP	(2)	
N,N^1-Bis(α-metylbenzyl) sulfamide	T	NP	(7)	
N-benzoylalanine methyl ester	V	RP	(2)	
Phensuximide	V,R,T	RP,NP	(2,7,17,22)	
proglumide	V,T	RP	(2,7,19)	
Promethazine	V, R	RP, PO	(50)	Antidepressive and antiallergic
Pyridoglutethimide	V	RP	(2)	
Salbutamol and its 4-*O*-Sulphate Metabolites	T	PO	(85)	
Sulfoxides, sulfinate esters and tosylated sulfilimines	T,R,V,TAG ,VAG	RP,PO,NP	(43)	42 compounds
Tropicamide	T	RP	(7)	
α,α-Dimethyl-β-methyl succinimide	T	NP	(7)	
α-methyl-α-phenyl succinimide	T, TAG,V,R	RP, PO,NP	(2,7,17,22,23, 29)	antiurolithic
α-methyl-α-propyl succinimide	R,T	NP	(7,17,22)	

5. References

1 Armstrong, D. W., Tang, Y., Chen, S., Zhou, Y., Bagwill, C. and Chen, J.-R. (1994). Macrocyclic Antibiotics as a New Class of Chiral Selectors for Liquid Chromatography. *Anal. Chem.* 66, 1473-84.

2 Armstrong, D. W. and Zhang, B. (2001). Chiral stationary phases for HPLC. *Analytical Chemistry* 73, 557A-561A.

3 Armstrong, D. W. and Zhou, Y. (1994). Use of a macrocyclic antibiotic as the chiral selector for enantiomeric separations by TLC. *J. Liq. Chromatogr.* 17, 1695-707.

4 Armstrong, D. W., Rundlett, K. L. and Chen, J.-R. (1994). Evaluation of the macrocyclic antibiotic vancomycin as a chiral selector for capillary electrophoresis. *Chirality* 6, 496-505.

5 Armstrong, D. W., Gasper, M. P. and Rundlett, K. L. (1995). Highly enantioselective capillary electrophoretic separations with dilute solutions of the macrocyclic antibiotic ristocetin A. *J. Chromatography A* 689, 285-304.

6 Chen, S., Liu, Y., Armstrong, D. W., Borrell, J. I., Martinez-Teipel, B. and Matallana, J. L. (1995). Enantioresolution of substituted 2-methoxy-6-oxo-1,4,5,6-tetrahydropyridine-3-carbonitriles on macrocyclic antibiotic and cyclodextrin stationary phases. *J. Liq. Chromatogr.* 18, 1495-507.

7 Armstrong, D. W., Liu, Y. and Ekborgott, K. H. (1995). A covalently bonded teicoplanin chiral stationary phase for HPLC enantioseparations. *Chirality* 7, 474-97.

8 Rundlett, K. L., Gasper, M. P., Zhou, E. Y. and Armstrong, D. W. (1996). Capillary electrophoretic enantiomeric separations using the glycopeptide antibiotic, teicoplanin. *Chirality* 8, 88-107.

9 Berthod, A., Liu, Y., Bagwill, C. and Armstrong, D. W. (1996). Facile LC enantioresolution of native amino acids and peptides using a teicoplanin chiral stationary phase. *J. Chromatogr., A* 731, 123-37.

10 Gasper, M. P., Berthod, A., Nair, U. B. and Armstrong, D. W. (1996). Comparison and Modeling Study of Vancomycin, Ristocetin A, and Teicoplanin for CE Enantioseparations. *Anal. Chem.* 68, 2501-2514.

11 Armstrong, D. W. (1996). Enantioselective interactions and separations with macrocyclic antibiotics. *Chimia* 50, 273.

12 Berthod, A., Nair, U. B., Bagwill, C. and Armstrong, D. W. (1996). Derivatized vancomycin stationary phases for LC chiral separations. *Talanta* 43, 1767-1782.

13 Nair, U. B., Chang, S. S. C., Armstrong, D. W., Rawjee, Y. Y., Eggleston, D. S. and McArdle, J. V. (1996). Elucidation of vancomycin's enantioselective binding site using its copper complex. *Chirality* 8, 590-595.

14 Peter, A., Torok, G. and Armstrong, D. W. (1998). High-performance liquid chromatographic separation of enantiomers of unusual amino acids on a teicoplanin chiral stationary phase. *J. Chromatogr., A* 793, 283-296.

15 Armstrong, D. W. and Nair, U. B. (1997). Capillary electrophoretic enantioseparations using macrocyclic antibiotics as chiral selectors. *Electrophoresis* 18, 2331-2342.

16 Armstrong, D. W., Lee, J. T. and Chang, L. W. (1998). Enantiomeric impurities in chiral catalysts, auxiliaries and synthons used in enantioselective synthesis. *Tetrahedron: Asymmetry* 9, 2043-2064.

17 Ekborg-Ott, K., Liu, Y. and Armstrong, D. W. (1998). Highly enantioselective HPLC separations using the covalently bonded macrocyclic antibiotic, ristocetin A, chiral stationary phase. *Chirality* 10, 434-483.

18 Peter, A., Torok, G., Toth, G., Van den Nest, W., Laus, G., Tourwe, D. and Armstrong, D. W. (1998). Enantiomeric separation of unusual secondary aromatic amino acids. *Chromatographia* 48, 53-58.

19 Ekborg-Ott, K. H., Kullman, J. P., Wang, X., Gahm, K., He, L. and Armstrong, D. W. (1998). Evaluation of the macrocyclic antibiotic avoparcin as a new chiral selector for HPLC. *Chirality* 10, 627-660.

20 Peter, A., Torok, G., Armstrong, D. W., Toth, G. and Tourwe, D. (1998). Effect of temperature on retention of enantiomers of -methyl amino acids on a teicoplanin chiral stationary phase. *J. Chromatography A* 828, 177-190.

21 Armstrong, D. W., He, L., Yu, T., Lee, J. T. and Liu, Y.-s. (1999). Enantiomeric impurities in chiral catalysts, auxiliaries, synthons and resolving agents. Part 2. *Tetrahedron: Asymmetry* 10, 37-60.

22 Ekborg-Ott, K. H., Wang, X. and Armstrong, D. W. (1999). Effect of selector coverage and mobile phase composition on enantiomeric separations with ristocetin A chiral stationary phases. *Microchem. J.* 62, 26-49.

23 Berthod, A., Chen, X., Kullman, J. P., Armstrong, D. W., Gasparrini, F., D'Acquarica, I., Villani, C. and Carotti, A. (2000). Role of the Carbohydrate Moieties in Chiral Recognition on Teicoplanin-Based LC Stationary Phases. *Analytical Chemistry* 72, 1767-1780.

24 Peter, A., Olajos, E., Casimir, R., Tourwe, D., Broxterman, Q. B., Kaptein, B. and Armstrong, D. W. (2000). High-performance liquid chromatographic separation of the enantiomers of unusual -amino acid analogues. *J. Chromatography A* 871, 105-113.

25 Peter, A., Torok, G., Toth, G., Tourwe, D., Mannekens, E., Van Den Nest, W., Sapi, J. and Armstrong, D. W. (1998). Chiral separation of unusual beta -methyl amino acids. *Proc. Eur. Pept. Symp., 25th* 25th, 300-301.

26 Torok, G., Peter, A., Toth, G., Tourwe, D., Van Den Nest, W., Iterbeke, K. and Armstrong, D. W. (1998). Chiral separation of secondary amino acids possessing

1,2,3,4-tetrahydroisoquinoline and related structures. *Proc. Eur. Pept. Symp* 25th, 302-303.

27 Torok, G., Peter, A., Vekes, E., Sapi, J., Laronze, M., Laronze, J.-Y. and Armstrong, D. W. (2000). Enantiomeric high-performance liquid chromatographic separation of beta-substituted tryptophan analogues. *Chromatographia* 51, S165-S174.

28 Karlsson, C., Karlsson, L., Armstrong, D. W. and Owens, P. K. (2000). Evaluation of a Vancomycin Chiral Stationary Phase in Capillary Electrochromatography Using Polar Organic and Reversed-Phase Modes. *Analytical Chemistry* 72, 4394-4401.

29 Berthod, A., Yu, T., Kullman, J. P., Armstrong, D. W., Gasparrini, F., D'Acquarica, I., Misiti, D. and Carotti, A. (2000). Evaluation of the macrocyclic glycopeptide A-40,926 as a high-performance liquid chromatographic chiral selector and comparison with teicoplanin chiral stationary phase. *J. Chromatography A* 897, 113-129.

30 Karlsson, C., Karlsson, L., Armstrong, D. W. and Owens, P. K. (2000). Enantioselective reversed-phase and non-aqueous capillary electrochromatography using a teicoplanin chiral stationary phase. *J. Chromatography A* 897, 349-363.

31 Peter, A., Torok, G., Armstrong, D. W., Toth, G. and Tourwe, D. (2000). High-performance liquid chromatographic separation of enantiomers of synthetic amino acids on a ristocetin A chiral stationary phase. *J. Chromatography A* 904, 1-15.

32 Lehotay, J., Hrobonova, K., Cizmarik, J., Reneova, M. and Armstrong, D. W. (2001). Modification of the chiral bonding properties of teicoplanin chiral stationary phase by organic additives. HPLC separation of enantiomers of alkoxysubstituted esters of phenylcarbamic acid. *J. Liq. Chromatogr. Relat. Technol.* 24, 609-624.

33 Peter, A., Lazar, L., Fulop, F. and Armstrong, D. W. (2001). High-performance liquid chromatographic enantioseparation of beta -amino acids. *J. Chromatography A* 926, 229-238.

34 Hrobonova, K., Lehotay, J., Cizmarikova, R. and Armstrong, D. W. (2001). Study of the mechanism of enantioseparation. I. Chiral analysis of alkylamino derivatives of aryloxypropanols by HPLC using macrocyclic antibiotics as chiral selectors. *Journal of Liquid Chromatography & Related Technologies* 24, 2225-2237.

35 Berthod, A., Valleix, A., Tizon, V. L., Estelle; , Caussignac, C. and Armstrong, D. W. (2001). Retention and selectivity of teicoplanin stationary phases after copper complexation and isotopic exchange. *Analytical Chemistry* 73, 5499-5508.

36 Xiao, T. L., Zhang, B., Lee, J. T., Hui, F. and Armstrong, D. W. (2001). Reversal of enantiomeric elution order on macrocyclic glycopeptide chiral stationary phases. *Journal of Liquid Chromatography & Related Technologies* 24, 2673-2684.

37 Anan'eva, I. A., Shapovalova, E. N., Shpigun, O. A. and Armstrong, D. W. (2001). Separation of amino acid enantiomers and enantiomers of their derivatives on macrocyclic antibiotic teicoplanin. *Vestn. Mosk. Univ., Ser. 2: Khim.* 42, 278-280.

38 Peter, A., Olajos, E., Casimir, R., Tourwe, D., Broxterman, Q. B., Kaptein, B. and Armstrong, D. W. (2000). High-performance liquid chromatographic separation of

the enantiomers of unusual alpha-amino acid analogues. *J. Chromatography A* 871, 105-113.

39 Torok, G. P., Antal; Armstrong, Daniel W.; Tourwe, Drik; Toth, Geza; Sapi, Janos. (2001). Direct chiral separation of unnatural amino acids by high-performance liquid chromatography on a ristocetin A-bonded stationary phase. *Chirality* 13, 648-656.

40 D'Acquarica, I., Gasparrini, F., Misiti, D., Villani, C., Carotti, A., Cellamare, S. and Muck, S. (1999). Direct chromatographic resolution of carnitine and O-acylcarnitine enantiomers on a teicoplanin-bonded chiral stationary phase. *Journal of Chromatography A* 857, 145-155.

41 Snegur, L. V., Boev, V. I., Nekrasov, Y. S., Ilyin, M. M., Davankov, V. A., Starikova, Z. A., Yanovsky, A. I., Kolomiets, A. F. and Babin, V. N. (1999). Synthesis and Structure of Biologically Active Ferrocenylalkyl Polyfluoro Benzimidazoles. *J. of Organometallic Chem.* 580, 26-35.

42 Iungelova, J., Lehotay, J., Hrobonova, K., Cizmarik, J. and Armstrong, D. W. (2002). Study of local anaesthetics. CLVIII. Chromatographic separation of some derivatives of substituted phenylcarbamic acid on a vancomycin-based stationary phase. *Journal of Liquid Chromatography & Related Technologies* 25, 299-312.

43 Berthod, A., Xiao, T. L., Liu, Y., Jenks, W. S. and Armstrong, D. W. (2002). Separation of chiral sulfoxides by liquid chromatography using macrocyclic glycopeptide chiral stationary phases. *J. Chromatography A* 955, 53-69.

44 Owens, P. K., Svensson, L. A. and Vessman, J. (2001). Direct separation of captopril diastereoisomers including their rotational isomers by RP-LC using a teicoplanin column. *Journal of Pharmaceutical and Biomedical Analysis* 25, 453-464.

45 Lamprecht, G., Kraushofer, T., Stoschitzky, K. and Lindner, W. (2000). Enantioselective analysis of (R)-and (S)-atenolol in urine samples by a high-performance liquid chromatography column-switching setup. *Journal of Chromatography B* 740, 219-226.

46 Esquivel, J. B., Sanchez, C. and Fazio, M. J. (1998). Chiral HPLC Separation of Protected Amino Acids. *J. Liq. chromatogr. & Rel. Technol.* 21, 777-791.

47 Kleidernigg, O. P. and Kappe, C. O. (1997). Separation of Enantiomers of 4-aryldihydropyrimidines by Direct Enantioselective HPLC. A Critical Comparison of Chiral Stationary Phases,. *Tetrahedron: Asymmetry* 8, 2057-2067.

48 He, J., Cheung, A. P., Struble, E., Wang, E. and Liu, P. (2000). Enantiomeric separation of an aryloxyphenoxypropanoic acid by CE and LC. *Journal of Pharmaceutical and Biomedical Analysis* 22, 583-595.

49 Wu, G. and Furlanut, M. (1999). Hydrogen bonding as a possible interaction for the chiral separation of DL-dopa and DL-3-O-methyl-dopa in a chiral teicoplanin column. *Farmaco* 54, 188-190.

50 Bosakova, Z., Klouckova, I. and Tesarova, E. (2002). Study of the stability of promethazine enantiomers by liquid chromatography using a vancomycin-bonded

chiral stationary phase. *Journal of Chromatography, B: Analytical Technologies in the Biomedical and Life Sciences* 770, 63-69.

51 J. M. Schneiderheinze, D. W. Armstrong and A. Berthod. (1999). Plant and Soil Enantioselective Biodegradation of Racemic Phenoxyalkanoic Herbicides,. *Chirality* 11, 330-337.

52 Hui, F., Ekborg-Ott, K. H. and Armstrong, D. W. (2001). High-performance liquid chromatographic and capillary electrophoretic enantioseparation of plant growth regulators and related indole compounds using macrocyclic antibiotics as chiral selectors. *J. Chromatography A* 906, 91-103.

53 K. H. Ekborg-Ott and D.W. Armstrong. (1997). Stereochemical Analyses of Food Components. *Chiral Separations: Application and Technology,* Ch. 9, 201-270.

54 Nieto, M. and Perkins, H. R. (1971). The specificity of combination between ristocetins and peptides related to bacterial cell wall mucopeptide precursors. *Bichemical Journal* 124, 845-52.

55 Nieto, M. and Perkins, H. R. (1971). Modifications of the acyl-D-alanyl-D-alanine terminus affecting complex-formation with vancomycin. *Biochemical Journal* 123, 789-803.

56 Nieto, M. and Perkins, H. R. (1971). Physicochemical properties of vancomycin and iodovancomycin and their complexes with diacetyl-L-lysyl-D-alanyl-D-alanine. *Biochemical Journal* 123, 773-87.

57 Armstrong, D. W., Rundlett, K. and Reid, G. L., III. (1994). Use of a Macrocyclic Antibiotic, Rifamycin B, and Indirect Detection for the Resolution of Racemic Amino Alcohols by CE. *Anal. Chem.* 66, 1690-5.

58 Ward, T. J., Dann, C. I. and Blaylock, A. (1995). Enantiomeric resolution using the macrocyclic antibiotics rifamycin B and rifamycin SV as chiral selectors for capillary electrophoresis. *Journal of Chromatography A* 715, 337-44.

59 Ward, T. J. (1994). For capillary electrophoresis. *Anal. Chem.* 66, 632A-640A.

60 Armstrong, D. (1995). Macrocyclic antibiotics as separation agents. *PCT Int. Appl.* 71 pp.

61 Aboul-Enein, H. Y. and Ali, I. (2000). Macrocyclic Antibiotics as Effective Chiral Selectors for Enantiomeric Resolution by Liquid Chromatography and Capillary Electrophoresis,. *Chromatographia* 52, 679-691.

62 Wang, A. X., Lee, J. T. and Beesley, T. E. (2000). Coupling Chiral Stationary Phases as a Fast Screening Approach for HPLC Method Development. *LC. GC* 18, 626-639.

63 Armstrong, D. W. (1999). Complicating chromatography to make it work more effectively. *Book of Abstracts, 217th ACS National Meeting, Anaheim, Calif.,* March 21-25.

64 Armstrong, D. W. (1998). The evolution of chiral stationary phases for liquid chromatography. *J. Chin. Chem. Soc. (Taipei)* 45, 581-590.

65 Tesarova, E. and Armstrong, D. W. (1998). Enantioselective separations. *J. Chromatogr. Libr* 60, 197-256.

66 Armstrong, D. W. (1996). Enantioselective interactions and separations with macrocyclic antibiotics. *Book of Abstracts, 211th ACS National Meeting, New Orleans, LA* March 24-28.

67 Chen, S., Liu, Y., Armstrong, D. W., Borrell, J. I., Martinez-Teipel, B. and Matallana, J. L. (1995). Enantioresolution of substituted 2-methoxy-6-oxo-1,4,5,6-tetrahydropyridine-3-carbonitriles on macrocyclic antibiotic and cyclodextrin stationary phases. *Biochim. Biophys. Acta* 1263, 2703.

68 Chen, S., Armstrong, D. W., Borrell, J. I., Martinez-Taipel, B. and Matallana, J. L. (1995). Enantioresolution of substituted 2-methoxy-6-oxo-1,4,5,6-tetrahydropyridine-3-carbonitriles on macrocyclic antibiotic and cyclodextrin stationary phases. *J. Liq. Chromatogr.* 18, 2703.

69 Bojarski, J., Zakl. Chem. Org., Collegium Medicum, Uniw. Jagiellonski and Krakow, P. (1999). Antibiotics as electrophoretic and chromatographic chiral selectors. *Wiad. Chem.* 53, 235-247.

70 O.P. Kleidernigg and Kappe, C. O. (1997). Separation of Enantiomers of 4-aryldihydropyrimidines by Direct Enantioselective HPLC. A Critical Comparison of Chiral Stationary Phases,. *Tetrahedron: Asymmetry* 8, 2057-2067.

71 Advanced Separation Technologies Inc and Whippany, N., USA. (2002). A Guide to Using Macrocyclic Glycoppeptide bonded phases for Chiral LC Separations. 4th Edn., 1-65.

72 K. M. Fried, P. Koch and Wainer, I. W. (1998). Determination of the Enantiomers of Albuterol in Human and Canine Plasma by Enantioselective High-Performance Liquid Chromatography on a Teicoplanin-Based Chiral Stationary Phase,. *Chirality* 10, 484-491.

73 H. Y. Aboul-Enein and Serignese, V. (1998). Enantiomeric Separation of Several Cyclic Imides on a Macrocyclic Antibiotic (Vancomycin) Chiral Stationary Phase Under Normal and Reversed Phase Conditions,. *Chirality* 10, 358-361.

74 E. Tesarova, A. Bosakova and Pacakova, V. (1999). Comparison of Enantioselective Separation of N-tert.-butyloxycarbonyl Amino Acids and Their Non-blocked Analogues on Teicoplanin-based Chiral Stationary Phase. *J. Chromatography A* 838, 121-129.

75 R.P.W. Scott and Beesley, T. E. (1999). Optimum Operating Conditions for Chiral Separations in Liquid Chromatography,. *Analyst* 124, 713-719.

76 E. Tesarova, K. Zaruba and Flieger, M. (1999). Enantioseparation of Semisynthetic Ergo Alkaloids on Vancomycin and Teicoplanin Stationary Phases. *J. Chromatography A* 844, 137-147.

77 H. Y. Aboul-Enein and V. Serignese, B. (1999). Quantitative Determination of Clenbuterol Enantiomers in Human Plasma by High-performance Liquid

Chromatography Using the Macrocyclic Antibiotic Chiral Stationary Phase Teicoplanin. *Chromatographia* 13, 520-524.

78 Risley, D. S. and Strege, M. A. (2000). Chiral Separations of Polar Compounds by Hydrophilic Interaction Chromatography with Evaporative Light Scattering Detection,. *Anal. Chem.* 72.

79 Yu, Y.-P. and Wu, W.-H. (2001). Simultaneous Analysis of Enantiomeric Composition of Amino Acids and N-Acetyl-Amino Acids by Enantioselective Chromatography. *Chirality* 13.

80 Schlauch, M., Kos, O. and Frahm, A. W. (2002). Comparison of three chiral stationary phases with respect to their enantio- and diastereoselectivity for cyclic beta-substituted alpha-amino acids. *Journal of Pharmaceutical and Biomedical Analysis* 27, 409-419.

81 Ward, T. J. and Farris, A. B., III. (2001). 53. Chiral separations using the macrocyclic antibiotics: a review. *J. Chromatography A* 906, 73-89.

82 Peyrin, E., Ravelet, C., Nicolle, E., Villet, A., Grosset, C., Ravel, A. and Alary, J. (2001). Dansyl amino acid enantiomer separation on a teicoplanin chiral stationary phase: effect of eluent pH. *Journal of Chromatography, A* 923, 37-43.

83 Ward, T. J. (1996). Macrocyclic antibiotics - the newest class of chiral selectors. *LC. GC* 14, 886,890-894.

84 Bojarski, J. and Aboul-Enein, H. Y. (1999). Recent chromatographic and electrophoretic enantioseparartions of cardiovascular drugs. *Biomedical Chromatography* 13, 197-208.

85 K. B. Joyce, A. E. Jones, R. J. Scott, R. A. Biddlecombe and S. Pleasance. (1998). Determination of the Enantiomers of Salbutamol and its 4-O-Sulphate Metabolites in Biological Matrices by Chiral Liguid Chromatography Tandem Mass Spectrometry,. *Rapid Commun. Mass Spectrom.* 12, 1899-1910.

86 Ramos, L., Bakhtiar, R., Majumdar, T., Hayes, M. and Tse, F. (1999). Liquid Chromatographic/Atmospheric Pressure Chemical Ionization Tandem Mass Spectrometry Enantiomeric Separation of dl-threo-Methylphenidate, (Ritalinâ) Using a Macrocyclic Antibiotic as the Chiral Selector. *Rapid Commun. Mass Spectrom.* 13, 2054-2062.

87 Bakhtiar, R. and Tse, F. L. S. (2000). High-Throughput Chiral Liquid Chromatography/Tandem Mass Spectrometry,. *Rapid Commun. Mass Spectrom.* 14, 1128-1135.

88 Petritis, K., Valleix, A., Elfakir, C. and Dreux, M. (2001). Simutaneous analysis of underivatized chiral amino acids by liquid chromatography-ionspray tandem mass spectrometry using a teicoplanin chiral stationary phase. *Journal of Chromatography A* 913, 331-340.

89 Mendez, S. P., Gonzalez, E. B. and Medel, A. S. (2000). Chiral speciation and determination of selenomethionine enantiomers in selenized yeast by HPLC-ICP-MS

using a teicoplanin-based chiral stationary phase. *J. Anal. At. Spectrom.* 15, 1109-1114.

90 Armstrong, D. W. and Rundlett, K. L. (1995). CE resolution of neutral and anionic racemates with glycopeptide antibiotics and micelles. *J. Liq. chromatogr.* 18, 3659-74.

91 A. S. Carter-Finch and N. W. Smith. (1999). Enantiomeric separations by capillary electrochromatography using a macrocyclic antibiotic chiral stationary phases. *J. Chromatography A* 848, 375-385.

92 Ward, T. J. (2000). Chiral Separations. *Anal. Chem.* 72, 4521-4528.

93 Desiderio, C. and Fanali, S. (1998). Chiral analysis by capillary electrophoresis using antibiotics as chiral selector. *Journal of Chromatography, A* 807, 37-56.

94 Wan, H. and Blomberg, L. G. (1997). Enantiomeric separation of small chiral peptides by capillary electrophoresis. *Journal of Chromatography A* 792, 393-400.

95 Carotti, A. and Gioia, F. D. (1999). Teicoplanin-based Enantiomeric Separations in CZE Using Partial Filling Technique. *J. High Resol. Chromatogr.* 22, 315-321.

96 Ward, T. J. (1994). Chiral media for capillary electrophoresis. *Anal. Chem.* 66, 632A-640A.

97 Ward, T. J., Dann, C. I. and Brown, A. P. (1996). Separation of enantiomers using vancomycin in a countercurrent process by suppression of electroosmosis. *Chirality* 8, 77-83.

98 Vespalec, R., Corstjens, H., Billiet, H. A. H., Frank, J. and Luyben, K. C. A. M. (1995). Enantiomeric Separation of Sulfur- and Selenium-Containing Amino Acids by Capillary Electrophoresis Using Vancomycin as a Chiral Selector. *Anal. Chem.* 67, 3223-8.

99 Sharp, V. S., Risley, D. S., Mccarthy, S., Huff, B. E. and Strege, M. A. (1997). Evaluation of a new macrocyclic antibiotic as a chiral selector for use in capillary electrophoresis. *J. Liq. chromatogr.* 20, 887-898.

100 Strege, M. A., Huff, B. E. and Risely, D. S. (1996). Evaluation of macrocyclic antibiotic A82846B as a chiral selector for capillary electrophoresis separations. *LC. GC* 14, 144-150.

101 Ward, T. J., Farris III, A. B. and Woodling, K. (2001). Synergistic chiral separations using the glycopeptides ristocetin A and vancomycin. *Journal of Biochemical and Biophysical Methods* 48, 163-174.

102 Wikstrom, L. A. Svensson, A. Torstensson and P. K. Owens. (2000). Immobilisation and evaluation of a vancomycin chiral stationary phase for capillary electrochromatography. *J. Chromatography A* 869, 395-409.

103 Carlsson, E., Wikström, H. and Owens, P. K. (2001). Validation of a Chiral Capillary Electrochromatographic Method for Metoprolol on a Teicoplanin Stationary Phase. *Chromatographia* 53, 419-424.

104 Andrei Medvedovicia, Pat Sandraa, Laura Toribiob and Frank David. (1997). Chiral packed column subcritical fluid chromatography on polysaccharide and macrocyclic antibiotic chiral stationary phases. *Journal of Chromatography, A* 785, 159-171.

105 Svensson, L. A. and Owens, P. K. (2000). Enantioselective supercritical fluid chromatography using ristocetin A chiral stationary phases. *Analyst* 125, 1037-1039.

106 Toribio, L., David, F. and Sandra, P. (1999). Enantiomeric separation of some cyclic ketones and dioxalene derivatives by chiral SFC. *Quimica Analitica (Barcelona)* 18, 269-273.

107 Liu, Y., Berthod, A., Mitchell, C. R., Xiao, T. L., Zhang, B. and Armstrong, D. W. (2002). Super/Subcritical Fluid Chromatography Chiral Separations with Macrocyclic Glycopeptide Stationary Phases. *Journal of Chromatography A* 978, 185-204.

108 F Q. Sun and Olesik, S. V. (1999). Chiral Separations Performed by Enhanced Fluidity Liquid Chromatography on a Macrocyclic Antibioitc Chiral Stationary Phase. *Anal. Chem.* 71, 2139-2145.

109 Jin, Z. H., Wang, M. R. and Cen, P. L. (2002). Production of teicoplanin by valine analogue-resistant mutant strains of Actinoplanes teichomyceticus. *Applied Microbiology and Biotechnology* 58, 63-66.

110 Constance M. Harris, Hana Kopecka and Harris, a. T. M. (1983). Vancomycin: structure and transformation to CDP-I. *Journal of the American Chemical Society* 105, 6915-6922.

111 Higgins, H. M., Harrison, W. H., Wild, G. M., Bungay, H. R., McCormick, M. H. and Eli Lilly & Co., I., IN,. (1957-1958). Vancomycin, a new antibiotic. VI. Purification and properties of vancomycin. *Antibiot. Annu.* 906.

112 Parenti, F., Beretta, G., Berti, M. and Arioli, V. (1978). Teichomycins, new antibiotics from Actinoplanes teichomyceticus Nov. Sp. I. Description of the producer strain, fermentation studies and biological properties. *Journal of Antibiotics* 1978, 276-83.

113 Philip, J. E., Schenck, J. R., Hargie, M. P., Abbott Labs. and N. Chicago. (1957). Ristocetins A and B, two new antibiotics. Isolation and properties. *Antibiot. Annu.* 1956-1957, 699-705.

114 Beesley, T. E. and Scott, R. P. W. Chiral Chromatography. *John Wiley & Sons Ltd., Baffins Lane, Chicheste, West Sussex PO19 1UD, England* 1998.

115 Tesarova, E., Tuzar, Z., Nesmerak, K., Bosakova, Z. and Gas, B. (2001). Study on the aggregation of teicoplanin. *Talanta* 54, 643-653.

116 O'Neil, M. J., Smith, A. and Heckelman, P., E.. (2001). The Merck Index. 13th Edition, 9194-9195.

117 Xiao, T. L. and Armstrong, D. W. (2002). Chiral separation using glycopeptide antibiotics chiral stationary phases. *Unpublished Results*.

118 Tesarova, E., Bosakova, Z. and Zuskova, I. (2000). Enantioseparation of selected N-tert.-butyloxycarbonyl amino acids in high-performance liquid chromatography and capillary electrophoresis with a teicoplanin chiral selector. *Journal of Chromatography A* 879, 147-156.

119 S.C Chang, G.L. Reid, S. Chen, C. D., Chang and Armstrong, D. W. (1993). Evaluation of a new polar-organic high-performance liquid chromatographic mobile phase for cyclodextrin-bonded chiral stationary phases. *Trends in analytical chemistry* 12, 144-153.

120 Armstrong, D. W., Chen, S., Chang, C. and Chang, S. (1992). A new approach for the direct resolution of racemic beta adrenergic blocking agents by HPLC. *Journal of Liquid Chromatography & Related Technologies* 15, 545-556.

121 Mislanova, C., Stefancova, A., Oravcova, J., Horecky , J., Trnovec , T. and Lindner, W. (2000). Direct high-performance liquid chromatographic determination of (R)- and (S)-propranolol in rat microdialysate using on-line column switching procedures. *Journal of Chromatography B* 739.

122 Armstrong, D. W., Kullman, J. P., Chen, X. and Rowe, M. (2001). Composition and chirality of amino acids in aerosol/dust from laboratory and residential enclosures. *Chirality* 13, 153-158.

123 Ekborg-Ott, K. H. and Armstrong, D. W. (1996). Evaluation of the concentration and enantiomeric purity of selected free amino acids in fermented malt beverages (beers). *Chirality* 8, 49-57.

124 Pawlowska, M. and Armstrong, D. W. (1994). Evaluation of enantiomeric purity of selected amino acids in honey. *Chirality* 6, 270-276.

125 Peter, A., Vekes, E. and Armstrong, D. W. (2002). Effects of temperature on retention of chiral compounds on a ristocetin A chiral stationary phase. *Journal of Chromatography A* 958, 89-107.

126 Schlauch, M. and Frahm, A. W. (2000). Enantiomeric and diastereomeric high-performance liquid chromatographic separation of cyclic beta-substituted alpha-amino acids on a teicoplanin chiral stationary phase. *Journal of Chromatography A* 868, 197-207.

127 Schurig, V. and Fluck, M. (2000). Enantiomer separation by complexation SFC on immobilized Chirasil-nickel and Chirasil-zinc. *Journal of Biochemical and Biophysical Methods* 43, 223-240.

128 Welch, C. J. (2002). Presentation at Iowa State University on Rapid Chiral separation methods. *Merck &Co., Rahway, NJ. USA* Feb. 15.

129 Xiao, T. L., Rozhkov, R. V., Larock, R. C., and Armstrong, D. W. (2003). Enantiomeric separation of substituted dihydrofurocoumarin compounds by HPLC using macrocyclic glycopeptide chiral stationary phases. *Analytical and Bioanalytical Chemistry, In Press.*

130 Jandera, P., Backovska, V. and Felinger, A. (2001). Analysis of the band profiles of the anantiomers of phenylglycine in liquid chromatography on bonded teicoplanin columns using the stochastic theory of chromatography. *Journal of Chromatography A* 919, 66-77.

131 Jandera, P., Skavrada, M., Klemmova, K., Backovska, V. and Guiochon, G. (2001). Effect of the mobile phase on the retention behaviour of optical isomers of carboxylic acids and amino acids in liquid chromatography on bonded Teicoplanin columns. *Journal of Chromatography A* 917, 123-133.

132 Courderot, C. M., Perrin, F. X., Guillaume, Y. C., Truong, T. T., Millet, J., Thomassin, M., Chaumont, J. P. and Nicod, L. (2002). Chiral discrimination of dansyl-amino-acid enantiomerson teicoplanin phase: sucrose-perchlorate anion dependence. *Analytica Chimica Acta* 457, 149-155.

133 Yu, Y.-P. and Wu, S.-h. (2001). Simultaneous Analysis of Enantiomeric Composition of Amino Acids and N-Acetyl-Amino Acids by Enantioselective Chromatography. *Chirality* 13, 231-235.

134 Torok, G., Peter, A., Armstrong, D. W., Tourwe, D., Toth, G. and Sapi, J. (2001). Direct chiral separation of unnatural amino acids by high-performance liquid chromatography on a ristocetin A-bonded stationary phase. *Chirality* 13, 648-656.

135 D'Acquarica, I., Gasparrini, F., Misiti, D., Zappia, G., Cimarelli, C., Palmieri, G., Carotti, A., Cellamare, S. and Villani, C. (2000). Application of a new chiral stationary phase containing the glycopeptide antibiotic A-40,926 in the direct chromatographic resolution of beta-amino acids. *Tetrahedron: Asymmetry* 11, 2375-2385.

136 D'Acquarica, I. (2000). New synthetic strategies for the preparation of novel chiral stationary phases for high-performance liquid chromatography containing natrual pool selectors. *Journal of Pharmaceutical and Biomedical Analysis* 23, 3-13.

137 Wang, A. X., Lee, J. T. and Beesley, T. E. (2000). Coupling Chiral Stationary Phases as a Fast Screening Approach for HPLC Method Development. *LC. GC* 18, 626-639.

138 Kosel, M., Eap, C. B., Amey, M. and Baumann, P. (1998). Analysis of the enantiomers of citalopram and its demethylated metabolites using chiral liquid chromatography. *Journal of Chromatography, B: Biomedical Sciences and Applications* 719, 234-238.

139 Aboul-Enein, H. Y. and Serignese, V. (1999). Quantitative Determination of Clenbuterol Enantiomers in Human Plasma by High-performance Liquid Chromatography Using the Macrocyclic Antibiotic Chiral Stationary Phase Teicoplanin. *Chromatographia* 13, 520-524.

140 Schneiderheinze, J. M., Armstrong, D. W. and Berthod, A. (1999). Plant and Soil Enantioselective Biodegradation of Racemic Phenoxyalkanoic Herbicides,. *Chirality* 11, 330-337.

141 Gasparrini, F., D'Acquarica, I., Vos, J. G., O'Connor, C. M. and Villani, C. (2000). Efficient enantiorecognition of ruthenium(II) complexes by silica-bound teicoplanin. *Tetrahedron: Asymmetry* 11, 3535-3541.

142 Aboul-Enein, H. Y. and Serignese, V. (1998). Enantiomeric separation of several cyclic imides on a macrocyclic antibiotic (vancomycin) chiral stationary phase under normal and reversed phase conditions. *Chirality* 10, 358-361.

FIGURE CAPTIONS

Figure 1. Structures of the macrocyclic antibiotics vancomycin, teicoplanin, ristocetin A, and teicoplanin aglycon showing a profile view of the aglycon "basket" using (A) space-filling molecular models produced through energy minimization and (B) stick figures. The colored atoms in part A denote the hydrophilic moieties, while the black portion designates the more hydrophobic regions. Red represents carboxylate groups, green are ammonium groups, and blue are hydroxyls. Black regions include the aromatic rings, connecting carbons, and amido linkages. (revised from (10)).

Figure 2. Plot showing the effect of solution pH on the electrophoretic mobility of ristocetin A (■), vancomycin (▲), and teicoplanin (●) macrocyclic antibiotics using 0.1 M phosphate buffer. The capillary for ristocetin A and vancomycin studies was 32.5 cm × 50 μm i.d. (25 cm to the detector window). The voltage was +5 kV. The electrophoretic mobility of teicoplanin was obtained using a 44 cm × 50 μm i.d. capillary (36.5 cm to the detector) and a run voltage of +10 kV. Either acetone or methanol was used as the electroosmotic flow marker (revised from (10)).

Figure 3. Simplified schematic shows two important morphological characteristics of the aglycon part of glycopeptide antibiotics. (A) End-to-end distance (represented by the length of the arrow) decreases from left to right. (B) The "C-shaped" aglycon also can be twisted to different degrees. The helical twist increases from left to right in this series of three figures (revised from (10)).

Figure 4. Reversed-phase separation of N-CBZ methionine and ketoprofen using high (1 g ristocetin A per 3.00 g silica gel), medium (0.75 g ristocetin A per 3.00 g silica gel), and low coverage (0.5 g ristocetin A per 3.00 g silica gel) of the ristocetin A chiral selector. MP: MeOH/0.1%TEAA buffer, pH 7.0 (20/80, v/v). Detection: UV 254 nm. Flow rate: 1.0 ml/min room temperature(revised from (22)).

Figure 5. The pH effect on retention factor (k') for various dansyl amino acids (▲: dansyl leucine; ■: dansyl valine; ♦: dansyl serine) at T=20°C using Chirobiotic T as CSP, mobile phase: 0.01 M citrate buffer-Methanol (90/10, v/v) (revised from (82))

Figure 6. The pH effect on selectivity factor (α) for dansyl serine enantiomers. All other conditions same as Figure 5 (revised from (82)).

Figure 7. Reversed-phase retention of the first eluted (□) and second eluted (▲) enantiomers of 5-methyl-5-phenylhydantoin as a function of mobile phase composition using Chirobiotic V as CSP (revised from (2)).

Figure 8. Effect of different organic modifier on resolution using Chirobiotic V as CSP. (Courtesy of Scott Sharpe, Eli Lilly & Co.)

Figure 9. Effect of organic modifier (EtOH)/water ratio on resolution, selectivity, and retention factor k for the enantiomeric separation of Methionine using Chirobiotic T as CSP (revised from (7)).

Figure 10. Effect of organic modifier (EtOH)/Hexane ratio on the retention of the first (1) and second (2) enantiomers of γ-phenyl- γ-butyrolactone (solid line, A) and 4-phenyl-2-methoxy-6-oxo-1,4,5,6-tetrahydropyridine-3-carbonitrile (dotted line, B) using teicoplanin as CSP (revised from (7)).

Figure 11. The separation of enantiomers of Propranolol employing different HOAC/ TEAA concentration ratios on Chirobiotic T. Room temperature and at a flow rate of 2ml/min (revised from (114)).

Figure 12. Temperature effect on separation of β-MePhe enantiomers. Column: Chirobiotic T; MP: H_2O/MeOH (10/90, v/v), detection 202 nm. Flow rate 1ml/min. (A) 1°C, (B) 20°C (C) 50 °C; peaks: 1) erytho-L isomer, 2) erytho-D isomer; 3) threo-L isomer; 4) threo-D isomer (revised from (14)).

Figure 13. An example of complementary separation using Chirobiotic T vs. Chirobiotic V. Separation conditions as shown on the figure (revised from (71)).

Figure 14. Method Development Protocol for Chirobiotic V

Figure 15. Method Development Protocol for Chirobiotic T

Figure 16. Method Development Protocol for Chirobiotic TAG

Figure 17. Method Development Protocol for Chirobiotic R

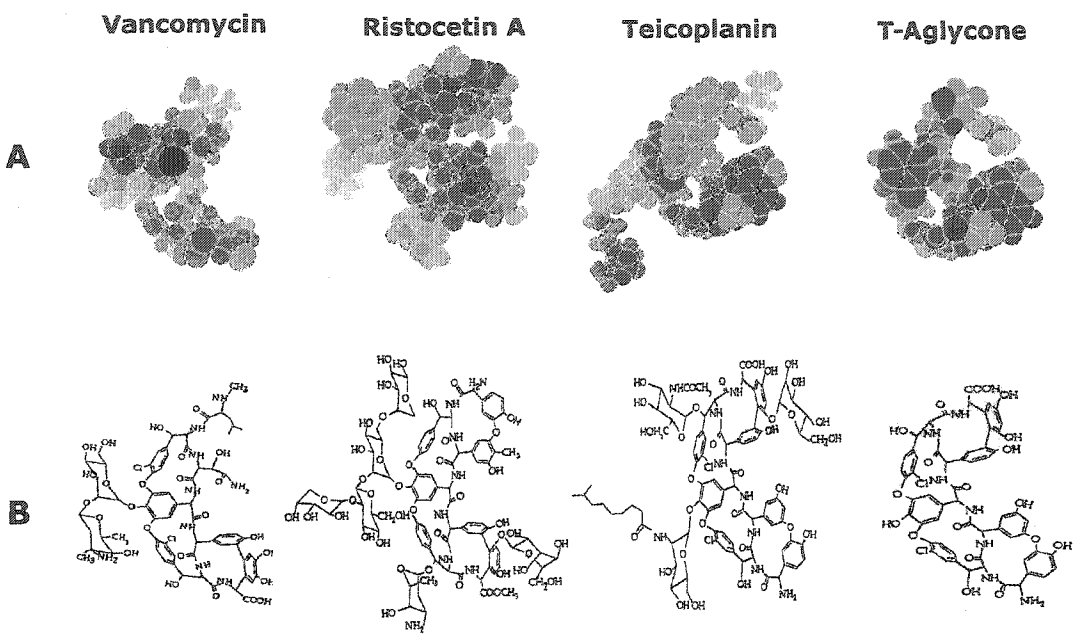

Figure 1

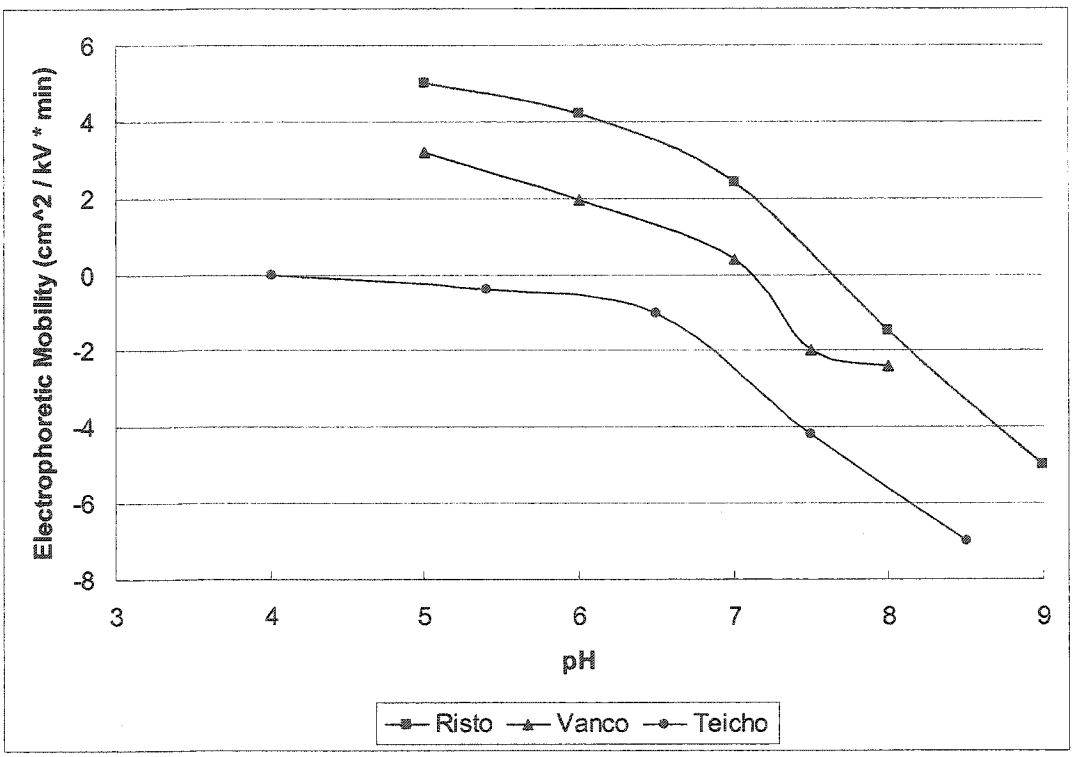
Electrophoretic Mobility (cm^2 / kV * min)
6
4
2
0
-2
-4
-6
-8
3
4
5
6
7
8
9
pH
Risto
Vanco
Teicho

Figure 2

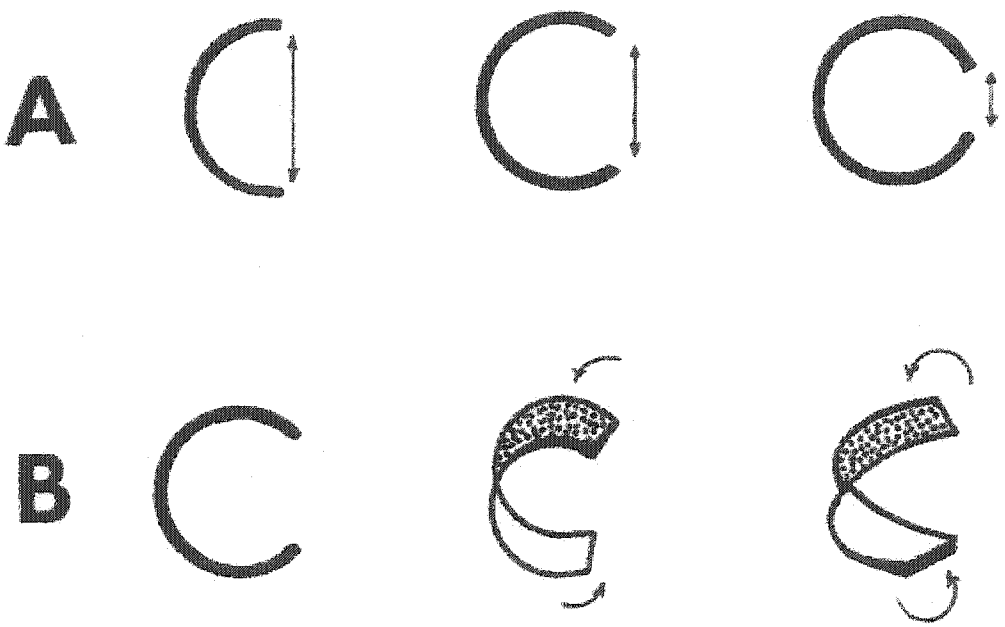

Figure 3

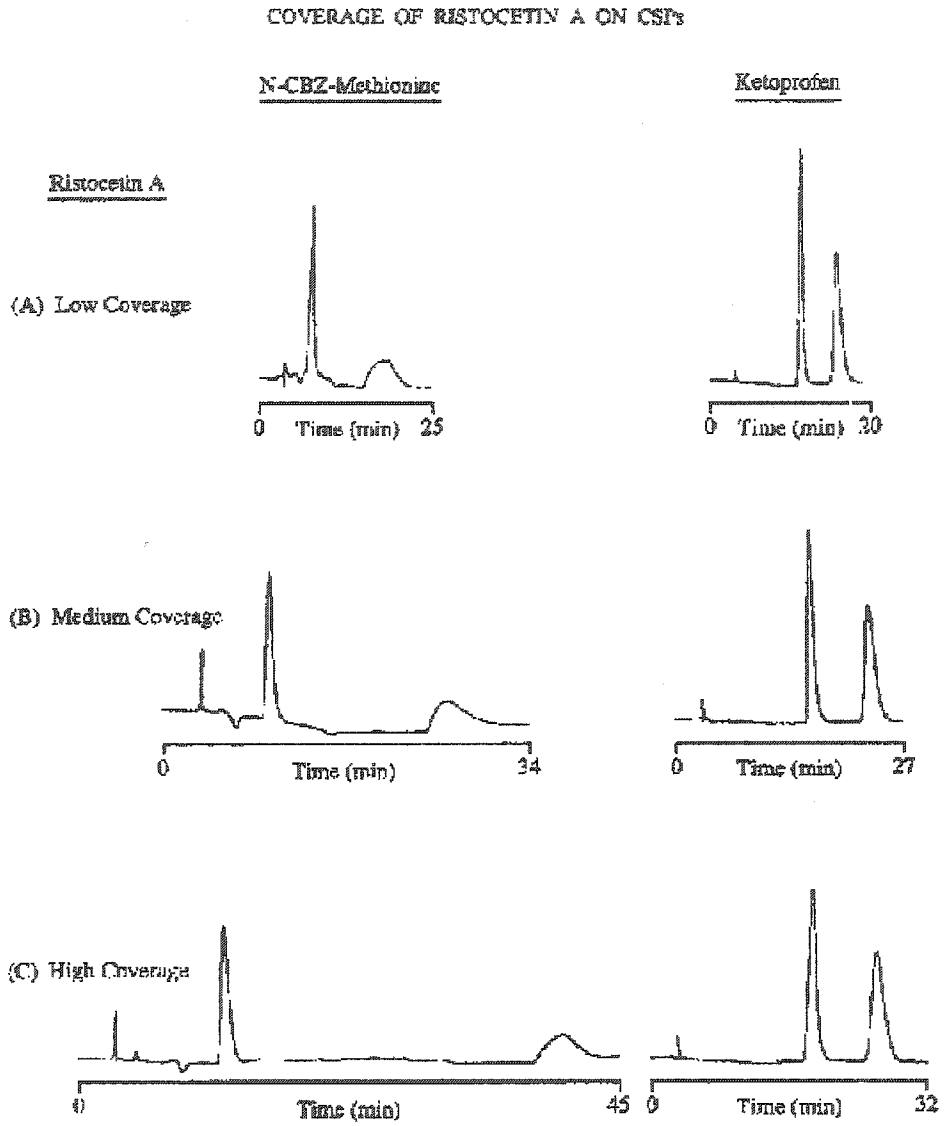
COVERAGE OF RISTOCETIN A ON CSPs
N-CBZ-Methionine
Ketoprofen
Ristocetin A
(A) Low Coverage
0 Time (min) 25
0 Time (min) 30
(B) Medium Coverage
0 Time (min) 34
0 Time (min) 27
(C) High Coverage
0 Time (min) 45
0 Time (min) 32

Figure 4

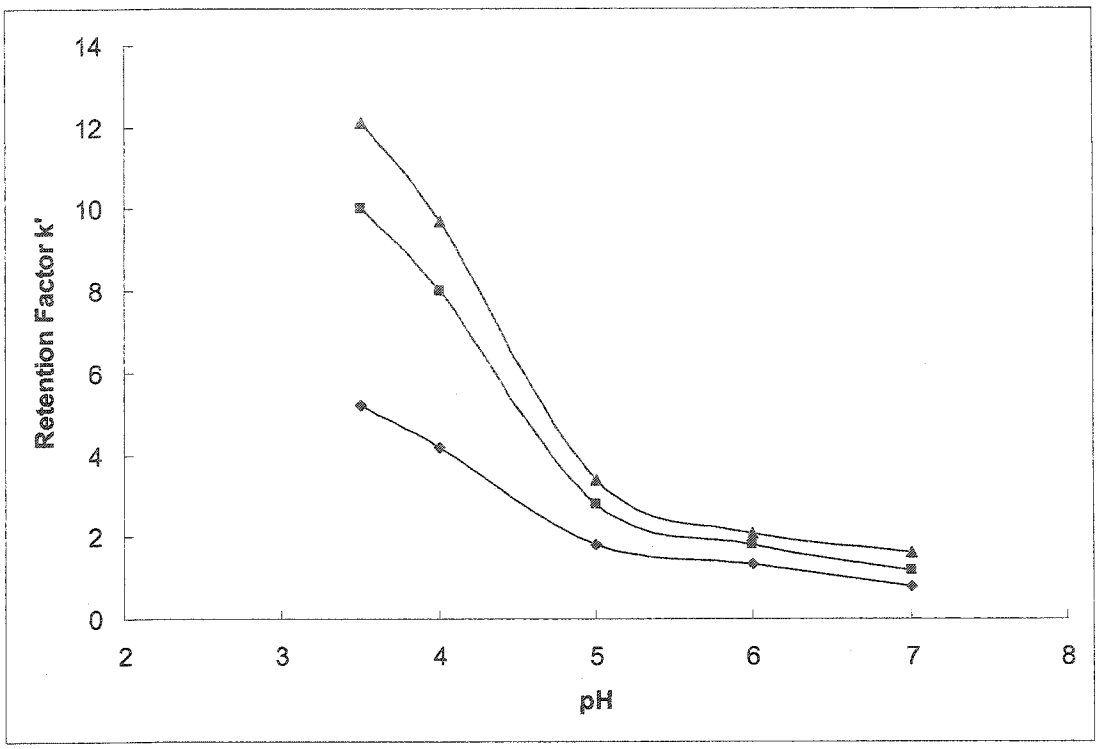

Figure 5

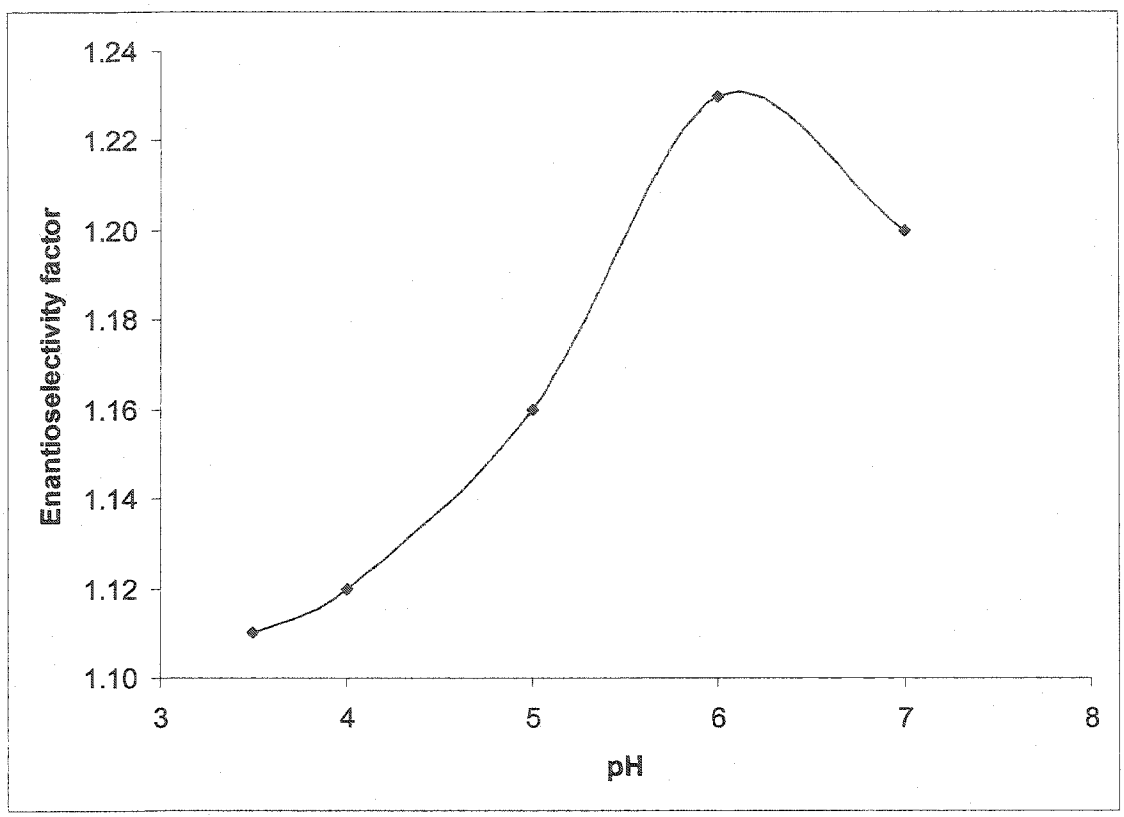
Enantioselectivity factor
1.24
1.22
1.20
1.18
1.16
1.14
1.12
1.10
3
4
5
6
7
8
pH

Figure 6

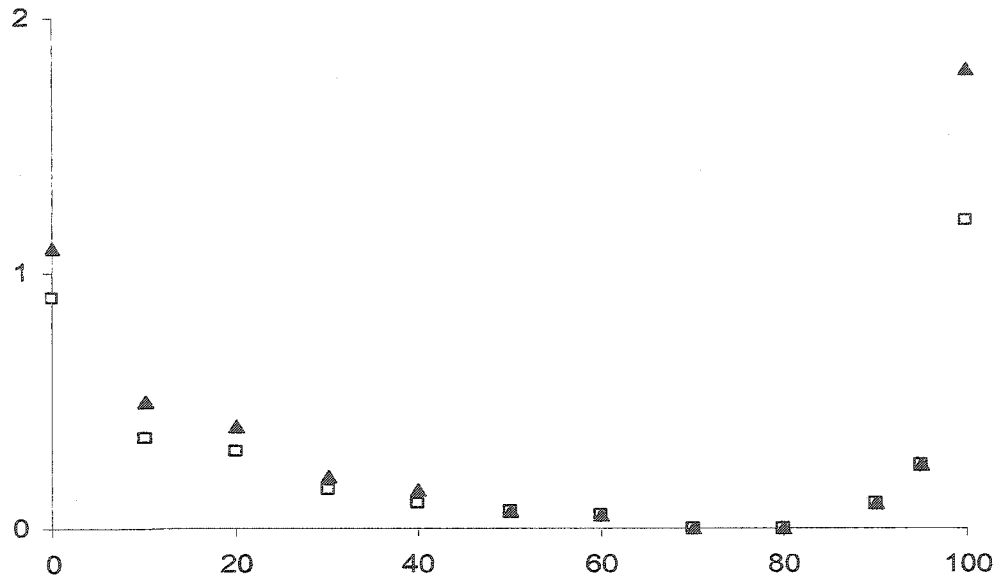

Figure 7

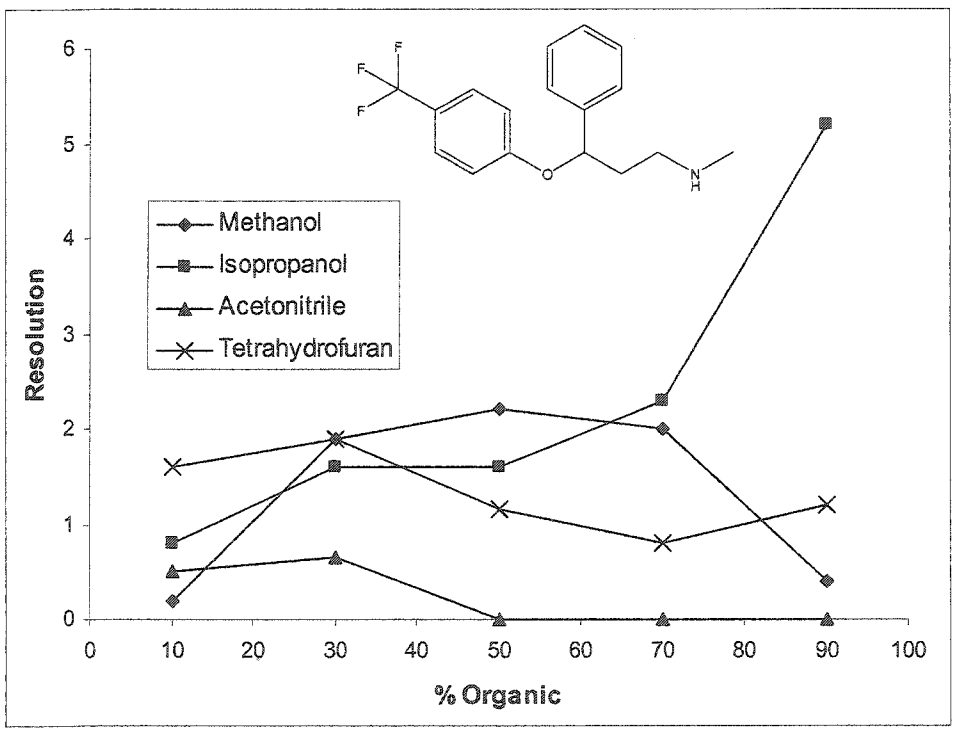
Resolution
% Organic
Methanol
Isopropanol
Acetonitrile
Tetrahydrofuran
0
1
2
3
4
5
6
0
10
20
30
40
50
60
70
80
90
100
F
F
F
O
N
H

Figure 8

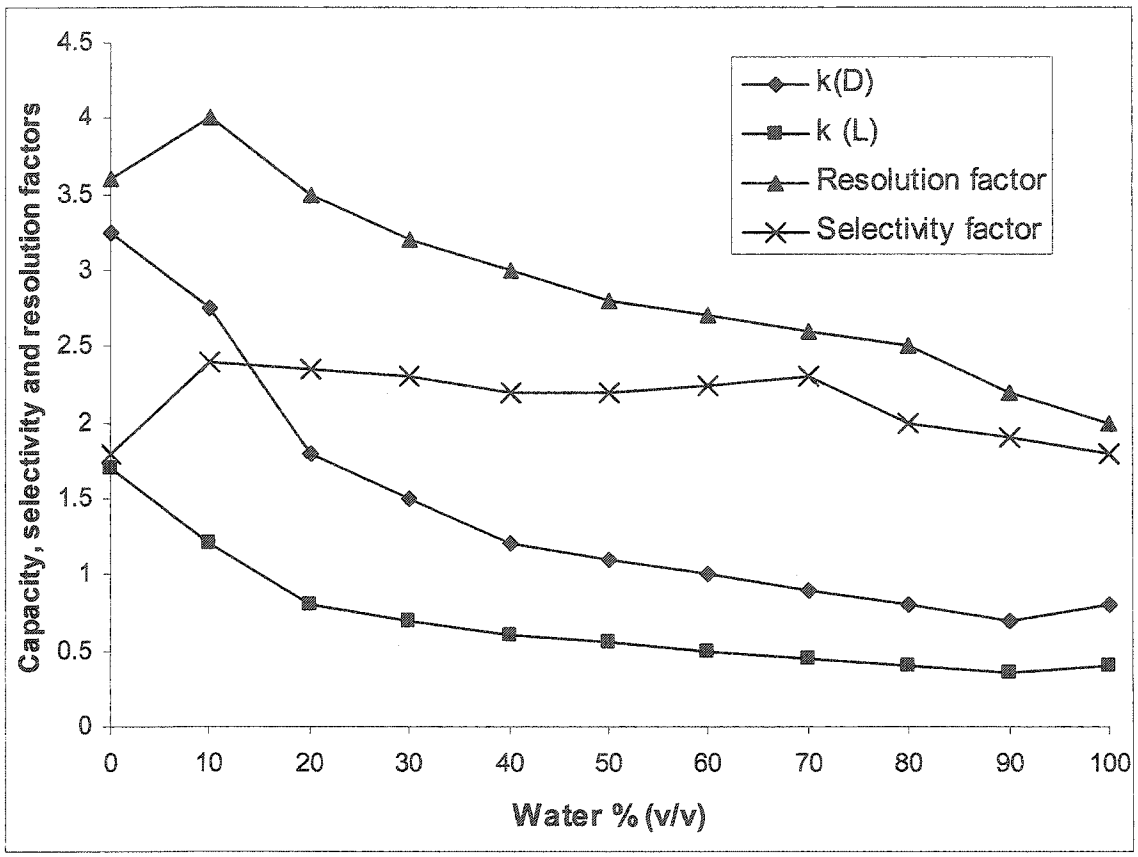
4.5
4
3.5
3
2.5
2
1.5
1
0.5
0
0
10
20
30
40
50
60
70
80
90
100
Capacity, selectivity and resolution factors
Water % (v/v)
k(D)
k (L)
Resolution factor
Selectivity factor

Figure 9

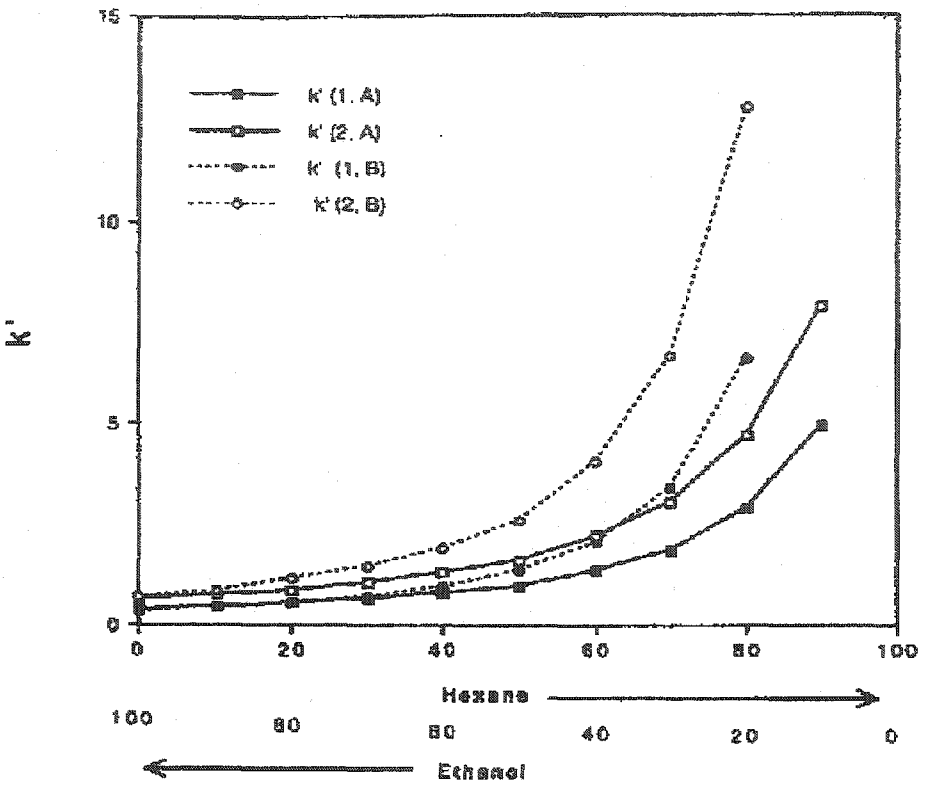
k' (1, A)
k' (2, A)
k' (1, B)
k' (2, B)
k'
15
10
5
0
0
20
40
60
80
100
Hexane
100
80
60
40
20
0
Ethanol

Figure 10

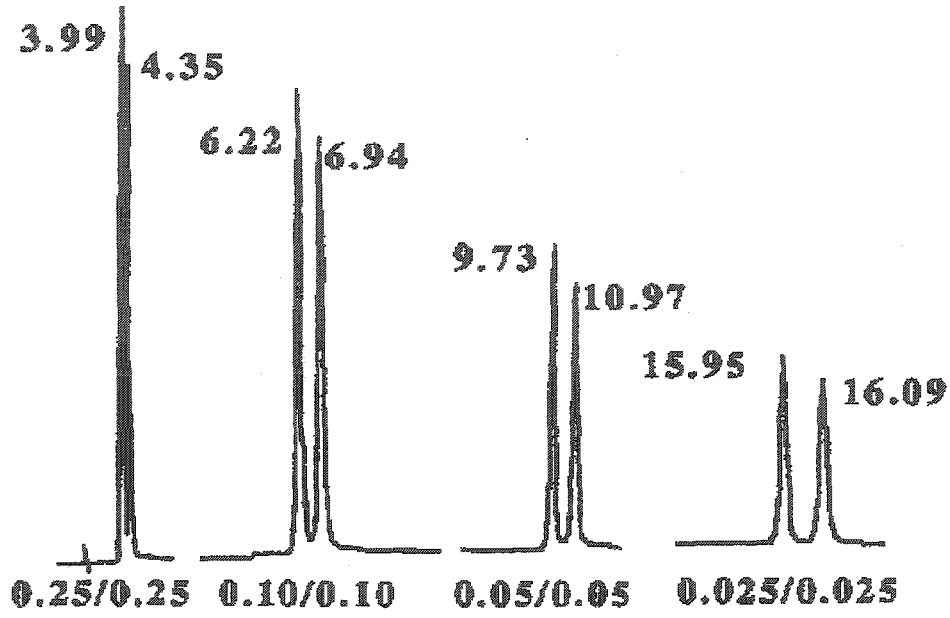
3.99
4.35
6.22
6.94
9.73
10.97
15.95
16.09
0.25/0.25
0.10/0.10
0.05/0.05
0.025/0.025

Figure 11

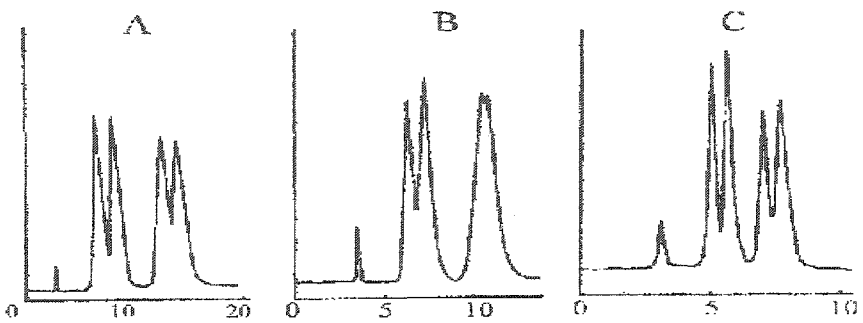

Figure 12

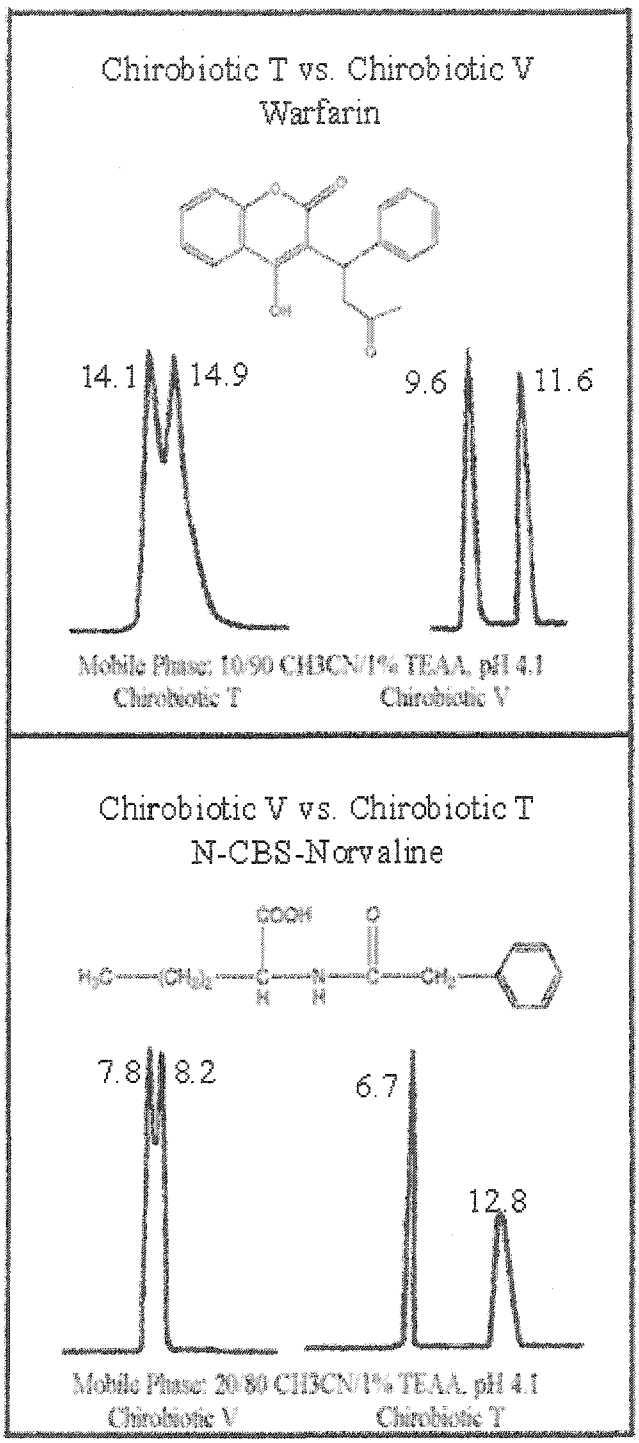
Chirobiotic T vs. Chirobiotic V
Warfarin
14.1
14.9
9.6
11.6
Mobile Phase: 10/90 CH3CN/1% TEAA, pH 4.1
Chirobiotic T
Chirobiotic V
Chirobiotic V vs. Chirobiotic T
N-CBS-Norvaline
7.8
8.2
6.7
12.8
Mobile Phase: 20/80 CH3CN/1% TEAA, pH 4.1
Chirobiotic V
Chirobiotic T

Figure 13

Method Development Protocol for Chirobiotic V

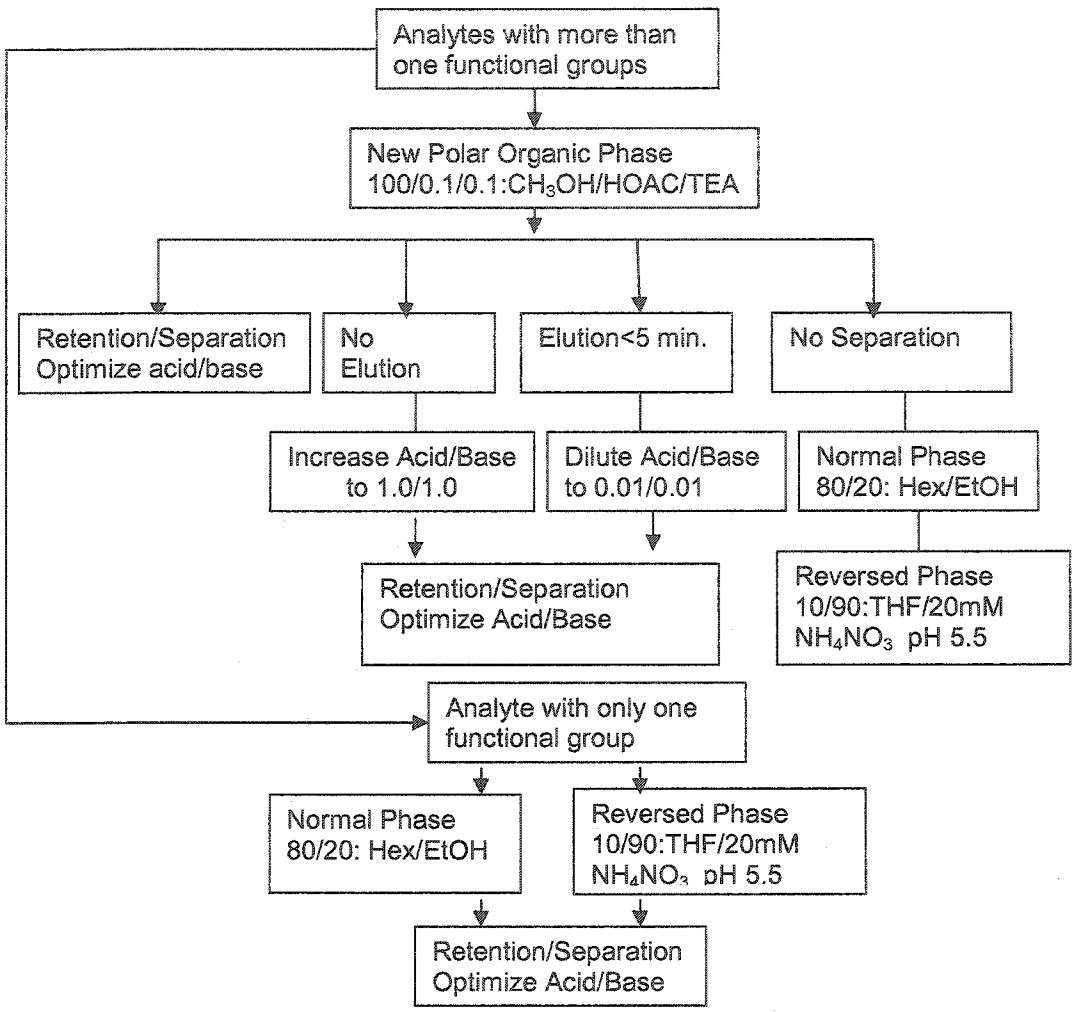

Figure 14

Method Development Protocol for Chirobiotic T

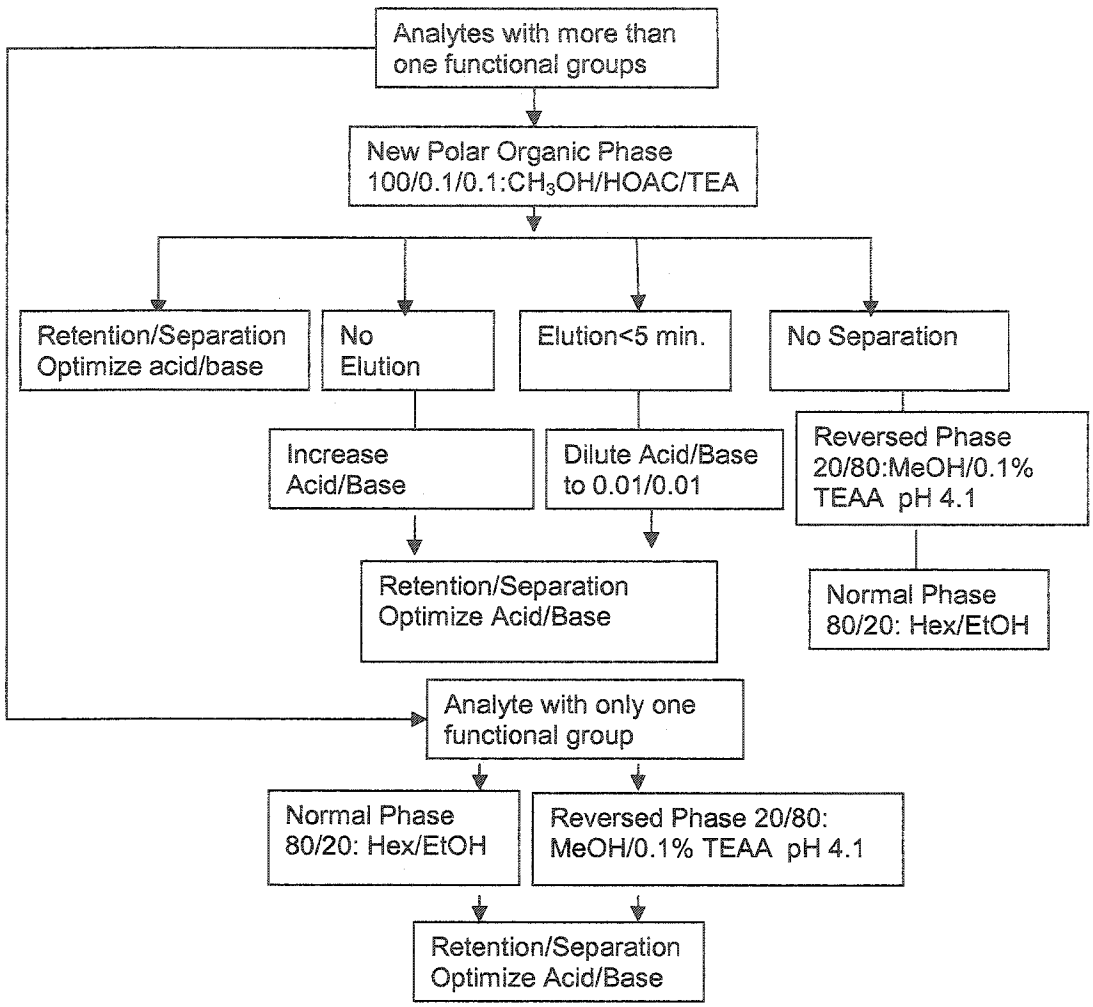

Figure 15

Method Development Protocol for Chirobiotic TAG

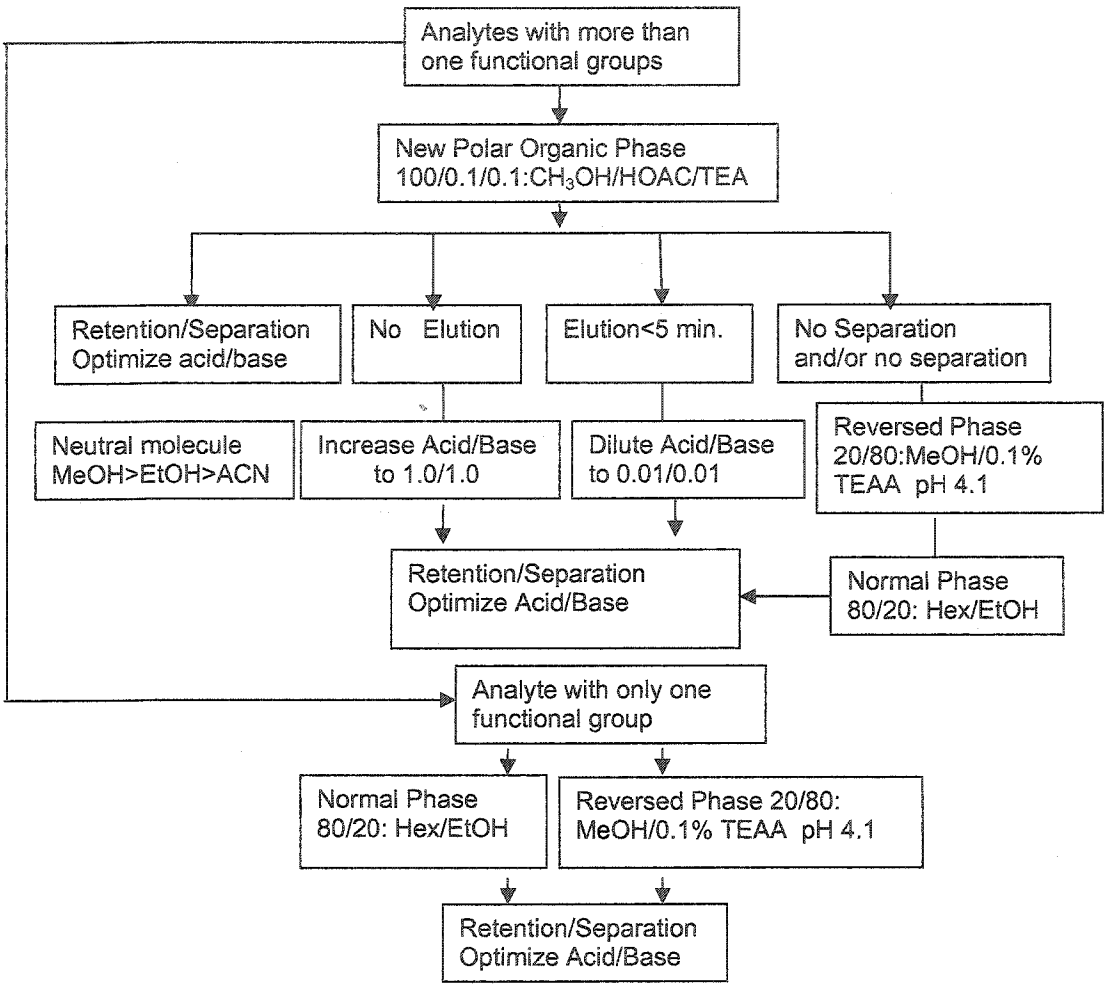

Figure 16

Method Development Protocol for Chirobiotic R

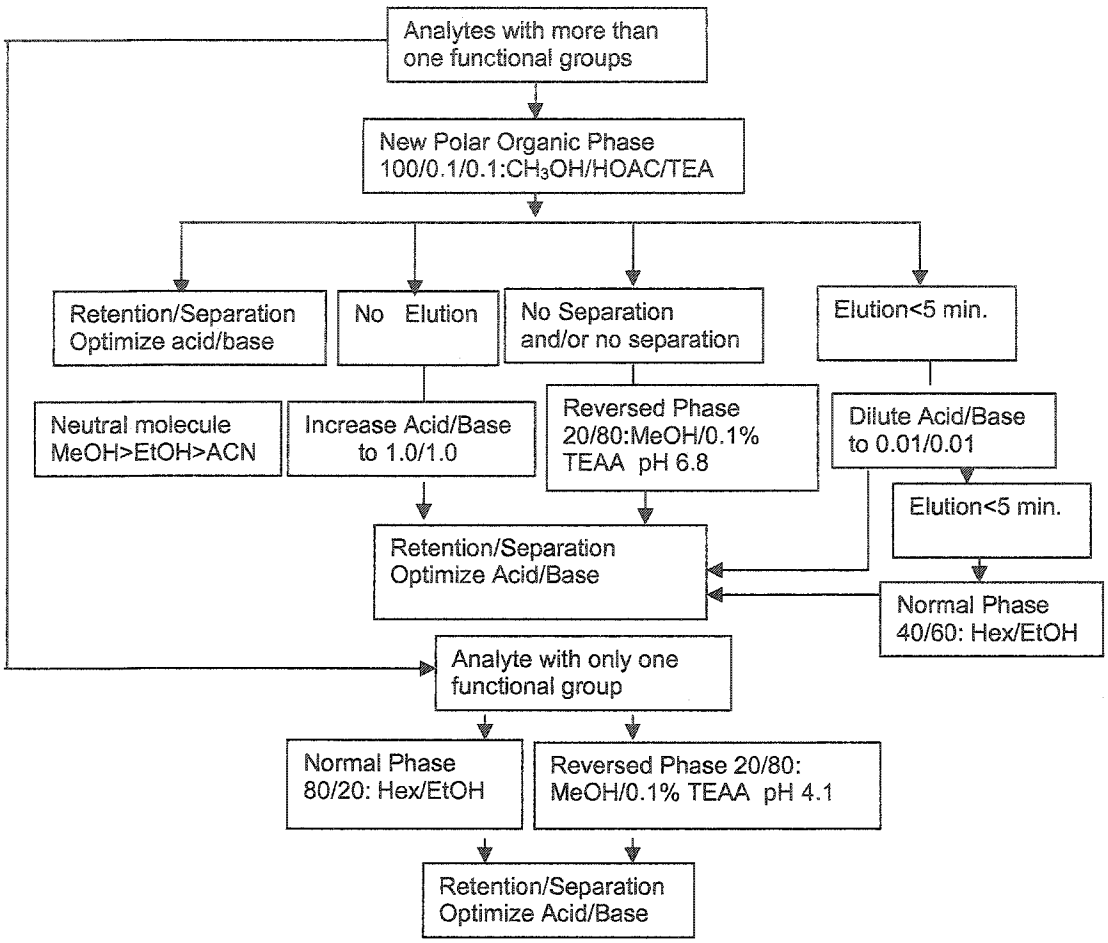

Figure 17

CHAPTER 2
SEPARATION OF CHIRAL SULFOXIDES BY LIQUID CHROMATOGRAPHY USING MACROCYCLIC GLYCOPEPTIDE CHIRAL STATIONARY PHASES

A paper published in Journal of Chromatography A[1]

Alain Berthod , Tom Ling Xiao, Ying Liu, William S. Jenks, Daniel W. Armstrong

ABSTRACT

A set of 42 chiral compounds containing stereogenic sulfur was prepared. There were 31 chiral sulfoxide compounds, three tosylated sulfilimines and eight sulfinate esters. The separations were done using five different macrocyclic glycopeptide chiral stationary phases (CSPs), namely ristocetin A, teicoplanin, teicoplanin aglycone (TAG), vancomycin and vancomycin aglycone (VAG) and seven eluents, three normal-phase mobile phases, two reversed phases and two polar organic mobile phases. Altogether the macrocyclic glycopeptide CSPs were able to separate the whole set of the 34 sulfoxide enantiomers and tosylated derivatives. Five of the eight sulfinate esters were also separated. The teicoplanin and TAG CSPs were the most effective CSPs able to resolve 35 and 33 of the 42 compounds. The three other CSPs each were able to resolve more than 27 compounds. The normal-phase mode was the most effective followed by the reversed-phase mode with methanol–water mobile phases. Few of these compounds could be separated in the polar organic mode with 100% methanol mobile phases. Acetonitrile was also not a good solvent for the resolution of enantiomers of sulfur-containing compounds, neither in the reversed-phase nor in the polar organic mode. The structure of the chiral molecules was compared to the enantioselectivity factors obtained with the teicoplanin and TAG CSP. It is shown that the polarity, volume and shape of the sulfoxide substituents influence the solute enantioselectivity factor. Changing

---

[1] Reprinted with permission from Journal of Chromatography A, 955 (2002) 53–69.
Copyright © 2002 Elsevier Science B.V. All rights reserved.

the oxidation state of the sulfur atom from sulfoxides to sulfinate esters is detrimental to the compound's enantioselectivity. The enantiomeric retention order on the teicoplanin and TAG CSPs was very consistent: the (*S*)-(1)-sulfoxide enantiomer was always the less retained enantiomer. In contrast, the (*R*)-(2)-enantiomer was less retained by the ristocetin A, vancomycin and vancomycin aglycon columns, showing the complementarity of these CSPs. The macrocyclic glycopeptide CSPs provided broad selectivity and effective separations of chiral sulfoxides.

2.1. Introduction

Trivalent sulfur compounds such as sulfoxides and sulfinate esters have non-planar geometries and, when asymmetrically substituted, can be found as stable enantiomers at room temperature [1]. Traditionally, the sulfoxide group has been represented in illustrations as S=O, implying the existence of a second bond between the two atoms. A more modern understanding is that the S-O bond is more ylide-like, i.e. the molecule bears no overall charge but has a negatively charged oxygen atom bonded to a positively charged sulfur atom [2]. The sulfur center is pyramidal, with a lone pair occupying the fourth position of the pseudotetrahedral center. The barrier to inversion depends on substituents, but for sulfoxides, it is in the neighborhood of 40 kcal/mol[3]. Thus, if the two substituents are different, stable stereoisomers exist.

Figure below is the traditional structure of sulfoxide

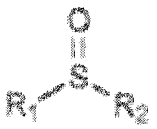

This is the sulfoxide enantiomers with current accepted structures.

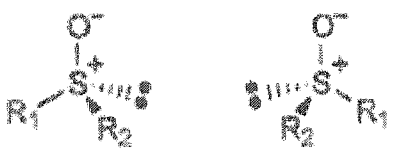

Since the first report on the separation of chiral sulfoxides in 1926 [4], this family of compounds has received much attention given the usefulness of these compounds in organic synthesis [5-7]. Consequently, an effective separation of the enantiomers of racemic sulfoxides is of analytical and preparative interest. In 1959, using column liquid chromatography and an α-lactose home made stationary phase, an Italian research group was able to partially resolve a few racemic sulfoxides [8]. Some chiral sulfoxides were used to test early π-π association-type LC chiral stationary phases (CSPs) [9]. Subsequently, this class of CSPs was used to separate a limited number of compounds containing stereogenic sulfur [10-14]. Protein bonded CSPs were also found to be able to separate some chiral sulfoxides [15-16]. Polysaccharide based CSPs were also used successfully to resolve a dozen sulfoxide enantiomeric pairs [17-21]. This appears to be the most useful class of CSPs for the enantioseparation of chiral sulfoxides thus far [22-23]. Cyclodextrin-based CSPs were also found to provide effective and efficient resolution of enantiomers of these compounds [24].

A recent review did not mention the use of the macrocyclic glycopeptide CSPs for the LC separation of sulfur containing compounds [25]. The goal of this work is to evaluate the capabilities of the macrocyclic glycopeptide-based CSPs for the separation of chiral sulfoxides. In order to obtain a thorough evaluation, the largest number of chiral sulfoxide molecules ever examined as well as several sulfinate esters and sulfilimines were especially synthesized and assayed for compound enantioselectivity. The first part of this work describes and discusses the separation results obtained on five different macrocyclic glycopeptide CSPs in three different mobile phase modes. These results are also compared

with those found in previous reports. The second part of the study will focus on specific solute-stationary phase interactions. By relating the solute structures to the separation data, the factors involved in the chiral recognition process can sometimes be identified.

2.2. Experimental Section

2.1. S-containing compounds

The 42 chiral sulfur-containing compounds used in this study are listed in Table 1. The chiral sulfoxide compounds were sorted by increasing molecular weight from **1** to **31**. **32** to **34** are the tosylated forms of **1**, **16** and **22**, respectively. **35** to **42** are sulfinate ester containing the R_1-SO-O-R_2 group. **1**, **4** and **5** were obtained from Aldrich (St. Louis, MO). All other 39 compounds were prepared and purified according to published methods by the group of W.S. Jenks at Iowa State University, Ames, Iowa [26-30].

2.2. Other chemicals

HPLC grade acetonitrile (ACN), methanol (MeOH), ethanol (EtOH), 2-propanol (IPA), *n*-hexane (hex) and methyl-*tert*-butyl ether (MTBE) were purchased from Fisher (St Louis, MO) and/or EM (Gibbstown, NJ). Water was deionized and filtered on active charcoal and a 5 μm filter. Triethylamine (TEA) and acetic acid (AA) were from Sigma Chemicals (St Louis, MO).

2.3. Chiral stationary phases

Five different macrocyclic glycopeptide chiral selectors were evaluated. They were ristocetin A, $C_{95}H_{110}N_8O_{44}$, m.w. 2066, teicoplanin, $C_{88}H_{97}Cl_2N_9O_{33}$, m.w. 1878, vancomycin, $C_{66}H_{75}Cl_2N_9O_{24}$, m.w. 1449, and the aglycone forms of the latter two: teicoplanin aglycone (TAG), $C_{58}H_{45}Cl_2N_7O_{18}$, m.w. 1197 and vancomycin aglycone (VAG),

$C_{53}H_{52}Cl_2N_8O_{17}$, m.w. 1142. The complete structural description of these chiral selectors has been given in several articles [25, 31-34]. The chiral stationary phases were prepared by bonding the chiral selectors to a 5 μm HPLC spherical porous silica gel through a linking chain [34, 35]. The bonding chemistry was done by Astec (Whippany, NJ). The chiral stationary phases were slurry-packed in 250 × 4.6 mm columns. These columns are marketed by Astec under the trade names: Chirobiotic R, T, V, TAG and VAG for the five glycopeptides, respectively.

2.4. Mobile phase compositions

The macrocyclic glycopeptide based CSPs were used in three different chromatographic modes: 1) the normal phase mode with a low polar mobile phase, 2) the reversed phase mode with hydro-organic mobile phases and 3) the polar organic mode that uses 100% polar organic solvent mobile phases. Three different low polarity normal mobile phases were used: *n*-hexane with 10% ethanol, *n*-hexane with 10% IPA and MTBE with 10% ACN (all % are given in v/v). Two compositions for reversed phase separations were used: methanol and aqueous buffer of 1% TEA (0.07 M), adjusted to pH 4.1 with acetic acid, and the same pH 4.1 aqueous buffer but with ACN as the organic modifier. The methanol contents were 10% v/v with the vancomycin and VAG CSPs, 20% with the teicoplanin CSP, 30% with the ristocetin A CSP and 50% with the VAG CSP. The ACN content was 10% with the vancomycin, VAG and teicoplanin CSPs, 20% with the ristocetin A CSP and 30% with the TAG CSP. Two mobile phase compositions for polar organic mode were used: 100% methanol or 100% ACN, plus 0.025% v/v TEA (2 mM) and AA which were added to the organic solvents for use with the vancomycin, VAG and TAG CSPs. 0.05% TEA and AA (4 mM) and 0.1% TEA and AA (8 mM) were added when using the ristocetin A and

teicoplanin CSPs, respectively. The mobile phase compositions for the reversed phase and polar organic mode analyses were adapted to the CSPs to increase elution strength and reduce analyses duration. They are not necessarily the optimal mobile phase composition giving the best enantioselectivity.

2.3. Results and Discussion

The 42 compounds listed in Table 1 were run in triplicate on five columns with seven different mobile phases. This produced 4410 chromatograms (i.e., 3 runs ×1470 analyses). The experimental reproducibility was good. The 1470 average values for the 4410 analyses gave relative standard deviations lower than 0.08. Exactly 500 analyses showed some resolution of enantiomers of the racemic sulfur-containing compounds. Although the mobile phase compositions were not optimized for maximal resolution of enantiomers, the separation of the enantiomers was excellent with a baseline return between peaks ($Rs > 1.5$) for 154 separations, that is almost one third (exactly 31%) of the chromatograms with an observable enantioseparation. It is notable that every partial enantioseparation could be improved by optimizing the corresponding mobile phase composition. In this study, only seven distinct mobile phase compositions, in the three chromatographic modes, were used in order to obtain a general view of the capability of the macrocyclic glycopeptide based CSPs for the resolution of enantiomers of chiral sulfur containing compounds. Table 2 lists the average value of the retention factor of the first enantiomer, k_1, the enantioselectivity factor, $\alpha = k_2/k_1$, and the resolution factor, Rs, for selected compounds on three CSPs: ristocetin A, teicoplanin and TAG. These three CSPs were the most widely applicable of the columns tested.

3.1. Stationary phase performance

Figure 1 shows the number of observable enantioseparations ($\alpha > 1.01$) obtained (for the 42 compounds listed in Table 1) on each CSPs with the seven mobile phases that were tested. The black bars indicate the number of baseline separation (Rs > 1.5) obtained with the unoptimized mobile phases. Table 3 lists the cumulative number of enantioseparation ($\alpha > 1$) obtained with each stationary phase along with the number of baseline separations (Rs> 1.5) obtained.

The two teicoplanin based CSPs are clearly the most effective chiral stationary phases being able to resolve 35 and 33 chiral sulfur analytes for the teicoplanin and TAG CSPs, respectively. They produced almost twice as many observable separations as the three other CSPs. The teicoplanin CSP separated 3 compounds (**25**, **27** and **34**) that the TAG CSP could not separate. In contrast, **40** was separated by the TAG and not by the teicoplanin CSP. 53% of the compounds enantioresolved by the TAG CSP were baseline separated. Even though unoptimized mobile phases were used, this figure is significantly higher than the corresponding value for the teicoplanin CSP results (~34% baseline resolutions). This means that the enantioselectivity factors obtained with the TAG CSP often were higher that the corresponding values obtained with the native teicoplanin column (Table 3).

The vancomycin and VAG columns were able to separate 31 and 29 compounds, respectively. However, the number of chromatograms with observable enantioseparations is significantly lower with these two CSPs than with the teicoplanin and TAG CSPs (Table 3). Figure 1 shows that most compounds could be resolved with one or two mobile phase compositions only. The number of compounds baseline resolved is dramatically lower; seven compounds on the VAG column and only four on the vancomycin column (**12**, **22**, **29**

and **31**) (Fig. 1). The vancomycin CSP could partly resolve five compounds (**10**, **19**, **27**, **40** and **41**) that the VAG CSP could not separate. Conversely, the VAG CSP could partly resolve **21** and **35**, which vancomycin did not separate. It should be noted, however, that vancomycin is the only CSP that could partly separate the enantiomers of the sulfinate esters **41** and **42** with the apolar MTBE/MeOH 97/3 %v/v mobile phase. The results obtained with these two CSPs and the normal-phase MTBE/ACN 90/10% mobile phase were optimized. Methanol was substituted for ACN to decrease slightly the solute-CSP hydrogen bonding interactions. Shorter retention times and sharper peaks were obtained with a MTBE/MeOH 97/3 % v/v mobile phase compared to the MTBE/ACN 90/10% v/v mobile phase (Table 3).

The glycopeptide antibiotics teicoplanin and vancomycin are naturally produced by the fermentation of *Actinoplanes teicomyceticus* and *Streptomyces orientalis*, respectively. Both molecules have an aglycone "basket" core bearing three or two carbohydrate substituents, respectively. To answer whether the carbohydrate moieties are useful for compound enantioselectivity of stereogenic sulfur-containing compounds, the aglycone form of teicoplanin, TAG, and vancomycin, VAG, were prepared [33]. It was found that a few more sulfur containing compounds could be resolved on the carbohydrate containing columns (teicoplanin or vancomycin) than on their aglycone counterpart columns (TAG or VAG). However, for the compounds that were separated on both CSPs with identical mobile phases, most had higher enantioselectivity and resolution factors on the aglycone columns (Table 2). Figure 2 illustrates this observation for the vancomycin and teicoplanin based CSPs. **26** (Fig. 2 top left) is not resolved on the vancomycin CSP with the MTBE/ACN 90/10 %v/v mobile phase; its α and Rs values are respectively 1.08 and 1.3 when the VAG column is used with the same mobile phase. For **31** (Fig. 2 top right), going from the

vancomycin to the VAG CSP with the same mobile phase, the α and Rs values increase from 1.15 to 1.3 and from 1.2 to 1.4, respectively.

A similar improvement with the teicoplanin and TAG columns is also shown in Figure 2 (bottom) for Compounds **1** and **8** and the hex/EtOH 50/50 %v/v mobile phase. However, in some cases, the teicoplanin and vancomycin CSPs performed better than their aglycone counterparts. For example, Compounds **25**, **27** and **34** are separated by the teicoplanin CSP and not by the TAG column; Compounds **10**, **19**, **27**, **40**, **41** and **42** are separated by the vancomycin CSP and not by the VAG column. The two forms of the macrocyclic glycopeptide selectors should be considered. The native form of glycopeptide seems capable of separating, at least partially, more enantiomeric pairs than the corresponding aglycone form. Similar results were reported previously for amino-acids and the teicoplanin and TAG columns [33].

The ristocetin A column was able to resolve 29 of the 42 chiral sulfoxide compounds. This is only 4 compounds fewer than the TAG CSP and not significantly different from the number of compounds that the vancomycin and VAG columns could resolve. Of the 83 chromatograms obtained on the ristocetin A CSP that showed observable separation, 26 had baseline separation of the enantiomers (Table 3). This is significantly higher than the figures obtained with the vancomycin or VAG columns, especially in the number of baseline resolutions. It is, however, significantly lower than the figures obtained with the teicoplanin or TAG columns. The ristocetin column is useful in the separation of chiral sulfoxide and sulfinate esters. It is the only column able to separate the sulfinate methyl ester, Compound 37. However, the mobile phase composition must be properly optimized.

The complementary nature of the macrocyclic glycopeptide CSPs is well known [34]. A partial separation obtained on one CSP is often converted in a baseline separation when changing to a related glycopeptide chiral selector. This effect was observed for the sulfoxides **25** and **31** that were poorly separated by the teicoplanin based CSPs and well separated by the ristocetin A CSP (Fig. 1) and, to a lesser extent, for several sulfinate esters (**39**, **40** and **42**) that were partly separated by the vancomycin CSP only.

3.2. Mobile phase performance

Table 3 lists the cumulative number of separations obtained with the different mobile phases. Clearly, the three normal-phase mobile phases and the methanol- containing reversed mobile phases are the most useful in separating these compounds with the macrocyclic glycopeptide CSPs. The *n*-hexane-alcohol mobile phases were both able to separate 34 compounds from the set of 42. Ethanol seems to be a better polar organic modifier than isopropyl alcohol since 97 observable chromatograms were obtained with *n*-hexane-ethanol normal mobile phases on the five CSPs. 45 of these separations were complete with a baseline return between peaks. The *n*-hexane-ethanol mobile phases were most useful with the TAG CSP. The *n*-hexane-IPA mobile phases could separate the same 34 compounds but on a lower number of stationary phases; only 87 chromatograms showed some separation with only 39 of them being baseline separations (Table 3). The MTBE-ACN mobile phases are low polarity mobile phases made of dipolar aprotic solvents. They were able to separate 31 compounds only, but with many different CSPs since they have the highest number of successful hits: 107. If these 107 separations are compared to the 31 compounds separated by this mobile phase, it means that an average of 3.5 CSPs were

producing a chromatogram with observable enantioseparation for each 31 compounds. However 84% of these chromatograms were partial separations since only 17 were baseline separations. The MTBE-ACN mobile phases were most useful with the ristocetin A, vancomycin and VAG CSPs. It was shown that methanol, a polar hydrogen bond donor solvent, was a better organic modifier in the MTBE based mobile phase. The MTBE/MeOH 97/3 % v/v mobile phase showed a 10% improvement in the number of enantioseparated compounds and a doubling of the number of baseline separations compared to the MTBE/ACN 90/10 % v/v composition (study done on vancomycin and VAG CSPs only, Table 3).

The reversed phase mode (with methanol-buffer mobile phases) was highly effective for the separation of chiral sulfoxides and related compounds as well. A total of 35 compounds, 32 of which belonged to the set of compounds separated by the normal mobile phases, were separated. **24** was not separated by the methanol-buffer mobile phase, but **34**, a tosyl derivative, and **37**, a sulfinate ester, were separated with the methanol reversed phase and not with the normal-phase mobile phases. If 92 chromatograms showed enantioselectivity, only 30 were baseline separations ($Rs > 1.5$) (Table 3). Table 3 shows that the methanol-buffer mobile phase are much more effective than the acetonitrile-buffer mobile phases. The ACN-buffer mobile phases could resolve only 26 solutes of the set of sulfur-containing compounds. 56 chromatograms showed observable enantioselectivity, that is an average value of two different CSPs per resolved compounds. Only 6 of the 56 chromatograms showed baseline separation. The ACN-buffer reversed-phase systems are not as effective in separating sulfoxide enantiomers with the TAG CSP than the methanol-

buffer mobile phases. Table 2 shows that each time a partial resolution is obtained with an ACN-buffer mobile phase a higher α value is obtained with the corresponding methanol-buffer mobile phase. Note that when the RP ACN line is missing for a compound in Table 2, it means that no resolution was obtained on all CSPs ($\alpha = 1$). One exception should be mentioned: the sulfinate ester enantiomers of **41** could be partially resolved only by the vancomycin CSP in association with a ACN-buffer reversed mobile phase (Fig. 1).

The polar organic methanol mobile phases could separate 28 compounds with 48 chromatograms with observable separation (14 were baseline separations). All the 28 compounds could be better separated by another mobile phase either in the normal or in the reversed phase modes (Table 2). The teicoplanin based CSPs where the most compatible with the polar organic methanol mobile phases. The results were worse with the polar organic ACN mobile phases that could only separate 13 compounds and only 3 where completely resolved. The ristocetin CSP gave the best results with the polar organic ACN mobile phases (Fig. 4).

3.3. Effectiveness of the macrocyclic glycopeptide CSPs

Altogether the macrocyclic glycopeptide CSPs were able to separate the whole set of the 34 sulfoxide enantiomers and tosylated derivatives. Five of the eight sulfinate esters were also separated. The largest set of chiral sulfoxide compounds studied for enantioselective separation found in the literature contained 23 sulfoxide derivatives [36]. Only five of these compounds were also present in our set of 42 compounds. These compounds were separated on four different cellulose or amylose polysaccharide CSPs with

a *n*-hexane-IPA 90/10 v/v normal mobile phase only. The best CSP was able to resolve 16 compounds, of which only two were baseline separated. The compounds in this previous study that are common with ours, are **1**, **4**, **5**, **16** and **21** (Table 1). With the same *n*-hexane-IPA normal mobile phase, **1** is baseline resolved by the teicoplanin and TAG columns and almost baseline resolved by the ristocetin A column (Rs = 1.3, Table 2). This compound is partially resolved by the best polysaccharide CSP of Ref. 36 with a Rs value of 0.8. It is not resolved by the three other CSPs. Similar observations can be made with the other four common compounds.

In another article, the capability of 8 commercial cellulose-based sorbents were screened for the enantiomeric separation of a set of 10 chiral sulfoxides [18]. Our compounds **1**, **4** and **18** were part of this set. The mobile phase used was *n*-hexane-IPA 90-10 v/v. The best enantioseparation of **1** was obtained with CSP Chiralcel OB with an α value of 1.72 giving a Rs value of 3.6. With the same mobile phase, teicoplanin resolves the enantiomers of **1** with an α value of 1.22 giving a Rs value of 4.27 (better efficiency) and TAG gave $\alpha = 2.02$ and Rs = 2.2 (better enantioselectivity) (Table 2). Similarly, **4** was also best separated by Chiralcel OB ($\alpha = 1.58$ and Rs = 3.11). The teicoplanin and TAG CSPs were also able to separate it with a baseline resolution ($\alpha = 1.44$ and 1.47, Rs = 1.8 and 2.1, respectively). However, the values were slightly lower. Methyl dodecyl sulfoxide was part of the set of compounds in Ref. 14 and was not separated by Chiralcel OB and poorly separated by the Chiralcel OD column ($\alpha = 1.07$, Rs = 0.6). Our compound **3**, methyl hexyl sulfoxide is closely related. It was baseline resolved by both the teicoplanin and TAG CSPs in either the normal or reversed phase mode.

In a recent study, polar organic mobile phases (100% alcohol), reversed alcoholic mobile phases and *n*-hexane-IPA mobile phases were used with six polysaccharide phenylcarbamate CSPs to separate a set of five sulfoxide compounds [22]. Our compounds **1** and **5** were part of this set. Every time a comparison was possible (same mobile phase), there was a macrocyclic glycopeptide CSP that could match the polysaccharide CSPs used [22].

3.4. Structure-enantioselectivity relationships

3.4.1. Nature of the benzene ring substituent. Figure 3 shows the enantioselectivity factors obtained for a variety of substituted aryl methyl sulfoxides with the teicoplanin and TAG columns with two mobile phases: *n*-hexane-isopropyl alcohol (IPA) 90/10 v/v and methanol-pH 4 buffer 50/50 v/v. The α factor is plotted versus the para substituent on the benzene ring. The enantioselectivity factors decrease in the order:

$F > Cl > Br > H > CH_3 > CF_3$

for the two CSPs and for the two mobile phases (normal phase mode and reversed phase mode). Clearly, the order corresponds to the decreasing electronegativity order for the halogen atoms, the hydrogen atom and the methyl group. The trifluoromethyl group does not fit in this correlation. With three strongly electronegative atoms, it has a strong electron withdrawing capability. Also, the size of the substituents should be noted. The fluorine atom is the smallest halogen; the CF_3 group is slightly bigger than the CH_3 group and the H atom.

3.4.2. Position of the benzene ring substituents. Figure 4 shows that the enantioselectivity factors obtained with the meta substituted molecules were significantly higher than the values obtained with the corresponding ortho or para isomers. The exception is ortho-bromophenyl

methyl sulfoxide separated by the teicoplanin CSP in the reversed phase mode. It has an α value of 1.2, slightly higher than that of meta-bromophenyl methyl sulfoxide ($\alpha = 1.17$, Table 2). In organic synthesis it is known that the methyl group and halogen substituents are ortho and para directors for electrophilic aromatic substitutions. The electron deficient intermediate complex can be stabilized only by ortho and para substituents. It is possible that the ortho and para positions of the methyl, chloro or bromo substituents produce an electron density on the sulfur atom less favorable for compound enantioselectivity than that obtained when the substitutents are in the meta position. However, the aromatic electron density and the electron environment of the sulfur atom are certainly not the only parameters acting on the compound enantioselectivity of sulfoxides by teicoplanin CSPs. Shape and steric repulsion are certainly involved in the mechanism [18].

3.4.3. Steric factors. Using a thermodynamic approach, Küster et al. claimed that steric hindrance was the main reason for chiral discrimination of sulfoxides by polysaccharide based CSPs in the normal phase mode [18]. Table 4 lists the enantioselectivity factors for a variety of phenyl sulfoxides and para-tolyl sulfoxides obtained with the teicoplanin and TAG CSPs and with normal and reversed-phase mobile phases. Four substituents in the table are common to phenyl and *para*-toluyl sulfoxides. They are the methyl, benzyl, (2-phenyl) ethyl and (1,1-dimethyl 2-phenyl) ethyl substituents. Every time the enantiomers of these sulfoxides are separated ($\alpha > 1$), the α factor is better in the same experimental conditions for the phenyl sulfoxide than for the corresponding tolyl compound. It seems that the main part of this effect is due to steric hindrance. The slight change in molecular volume between the phenyl and the *para*-tolyl group makes a significant difference for the chiral selector.

Steric bulk seems to be the dominant factor explaining the increased α values obtained when the bulky tert-butyl group replaces the methyl group (**1** and **12**, Table 4). Intramolecular stacking may also be part of steric repulsion. Comparing the results obtained with **22** and **29** (phenyl sulfoxides) and **24**, **27** and **30** (tolyl sulfoxides), a dramatic increase of the enantioselectivity factor for the dimethylaryl-α-substitued sulfoxides can be noted (Table 4). Figure 5 illustrates the intramolecular π-π stacking that could be favored with **29** and **30** having two methyl groups that promote bending of the alkyl chain, allowing the two aromatic rings to interact. **22**, **24** and **27** have also two aromatic rings that could stack but possible free rotations around the CH_2 groups decrease the stacking. The stacked form of the compounds seems to interact strongly with some chiral selector sites. Either reduced or no enantiorecognition is obtained when stacking is reduced (Table 4). The stacking effect is more pronounced with the apolar *n*-hexane/IPA mobile phase (where π-π interactions are favored) than with the polar methanol/buffer mobile phase.

3.4.4. Altering the sulfoxide group. Table 5 lists the results obtained with the teicoplanin CSP for the analyses of different compounds in which the sulfoxide group has been modified. For example, **32** is the N-tosyl analog of **1**. The S^+-O^- group of **1** is replaced by S^+-N^--SO_2-ϕ-CH_3. Changing the sulfoxide group to the N-tosylated form significantly decreased the chromatographic polarity of the molecule. Apparently, the N^- group is much more hindered than a lone O^- group which is very active for H-bonding. The N-tosyl analogs are less retained in the normal phase mode and more retained in the reversed phase mode

(Table 5). The enantioselectivity factor, α, was less for all of the tosylated compounds except one in the normal-phase mode (Table 5). In the reversed phase mode, the results were mixed. Clearly the tosyl group alters the interaction between the chiral analyte and the CSPs in both normal and reversed phase modes. Steric interactions will increase in both modes. While hydrophobic interactions are more significant for the N-tosylated compounds in the reversed phase mode (Table 5), the corresponding π-π interactions do not seem to be enhanced in the normal-phase mode except for **34**. Apparently, the increased retention and possible stacking with this molecule results in the elimination of enantioselective recognition.

35 to **42** are sulfinate esters. The oxidation number of sulfur in these compounds is different from that of the sulfoxide compounds. This change is detrimental for compound enantioselectivity. Only the enantiomers of methyl *p*-toluene sulfinate (**35**) could be resolved by the teicoplanin and TAG columns. Three of the seven sulfinate esters could not be resolved by any of the five CSPs studied. Ristocetin A was the only CSP able to partially resolve **37** and the vancomycin CSP could also partially resolve **40**, **41** and **42** (Figure 1). All partial separations were obtained in the reversed phase mode. It should be pointed out that there are very few, if any, previously reported LC enantiomeric separations of sulfinate esters. However, these compounds are easily resolved by gas chromatography using cyclodextrin-based CSPs [37].

3.4.5. Enantiomeric retention order. The enantiomeric elution order was determined for all separations using a laser-based polarimetry detector and/or by injecting an enantiomer standard of known configuration. The first eluted enantiomer, for all compounds separated on the teicoplanin and TAG CSPs (but one) was the (*S*)-(+)-enantiomer. The one exception

was methyl *p*-biphenyl sulfoxide (**17**) where the (*R*)-(-)-enantiomer eluted first with all mobile phases. Its long and rigid *para*-biphenyl substituent is very likely sterically altering its interaction with the teicoplanin or TAG chiral selector. Also, the *ortho* derivatives, **11** and **20**, showed a reversed enantiomeric retention order, i.e., the (*R*)-(-)-enantiomer eluted first, but only in the normal-phase mobile phase of acetonitrile and methyl *tert*-butyl ether only. With the six other mobile phases, the (*S*)-(+)-enantiomer of these two analytes eluted first.

Conversely, all chiral sulfoxides separated on the ristocetin A, the vancomycin and the VAG CSPs showed the (*R*)-(-)-enantiomer eluting first. This behavior was maintained with the optimized MTBE-MeOH mobile phase and the vancomycin and VAG CSPs. Figure 6 shows the separation of the enantiomers of **29** on the TAG column (left) and the VAG column (right). The trace of the optical rotation detector shows that the enantiomeric retention order of the two enantiomers is reversed. The (*S*)-(+)-enantiomer elutes first on the TAG column and last on the VAG column. There were no exceptions for the vancomycin and VAG columns. It should be recalled, however, that these columns could only separate 30 and 27 compounds, respectively, from the set of 42. With the ristocetin A column, the only exceptions found were the benzyl derivatives, **16**, **25** and **26**, and the diphenylmethyl derivative, **31**. The (*S*)-(+)-enantiomers of these four analytes eluted first but with the reversed phase mode methanol-buffer system, only.

These results show again the complementarity of the macrocyclic glycopeptide CSPs. There are multiple chiral interaction sites on a given CSP and the individual chiral selectors

of this class of compounds are not the same. For a given compound, if no enantioseparation is obtained in the different mobile phase modes with a particular CSP, chances are that another macrocyclic glycopeptide based CSP will separate the enantiomers [38]. Furthermore, for neutral sulfoxides, at least two different glycopeptide CSPs can have the opposite enantiomeric retention order.

2.4. Summary and conclusion

The macrocyclic glycopeptide CSPs are very useful for the separation of enantiomers of chiral sulfoxides. The teicoplanin and TAG CSPs with the *n*-hexane-IPA mobile phase (i.e., normal phase mode) and the methanol-buffer mobile phase in the reversed phase mode are the most effective CSP-mobile phase associations for the enantioseparation of these compounds. An important feature involving the chiral recognition mechanism of sulfoxide compounds seems to be steric repulsion. Also it appears that intramolecular stacking of some of the larger chiral sulfoxides can greatly affect its enantiorecognition. Compared to chiral sulfoxides, the sulfinate esters, with an increased oxidation state of the sulfur atom, are poorly separated by the macrocyclic antibiotic CSPs. The enantiomeric retention order of the enantiomer showed a great deal of consistency for any single CSP and mobile phase. However, reversing the enantiomeric retention order is possible by changing the CSP.

Acknowledgments

Support by the National Institute of Health NIH R01 GM 53825 is gratefully acknowledged. AB thanks the French Centre National de la Recherche Scientifique, ERS 2007 FRE 2394, for a one-year sabbatical leave at ISU.

References

[1] K. Mislow, A.J. Gordon, D.R. Rayner, J. Amer. Chem. Soc. 90 (1968) 4854.

[2] J.A. Dobado, H. Martinez-Garcia, J.M. Molina, M.R. Sundberg, J. Am. Chem. Soc. 121 (1999) 3156.

[3] D.R. Rayner, A.J. Gordon, K. Mislow, J. Am. Chem. Soc. 90 (1968) 4854.

[4] P.W.B. Harrison, J. Keynon, H. Phillips, J. Chem.. Soc. (1926) 2079.

[5] M.C. Carreño, Chem. Rev. 95 (1995) 1717.

[6] H. Matsuyama, Sulfur Rep. 22 (1999) 85.

[7] J.C. Carretero, R.G. Arrayas, N.D. Buezo, J.L. Garrido, I. Alonso, J. Adrio, Phosphorus, Sulfur Silicon Relat. Elem. 153-4 (1999) 259.

[8] G. Farina, F. Montanari, A. Negrini, Gazz. Chim. Ital. 89 (1959) 1548.

[9] W.H. Pirkle, D.W. House, J. Org. Chem. 44 (1979) 1957.

[10] W.H. Pirkle, J.M. Finn, J.L. Schreiner, B.C. Hamper, J. Am. Chem. Soc. 103 (1981) 3964.

[11] S. Allenmark, L. Nielsen, W.H. Pirkle, Acta Chem. Scand. 37 (1983) 325.

[12] G. Gargaro, F. Gasparrini, D. Misiti, G. Palmieri, M. Pierini, D. Villani, Chromatographia 24 (1987) 505.

[13] M. Lienne, M. Caude, R. Rosset, A. Tambute, P. Delatour, Chirality 1 (1989) 142.

[14] C.J. Welch, T. Szczerba, S.R. Perrin, J. Chromatogr. A 758 (1997) 93.

[15] S. Allenmark, B. Bomgren, J. Chromatogr. 252 (1982) 297.

[16] K. Balmer, B.A. Persson, P.O. Lagerström, J. Chromatogr. A 660 (1994) 269.

[17] A. Ichida, T. Shibata, Y. Okamoto, Y. Yuki, H. Namikoshi, Y. Toga Chromatographia 19 (1984) 280.

[18] I. Wainer, M.C. Alembik, C.R. Johnson, J. Chromatogr. 361 (1986) 374.

[19] E. Küsters, V. Loux, E. Schmid, P. Floersheim, J. Chromatogr. A 666 (1994) 421.

[20] M. Tanaka, H. Yamazaki, H. Hakusui, Chirality 7 (1995) 612.

[21] M.I. Donnoli, S. Superchi, C. Rosini, Enantiomers 5 (2000) 181.

[22] B. Chankvetadze, C. Yamamoto, Y. Okamoto, J. Chromatogr. A 922 (2001) 127.

[23] S.A. Matlin, M.E. Tiritan, Q.B. Cass, D.B. Boyd Chirality 8 (1996) 147.

[24] E. Küsters, G. Gerber, Chromatographia 44 (1997) 91.

[25] T.J. Ward, A.B. Farris, J. Chromatogr. A 906 (2001) 73.

[26] S. Oae, N. Furukawa, *Sulfilimines and Related Derivatives*, ACS Symp. Ser. 179 (1983) 2.

[27] J.M. Klunder, K.B. Sharpless, J. Org. Chem. 52 (1987) 2598.

[28] G. Capozzi, J. Drabowicz, D. Kiełbasinski, S. Menichetti, M. Mikołajczyk, C. Nativi, K. Schank, N. Schott, U. Zoller, *Synthesis of Sulphones, Sulphoxides and Cyclic Sulphides*, J. Wiley & Sons, Chichester, 1994.

[29] W.S. Jenks, W. Lee, D. Schutters, J. Phys. Chem. 98 (1994) 2282.

[30] W. Lee, W.S. Jenks, J. Org. Chem. 66 (2001) 474.

[31] M.P. Gasper, A. Berthod, U.B. Nair, D.W. Armstrong, Anal. Chem. 68 (1996) 2501.

[32] A. Berthod, Y. Liu, C. Bagwill, D.W. Armstrong, J. Chromatogr. A 731 (1996) 123.

[33] A. Berthod, X. Chen, J.P. Kullman, D.W. Armstrong, F. Gasparrini, I. D'Acquarica, C. Villani, A. Carotti, Anal. Chem. 72 (2000) 1727.

[34] U.B. Nair, S.C. Chang, D.W. Armstrong, Y.Y. Rawjee, D.S. Eggleston, J.V. McArdle, Chirality 8 (1996) 590.

[35] D.W. Armstrong, Y. Tang, S. Chen, Y. Zhou, C. Bagwill, J.R. Chen, Anal. Chem. 66 (1994) 1473.

[36] C.A. Montanari, Q.B. Cass, M.E. Tiritan, A.L.S. De Souz, Anal. Chim. Acta 419 (2000) 93.

[37] J.A. Anderson, J. Ding, R. McCulla, W.S. Jenks, D.W. Armstrong, J. Chromatogr. A 947 (2002) 197.

[38] T.E. Beesley, R.P.W. Scott, *Chiral Chromatography*, Separation Science Series, Wiley, Chichester, 1998.

Figure Legends

Figure 1: Overview of the results arranged per solute and per CSP. The length of the bars indicates how many mobile phase were capable to produce observable separation of the enantiomers of the solute. White bars: number of observable enantioselective separations ($\alpha > 1.02$); dark bars: number of baseline separations (Rs > 1.5).

Figure 2: Effect of the macrocyclic glycopeptide sugar units on compound enantioselectivity Top: Vancomycin and Compounds **26** (left) and Compounds **31** (right). Mobile phase: MTBE/ACN 90/10 v/v, 1 mL/min. Bottom: Teicoplanin and Compounds **1** (left) and Compounds **8** (right). Mobile phase: hex/EtOH, 50/50 v/v 2 mL/min.

Figure 3: Effect of the substituents of the para substituted phenyl methyl sulfoxides on the compounds enantioselectivity. Thick lines: teicoplanin CSP, dotted lines: TAG CSP; squares: methanol/buffer(20/80 v/v) reversed mobile phase, triangles: *n*-hexane/IPA (90/10 v/v) normal mobile phase.

Figure 4: Structural effect of the phenyl substituents of the ortho, meta or para substituted phenyl methyl sulfoxides on the compounds enantioselectivity. Top figures: *n*-hexane/IPA (90/10 v/v) normal mobile phase; bottom figures: methanol-buffer (20/80 v/v) reversed mobile phase.

Figure 5: Left: Possible intramolecular stacking by π-π interactions. Right: the stacking is favored by the two methyl groups in α position of the sulfur atom.

Figure 6: Illustration of the enantiomeric retention order reversal. Left: Compound **29** separated with the TAG column, the (*S*)-(+)-enantiomer elutes first, normal mobile phase (*n*-hexane/EtOH 50/50 v/v); right: on the VAG column, the (R)-(-) enantiomer elutes first, normal mobile phase (MTBE/ACN 90/10 v/v).

Table 1
Structures of 42 stereogenic sulfur-containing compounds and the number of observable enantiomeric separations achieved for each.

compound number	R_1[a]	R_2[a]	SO[a]	mw	separations[b]
1	C6H5	CH3		140	17
2	CH3CH2CH2CH2CH=CH	CH3		146	13
3	CH3CH2CH2CH2CH2CH2	CH3		148	7
4	C6H5	CH2=CH		152	8
5	pCH3C6H4	CH3		154	10
6	mCH3C6H4	CH3		154	14
7	oCH3C6H4	CH3		154	15
8	FC6H4	CH3		159	16
9	pClC6H4	CH3		174.5	12
10	mClC6H4	CH3		174.5	13
11	oClC6H4	CH3		174.5	23
12	C6H5	(CH3)3C		182	20
13	aC10H7	CH3		190	21
14	C6H5CH2CH2CH=CH	CH3		194	15
15	CF3C6H4	CH3		208	10
16	C6H5	C6H5CH2		216	18
17	C6H5C6H4	CH3		216	17
18	pBrC6H4	CH3		219	12
19	mBrC6H4	CH3		219	14
20	oBrC6H4	CH3		219	22
21	CH3C6H4	C6H5CH2		230	10
22	C6H5	C6H5CH2CH2		230	18
23	C6H5	CH3C6H4CH2		230	14
24	CH3C6H4	C6H5CH2CH2		244	13
25	C6H4OCH3	C6H5CH2		246	12
26	ClC6H4	C6H5CH2		250.5	19
27	CH3C6H4	C6H5CH2CH2CH2		258	2
28	bC10H7	C6H5CH2		266	19
29	C6H5	C6H5CH2CH2C(CH3)2		272	28
30	CH3C6H4	C6H5CH2CH2C(CH3)2		286	14
31	C6H5	(C6H5)2CH		292	24
32	C6H5	CH3	Tosyl	279	12
33	C6H5	C6H5CH2	Tosyl	355	7
34	C6H5	C6H5CH2CH2	Tosyl	369	3
35	CH3O	C6H5CH2	s.e.	170	7
36	CH3CH2O	CH3C6H4	s.e.	184	0
37	C6H5CH2CH2CH2O	CH3	s.e.	198	1
38	CH3(CH3)CHO	CH3C6H4	s.e.	198	0
39	CH3CH2CH2O	CH3C6H4	s.e.	198	0
40	CH3CH2CH2CH2O	CH3C6H4	s.	212	3

41	CH3CH(CH3)CH2O	CH3C6H4	e.s.e.	226	1
42	CH3CH2CH(CH3)O	CH3C6H4	e.s.e.	226	3

a) The general structure is R_1-SO-R_2. Compounds **1** to **31** are sulfoxides; Compounds **32** to **35** are tosylated sulfoxides (tosyl = p-toluene sulfonate, SO was replaced by SN-SO_2-C_6H_4-CH_3); Compounds **36** to **42** are sulfinate esters.

b) separation = cumulative number of observable enantioseparations on the five CSPs with the 7 mobile phases (total = 35 essays per compound).

C6H5 = phenyl ring; p, m, o = para, meta, ortho phenyl substitution, C10H7 = naphthalenyl group; a, b = alpha or beta connected to the SO group, s.e. = sulfinate ester with the R1-O-SO-R2 asymmetric center.

Table 2
Chromatographic results obtained with selected chiral sulfur-containing compounds on three macrocyclic antibiotic CSPs.

		ristocetin A			teicoplanin			teicoplanin aglycone		
mobile phase		k_1	alpha	Rs	k_1	alpha	Rs	k_1	alpha	Rs
1	**methyl phenyl sulfoxide**									
RP	MeOH	0.68	1	0	1.27	1.11	0.5	1.15	1.13	1.2
PO	MeOH	0.21	1	0	0.15	1.40	0.8	0.46	1.38	1.3
PO	ACN	1.23	1.94	3.8	1.79	1.14	0.6	2.17	1	0
NP	hex-EtOH	3.15	1.15	1.7	8.90	1.11	2.1	3.36	1.34	2.7
NP	hex-IPA	11.7	1.05	1.3	19.34	1.22	4.3	13.1	2.02	2.2
NP	MTBE-ACN	8.13	1.11	1.5	9.80	1.03	0.2	15.8	1	0
5	**p-toluyl methyl sulfoxide**									
RP	MeOH	1.23	1	0	2.50	1.12	1.3	2.15	1.19	1.7
PO	MeOH	0.19	1	0	0.21	1.43	1.0	0.56	1.50	1.9
NP	hex-EtOH	2.72	1	0	6.90	1.17	2.7	3.14	1.64	3.3
NP	hex-IPA	3.52	1.16	0.8	7.17	1.57	2.1	6.93	2.08	2.3
NP	MTBE-ACN	5.80	1.02	0.3	6.90	1	0	11.5	1	0
6	**m-toluyl methyl sulfoxide**									
RP	MeOH	2.00	1	0	1.82	1.17	1.3	1.08	1.33	2.1
RP	ACN	1.07	1	0	1.37	1.07	1.0	1.34	1	0
PO	MeOH	0.13	1	0	0.24	1.41	1.2	0.39	1.59	2.9
NP	hex-EtOH	5.44	1.06	1.25	6.87	1.32	3.4	13.2	1.53	3.2
NP	hex-IPA	18.9	1	0	28.45	2.00	3.0	7.90	2.15	3
NP	MTBE-ACN	7.47	1.05	0.9	8.40	1	0	57.0	1.16	1.8
7	**o-toluyl methyl sulfoxide**									
RP	MeOH	1.47	1	0	4.93	1.07	1.3	1.59	1.16	1.4
PO	MeOH	0.17	1	0	0.21	1.29	1.0	0.53	1.33	1.5
PO	ACN	1.52	1.05	0.8	2.00	1	0	1.55	1	0
NP	hex-EtOH	2.48	1.12	1.4	6.00	1.09	1.0	4.90	1.31	3
NP	hex-IPA	8.60	1.10	0.5	8.07	1.29	1.0	13.6	1.70	2.3
NP	MTBE-ACN	31.8	1.15	1.2	7.20	1.11	1.4	14.1	1	0
8	**p-fluorophenyl methyl sulfoxide**									
RP	MeOH	0.68	1	0	1.23	1.14	1.3	1.07	1.28	1.7
PO	MeOH	0.19	1	0	0.19	1.48	1.0	0.42	1.67	2.4
NP	hex-EtOH	3.35	1	0	8.40	1.26	1.6	3.21	1.69	3.7
NP	hex-IPA	19.6	1.11	1.1	6.13	1.71	1.9	13.1	2.02	2.6
NP	MTBE-ACN	7.13	1.04	0.6	8.00	1	0	12.3	1.08	0.6
9	**p-chlorophenyl methyl sulfoxide**									
RP	MeOH	1.03	1	0	2.00	1.13	1.6	1.74	1.21	1.8
PO	MeOH	0.17	1	0	0.19	1.48	1.0	0.49	1.61	2
NP	hex-EtOH	2.72	1	0	6.70	1.19	3.1	2.93	1.68	3.3
NP	hex-IPA	3.45	1.18	0.8	6.93	1.63	2.0	14.5	2.34	2.9
NP	MTBE-ACN	5.80	1.02	0.4	6.70	1	0	11.0	1	0

	ristocetin A			teicoplanin			teicoplanin aglycone		
mobile phase	k_1	alpha	Rs	k_1	alpha	Rs	k_1	alpha	Rs
10	**m-chlorophenyl methyl sulfoxide**								
RP MeOH	2.32	1	0	2.18	1.18	1.6	1.68	1.28	1.5
RP ACN	1.28	1	0	1.67	1.05	1.2	1.62	1	0
PO MeOH	0.14	1	0	0.22	1.23	1.0	0.42	1.62	2.2
NP hex-EtOH	5.27	1.03	0.5	6.76	1.22	3.2	11.9	1.59	4.8
NP hex-IPA	14.6	1	0	20.9	1.57	2.9	7.00	2.69	3.1
NP MTBE-ACN	4.44	1.05	0.8	4.50	1	0	36.1	1.09	1.1
11	**o-chlorophenyl methyl sulfoxide**								
RP MeOH	2.70	1	0	2.73	1.19	1.6	2.15	1.24	1.6
RP ACN	1.44	1	0	1.96	1.07	1.2	1.91	1	0
PO MeOH	0.15	1	0	0.28	1.34	1.2	0.60	1.67	3.4
PO ACN	0.50	1.16	0.7	0.88	1	0	1.17	1.11	0.6
NP hex-EtOH	3.10	1.04	0.6	4.37	1.16	2.2	9.80	1.40	3.5
NP hex-IPA	7.00	1	0	12.0	1.38	1.6	8.08	2.00	2.4
NP MTBE-ACN	2.95	1.11	1.4	3.00	1.11	1.5	30.5	1.06	0.6
12	**phenyl *tert*-butyl sulfoxide**								
RP MeOH	1.64	1.08	0.8	2.13	1.06	0.8	1.30	1.20	1.5
PO MeOH	0.00	1	0	0.02	1	0	0.11	1.76	0.6
PO ACN	0.91	1.04	0.5	1.40	1	0	0.88	1	0
NP hex-EtOH	0.79	1	0	1.47	1.30	3.4	0.93	1.56	4.1
NP hex-IPA	1.46	1.20	1.3	0.80	2.50	1.9	1.50	1.81	2.5
NP MTBE-ACN	4.80	1.33	2.4	2.23	1.12	0.8	4.50	1.18	1.2
13	**α-naphthalenyl methyl sulfoxide**								
RP MeOH	3.50	1	0	11.61	1.18	3.0	3.56	1.43	4.8
RP ACN	0.94	1	0	3.83	1.03	0.3	3.05	1.07	0.7
PO MeOH	0.21	1	0	0.29	1.53	2.0	0.79	1.65	3.5
PO ACN	1.28	1.09	1.45	1.67	1	0	1.66	1	0
NP hex-EtOH	2.04	1.14	1.4	5.80	1.44	3.6	5.56	1.70	4.4
NP hex-IPA	7.80	1	0	7.13	2.18	2.5	16.5	1	0
NP MTBE-ACN	8.50	1.20	2.5	6.13	1.07	0.8	12.8	1.12	0.9
18	**p-bromophenyl methyl sulfoxide**								
RP MeOH	1.23	1	0	2.50	1.12	1.3	2.15	1.19	1.7
PO MeOH	0.19	1	0	0.21	1.43	1.0	0.56	1.50	1.9
NP hex-EtOH	2.72	1	0	6.90	1.17	2.7	3.14	1.64	3.3
NP hex-IPA	3.52	1.16	0.8	7.17	1.57	2.1	6.93	2.08	2.2
NP MTBE-ACN	5.80	1.02	0.3	6.90	1	0	11.5	1	0
19	**m-bromophenyl methyl sulfoxide**								
RP MeOH	2.70	1	0	2.71	1.17	1.3	1.75	1.32	3.0
RP ACN	1.51	1	0	1.81	1.09	1.2	0.66	1	0
PO MeOH	0.16	1	0	0.26	1.25	1.2	0.48	1.67	4.9
NP hex-EtOH	6.10	1.01	0.2	6.76	1.24	3.6	13.7	1.72	4.5
NP hex-IPA	19.1	1.04	0.5	24.5	1.80	2.9	7.50	2.73	3.1
NP MTBE-ACN	4.37	1.04	0.6	4.70	1	0	37.5	1.11	1.2
20	**o-bromophenyl methyl sulfoxide**								
RP MeOH	5.20	1	0	3.55	1.20	1.7	2.66	1.28	2.4
RP ACN	1.78	1	0	2.42	1.09	1.3	2.34	1	0
PO MeOH	0.17	1	0	0.31	1.32	1.3	0.68	1.56	3.9
PO ACN	0.82	1	0	0.88	1	0	1.38	1.09	0.6

	ristocetin A			teicoplanin			teicoplanin aglycone		
mobile phase	k_1	alpha	Rs	k_1	alpha	Rs	k_1	alpha	Rs
NP hex-EtOH	3.30	1.50	1	4.78	1.17	2.1	12.4	1.49	3.2
NP hex-IPA	7.55	1	0	13.43	1.47	1.7	9.33	2.02	3.0
NP MTBE-ACN	3.13	1.11	1.45	3.20	1.11	1.2	34.2	1.07	0.7
22 phenylethyl phenyl sulfoxide									
RP MeOH	5.20	1	0	7.20	1	0	3.90	1	0
RP ACN	1.44	1	0	4.20	1.06	0.7	3.95	1	0
PO MeOH	0.05	1	0	0.14	1	0	0.26	1.26	1.0
PO ACN	0.62	1.10	0.5	0.67	1	0	1.33	1	0
NP hex-EtOH	2.40	1.09	1.3	3.48	1	0	7.05	1.26	1.8
NP hex-IPA	4.66	1.12	1.4	9.54	1.17	0.7	3.92	1.47	1.3
NP MTBE-ACN	2.90	1.18	1.7	2.93	1.10	0.9	34.5	1	0
26 p-chlorophenyl benzyl sulfoxide									
RP MeOH	2.06	1.80	8	4.64	1.05	0.8	4.20	1	0
RP ACN	1.15	1.25	1.8	4.64	1.05	0.7	4.62	1	0
PO MeOH	0.05	3.10	1.5	0.06	1	0	0.37	1	0
NP hex-EtOH	1.17	1.16	1.2	2.57	1.09	1.0	1.36	1.16	1.2
NP hex-IPA	1.13	1	0	2.65	1.17	0.7	6.38	1.29	1.0
NP MTBE-ACN	2.33	1	0	2.10	1.06	0.3	4.90	1	0
28 β-naphthalenyl benzyl sulfoxide									
RP MeOH	7.40	1.45	4	11.5	1	0	7.00	1.11	1.25
RP ACN	1.69	1.29	2.2	8.92	1.05	0.5	7.60	1	0
PO MeOH	0.06	1.50	0.6	0.11	1	0	0.52	1.07	0.3
NP hex-EtOH	1.51	1	0	3.20	1.08	1.3	2.80	1.22	2.2
NP hex-IPA	3.44	1	0	3.47	1.38	0.8	6.00	1.33	1.1
NP MTBE-ACN	7.00	1	0	2.83	1.06	0.4	7.70	1.04	0.2
29 1,1-dimethyl 3-phenylpropyl phenyl sulfoxide									
RP MeOH	5.00	1.15	1.5	6.67	1.42	1.4	3.90	1.19	1.6
RP ACN	1.42	1.13	1.4	6.25	1.20	1.7	5.64	1	0
PO MeOH	0.00	1	0	0.02	1	0	0.14	1.50	1.1
PO ACN	0.55	1.27	1.5	0.63	1	0	0.67	1	0
NP hex-EtOH	0.55	1.27	1.0	1.20	1.64	4.3	0.85	1.57	2.4
NP hex-IPA	0.39	1.33	1.2	1.40	3.96	4.6	3.55	1.95	2.1
NP MTBE-ACN	3.40	1.47	4.7	1.67	1.16	0.9	3.50	1.20	1
31 diphenylmethyl phenyl sulfoxide									
RP MeOH	5.00	1.27	2.7	8.53	1.15	1.1	5.26	1.10	0.8
RP ACN	1.36	1.24	1.5	8.00	1.16	1.3	6.90	1.05	0.6
PO ACN	0.32	1.28	1.5	0.29	1	0	0.67	1	0
NP hex-EtOH	0.79	1.25	1.6	1.93	1.05	0.7	1.26	1.06	0.6
NP hex-IPA	0.52	1.56	1.6	2.85	1	0	6.38	1	0
NP MTBE-ACN	1.27	2.00	6.4	1.30	1.41	3.2	3.70	1	0

RP = reversed phase, PO = polar organic mode, NP = normal phase; k_1 = retention factor of the first eluting enantiomer, alpha = enantioselectivity factor, Rs = enantioresolution factor. Average values from triplicate analyzes, standard deviation below 0.08. A missing mobile phase line means that no separations were obtained on any CSPs.

Table 3

Observable enantioseparations sorted by stationary phase type and mobile phase composition.

	compounds separated		separation ($\alpha > 1.02$)		baseline separation (Rs ≥1.5)	
	number	percentage	number	percentage[a]	number	percentage[b]
STATIONARY PHASES						
ristocetin A	29	69%	81	28%	26	32%
teicoplanin	35	83%	142	48%	48	34%
TAG	33	79%	134	46%	71	53%
vancomycin	30	71%	60	24%	3	5%
VAG	27	64%	83	28%	6	7%
MOBILE PHASES						
RP MeOH-buffer	35	83%	92	43%	30	33%
RP ACN-buffer	26	62%	56	27%	6	11%
PO MeOH	28	67%	42	20%	14	33%
PO ACN	13	31%	19	9%	3	16%
NP hex-EtOH	34	81%	97	46%	45	47%
NP hex-IPA	34	81%	87	41%	39	45%
NP MTBE-ACN	31	74%	107	50%	17	16%
NP MTBE-MeOH	29[c]	69%	50[c]	59%[c]	11	22%
total	39	93%	500	34%	154	31%

RP = reversed phase, PO = polar organic mode, NP = normal phase

a) percentage of observable separations from the total number of analyses done (42 compounds x 7 mobile phases = 294 analyses per stationary phase, and 42 compounds x 5 mobile phases = 210 analyses per mobile phase).

b) percentage of baseline separations obtained from the non optimized separations.

c) results obtained with the 97/3 optimized mobile phase composition but on vancomycin and VAG CSPs only (84 analyses instead of 210).

Table 4

Enantioselectivity factor for phenyl and toluyl sulfoxide chiral compounds

CSP		teicoplanin		TAG	
compound number	R susbtituent	Hex/IPA 90/10 v/v	MeOH/buffer 20/80 v/v	Hex/IPA 90/10 v/v	MeOH/buffer 50/50 v/v
1	CH_3	1.22	1.11	2.02	1.13
4	vinyl	1.44	1.06	1.46	1.19
12	t-Bu	2.50	1.06	1.81	1.20
16	benzyl	1.09	1.00	1.12	1.07
22	$CH_2CH_2\phi$	1.17	1.00	1.47	1.00
23	$CH_2\phi CH_3$	1.00	1.00	1.09	1.07
29	$C(CH_3)_2CH_2CH_2\phi$	4.00	1.42	1.95	1.19
31	$CH(\phi)_2$	1.00	1.15	1.00	1.10
5	CH_3	1.22	1.10	1.65	1.11
21	benzyl	1.00	1.00	1.00	1.08
24	$CH_2CH_2\phi$	1.00	1.02	1.30	1.00
27	$CH_2CH_2CH_2\phi$	1.00	1.00	1.00	1.00
30	$C(CH_3)_2CH_2CH_2\phi$	2.24	1.31	1.33	1.15
35	OCH_3	1.71	1.09	2.00	1.20
36	OCH_2CH_3	1.00	1.00	1.00	1.00
38	$OCH(CH_3)CH_3$	1.00	1.00	1.00	1.00
39	$OCH_2CH_2CH_3$	1.00	1.00	1.00	1.00
40	$OCH_2CH_2CH_2CH_3$	1.00	1.00	1.30	1.00
41	$OCH_2CH(CH_3)CH_3$	1.00	1.00	1.00	1.00
42	$OCH(CH_3)CH_2CH_3$	1.00	1.00	1.00	1.00

Vinyl = $CH{=}CH_2$; t-Bu = $C(CH_3)_3$; benzyl = $CH_2\phi$; ϕ = phenyl ring.

Table 5
Chromatographic results obtained with sulfoxides and the corresponding N-tosylated compounds and sulfinate esters with the teicoplanin CSP.

Mobile phase		Hexane/IPA 90/10 v/v				Methanol/buffer 20/80 v/v			
Number	formula	k_1	k_2	α	Rs	k_1	k_2	α	Rs
1	ϕ-SO-CH_3	19.3	23.6	1.22	4.3	1.27	1.41	1.11	0.5
32	ϕ-SNTs-CH_3	4.60	5.20	1.13	0.7	3.00	3.33	1.11	1.1
16	ϕ-SO-CH_2ϕ	6.30	6.86	1.09	0.6	3.50	3.50	1.00	0.0
33	ϕ-SNTs-CH_2ϕ	4.73	5.44	1.15	0.7	9.83	11.1	1.13	1.1
22	ϕ-SO-CH_2CH_2ϕ	9.54	11.2	1.17	0.7	7.21	7.21	1.00	0.0
34	ϕ-SNTs-CH_2CH_2ϕ	17.8[a]	17.8[a]	1.00	0.0	13.4	14.6	1.09	1.0
35	CH_3-ϕ-SO-O-CH_3	0.47	0.80	1.71	1.5	0.20	0.22	1.09	1.1
36	CH_3-ϕ-SO-O-CH_2CH_3	0.27	0.27	1.00	0.0	3.17	3.17	1.00	0.0

a) experiments done with a 80/20 v/v hexane/IPA normal mobile phase
ϕ = phenyl ring; NTs = N-SO_2-ϕ-CH_3
Column Chirobiotic T, 25 cm, 4.6 mm i.d., 5 μm silica particle size.

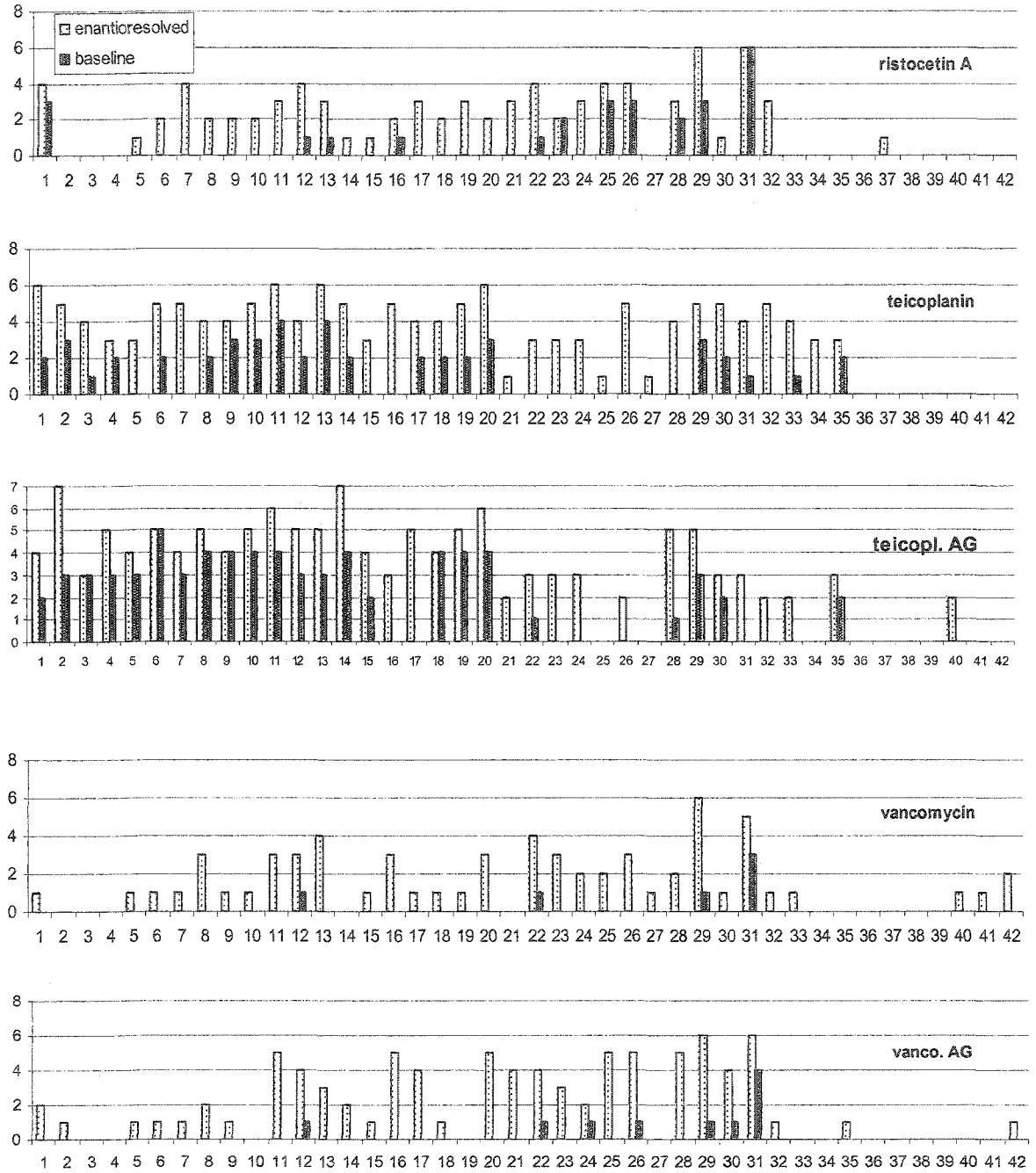

Figure 1: Overview of the results arranged per solute and per CSP. The length of the bars indicates how many mobile phases were capable to produce observable separation of the enantiomers of the solute. White bars: number of observable enantioselective separations (α > 1.02); dark bars: number of baseline separations (Rs > 1.5).

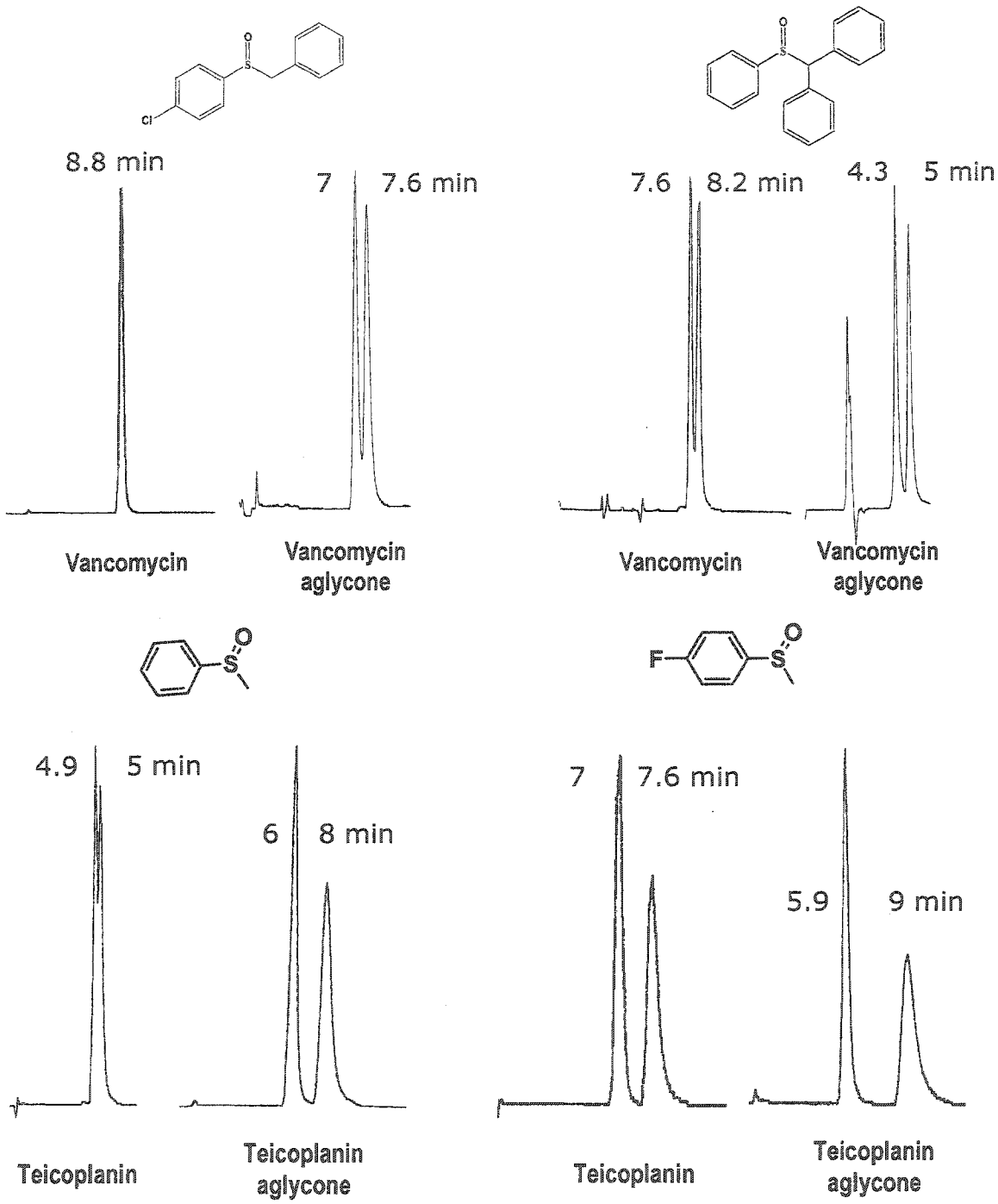

Figure 2. Effect of the macrocyclic glycopeptide sugar units on compound enantioselectivity Top: Vancomycin and Compounds **26** (left) and Compounds **31** (right). Mobile phase: MTBE/ACN 90/10 v/v, 1 mL/min. Bottom: Teicoplanin and Compounds **1** (left) and Compounds **8** (right). Mobile phase: hex/EtOH, 50/50 v/v 2 mL/min.

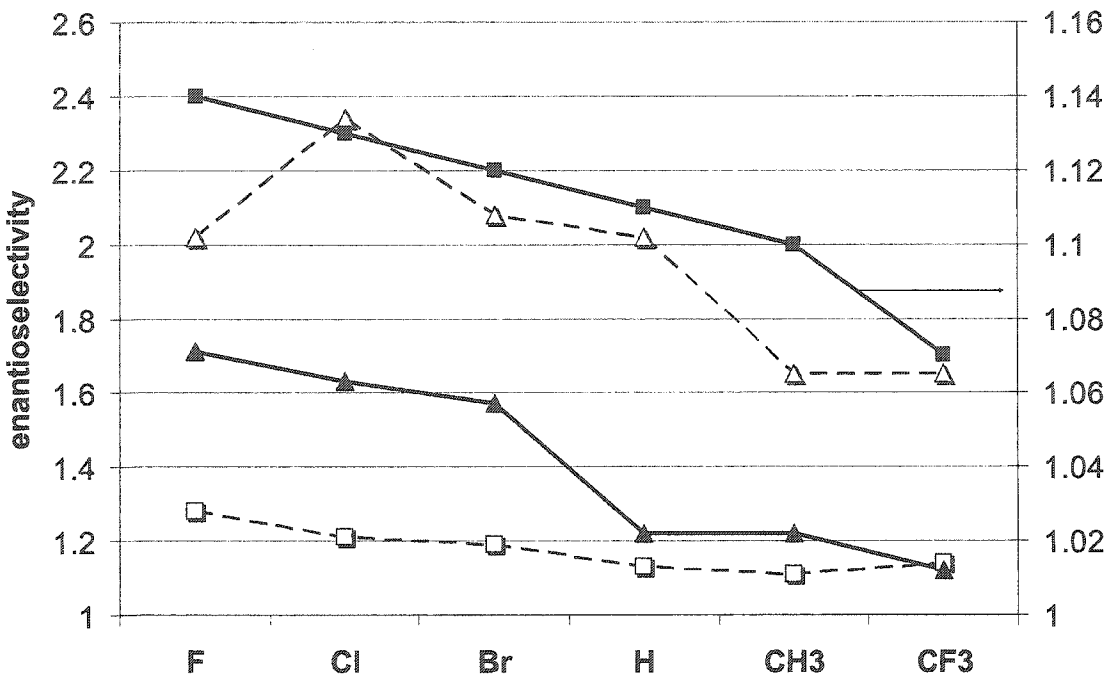

Figure 3. Effect of the substituents of the para substituted phenyl methyl sulfoxides on the compounds enantioselectivity. Thick lines: teicoplanin CSP, dotted lines: TAG CSP; squares: methanol/buffer(20/80 v/v) reversed mobile phase, triangles: *n*-hexane/IPA (90/10 v/v) normal mobile phase.

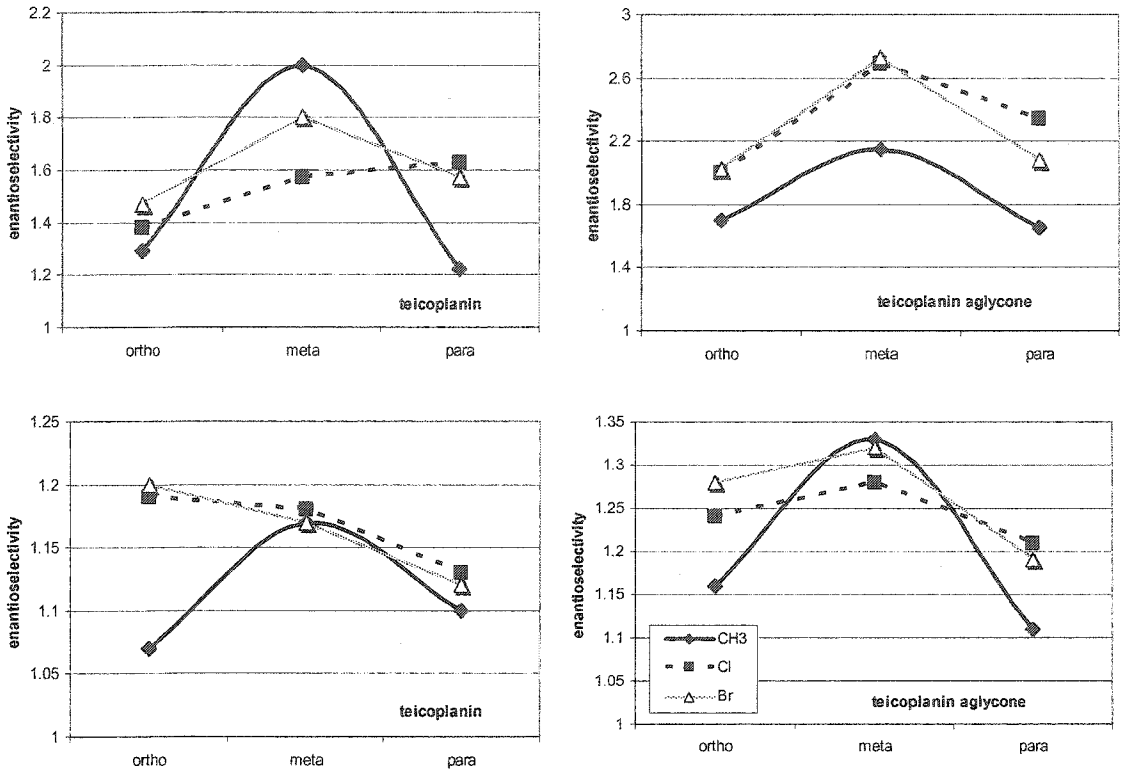

Figure 4. Structural effect of the phenyl substituents of the ortho, meta or para substituted phenyl methyl sulfoxides on the compounds enantioselectivity. Top figures: *n*-hexane/IPA (90/10 v/v) normal mobile phase; bottom figures: methanol-buffer (20/80 v/v) reversed mobile phase.

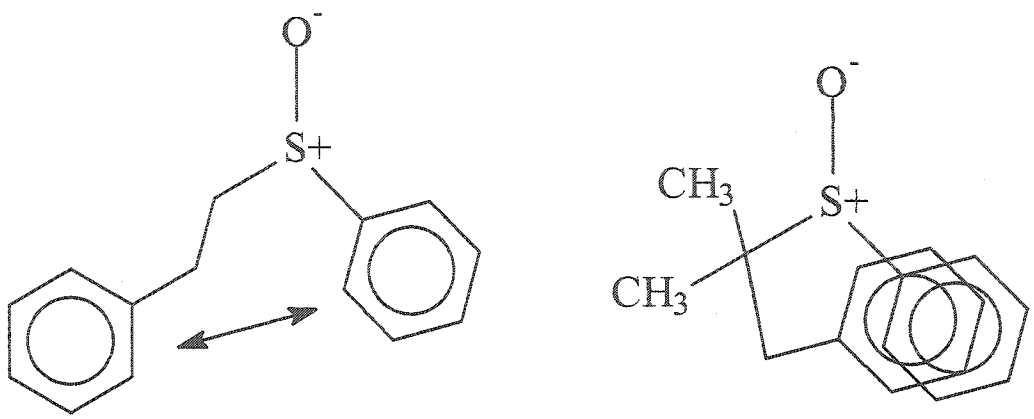

possible π-π stacking **π-π stacking favored by two methyl groups**

Figure 5. Left: Possible intramolecular stacking by π-π interactions. Right: the stacking is favored by the two methyl groups in α position of the sulfur atom.

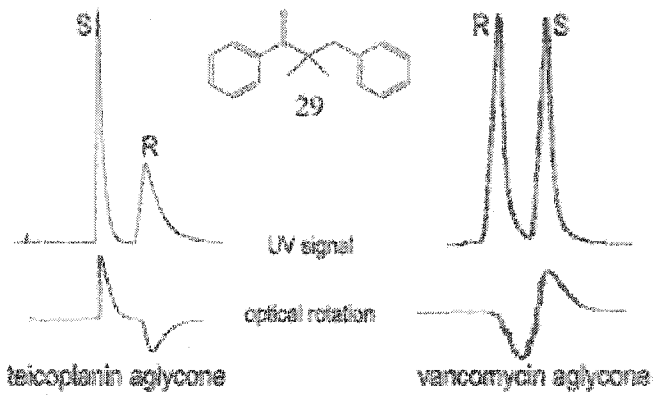

Figure 6. Illustration of the enantiomeric retention order reversal. Left: Compound **29** separated with the TAG column, the (*S*)-(+)-enantiomer elutes first, normal mobile phase (*n*-hexane/EtOH 50/50 v/v); right: on the VAG column, the (R)-(-) enantiomer elutes first, normal mobile phase (MTBE/ACN 90/10 v/v).

CHAPTER 3

ENANTIOMERIC SEPARATION OF SUBSTITUTED DIHYDROFUROCOUMARIN COMPOUNDS BY HPLC USING MACROCYCLIC GLYCOPEPTIDE CHIRAL STATIONARY PHASES

A paper published in Analytical and Bioanalytical Chemistry[1]

Tom Ling Xiao, Roman V. Rozhkov, Richard C. Larock and Daniel W. Armstrong

ABSTRACT

Enantiomeric separations by HPLC using the macrocyclic glycopeptides, teicoplanin (Chirobiotic T), teicoplanin aglycon (Chirobiotic TAG) and ristocetin A (Chirobiotic R), chiral stationary phases (CSPs) were achieved on a unique series of biologically active racemic analogues of dihydrofurocoumarin. The macrocyclic glycopeptides proved to be exceptionally selective for this class of compounds. All of the 28 chiral analogues were baseline separated on at least one of the macrocyclic glycopeptide CSPs. The teicoplanin CSP showed the broadest enantioselectivity with 24 of the compounds baseline separated. The TAG and the R CSPs produced 23 and 14 baseline separations respectively. All three mobile phase modes, i.e., normal phase (NP), reversed phase (RP), and new polar organic modes (PO), were evaluated. The NP mode proved to be most effective for the separation of chiral dihydrofurocoumarins on all CSPs tested. In the reversed phase (RP) mode, all three

---

[1] Reprinted with permission from Analytical and Bioanalytical Chemistry, 955 (2002) 53–69.
Copyright © Springer-Verlag 2003. All rights reserved.
CSPs separated a similar number of compounds. It was observed that the structural

characteristics of the analytes and steric effects are very important factors leading to chiral recognition. Hydrogen bonding was found to play a secondary role in chiral discrimination in the normal phase and polar organic modes. Hydrophobic interactions are important for chiral separation in the reversed phase mode. When coupled with circular dichroism, using the exciton coupling chirality method, the enantiomeric elution order and the absolute configuration of some chiral dihydrofurocoumarins were successfully determined.

3.1. INTRODUCTION

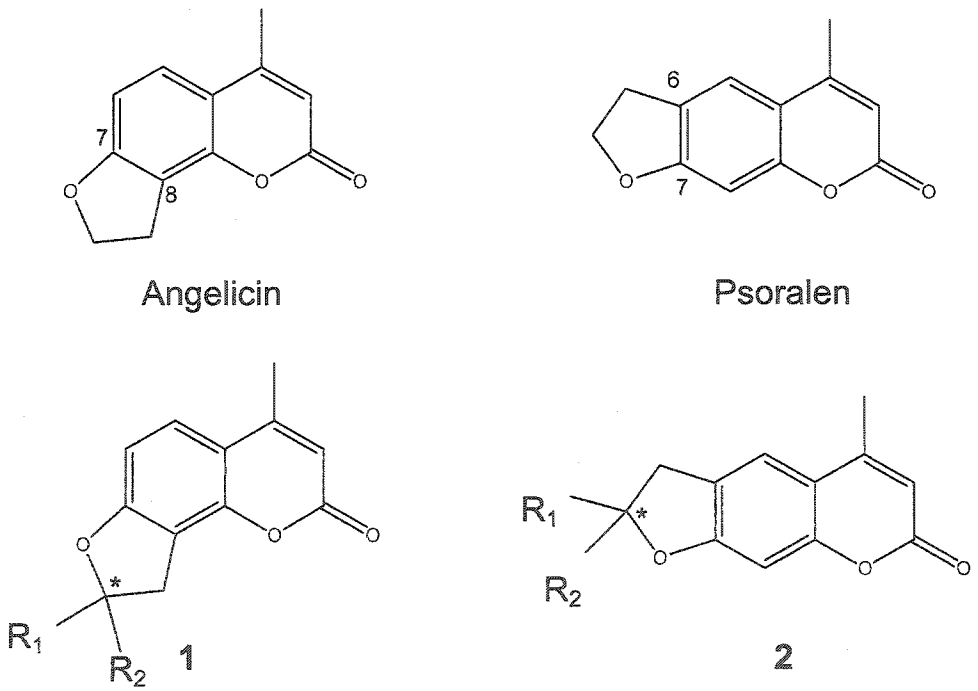

Fig 1.The top two structures are Angelicin and Psoralen, which are often found in nature. Structure **1** is a substituted dihydroangelicin and structure **2** is a substituted dihydropsoralens. R1 and R2 can be various types of aliphatic or aromatic substituents. Note, when R1 ≠R2, the carbon marked with an asterisk is the stereogenic center.

The first historically documented use of dihydrofurocoumarins (Figure 1) was in ancient Egypt, where dihydrofurocoumarin-rich extracts were used for the treatment of skin

disorders such as psoriasis and vitiligo[1-3]. Extensive investigation of this class of compounds started in the late 1970s and a variety of useful medical effects were found[4-6]. Recently, different chiral analogues of dihydrofurocoumarin have been isolated as natural products, and shown to be active against a number of diseases[7]. For example, marmesin and columbionetin derivatives have been shown to exhibit cytotoxicity against KB cells, to inhibit c-AMP (which affects coronary vasodilation) and to mediate the action of acetylcholinesterase (which plays a role in Alzheimer's disease)[4-9]. Dihydrofurocoumarin compounds appear to be nontoxic[4,10-12]. Clearly, the potential pharmaceutical applications of these compounds are promising. However, the pharmacological activity of both enantiomers must be assessed. This means that asymmetric synthesis or enantioselective separations must be used to prepare the pure enantiomers. Methods for the asymmetric synthesis of these compounds are under development, but are proving to be very difficult and of low yield[13].

A recent report used the palladium-catalyzed annulation of 1,3-dienes by *o*-iodoacetoxycoumarins to produced racemic substituted dihydrofurocoumarin (Figure 1) in high yields[14]. Effective methods for separating and identifying these synthetic products as well as the stereoisomers of related natural products are desperately needed.

Macrocyclic glycopeptides are one of the fastest growing classes of chiral selectors. Since the first introduction as CSPs for HPLC , TLC, and run buffer additive for CE in 1994 by Armstrong[15-18], enantiomeric separations of over a thousand different compounds have been reported[19]. The structure of the macrocyclic glycopeptides includes many functional groups, including aromatic, hydroxyl, amine, carboxylic acid moieties, amide linkages, hydrophobic pockets, etc. (Figure 2). A complete description of this family of compounds

was given previously[15,18-23]. All possible molecular interactions, including ionic interaction, hydrogen bonding, steric, dipole-dipole and π-π interactions as well as hydrophobic interactions responsible for chiral recognition, are

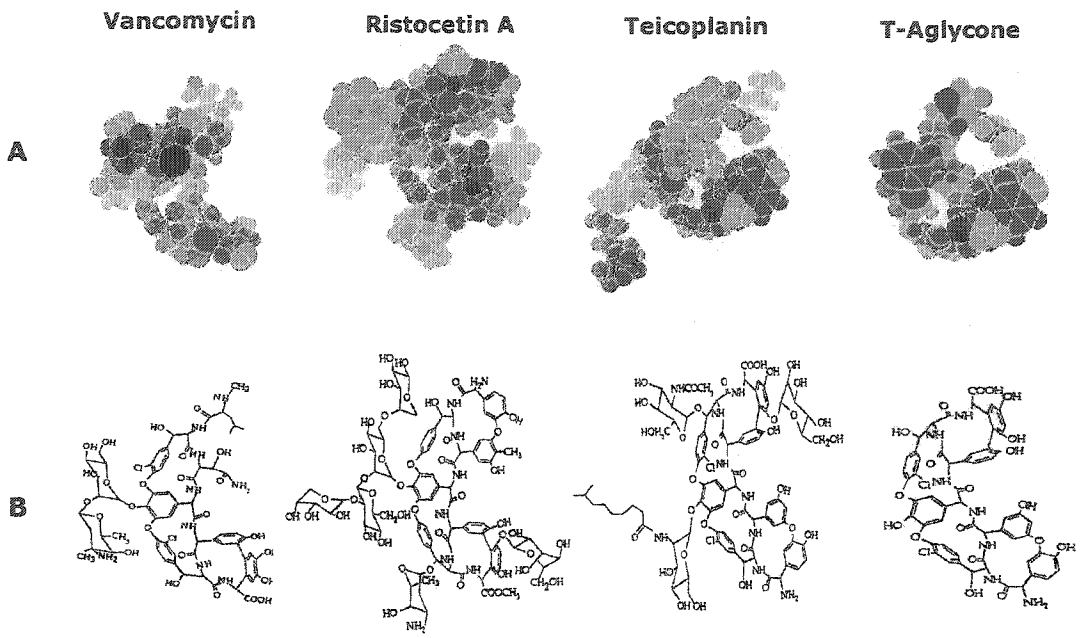

Fig. 2 These are the Structures of the four macrocyclic antibiotics vancomycin, teicoplanin, ristocetin A, and teicoplanin aglycon tested in this study showing a profile view of the aglycon "basket" using (A) space-filling molecular models produced through energy minimization and (B) stick figures. The colored atoms in part A denote the hydrophilic moieties, while the black portion designates the more hydrophobic regions. Red represents carboxylate groups, green are ammonium groups, and blue are hydroxyls. Black regions include the aromatic rings, connecting carbons, and amido linkages. (revised from reference 19)

available within their relatively compact structures. This class of CSPs is multimodal, which means they can be utilized in any of the known mobile phase modes including normal phase, reverse phase and polar organic phase modes[15,17-56]. Two of the most common coumarin-based pharmacologically active compounds are warfarin and coumachlor. Their racemates have been separated by a wide variety of CSPs. However, to our knowledge, no enantioseparation of chiral dihydrofurocoumarin compounds (Figure 1) have been reported on any CSP. In this study, 28 chiral dihydrofurocoumarin derivatives were evaluated. The

first part of this work discusses the overall separation performance using different macrocyclic glycopeptide CSPs and different mobile phase conditions. Subsequently, the effect of analyte structure on the enantioselective separation is discussed. The information gleaned from the separation of structurally related compounds using different mobile phases and closely related CSPs provides some insight into the chiral recognition mechanism for the substituted dihydrofurocoumarins.

3.2. EXPERIMENTAL

3.2.1. Dihydrofurocoumarin derivatives

All the racemic dihydrofurocoumarin derivatives were synthesized and purified as previously reported[14]. The structures of the 28 chiral coumarin derivatives used in this study are given in Figure 3.

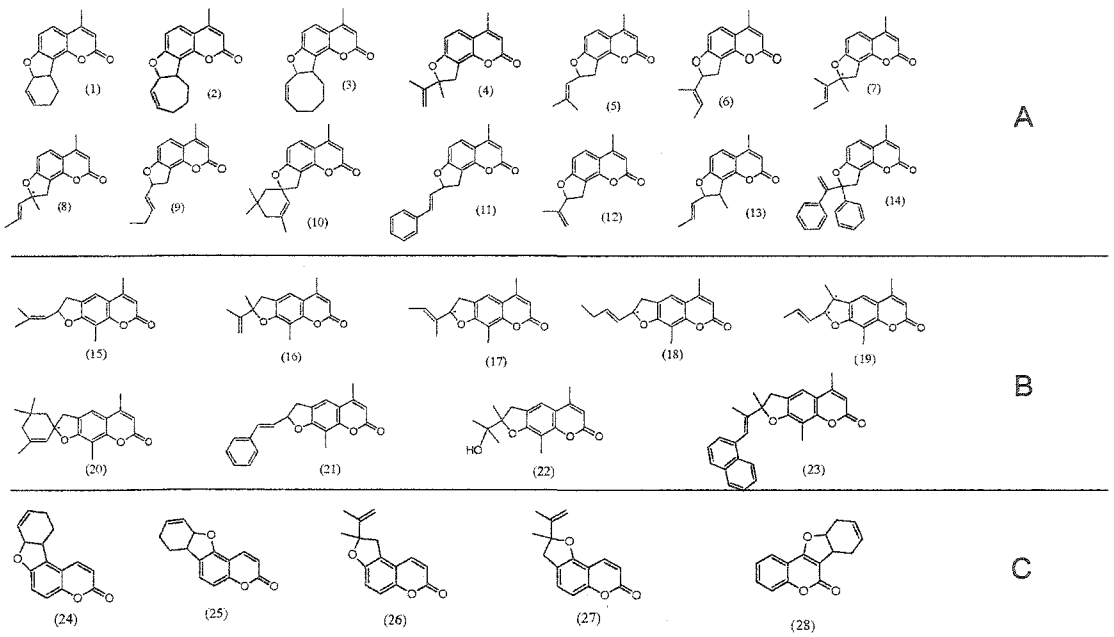

Fig. 3 Structures of the chiral furocoumarin derivatives tested in this study. Compounds listed in group **A** are 14 dihydroangelicins, group **B** are 9 dihydropsoralens, and group **C** are 5 related different dihydrofurocoumarin derivatives.

The dihydrofurocoumarins shown in Figure 3 can be divided into three structural categories. The compounds in the first group are dihydroangelicin derivatives. The furan ring is fused to the 7, 8 position of the coumarin giving these molecules a "bent" appearance. The second group (Figures 1 and 3) is referred to as dihydropsoralens. The furan ring in these

compounds is fused to the 6, 7 position of the coumarin giving these molecules a linear orientation. The last group of compounds has the furan ring fused to the 5 and 6 positions or 3 and 4 positions (Figure 3). All 28 dihydrofurocoumarins have stereogenic centers located in the furan ring. Note that both compounds **13** and **19** have two stererogenic centers (Figure 3). Separations of two pairs of enantiomers were both achieved in these cases.

3.2.2. Other chemicals

HPLC-grade acetonitrile (ACN), methanol (MeOH), 2-propanol (IPA), n-hexane (Hex) and were purchased from Fisher (St. Louis, MO, USA) and/or EM (Gibbstown, NJ, USA). Ethanol (EtOH), 200 proof, was purchased from AAPER Alcohol and Chemical CO. (Shelbyville, KY, USA). Water was deionized and filtered through active charcoal and a 5 μm filter. Triethylamine (TEA) and acetic acid (AA) were from Sigma (St. Louis, MO, USA).

3.2.3. HPLC system and the chiral stationary phases

Separations were achieved on a HP 1050 HPLC system with UV detector, auto injector, using a computer controlled Chem-station data processing software. All three CSPs, trade named Chirobiotic T, Chirobiotic TAG, and Chirobiotic R columns (250×4.6 mm I.D.) were obtained from Advanced Separation Technologies, Inc. (Astec), Whippany, NJ, USA. The detailed structures of the chiral selectors used in these CSPs are shown in Fig 2. The chiral stationary phases were prepared by bonding the chiral selectors to a 5 μm spherical porous silica gel through a linkage chain[15,53]. All separations were repeated at least three times with very good reproducibility. Detection wavelengths were varied between 220nm and 327 nm, which correspond to the two molecular absorption maxima of the dihydrofurocoumarins. The injection volume was 2 μl. Separations were carried out under

isocratically at a flow rate of 1 mL/min or 0.5mL/min at room temperature. The mobile phase was premixed and degassed under vacuum condition.

3.2.4. Mobile phase compositions

Three different mobile phase modes (i.e., normal phase, reversed phase and new polar organic modes) were used and compared. In the normal phase mode, n-hexane was used as the non-polar solvent and the polar organic modifier was ethanol, which proved to give better resolution than using isopropanol as the modifier. In the reversed phase mode, a mixture of pure deionized water and methanol was used throughout the study. Aqueous buffer solutions of 1% triethylamine (TEA, 0,07M), with pH value 4.1 adjusted by acetic acid, was tried but did not produce any significant difference in the separation. Reversed phase separations using acetonitrile as the modifier were compared to the separations achieved using methanol as the modifier. It was found that using methanol as modifier gave much better selectivity and resolution. In the polar organic mode, 100% pure methanol and acetonitrile was used and compared. Addition with some acid (acetic acid) and base (TEA) at various ratios to the mobile phase was tried but did not produce any improvements in the separations. All the reported mobile phase compositions used are not necessarily the optimum conditions for the enantiomeric separations, instead, are mobile phase compositions being adjusted to achieve a reasonable elution time and selectivity. In this way, direct comparison in the separation of this family of compounds can be made. Optimized separations for individual compounds can be done easily if the need arises.

3.2.5. Calculations of the chromatographic parameters

The dead volume (t_0 × flow rate) was estimated using the change in refractive index caused by different composition of the injection solvent. All other related parameters.

Retention factor (k'_1) was calculated using the equation $k'_1 = (t_{r1} - t_0)/t_0$, where t_{r1} is the corresponding retention time for the first eluted enantiomer. The enantioselectivity factor (α) was calculated using $\alpha = k'_2/k'_1$, where k'_2 is the retention factor for the second eluted enantiomer. The resolution factor (R_s) was calculated using the equation $R_s=2 \times (t_{r2} - t_{r1}) / (w_1 + w_2)$ where t_{r2} and t_{r1} are the retention times of the second and first eluted enantiomers and w_1 and w_2 are the corresponding base peak widths. The efficiency or number of theoretical plates (n) was calculated using the equation $n=16(t_r/w)^2$.

3.3. RESULTS AND DISCUSSION

3.1. Comparison of the performance of the three CSPs

See Table 1 at the end of this paper and Figure 4 listed below.

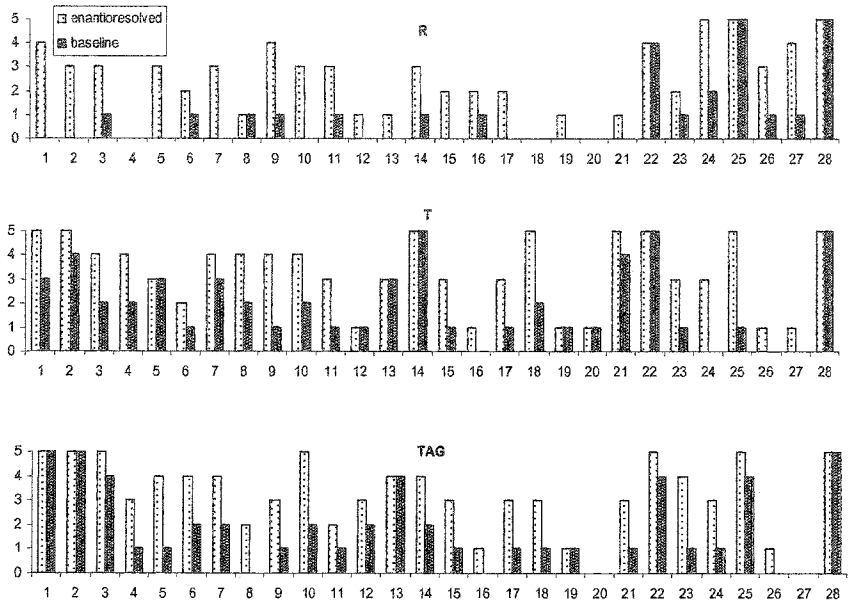

Figure 4. This is the summary of separations for individual compounds on different CSPs. The Y axis stands for the number of separations achieved using the five different mobile phase modes listed in Table 1. The X-axis stands for the compound sequence number assigned corresponding to Table 1and Figure 3. The light bar stands for the number of mobile phase modes that resolved (α>1.01) the corresponding compound. The black bar stands for the number of baseline separation (Rs ≥1.5) achieved.

Table 1 and Figure 4 summarize the overall number of observable ($\alpha \geq 1.02$) and baseline (Rs ≥ 1.5) enantiomeric separations obtained on each CSPs with the five mobile phases tested. In Figure 4, the white bar stands for the number of observable enantioseparations and the black bar stands for the number of baseline enantioseparations. As can be seen from Figure 4, the Chirobiotic T and TAG CSPs appears to be the most broadly useful for separating enantiomers of dihydrofurocoumarin-based compounds. The teicoplanin CSP resolved enantiomers of the entire set of 28 compounds with 24 of them being baseline separated. The teicoplanin aglycon CSP resolved the enantiomers of 26 compounds with 23 of them baseline. These two closely related CSPs showed similar selectivities for most of the compounds, however, there are some slight differences. Dihydropsoralens, which have a

"straight shape structure" (Figure 3) tend to be better resolved on the teicoplanin based CSP (Table 1). This indicates the importance of the sugar units on teicoplanin in the chiral discrimination of these compounds. The teicoplanin aglycon (TAG) CSP showed better selectivities for dihydroangelicins and other "bent-shaped" molecules (Table 1) using the same mobile phase conditions. This in turn implies that the steric effect of the bulky sugar units on the teicoplanin CSP decreases chiral recognition for some of these compounds. This effect was discussed in a previous paper[53]. Neither the Chirobiotic T nor the TAG CSPs could baseline resolve compounds **16**, **26** and **27** (Table 1, Figure 3). However, all of these compounds were baseline separated on the ristocetin A CSP (i.e., Chirobiotic R), which baseline separated 14 out of the 28 compounds. The ristocetin A CSP shows extremely good selectivity toward most of the third group of compounds (Figure 3), some of which (compounds **26** and **27**) did not separate very well on either the teicoplanin or teicoplanin aglycon CSPs. Compounds that could not be separated on the Chirobiotic R column were all baseline resolved on either or both the T and TAG columns. This demonstrates the complementary nature of these CSPs which was demonstrated in previous studies [29]. The principle of complementary separation says that if a partial enantiomeric separation is obtained with one glycopeptide based CSP, there is a strong probability that a baseline or better separation can be obtained with a related macrocyclic glycopeptide CSP using the same or similar mobile phase conditions. This allows for improved resolution by simply switching to a related Chirobiotic column. Figure 5 illustrates the complementary nature of the Chirobiotic TAG and R columns for the separation of compounds **1** and **22**. As can be seen, compound **22** was not baseline separated on the Chirobiotic TAG column in the RP mode, but was well separated on the related Chirobiotic R column in the same mobile phase

condition. Conversely, compound 1 was well separated with the Chirobiotic TAG column in the NP mode, but not with the Chirobiotic R column.

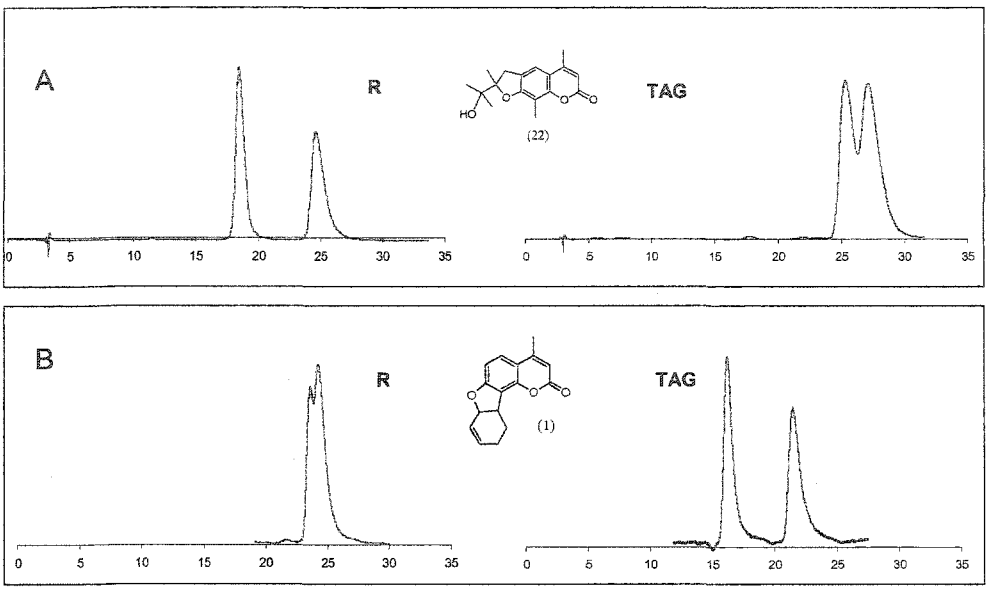

Figure 5. This figure shows the complementary nature. Figure A shows the separation of compound 22 using the Chirobiotic R versus Chirobiotic TAG in reversed phase mode(H2O: MeOH/60:40, 1ml/min). Figure B shows comparison of the separation for compound 1 using the same two columns in normal phase mode(Hexane:EtOH/95/5, 1 ml/min). It is obvious that the two columns complementary to each other for the separation of these two compounds.

3.2. Effects of mobile phase modes

It is well known that CSPs based on macrocyclic glycopeptides are multimodal, which means they can be used in any mobile phase mode and can achieve different separations in each mode[15,56]. This can be very advantageous since the chiral recognition mechanisms in different separation modes are different and this allows the CSP to separate a greater variety of chiral analytes. Compounds that do not separate in one chromatographic mode are often easily separated in another mode on the same CSP. Fig 6 summarizes the number of baseline separations achieved on the three CSPs in different mobile phase modes,

i.e., the normal phase mode (NP), reversed phase mode (RP) and polar organic mode (PO). Clearly the normal phase mode with hexane/ethanol is the most effective approach for separating substituted dihydrofurocoumarins when using teicoplanin and teicoplanin aglycon CSPs. The teicoplanin (T) and teicoplanin aglycon (TAG) CSPs baseline separated 23 and 21 compounds respectively using this single mobile phase. Teicoplanin (T) is the most effective chiral selector with all mobile phases except 100% methanol. The ristocetin A CSP was less effective for the chiral dihydrofurocoumarins regardless of the mobile phase conditions. In the reversed phase mode (RP), all three CSPs were less effective but they separated similar numbers of compounds. In the polar organic mode (PO), however, both the teicoplanin and teicoplanin aglycon again showed much better selectivity compared to the ristocetin A CSP (Figure 6).

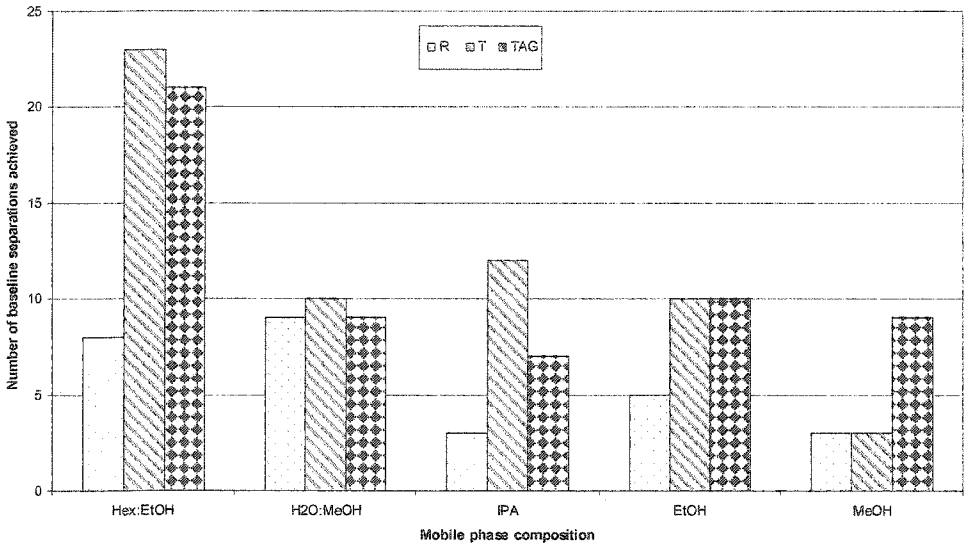

Fig. 6 This bar figure summarizes the number of baseline separations (after optimization) achieved using different mobile phase modes(i.e. NP, RP, and PO modes) on Chirobiotic R (R), Chirobiotic T (T) and Chirobiotic TAG (TAG) columns.

3.2.1 Normal phase mode separation

More and better enantioseparations of the dihydrofurocoumarins were achieved in the normal phase mode than in other chromatographic modes. In the normal phase mode, the CSP behaves as a polar stationary phase. The strongly polar functional groups and aromatic rings of the CSP provide the interactions needed for both retention and chiral recognition. In normal phase HPLC, retention is controlled by adjusting the percentage of a polar organic modifier such as ethanol or propanol.

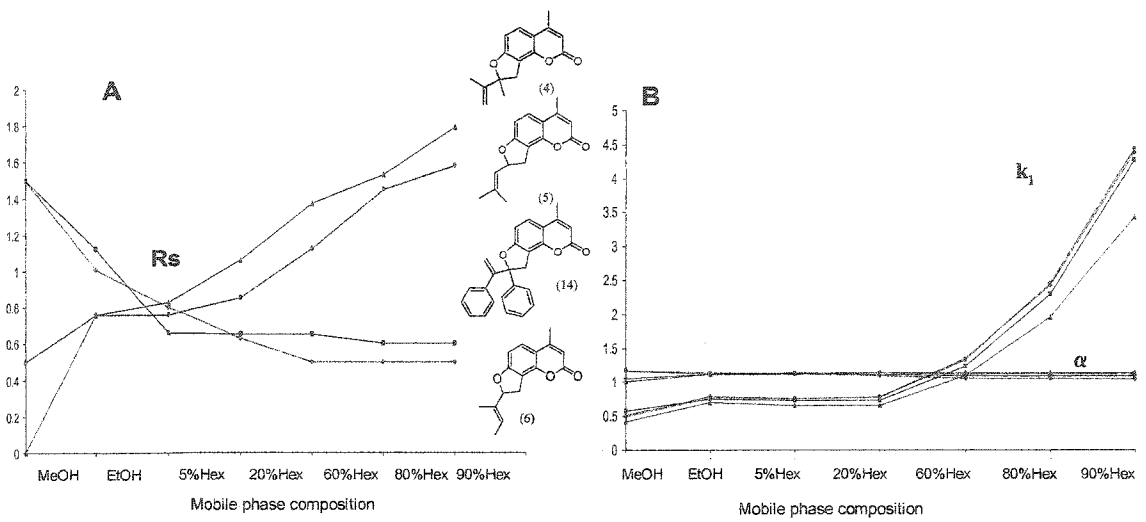

Fig. 7 Effect of Mobile Phase Modifier on retention, selectivity and resolution factors
Figure A shows the resolution factor changes with the mobile phase becomes less polar. Y axis is in the unit of resolution factor and X axis is the discrete mobile phase composition. Figure B shows the selectivity factor and resolution factor changes with the mobile phase composition changes. It can be seen in Figure A that compounds **4** and **5** shows different trend compare to compounds **6** and **14** when the mobile phase becomes less polar.

Figure 7 shows the effect of added organic modifier on the retention, selectivity, as well as the resolution factors for selected compounds in the normal phase mode on the TAG CSP. In Figure 7A and 7B, the x-axis represents the mobile phase compositions starting with the most polar solvent (100% methanol) and extending to the most nonpolar solvent mixture (i.e. 90% hexane + 10% ethanol by volume). The Y axis in Figure 7(A) represents resolution factor Rs, and that in Figure 7(B) represents retention factor, k_1', and enantioselectivity factor, α, for compounds **4**, **5**, **6**, and **14**. The TAG CSP showed a very typical normal phase behavior. When the mobile phase becomes less polar, the retention increases, however, the selectivity factor stays almost constant (Figure 7(B)). Nevertheless, increasing the retention does not necessarily increase the enantiomeric resolution. As can be seen from Figure 7(A), improved

resolutions were achieved for compounds **4** and **5** by simply decreasing the polarity of the mobile phase. Most of the compounds in Table 1 behaved in this way. In contrast, some of the dihydrofurocoumarin compounds (such as compounds **6** and **14**) behaved in just the opposite way (Figure 7(A)).

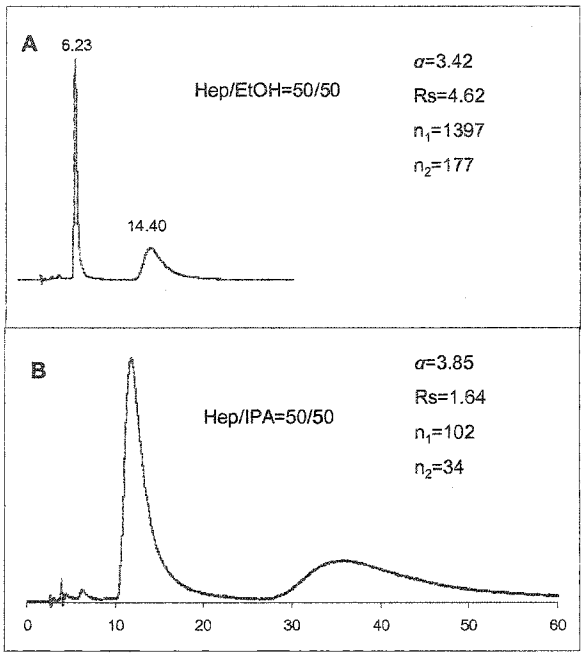

Fig. 8. Comparison of separations of compound **22** using ethanol and isopropanol as modifiers in the NP mode on Chirobiotic R Column. Figure A was obtained using heptane/ethanol=50/50, Figure B was obtained using heptane/isopropanol=50/50(v/v). Both use flow rate at 1ml/min.

Ethanol was selected as the organic modifier of choice since it produced improved enantioresolutions for the entire set of compounds in the normal phase mode. Figure 8 is a comparison of separations of compound **22** using ethanol and isopropanol (50% in heptane by volume) as modifiers on the ristocetin A CSP. As can be seen from these two chromatograms, the selectivity factors are very similar (3.42 and 3.85 using ethanol and isopropanol respectively), but the resolution factors are much different (4.62 and 1.64

respectively). The efficiency (n, number of theoretical plates) for peak 1 are 1397 and 102 using ethanol versus isopropanol, respectively. Using ethanol as the organic modifier improved the separation efficiency of all compounds separated. For convenience, Table 2 lists all the related solvent properties. As can be seen from Table 2, the biggest difference in properties between ethanol and isopropanol is viscosity. Isopropanol is about twice as viscous as ethanol. Viscosity contributes to the band broadening by two mass transfer terms found in the van Deemter equation, one is the mobile phase mass transfer term, and the other is the stagnant mobile phase mass transfer term. However, poor stationary phase mass transfer may be the most important factor affecting band broadening when using isopropanol versus ethanol as modifiers in the normal phase mode. Ethanol more effectively competes with the analyte for strong adsorption sites on the CSP. It also has a greater elutropic strength in the normal phase mode than does propanol. This accounts for the shorter retention times obtained for all of these analytes when ethanol is used as a modifier.

The Ristocetin A CSP is extremely selective for the compounds of the third group in Figure 3 (miscellaneous dihydrofurocoumarins) in the normal phase mode. Additionally, compound **22**, a dihydropsoralen, is well separated by the R CSP. Few other baseline separations were observed on this CSP in the NP mode.

Table 2.

solvents	Boiling point	Dipole moment	Dielectric constant	Viscosity (cP at 20°C)	Polarity index (Snyder)	Hydrogen bonding([a])
Water	100.0	1.85	78.54	1.00	10.2 (9)	2D + 2A
Methanol	64.7	1.7	32.70	0.6	5.1 (6.6)	1D + 2A
Ethanol	78.3	1.69	24.55	1.2	(5.2)	1D + 2A
Isopropanol	82.26	1.66	19.92	2.4	3.9 (4.3)	1D + 2A
Acetonitrile	81.6	3.92	37.50	0.37	5.8 (6.2)	1D
n-Hexane	68.7	0	1.89	0.31	0.1 (0)	-
n-Heptane	98.4	0	0.0	0.4	0.1	-

Data were obtained from

1) LC-GC INT. vol. 8, No. 4, page 190-195, April 1995, by Cynthia Seaver and James Przybytek. "LC troubleshooting, solvent section, Part II-Physical properties.
2) "Burdick & Jackson Solvent Guide; Third Edition." Burdick & Jackson (Muskegon, Michigan, USA. 1990.
3) Eastman Organic Chemical Bulletin, vol. 47, No. 1, 1975 by R. L. Schneider. "Physical properties of some organic solvents".

[a] D stands for H-bond donor and A stands for H-bond acceptor

3.2.2 Reversed phase mode applications

The reversed phase mode (RP) is not as effective as the normal phase mode (NP) for the separation of this class of compounds with teicoplanin based CSPs. Interestingly, the ristocetin A CSP separated the great number of compounds in this mode. In fact, the best separation, with a resolution factor of 9.05 for compound **28** was achieved in the reversed phase mode using the Chirobiotic R column. Hydrophobic interactions are believed to be one of the most important intermolecular interactions between this class of CSPs and these analytes in the reversed phase mode [15]. Compounds **11**, **14**, **21** and **23** (with one or more than one aromatic groups attached directly or indirectly to the stereogenic center) are the most hydrophobic compounds in this study. Note the large k_1' of 53 for compound **23** (Table 1) when a mobile phase of 50/50, methanol/water was used. The strong hydrophobic interactions for compounds **11**, **14** and **23** did improve their enantioselectivity. But for

compound **21**, which is a dihydropsoralen, the strong hydrophobic interaction, indicated a large k_1' of 29 on the TAG CSP, but no enantioselectivity was observed for this compound in the reversed phase mode. This means that the hydrophobic interactions between this analyte and the CSP in the reversed phase mode do not contribute to chiral recognition as they do for compounds **11**, **14** and **23**. Clearly, some hydrophobic interactions contribute to nonselective retention, as for compound **21**. If retention is dominated by nonselective hydrophobic interactions between the analytes and the CSP, these dominant interactions reduce the access of the analyte to favorable chiral recognition sites.

While baseline enantiomeric separations occurred more frequently in the NP mode, there are a few cases where a baseline separation of enantiomers was only achieved in the RP mode (compounds **6**, **9**, **11**, and **12**) when using macrocyclic glycopeptide CSPs. This is probably due to steric effects as will be discussed in the following section 3.4.2.

3.2.3 New polar organic mode separations

The new polar-organic mode is a modification of the polar organic mode that was originally developed for chiral separations with cyclodextrin bonded phases[57,58]. Generally, the main solvent component in the new polar-organic mobile phase is an alcohol (e.g., methanol, ethanol, or isopropanol) with a very small amount of acid/base added to affect retention and selectivity. The retention time can also be adjusted by adding acetonitrile. Figure 6 shows that the teicoplanin and teicoplanin aglycon CSPs separated the largest number of dihydrofurocoumarins using this simple mobile phase mode (100% alcohol). The ristocetin A CSP separated fewer of these compounds in the polar organic mode. It was noted that optimization of the mobile phase by adjusting the acid to base ratio did not improve enantioselectivity in the PO mode. This indicates that ionic interactions do

not play a role in the chiral recognition of these neutral molecules in this mode. Instead, dipole-dipole, H-bonding, π-π interactions and steric effects (or some combination thereof) are the main driving forces for chiral recognition.

Note that the selectivity factors for the separations of all dihydrofurocoumarin compounds using MeOH, EtOH and IPA are quite similar (Table 1), while the resolution and retention factors are very different. Narrower and sharper peaks were always obtained for the separations using EtOH or MeOH as mobile phases as compared to IPA. As can be seen from Table 2, this may be caused by the higher viscosity of isopropanol.

When one compares the separations achieved using pure methanol and pure ethanol, an interesting observation was made (Figure 7 and Table 1). When a better separation of enantiomers (enantioresolution factor (Rs) and enantioselectivity factor (α)) was achieved using pure methanol (compared to pure ethanol), it was found that the reversed phase mode was better than the normal phase mode for separating these enantiomers. This is true for compounds **6**, **14**, and **24**. When a better separation of enantiomers was achieved using pure ethanol (compared to methanol), then the normal phase mode was more effective than the reversed phase mode in separating these enantiomers. This is true for most of the remainder compounds. When pure methanol produced results that were approximately equal to those obtained while using pure ethanol, both the NP and the RP modes were found to work well. These observations hold true for the Chirobiotic T and TAG CSPs when analyzing the dihydrofurocoumarin derivatives shown in Fig. 3. This observation may be useful in choosing a mode of separation (the RP or NP mode) for the teicoplanin and teicoplanin aglycon CSPs. Unfortunately, the results from the Chirobiotic R CSP do not follow a discernable trend.

3.3 Role of hydrogen bonding in chiral discrimination

In the polar organic mode, when the pure alcohol mobile phase was mixed with acetonitrile, the number of separations was significantly decreased for the dihydrofurocoumarins. In fact, when using 100% acetonitrile as mobile phase, no separations were achieved on any CSPs for the entire set of analytes even though analyte retention was similar to that found with methanol. One can note from Table 2 that the polarity of acetonitrile is very similar to that of methanol. However, acetonitrile is a dipolar aprotic solvent, while all the alcohols are polar protic solvents. Therefore, the hydrogen bonding acidity (i.e. the ability to donate a H-bond) of acetonitrile is small, while the alcohols are both hydrogen-bond donor and acceptors (Table 2). This taken together with the fact that no separations were observed when using pure acetonitrile as mobile phase, support the contention that the hydrogen bonding between the mobile phase molecules and the analyte or the CSP plays a role in chiral recognition in the polar organic mode.

When the separations of compounds **16** and **22** are compared using the teicoplanin and teicoplanin aglycon CSPs in 100% ethanol, the effect of hydrogen bonding is obvious (Figure 9). With a hydroxyl group attached to the carbon next to the stereogenic center, compound **22** was separated on all CSPs with high selectivity and resolution in any of the pure alcohol mobile phases (Figure 9, Table 1 and Fig 4). However, removing this hydroxyl group produces compound 16, which cannot be separated on any CSP in the PO mode (Figure 9, Table 1 and Fig 4). In the normal phase mode, the separation of compound **22** was much improved compare to compound **16** on all CSPs examined (Table 1, Figure 8). This illustrates the additional benefits of hydrogen bonding between the analyte and the chiral selector for chiral recognition in normal phase mode.

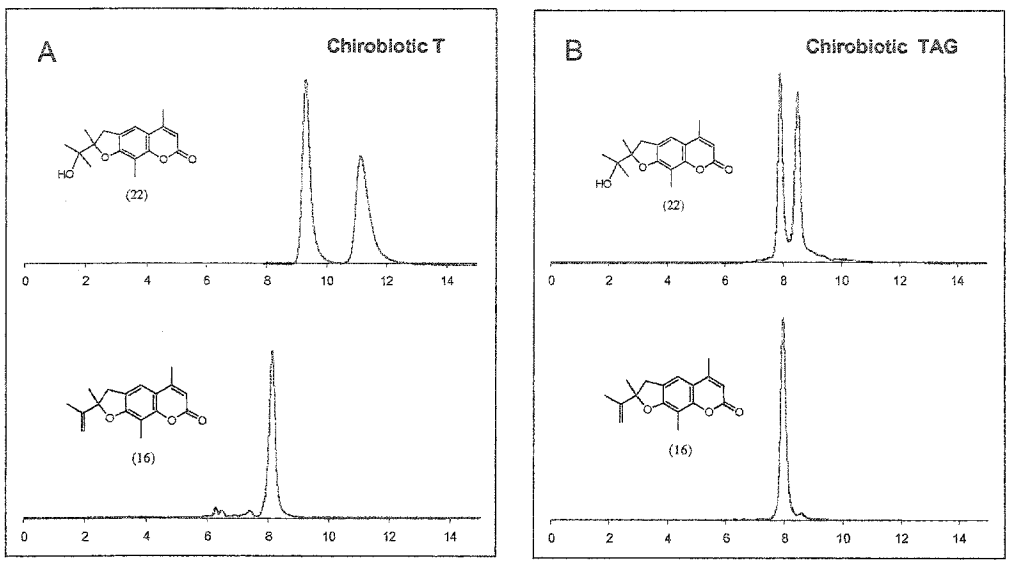

Fig. 9 Effect of hydrogen bonding ability of the analytes on chiral recognition in the polar organic mode
Figure A was obtained on Chirobiotic T column and Figure B was obtained on Chirobiotic TAG column using 100% ethanol, flow rate 1 ml/min.

In the reversed phase mode, however, the hydrogen bonding ability of the aqueous mobile phase is too strong. The hydrogen bonding interaction between the analytes and the CSP is much less pronounced in the reversed phase mode (RP) where the hydrophobic interactions predominate. Separations of compound **22** were greatly diminished on the teicoplanin and teicoplanin aglycon CSPs in the RP mode. This is likely due to the H-bonding sites on the chiral selector being preferentially associated with interactions from the mobile phase molecules. Therefore, one can conclude that hydrogen bonding between the hydroxyl group on the analyte and the hydrogen bonding groups on the CSP in PO mode as well as in NP mode is a one of the key interactions leads to chiral recognition.

The hydrogen bonding groups on the CSPs leading to chiral recognition for the enantioseparation of the dihydrofurocoumarins may be the hydroxyl groups on the rim of the aglycon. In general, teicoplanin and teicoplanin aglycon CSPs show very similar enantioselectivity for separation of chiral dihydrofurocoumarins. Therefore, the aglycon portion of teicoplanin must play the key role in chiral recognition. In addition, when the separations using teicoplanin aglycon (TAG) and methylated TAG (where the hydroxyl groups on the rim of the aglycon have been methylated) was compared in the normal phase and the PO mode, far fewer separations of these analytes were found[59]. This indicates the importance of the hydroxyl groups on the CSPs and it supports the presence of a stereoselective hydrogen bonding interaction (probably with the oxygen of the dihydrofuran ring) in the normal phase and polar organic modes.

3.4 Effects due to the nature of the individual compounds

3.4.1 Geometry of the dihydrofurocoumarins

As discussed in section 3.2, dihydroangelicins, dihydropsoralens, and the third group of analogues (Figure 3) have different enantioselectivities on different CSPs. It was also observed that the orientation of the furan oxygen in relation to the coumarin effects the chiral separation. Fig 10 shows the chromatograms of compounds **1**, **24**, **25** and **28** obtained on the Chirobiotic T and Ristocetin A columns in the RP mode. The only difference for these analytes is the positional substitution of the furan ring on the coumarin body. Note that the only difference between compound **24** and **25** is the opposite location of the ether linkage. It can be seen from the chromatograms that the best separations for the 7, 8 substituted dihydrofurocoumarins (Figure 1) were achieved on the Chirobiotic T and TAG columns (i.e. compound 1), while the other kinds of substituted dihydrofurocoumarins (i.e., 5, 6 substituted

and 6, 7 substituted, Figure 1) were better separated on the Chirobiotic R column (i.e. compounds **24**, **25**, and **28**). Another series of examples, which showed the exact same effects, are compounds **4**, **16**, **26**, and **27** (Table 1, Figure 3).

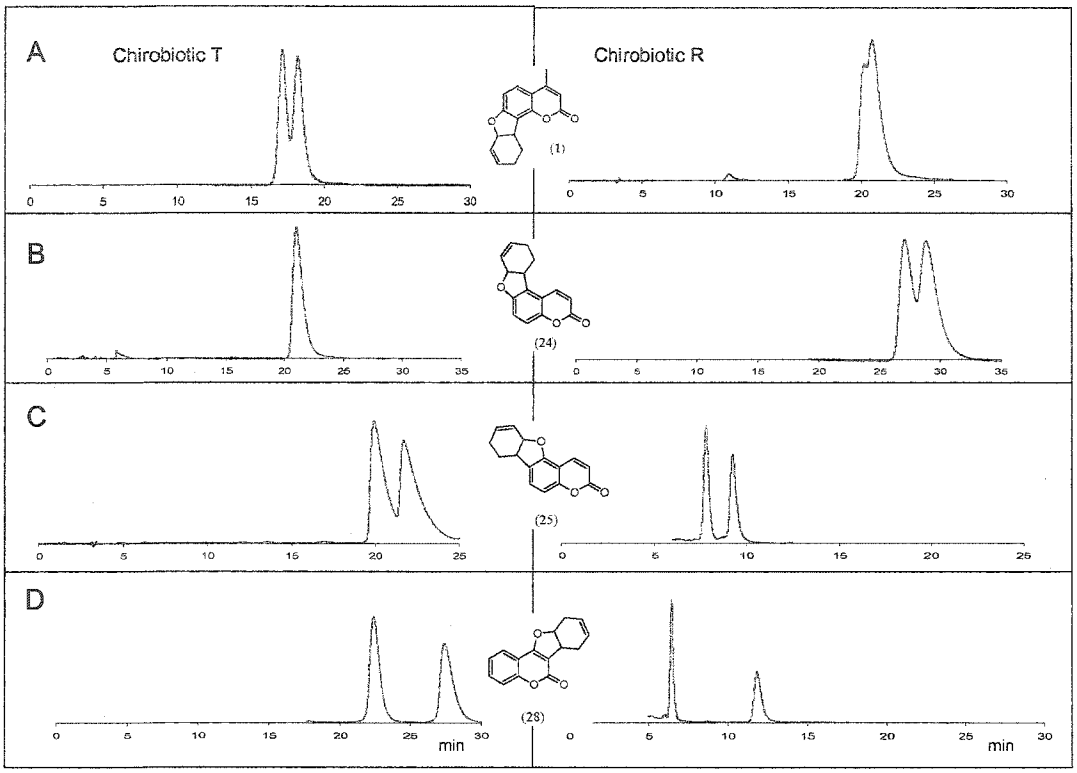

Figure 10. Effects of molecular spacial orientation. Figure A, B, C, and D list the comparison of separations achieved on Chirobiotic T and R columns in RP mode (H2O:MeOH=65:35) for compounds 1, 23, 24, and 27 respectively, 1ml/min.

3.4.2 Steric effects

Steric repulsive effects are important interactions responsible for chiral recognition in any mobile phase mode for this class of compounds. Steric effects in the normal phase mode were found to produce results which were contrary to the trends observed in the reversed phase mode. Steric bulk in positions α or β to the stereogenic center can either enhance or diminish the enantioselectivity.

In the normal phase mode, there are four dihydroangelicins (compounds **6**, **9**, **11**, and **12**) that were not well separated on the teicoplanin and teicoplanin aglycon (TAG) CSPs. They have in common smaller substituents attached to the stereogenic center compared to many of the other dihydroangelicins (compounds **4**, **7**, and **8** for example). Many of the well resolved dihydroangelicins have methyl groups as one of the substituents. However, compounds **6**, **9**, **11**, and **12** have hydrogen atoms instead. Conversely, many of the compounds in the second group of Figure 3 (dihydropsoralens) are better separated into enantiomers when a hydrogen atom is present as one of substituents on the stereogenic center (compounds **15**, **17**, and **18** versus compound **16**). An exception to this is compound **22**, which may interact with the CSP quite differently from the rest of compounds due to the hydroxyl group attached alpha to the stereogenic center.

In the reversed phase mode, compounds **6**, **9**, **11**, and **12** (which have less bulk around the stereogenic center) were all separated better than compounds **4**, **7**, and **8**; which is the opposite trend found in the normal phase mode. This indicates that the steric repulsive interactions between the analyte and the CSP in the reversed phase mode play a negative role in chiral discrimination of dihydroangelicins, while the steric effects play a positive role for the same compounds in the NP mode. Similarly, for dihydropsoralens (in Figure 3), the steric bulk (compound **16**) did improve the enantioselectivity with ristocetin A and teicoplanin aglycon CSPs. Therefore, the steric effects in the RP mode behave in just the opposite way as that seen in the NP mode for the enantiomeric separation of dihydrofurocoumarins.

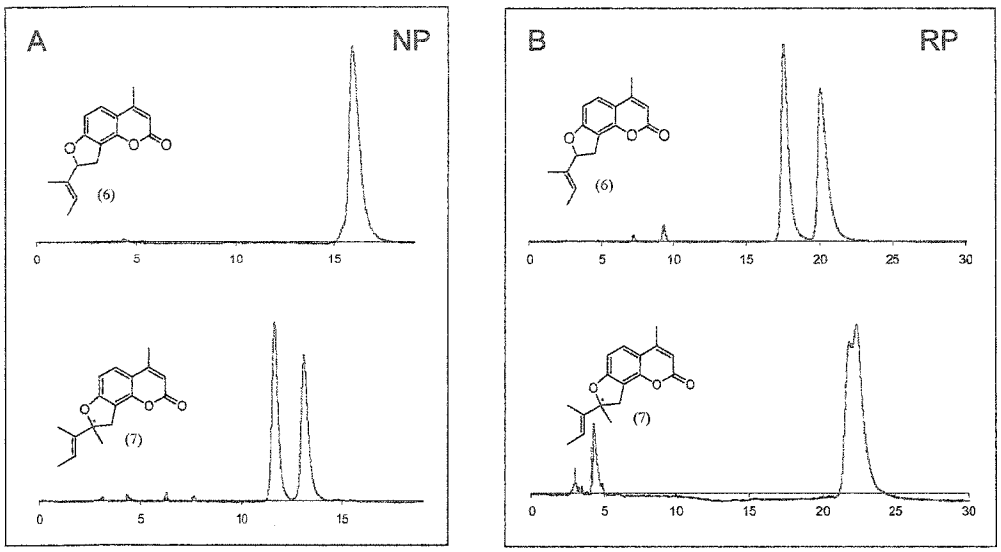

Fig. 11 Comparison of the role of steric effects for enantioseparations on the Chirobiotic T column using the NP versus the RP mode. Figure A is a pair of chromatograms obtained in the NP mode (NP =Hexane: EtOH=95/5), 1ml/min. Figure B is a pair of chromatograms obtained in the RP mode (RP=H_2O:MeOH=60/40), 1ml/min. Clearly, steric effects generate by the extra methyl group of compound **7** in the position alpha to the stereogenic center just play an opposite role in the NP mode versus in the RP.

Fig 11 shows the comparison of the enantioseparations of compounds 6 and 7. The opposite role of steric effects for enantioseparations in the NP mode and the RP mode achieved on the Chirobiotic T column are shown in this figure. The only difference between these two compounds is that compound 7 has an extra methyl group connected directly to the stereogenic center, which greatly enhanced the enantioselectivity in the NP mode. However, in the RP mode, the extra methyl group on compound 7 significantly diminished the enantioselectivity. The exactly same behavior can also be found for another pair of compounds 4 and 12 (Table 1).

3.5 Absolute configuration determination and enantiomeric elution order

Absolute configuration of the separated enantiomers for selected dihydrofurocoumarin derivatives was determined using exciton coupling chirality method[8]. It was shown that, the first eluted peak on the Chirobiotic T column in the NP mode for compounds **4** and **11** had the R configuration. The first eluted peak of compound **8** on the Chirobiotic R column in the RP mode has the S configuration[8]. This work is on-going.

3.4. Conclusions

The macrocyclic glycopeptides CSPs proved to be extremely selective for the enantiomeric resolution of a series of newly synthesized, biologically active chiral dihydrofurocoumarin derivatives. The teicoplanin and teicoplanin aglycon CSPs were most effective for the enantioseparation of this class of compounds. The ristocetin A CSP separated fewer overall compounds, but produced the best separations for those dihydrofurocoumarins that were not easily separated on the teicoplanin based CSPs. The normal phase mode is the most effective and useful separation mode for all of these CSPs. Hydrogen bonding was believed to play a key role in the normal phase and the polar organic mode chiral separations. Hydroxyl groups on the rim of the aglycon portion of all CSPs are responsible for hydrogen bonding interactions with the analyte. A hydroxyl group on the analyte near the stereogenic center greatly enhanced the enantioselectivity on all CSPs in all mobile phase modes. Hydrophobic interactions are important in the RP mode. Dihydroangelicins, dihydropsoralens, and a related third group of dihydrofurocoumarins (Figure 3) behave very differently with regard to enantioselectivity on the different CSPs. Steric repulsive effects are very important for achieving chiral recognition on all three CSPs, and in both the NP and RP modes. However, the steric bulk near the chiral center of the

dihydroangelicin tends to enhance the NP enantiomeric separations and inhibit the corresponding RP reparations. The exact opposite trend is seen for dihydropsoralens. The absolute configuration of selected, collected enantiomers was determined and therefore the enantiomeric elution orders for these particular compounds on a particular CSP under specific mobile phase condition were determined.

Acknowledgements

Support of this research fund by the National Institute of Health, NIH RO1 GM53825-06 is gratefully acknowledged. R. V. Rozokov and R. C. Larock also acknowledge the donors of the Petroleum Research Fund, administered by the American Chemical Society, for partial support of this research and Johnson Matthey Inc., and Kawaken Fine Chemicasl Co. Ltd., for donations of palladium acetate.

References

[1] M.A. Pathak, D.M. Kramer, T.B. Fitzpatrick, Sunlight and Man University of Tokyo Press (1973).
[2] J.D. Regan, J.A. Parrish, The Science of Photomedicine Plenum Press:New York (1982).
[3] E.P. Gasparro, Psoralen DNA Photobiology CRC Press, Inc.:Boca Raton, FL (1989).
[4] D. Guilet, J.J. Helesbeux, D. Seraphin, T. Sevenet, P. Richomme, J. Bruneton, Journal of Natural Products 64 (2001) 563.
[5] L.D. Via, O. Gia, S.M. Magno, L. Santana, M. Teijeira, E. Uriarte, Journal of Medicinal Chemistry 42 (1999) 4405.
[6] A. Jasinskas, N. Jasinskiene, J.P. Langmore, Biochimica et Biophysica Acta 1397 (1998) 285.
[7] S.Y. Kang, K.Y. Lee, S.H. Sung, M.J. Park, Y.C. Kim, Journal of Natural Products 64 (2001) 683.
[8] N.B. Gennaro Pescitelli, Tom L. Xiao, Roman V. Rozhkov, Richard C. Larock and Daniel W. Armstrong, Org. Biomol. Chem. 1 (2003) 186.
[9] D. Lee, K.P.L. Bhat, H.H.S. Fong, N.R. RFarnsworth, J.M. Pezzuto, A.D. Kinghorn, Journal of Natural Products 64 (2001) 1286.
[10] R.C. Beiber, G.W. Ivie, E.H. Obertli, D.L. Holt, Food and Chemical Toxicology 21 (1983) 163.
[11] C.A.J. Erdelmeier, B. Meier, O. Sticher, Journal of Chromatography 346 (1985) 456.
[12] F.R. Stermitz, R.D. Thomas, Journal of Chromatography 77 (1973) 431.

[13] V. Stanjek, M. Miksch, W. Boland, Tetrahedron 53 (1997) 17699.
[14] R. Rozhkov, R. Larock, Organic Letters 5 (2003) 797.
[15] D.W. Armstrong, Y. Tang, S. Chen, Y. Zhou, C. Bagwill, J.-R. Chen, Anal. Chem. 66 (1994) 1473.
[16] D.W. Armstrong, K. Rundlett, G.L. Reid, III., Anal. Chem. 66 (1994) 1690.
[17] D.W. Armstrong, K.L. Rundlett, J.-R. Chen, Chirality 6 (1994) 496.
[18] D.W. Armstrong, Y. Zhou, J. Liq. Chromatogr. 17 (1994) 1695.
[19] T.L. Xiao, Armstrong, Daniel W., Methods in Biotechnology, Chiral Separations-Methods and Protocols (In press).
[20] D.W. Armstrong, Chimia 50 (1996) 273.
[21] M.P. Gasper, A. Berthod, U.B. Nair, D.W. Armstrong, Anal. Chem. 68 (1996) 2501.
[22] A. Berthod, Y. Liu, C. Bagwill, D.W. Armstrong, J. Chromatogr., A 731 (1996) 123.
[23] D.W. Armstrong, Book of Abstracts, 211th ACS National Meeting, New Orleans, LA March 24-28 (1996).
[24] M. Pawlowska, D.W. Armstrong, Chirality 6 (1994) 270.
[25] S. Chen, Y. Liu, D.W. Armstrong, J.I. Borrell, B. Martinez-Teipel, J.L. Matallana, Biochim. Biophys. Acta 1263 (1995) 2703.
[26] D.W. Armstrong, Y. Liu, K.H. Ekborgott, Chirality 7 (1995) 474.
[27] S. Chen, Y. Liu, D.W. Armstrong, J.I. Borrell, B. Martinez-Teipel, J.L. Matallana, J. Liq. Chromatogr. 18 (1995) 1495.
[28] T.J. Ward, C.I. Dann, A. Blaylock, Journal of Chromatography A 715 (1995) 337.
[29] U.B. Nair, S.S.C. Chang, D.W. Armstrong, Y.Y. Rawjee, D.S. Eggleston, J.V. McArdle, Chirality 8 (1996) 590.
[30] A. Berthod, U.B. Nair, C. Bagwill, D.W. Armstrong, Talanta 43 (1996) 1767.
[31] M.A. Strege, B.E. Huff, D.S. Risely, LC. GC 14 (1996) 144.
[32] T.J. Ward, LC. GC 14 (1996) 886.
[33] K. H. Ekborg-Ott, D.W. Armstrong, Chiral Separations: Application and Technology, Ch. 9 (1997) 201.
[34] O.P. Kleidernigg, C.O. Kappe, Tetrahedron: Asymmetry 8 (1997) 2057.
[35] V.S. Sharp, D.S. Risley, S. Mccarthy, B.E. Huff, M.A. Strege, J. Liq. chromatogr. 20 (1997) 887.
[36] G. Torok, A. Peter, G. Toth, D. Tourwe, W. Van Den Nest, K. Iterbeke, D.W. Armstrong, Proc. Eur. Pept. Symp 25th (1998) 302.
[37] A. Peter, G. Torok, G. Toth, D. Tourwe, E. Mannekens, W. Van Den Nest, J. Sapi, D.W. Armstrong, Proc. Eur. Pept. Symp., 25th (1998) 300.
[38] K.H. Ekborg-Ott, J.P. Kullman, X. Wang, K. Gahm, L. He, D.W. Armstrong, Chirality 10 (1998) 627.
[39] A. Peter, G. Torok, G. Toth, W. Van den Nest, G. Laus, D. Tourwe, D.W. Armstrong, Chromatographia 48 (1998) 53.
[40] K. Ekborg-Ott, Y. Liu, D.W. Armstrong, Chirality 10 (1998) 434.
[41] D.W. Armstrong, J.T. Lee, L.W. Chang, Tetrahedron: Asymmetry 9 (1998) 2043.
[42] H.Y. Aboul-Enein, V. Serignese, Chromatographia 13, (1999) 520.
[43] H.Y. Aboul-Enein, V. Serignese, Chirality 10 (1998) 358.
[44] K. B. Joyce, A. E. Jones, R. J. Scott, R. A. Biddlecombe, S. Pleasance, Rapid Commun. Mass Spectrom. 12 (1998) 1899.

[45] K. M. Fried, P. Koch, I.W. Wainer, Chirality 10 (1998) 484.
[46] J. Lehotay, K. Hrobonová, J. Krupcík, J. Cizmárik, Pharmazie 53 (1998) 863.
[47] J.M. Schneiderheinze, D.W. Armstrong, A. Berthod, Chirality 11 (1999) 330.
[48] D.W. Armstrong, L. He, T. Yu, J.T. Lee, Y.-s. Liu, Tetrahedron: Asymmetry 10 (1999) 37.
[49] I. D'Acquarica, F. Gasparrini, D. Misiti, C. Villani, A. Carotti, S. Cellamare, S. Muck, Journal of Chromatography A 857 (1999) 145.
[50] L. Ramos, R. Bakhtiar, T. Majumdar, M. Hayes, F. Tse, Rapid Commun. Mass Spectrom. 13 (1999) 2054.
[51] E. Tesarova, Z. Bosakova, I. Zuskova, Journal of Chromatography A 879 (2000) 147.
[52] C. Karlsson, L. Karlsson, D.W. Armstrong, P.K. Owens, Analytical Chemistry 72 (2000) 4394.
[53] A. Berthod, X. Chen, J.P. Kullman, D.W. Armstrong, F. Gasparrini, I. D'Acquarica, C. Villani, A. Carotti, Analytical Chemistry 72 (2000) 1767.
[54] E. Peyrin, C. Ravelet, E. Nicolle, A. Villet, C. Grosset, A. Ravel, J. Alary, Journal of Chromatography, A 923 (2001) 37.
[55] T.L. Xiao, B. Zhang, J.T. Lee, F. Hui, D.W. Armstrong, Journal of Liquid Chromatography & Related Technologies 24 (2001) 2673.
[56] A. Berthod, T.L. Xiao, Y. Liu, W.S. Jenks, D.W. Armstrong, J. Chromatography A 955 (2002) 53.
[57] S.C. Chang, G.L. Reid, S. Chen, C.D. Chang, D.W. Armstrong, Trends in Analytical Chemistry 12 (1993) 144.
[58] D.W. Armstrong, S. Chen, C. Chang, S. Chang, Journal of Liquid Chromatography & Related Technologies 15 (1992) 545.
[59] T.L. Xiao, E. Tesarova, M.D. Egger, J.L. Anderson, D.W. Armstrong, unpublished results (2003).

Table 1
Chromatographic results obtained with chiral dihydrofurocoumarin derivatives on three macrocyclic antibiotic CSPs.

Compound number[a]	ristocetin A			teicoplanin			teicoplanin aglycone		
mobile phase[b]	k_1	alpha	Rs	k_1	alpha	Rs	k_1	alpha	Rs
1									
NP: Hep-EtOH	6.69	1.03	0.5	5.13	1.15	1.93	3.48	1.35	4.23
RP: H_2O-MeOH	5.57	1.03	0.45	4.35	1.08	0.95	7.41	1.13	1.5
PO: IPA	0.68	1.14	0.56	0.67	1.34	1.4	1.36	1.62	1.93
PO: EtOH	0.28	1.11	0.55	0.21	1.27	1.32	0.62	1.41	2.84
PO: MeOH	0.16	1	0	0.1	1.14	0.2	0.46	1.34	2.91
2									
NP: Hep-EtOH	5.68	1.08	1.12	4.35	1.25	3.53	3.09	1.49	5.27
RP: H_2O-MeOH	7.89	1	0	10.64	1.09	1.48	14.01	1.15	1.51
PO: IPA	0.55	1.3	1.05	0.56	1.62	2.01	1.16	1.89	2.37
PO: EtOH	0.23	1.26	1.06	0.18	1.49	1.65	0.56	1.61	3.68
PO: MeOH	0.15	1	0	0.1	1.27	0.63	0.47	1.4	3.27
3									
NP: Hep-EtOH	5.12	1.08	1.2	4.05	1.16	2.45	2.84	1.33	3.71
RP: H_2O-MeOH	11.9	1	0	17.20	1.02	0.61	20.43	1.06	0.55
PO: IPA	0.51	1.29	0.87	0.51	1.45	1.5	1.13	1.53	1.51
PO: EtOH	0.22	1.23	0.8	0.17	1.24	0.88	0.58	1.34	2.07
PO: MeOH	0.15	1	0	0.1	1	0	0.52	1.11	1.0
4									
NP: Hep-EtOH	5.83	1	0	5.13	1.1	1.61	3.43	1.13	1.79
RP: H_2O-MeOH	6.04	1	0	5.43	1.03	0.46	7.96	1	0
PO: IPA	0.87	1	0	1.11	1.23	1.24	1.84	1.17	0.6
PO: EtOH	0.31	1	0	0.29	1.15	0.69	0.7	1.1	0.76
PO: MeOH	0.11	1	0	0.1	1	0	0.42	1	0
5									
NP: Hep-EtOH	7.76	1.07	0.8	7.27	1.18	2.32	4.43	1.12	1.58
RP: H_2O-MeOH	7.11	1	0	6.96	1	0	10.57	1	0
PO: IPA	0.89	1.12	0.46	1.23	1.31	1.42	2.07	1.15	0.55
PO: EtOH	0.31	1.17	0.67	0.32	1.21	1.35	0.79	1.1	0.76
PO: MeOH	0.14	1	0	0.12	1	0	0.51	1.05	0.5
6									
NP: Hep-EtOH	7.36	1	0	7.47	1	0	4.38	1.04	0.56
RP: H_2O-MeOH	7.13	1.15	1.5	6.25	1.27	2.74	9.39	1.2	1.95
PO: IPA	0.94	1	0	1.29	1	0	2.15	1	0
PO: EtOH	0.32	1.1	0.3	0.35	1	0	0.76	1.14	1.01
PO: MeOH	0.14	1	0	0.11	1.22	0.65	0.49	1.17	1.5
7									
NP: Hep-EtOH	4.88	1.03	0.2	4.48	1.18	2.68	2.76	1.18	2.15
RP: H_2O-MeOH	7.31	1.03	0.3	6.2	1.04	0.46	9.43	1	0
PO: IPA	0.72	1	0	0.88	1.39	1.62	1.5	1.2	0.63
PO: EtOH	0.24	1.13	0.45	0.23	1.33	1.45	0.58	1.17	1.5
PO: MeOH	0.1	1	0	0.1	1	0	0.39	1.08	0.6

Compound number[a]	ristocetin A			teicoplanin			teicoplanin aglycone		
mobile phase[b]	k_1	alpha	Rs	k_1	alpha	Rs	k_1	alpha	Rs
8									
NP: Hep-EtOH	6.07	1	0	5.96	1.05	1.42	3.73	1.06	0.84
RP: H_2O-MeOH	5.81	1.1	1.25	5.21	1.11	1.42	7.89	1.08	0.64
PO: IPA	0.78	1	0	1.24	1.13	0.61	2.04	1	0
PO: EtOH	0.3	1	0	0.32	1.06	0.4	0.73	1	0
PO: MeOH	0.11	1	0	0.1	1	0	0.46	1	0
9									
NP: Hep-EtOH	7.14	1.02	0.2	6.78	1.12	0.73	4.26	1.05	1.33
RP: H_2O-MeOH	7.47	1.14	1.55	7.1	1.07	0.73	10.57	1.06	0.6
PO: IPA	0.82	1.11	0.43	1.1	1.23	1.12	1.89	1.1	0.2
PO: EtOH	0.29	1.09	0.5	0.29	1.1	0.56	0.74	1	0
PO: MeOH	0.13	1	0	0.1	1	0	0.48	1	0
10									
NP: Hep-EtOH	4.41	1.06	0.7	4.48	1.09	1.52	2.24	1.12	1.65
RP: H_2O-MeOH	11.1	1.07	0.59	11.13	1.07	0.67	16.57	1.1	0.85
PO: IPA	0.59	1	0	0.81	1.2	0.88	1.32	1.27	0.76
PO: EtOH	0.2	1.1	0.41	0.2	1.24	1.2	0.53	1.23	1.4
PO: MeOH	0.1	1	0	0.1	1	0	0.38	1.13	0.76
11									
NP: Hep-EtOH	14.14	1.04	0.2	13.9	1.07	1.02	8.58	1.03	0.53
RP: H_2O-MeOH	19.00	1.22	2.16	17.75	1.06	0.95	27.75	1.15	1.5
PO: IPA	1.28	1.12	0.5	1.86	1.1	0.47	3.58	1	0
PO: EtOH	0.43	1	0	0.47	1	0	1.22	1	0
PO: MeOH	0.19	1	0	0.19	1	0	0.81	1	0
12									
NP: Hep-EtOH	7.36	1	0	7.65	1	0	4.89	1	0
RP: H_2O-MeOH	5.86	1.07	0.95	5.04	1.28	2.69	7.61	1.18	1.77
PO: IPA	1.03	1	0	1.35	1	0	2.18	1	0
PO: EtOH	0.38	1	0	0.37	1	0	0.76	1.1	0
PO: MeOH	0.15	1	0	0.11	1	0	0.48	1.15	0
13									
NP: Hep-EtOH	4.13	1.07	0.8	3.23	1.17	2.61	2.07	1.38	4.88
	5.08	1.07	1.0	4.03	1.24	3.37	2.52	1.49	6.35
RP: H_2O-MeOH	4.95	1	0	3.94	1	0	6.39	1	0
				4.16	1	0	7.29	1	0
PO: IPA	0.46	1	0	0.36	1.56	1.4	0.8	1.62	2.4
	0.56	1	0	0.42	1.75	2	0.86	2.08	2.5
PO: EtOH	0.17	1	0	0.1	1.3	0.5	0.33	1.58	2.35
	0.21	1	0	0.11	1.64	1.5	0.37	1.67	2.92
PO: MeOH	0.1	1	0	0.05	1	0	0.23	1.51	2.6
				0.07	1	0	0.26	1.53	2.6

Compound number[a]	ristocetin A			teicoplanin			teicoplanin aglycone		
mobile phase[b]	k_1	alpha	Rs	k_1	alpha	Rs	k_1	alpha	Rs
14									
NP: Hep-EtOH	8.35	1.07	0.8	7.07	1.21	3.07	4.27	1.09	1.24
RP: H_2O-MeOH	24.62	1.12	1.2	42.94	1.19	1.88	49.0	1.21	1.55
PO: IPA	0.95	1	0	1.04	1.29	1.3	2.08	1	0
PO: EtOH	0.31	1.1	0.52	0.28	1.32	1.54	0.75	1.12	0.67
PO: MeOH	0.14	1	0	0.11	1.36	1.12	0.58	1.17	1.5
15									
NP: Hep-EtOH	11.0	1.	0.3	8.38	1.11	1.	4.53	1.09	1.5
RP: H_2O-MeOH	9.27	1.	0.41	7.59	1	0	10.93	1	0
PO: IPA	0.77	1	0	0.77	1.21	0.	1.42	1.1	0.37
PO: EtOH	0.32	1	0	0.2	1.12	0.	0.59	1.09	0.6
PO: MeOH	0.15	1	0	0.1	1	0	0.44	1	0
16									
NP: Hep-EtOH	8.45	1.	0.3	6.88	1.02	0.	3.87	1	0
RP: H_2O-MeOH	10.1	1.	1.21	6.09	1	0	8.82	1.05	0.45
PO: IPA	0.58	1	0	0.7	1	0	1.21	1	0
PO: EtOH	0.26	1	0	0.19	1	0	0.53	1	0
PO: MeOH	0.12	1	0	0.1	1	0	0.37	1	0
17									
NP: Hep-EtOH	10.8	1.	0.5	8.69	1.11	1.	4.57	1.09	1.45
RP: H_2O-MeOH	10.9	1.	0.46	7.5	1	0	10.75	1	0
PO: IPA	0.79	1	0	0.77	1.21	0.	1.33	1.12	0.2
PO: EtOH	0.32	1	0	0.21	1.11	0.	0.58	1.09	0.6
PO: MeOH	0.15	1	0	0.1	1	0	0.44	1	0
18									
NP: Hep-EtOH	10.1	1	0	7.90	1.17	2.	4.33	1.08	1.51
RP: H_2O-MeOH	10.1	1	0	7.34	1.07	0.	11.07	1	0
PO: IPA	0.72	1	0	0.67	1.33	1.	1.27	1.1	0.44
PO: EtOH	0.29	1	0	0.18	1.23	0.	0.55	1.08	0.54
PO: MeOH	0.14	1	0	0.1	1.21	0.	0.41	1	0
						2			
19									
NP: Hep-EtOH	8.66	1.	0.5	5.47	1.06	1.	3.5	1.1	1.5
	9.55	1.	0.5		1.12	2.		1.21	3.14
RP: H_2O-MeOH	7.79	1	0	6.41	1	0	8.64	1	0
PO: IPA	0.68	1	0	0.68	1	0	1.15	1	0
					1	0		1	0
PO: EtOH	0.26	1	0	0.17	1	0	0.48	1	0
	0.29	1	0		1	0	0.60	1	0
PO: MeOH	0.11	1	0	0.05	1	0	0.34	1	0
							0.39	1	0

Compound number[a]	ristocetin A			teicoplanin			teicoplanin aglycone		
mobile phase[b]	k_1	alpha	Rs	k_1	alpha	Rs	k_1	alpha	Rs
20									
NP: Hep-EtOH	6.66	1	0	5.52	1.05	1.	2.57	1	0
RP: H_2O-MeOH	14.3	1	0	11.1	1	0	18.0	1	0
PO: IPA	0.45	1	0	0.51	1	0	0.98	1	0
PO: EtOH	0.19	1	0	0.11	1	0	0.43	1	0
PO: MeOH	0.1	1	0	0.05	1	0	0.33	1	0
21									
NP: Hep-EtOH	19.5	1.	0.5	11.46	1.17	2.	8.38	1.09	1.46
RP: H_2O-MeOH	25.9	1	0	13.0	1.18	1.	29.0	1	0
PO: IPA	1.07	1	0	1.01	1.4	1.	2.38	1.05	0.2
PO: EtOH	0.4	1	0	0.27	1.27	1.	0.88	1.09	0.6
PO: MeOH	0.2	1	0	0.12	1.25	0.	0.69	1	0
22									
NP: Hep-EtOH	3.68[c]	3.42[c]	4.62[c]	47.31	1.75	5.8	16.37	1.27	2.69
RP: H_2O-MeOH	2.85	1.8	4.97	4.74	1.41	0.7	4.9	1.1	0.65
PO: IPA	1.3	3.6	1.71	0.12	1.56	1.5	2.33	1.95	2.51
PO: EtOH	0.4	3.66	3.76	0.39	1.71	3.01	1.3	1.3	1.95
PO: MeOH	0.15	2.03	2.72	0.39	1.71	2.99	0.55	1.15	1.21
23									
NP: Hep-EtOH	12.4	1.05	0.7	7.66	1.07	1.45	14.8	1	0
RP: H_2O-MeOH	28.5	1.35	1.51	16.8	1	0	53.3	1.16	1.52
PO: IPA	0.65	1	0	0.84	1.13	0.54	1.75	1.1	0.2
PO: EtOH	0.25	1	0	0.26	1.07	0.38	0.67	1.1	0.3
PO: MeOH	0.12	1	0	0.15	1	0	0.57	1.12	1.1
24									
NP: Hep-EtOH	20.88	1.21	2.5	*14.16	1.03	0.65	17.14	1	0
RP: H_2O-MeOH	7.47	1.09	0.6	14.23	1	0	8.93	1.15	1.61
PO: IPA	1.44	1.34	0.82	3.33	1.13	0.8	4.5	1.08	0.2
PO: EtOH	0.43	1.21	1.35	0.64	1.12	0.4	1.56	1	0
PO: MeOH	0.19	1.11	0.5	0.64	1.12	0.3	0.83	1.05	0.62
25									
NP: Hep-EtOH	12.42	1.46	3.34	11.5	1.11	1.45	7.49	1.15	2.03
RP: H_2O-MeOH	1.54	1.31	2.61	16.81	1.09	1.1	12.71	1.10	1.45
PO: IPA	1.93	1.51	1.2	2.13	1.14	0.7	2.62	1.16	0.58
PO: EtOH	0.66	1.54	2.3	0.57	1.13	0.58	1.08	1.17	1.5
PO: MeOH	0.24	1.36	1.6	0.56	1.12	0.58	0.70	1.25	2.53
26									
NP: Hep-EtOH	11.62	1.08	1.5	10.44	1.02	0.2	7.95	1.03	0.51
RP: H_2O-MeOH	4.71	1	0	3.88	1	0	5.08	1	0
PO: IPA	0.79	1.19	0.95	2.44	1	0	2.43	1	0
PO: EtOH	0.26	1.25	0.65	0.45	1	0	0.84	1	0
PO: MeOH	0.21	1	0	0.45	1	0	0.47	1	0

Compound number[a]	ristocetin A			teicoplanin			teicoplanin aglycone		
mobile phase[b]	k_1	alpha	Rs	k_1	alpha	Rs	k_1	alpha	Rs
27									
NP: Hep-EtOH	7.63	1.11	1.5	6.63	1	0	5.18	1	0
RP: H_2O-MeOH	1.08	1.1	0.76	6.45	1.04	0.52	11.32	1	0
PO: IPA	0.99	1.35	0.76	1.76	1	0	2.22	1	0
PO: EtOH	0.31	1.22	0.79	0.43	1	0	0.87	1	0
PO: MeOH	0.12	1	0	0.43	1	0	0.56	1	0
28									
NP: Hep-EtOH	5.84	1.32	3.0	3.83	1.19	2.69	2.92	1.32	3.66
RP: H_2O-MeOH	1.1	2.6	9.05	5.99	1.26	3.6	6.94	1.16	1.82
PO: IPA	0.65	1.75	1.5	0.53	1.68	1.96	0.85	1.7	1.8
PO: EtOH	0.24	1.86	2.10		1.66	1.81	0.46	1.47	2.75
PO: MeOH	0.16	2.12	3.44		1.68	1.81	0.39	1.4	3.07

a. The number of the compound corresponds to the structure shown in Figure 3.

b. NP = normal phase, Heptane/EtOH for R=98.5/1.5, for T=97.5/2.5, for TAG=90/10 (0.5 ml/min) at 1mL/min unless otherwise indicated. RP = reversed phase, H_2O/MeOH for R=70/30, for T=65/35, for TAG=50/50 at 1ml/min. PO= polar organic mode, all 100% alcohol with flow rate at 0.5 mL/min. k_1 = retention factor of the first eluting enantiomer, alpha = enantioselectivity factor, Rs = enantioresolution factor. All the data above are average values from triplicate analyzes, standard deviation below 0.06. * Hep/EtOH=95/5 due to the long retention time.

c. Data were obtained using Heptane/ethanol=75/25 due to strong retention. When Heptane/ethanol=95/5 was applied, the first peak came out at 67.05 min, corresponding to k_1=20.8, and second peak was too broad.

CHAPTER 4
REVERSAL OF ENANTIOMERIC ELUTION ORDER ON MACROCYCLIC GLYCOPEPTIDE CHIRAL STATIONARY PHASES

A paper published in J. Liquid Chromatography & Related Technologies[1]

Tom Ling Xiao, B. Zhang, J.T. Lee, F. Hui, and Daniel W. Armstrong

ABSTRACT

The macrocyclic glycopeptides, vancomycin, teicoplanin, and ristocetin A are naturally occurring chiral molecules that have been developed into one of the most useful classes of chiral stationary phases (CSPs) for HPLC. Since these chiral selectors are structurally related, they tend to have similar, but not identical, enantioselectivities for most compounds. CSPs, of this type, with opposite enantioselectivities are rare. Two exceptions have been found to this. The oxazolidiones (starting materials for asymmetric synthesis) and dansyl amino acids all show a reversal in enantioselective retention on one of these three related CSPs. By using the HPLC assays developed for these compounds, the levels of enantiomeric impurities can be measured down to ≈0.01%. The enantiomeric purity of commercial oxazolidiones was determined.

---

[1]Reprinted with permission from Journal of Liquid Chromatography & Related Technologies, 24(17), (2001) 2673–2684. Copyright © 2001 by Marcel Dekker, Inc

4.1. INTRODUCTION

The macrocyclic glycopeptides are the newest and fastest growing class of chiral selectors for HPLC [1-24]. Figure 1 gives the structure of three related glycopeptides (i.e., vancomycin, teicoplanin and ristocetin A) that are available as chiral stationary phases (CSPs). In addition, the aglycone portion of teicoplanin (i.e., teicoplanin with the carbohydrate moities removed) was recently produced as a separate chiral stationary phase[24].

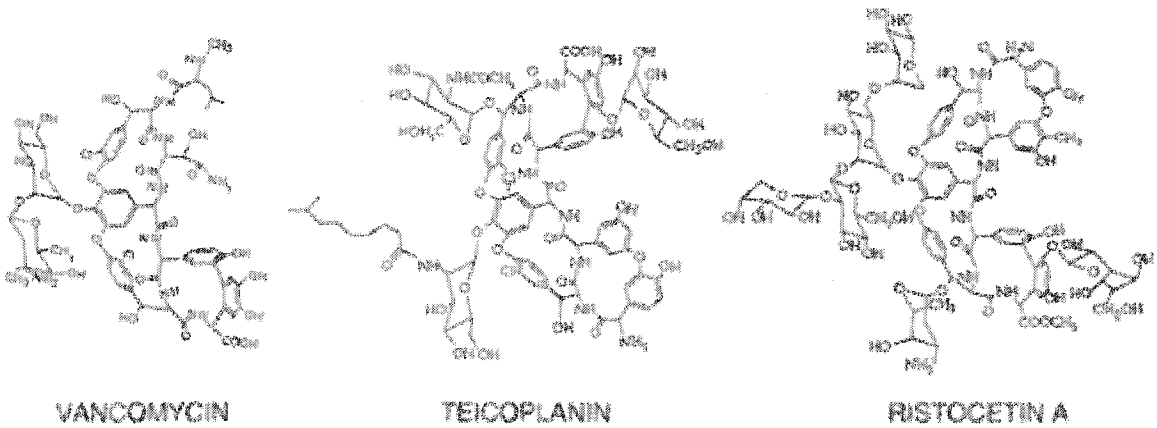

Figure 1. Schematic showing the structures of the related macrocyclic glycopeptides: vancomycin, teicoplanin, and ristocetin A.

The aglycone portion of all the macrocyclic glycopeptides contain either three or four fused macrocyclic rings (Figure 1). Together, these fused rings form a semirigid basket-shaped entity. Each aglycone basket has associated with it: an amine moiety, a carboxylic acid group (which is esterified in ristocetin A) and phenolic moieties. These groups, along with an amino-saccharide, control the charge of these molecules. In addition, the aglycone contains several amide or peptide bonds (Figure 1). Each aglycone has one or more carbohydrate moieties attached at various locations. A single disaccharide is attached to vancomycin, while

teicoplanin has three monosaccharides associated with it (Figure 1). Compared to the aglycone portion of these molecules, the carbohydrate moieties are relatively free to alter their orientation.

As a class of chiral selectors, the macrocyclic glycopeptides have very broad enantioselectivity, and can be used in all chromatographic modes (i.e., reversed phase, normal phase and polar organic modes). The teicoplanin-based CSP (Chirobiotic T) is now the preferred means of resolving native amino acids (both natural and synthetic types). (1) , (5) , (9-10) A distinct amino acid and carboxylic acid binding site has been identified for these related macrocycles. (5) , (7) , (24) Furthermore, it appears that there are other binding sites for neutral and cationic chiral analytes. (24)

Clearly, vancomycin, teicoplanin, and ristocetin A are similar, structurally related molecules. They have the same biological function, which is to bind to D-alanyl-alanine moieties in the cell wall of Gram positive bacteria. (1-3) , (8) Although they are related, these macrocycles are far from being identical. Thus, they have somewhat similar, but not identical selectivities. This property gave rise to the operating "principle of complimentary separations." This means that if only a partial enantioseparation can be obtained on one CSP, then it is likely that a baseline separation will be achieved on one of the related CSPs. (4) , (6)

Given the similarities of the glycopeptide chiral selectors, it is not surprising that enantiomeric elution order appears to be the same on all of these CSPs. Since these macrocyclic glycopeptides are complex, natural molecules, their enantiomers are unavailable. Consequently, reversing the enantioselectivity of a separation on these CSPs is difficult, and

would be considered unusual. After performing thousands of separations on these CSPs over the last few years, we have found a few cases in which the enantioselectivity of a separation could be reversed either by using a related glycopeptide CSP or, in one case, by altering the mobile phase composition. This behavior has not been reported previously for this class of CSPs.

4.2. EXPERIMENTAL

Materials

The HPLC-grade solvents [methanol, reagent alcohol, acetonitrile, glacial acetic acid, triethylamine (99+% pure) and hexane] were purchased from Fisher Scientific (Fair Lawn, NJ, USA). All racemates and single enantiomers of derivatized amino acids and neutral molecules used in this study were purchased from Aldrich (Milwaukee, WI, USA) and Fluka (Milwaukee, WI, USA). All HPLC Chirobiotic columns [Chirobiotic V (vancomycin), Chirobiotic T (teicoplanin), Chirobiotic R (ristocetin A)] were (stainless-steel 25 cm × 4.6 mm) obtained from Advanced Separation Technologies, Inc. (Whippany, NJ).

Methods

The separations were performed on Shimadzu (Columbia, MD) HPLC systems equipped with Model LC-6A pumps, Model SPD-6A, and SPD-6AV UV detectors, SCL-6A and SCL-6B system controllers, CR-601 and C-R3A Chromatopac integrators, and Rheodyne (Cotati, CA, USA) manual injectors. All samples were dissolved in methanol with concentration of 1 mg/mL and all separations were achieved at room temperature (22°C).

Mobile phases were prepared by mixing the indicated volumes of solvents or deionized and filtered water and degassed with a Crest Ultrasonic sonicator (Trenton, NJ, USA). The HPLC

mobile phase flow rate was 1 mL/min and UV detection wavelengths were 254 nm for compounds containing aromatic rings and 220 nm for all others. The pH value of buffer mobile phase was measured with an Orion (Boston, MA, USA) pH meter Model 410A. Elution orders were determined by spiking a single pure enantiomer into the solution of the corresponding racemic compound.

4.3. RESULTS AND DISCUSSION

There are few reports on the reversal of enantiomeric retention on CSPs containing natural chiral selectors. (25-26) These CSPs usually are either protein-based or linear derivatized carbohydrates. (25-26) The reversal of enantiomeric elution usually was the result of a change in mobile phase composition, although temperature effects also could be relevant. A solvent induced confirmational change in the chiral selector often was given as the reason for the change in selectivity. Note, that the changes in solvent composition that were reported were not drastic changes, such as going from the reversed phase mode to the normal phase mode (where the mechanism changed). Rather, they are milder changes, such as altering the organic modifier type or altering the pH in a reversed phase separation.

The macrocyclic glycopeptides are much smaller than the biological polymers that are used as chiral selectors. Thus, they seem to be less susceptible to solvent-induced changes in enantioselectivity. Indeed, the only reverse in enantioselective retention we've documented on the vancomycin CSP (involving different mobile phases), was for N-benzyl-α-methylbenzylamine (Figure 2). In this case, it took a rather drastic change in the mobile phase (i.e., from the polar organic mode to the reversed phase mode). It is less surprising to get a change in enantioselectivity if the retention mechanism is completely altered. Despite

this fact, the enantiomeric retention order of a wide variety of solutes on the macrocyclic glycopeptide CSPs is reasonably constant. Table 1 lists several classes of molecules that appear to have the same basic enantioselectivity on the vancomycin, teicoplanin, and ristocetin chiral stationary phases.

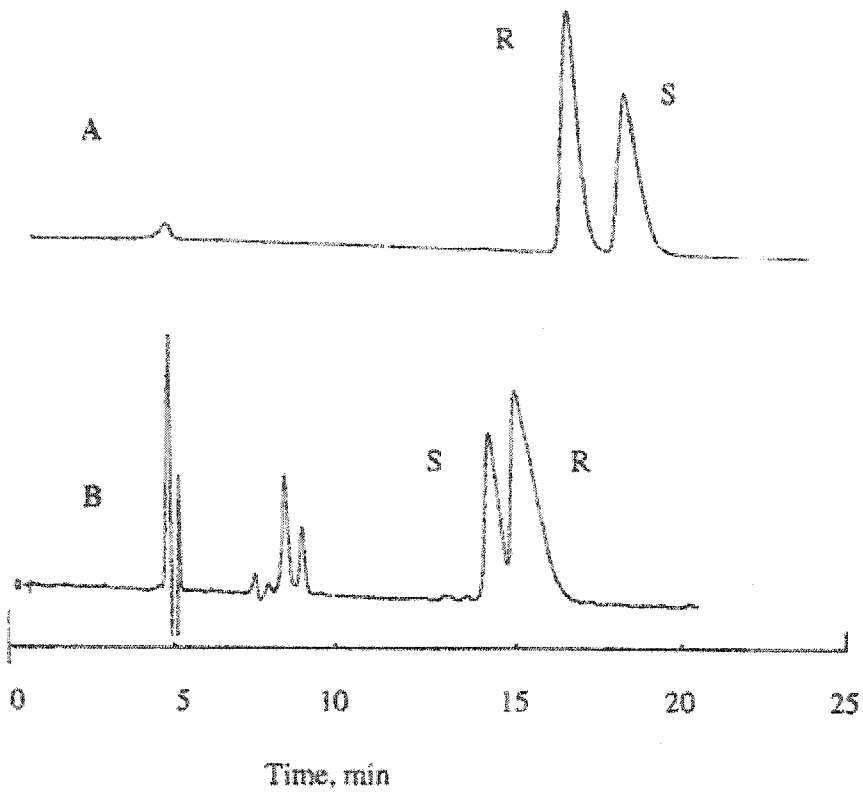

Figure 2. Chromatograms showing the reversal in elution order for enantiomers of N-benzyl-α-methylamine on the Chirobiotic V column (250 × 4.6 mm) resulting from a change in the mobile phase composition. Chromatogram (A) was generated in the polar organic mode (acetonitrile/0.1% TEAA buffer, pH 4.1; 20/80, by volume).

Table 1. Some Classes of Compounds That Appear to Have the Same Enantiomeric Retention Order on Chirobiotic V, T, and R Chiral Stationary Phases

1. FMOC-amino acids
2. N-t-BOC-amino acids
3. N-CBZ-Amino acids
4. Nonsteroidal anti-inflammatory compounds
5. β-Adrenergic blockers
6. 4-Aryldihydropyrimidines

Throughout the course of our studies, it was noted that a compound would sometimes have a different enantiomeric retention order on one of the macrocyclic glycopeptides CSPs. Thus far, all compounds that have shown this behavior fall into one of two classes: 1) the oxazolidinones, and 2) dansylated amino acids (Table 2A , 2B . Of these, the dansyl-amino acids show the most consistent behavior. The D-enantiomers are preferentially retained on the vancomycin and teicoplanin CSPs, while the L-enantiomer is more retained on the ristocetin CSP (Table 2A , 2B . It is the retention order on the ristocetin CSP that is unusual or anomalous. In most other cases, both the native and derivatized D-amino acids enantiomers are more retained on macrocyclic glycopeptide CSPs. Indeed, the biological function of these glycopeptides is to bind to D-alanyl-D-alanine on bacterial cell walls. The dansyl-fluorophore is a relatively bulky group and it contains an amine functionality. Apparently, this combination of additional steric-bulk and the hydrogen bonding or charge effect of the amine is sufficient to alter the enantioselectivity of ristocetin A, toward dansyl amino acids.

Table 2A. Members of two classes of compounds where there is a change in the enantiomeric elution order on macrocyclic glycopeptide CSPs.

Compound Oxazolidiones	Structure	Elution order[a]			*Mobile Phase*[b]
		Vancomycin V	RistocetinA R	Teicoplanin T	
RS - 4- phenyl - 2- oxazolidinone	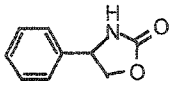	R	S	R	T& R= 100% MeOH V=H_2O/MeOH (90/10)
RS- 4- benzyl- 2- oxazolidinone	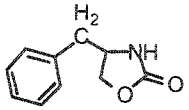	R	S	R	T=100% MeOH V=H_2O/MeOH (90/10) R=H_2O/MeOH (75/25)
RS- 4- benzyl- 3- propionyl- oxazolidinone	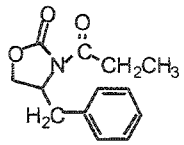	R	Unresolved	S	T=Buffer[c]/MeOH (90/10) V=MeOH/H_2O (82/18)
RS- 5,5,dimethyl-4- phenyl-2- oxazolidionone	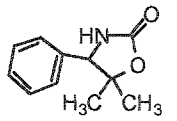	R	S	R	V, R, T = Hex/EtOH (80/20)
RS-3-benzyloxy carbonyl-4- oxazolidine carboxylic acid	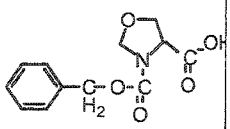	R	R	S	T=Buffer/MeOH (80/20) R=Buffer/MeOH (80/20) V= EtOH/H_2O (40/60)
4S,5R(+) - cis- 4,5- diphenyl-2- oxazolidinone	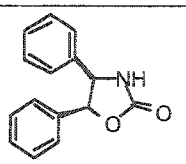	4R,5S	4S,5R	4S,5R	V, R, T =EtOH/Hex (50/50)

[a] The configuration of the first eluted enantiomer is given.
[b] The flow rate for all separation was 1.0 ml/min except for the first two compounds in this table which was 0.5 ml/min.
[c] The buffer was 1% triethylamine acetate, pH= 4.1.

Table 2B. continued

Dansyl-Amino acid	Structure	Elution order[a]			*Mobile Phase*[a]
		Vancomycin	RistocetinA	Teicoplanin	
DL-Valine	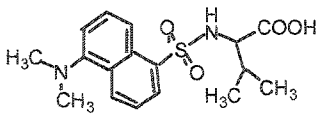	L	D	L	Buffer[b]/MeOH (80/20)
DL - Threonine	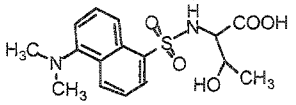	L	D	L	Buffer/MeOH (80/20)
DL - Glutamatic acid	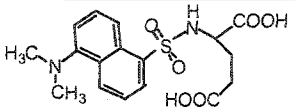	L	D	L	Buffer/MeOH (80/20)
DL - Aspartic acid	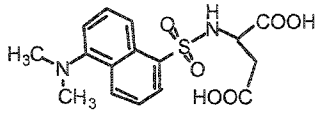	L	D	L	Buffer/MeOH (80/20)
DL – Serine	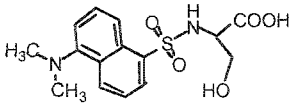	L	D	L	Buffer/MeOH (80/20)
DL - Phenylalanine	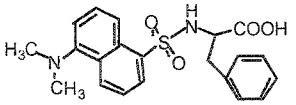	L	D	L	Buffer/MeOH (80/20)
DL - Trytophan	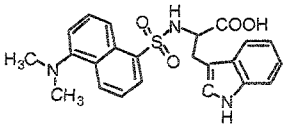	unresolved	D	L	Buffer/MeOH (80/20)
DL - Methionine	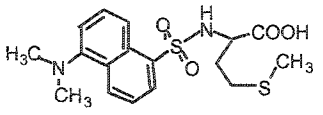	L	D	L	Buffer/MeOH (80/20)
DL - Norvaline	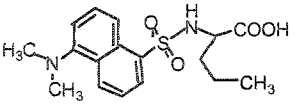	L	D	L	Buffer/MeOH (80/20)

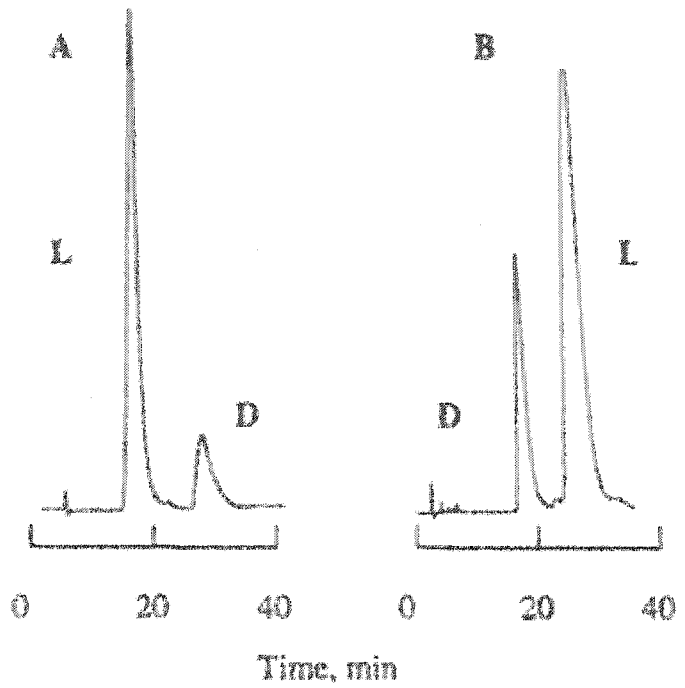

Figure 3. Chromatograms showing the reversal in elution order for dansyl-D, L-methionine on two different macrocyclic glycopeptide CSPs. Chromatogram A was generated using the Chirobiotic T column, and chromatogram B was generated using the Chirobiotic R column. The mobile phase compositions and other conditions are the same as given in Table 2A , 2B .

It is known that amino acids associate with the amine moiety of these macrocyclic glycopeptides via their carboxylic acid groups. (1) , (5) , (9-10) This association can be either electrostatic in nature or hydrogen bonding depending on the pH and/or mobile phase composition. The additional simultaneous interactions (required for chiral recognition) are thought to consist of hydrogen bonds to the amide groups of the aglycone, and in some cases, hydrophobic interactions (at least in the reversed-phase mode). Derivatizing the amine group of an amino acid with a fluorophore can alter the secondary interactions between the analyte and the aglycone. For example, the amino moiety of the amino acid would no longer be available for hydrogen bonding to the macrocyclic glycopeptide. However, the steric bulk of

the fluorophore could accentuate either hydrophobic interaction (in the reversed phase mode) or steric repulsive interactions. As mentioned previously, the dansyl group also contains an amine moiety that could result in additional interactions.

The oxazolidinones do not show consistent retention behavior, as do the dansyl-amino acids (Table 2A , 2B . It is not known how the oxazolidinones interact with the macrocyclic glycopeptides. Hence, the relative retentions reported can only be taken as empirical observations. The R-enantiomer always elutes before the S-enantiomer on the vancomycin CSP. However, there was no consistent pattern on either the ristocetin A or teicoplanin CSPs.

Chiral oxazolidinones are widely used in asymmetric synthesis. Since they are commercially available starting materials, it is often assumed that they are enantiomerically pure. In previous work, it was shown that enantiomeric impurities were prevalent in most of the available chiral catalysts, auxiliaries, synthons, and resolving agents. (27) Table 3 gives the enantiomeric purity found for the oxazolidinones used in this study. Note the wide variation in the enantiomeric purity found for this class of chiral compounds. As was noted previously, the batch-to-batch enantiomeric purity of each of these commercial chiral auxiliaries varies widely, since there is no enantiomeric quality control in their production or sale. (26-27)

Table 3. The enantiomeric composition of chiral compounds which show reversal in enantiomer elution order

Compound name	Commercial source	Enantiomeric composition		Separation Method number[a]
		Enantiomeric contaminant(%)	Enantiomeric excess(%)	
RS - 4- phenyl - 2-oxazolidinone	Aldrich	S=0.05 R=0.20	R=99.90 S=99.60	1
RS- 4- benzyl- 2-oxazolidinone	Aldrich	S=0.06 R=0.03	R=99.88 S=99.94	2
RS- 4- benzyl- 3-propionyl-oxazolidinone	Aldrich	S=0.30 R=0.14	R=99.40 S=99.72	3
RS- 5,5,dimethyl-4-phenyl-2-oxazolidionone	Aldrich	R=0.03 S=0.08	S=99.94 R=99.84	4
RS-3-benzyloxy carbonyl-4-oxazolidine carboxylic acid	Aldrich	S=2.38 R=0.85	R=95.24 S=98.30	5
4S,5R(+) - cis-4,5- diphenyl-2-oxazolidinone	Aldrich	4R, 5S = 0.08 4S, 5R =3.11	4S, 5R=99.84 4R, 5S =93.78	6

[a] Method No. 1= Chirobiotic T. Mobile phase 1% TEAA/MeOH=80/20(pH=4.1), Flow rate 1ml/min.
Method No. 2 = Chirobiotic T. Mobile phase 1% TEAA/MeOH=90/10(pH=4.1), Flow rate 1ml/min.
Method No. 3 = Chirobiotic T. Mobile phase 1% TEAA/MeOH=85/15(pH=4.1), Flow rate 1ml/min.
Method No. 4 = refer to D. W. Armstrong et al./ Tetrahedron: Asymmetry 9 (1998) 2043-2064.
Method No. 5 = Chirobiotic T_{AG}. Mobile phase 1% TEAA/MeOH=70/30(pH=4.1), Flow rate 1ml/min.
Method No. 6 = Chirobiotic T. Mobile phase Hex/EtOH=50/50, Flow rate 1ml/min

REFERENCES

[1] Armstrong D. W., Tang Y., Chen S., Zhou Y., Bagwill C., Chen J.-R., *Anal. Chem., 66* (1994) 1473.

[2] Armstrong D. W., Rundlett K. L., Chen J.-R., *Chirality, 6* (1994) 496.

[3] Armstrong D. W., Liu Y., Ekborg-Ott K. H., *Chirality, 7* (1995) 474.

[4] Chen S., Liu Y., Armstrong D. W., Victory P., Martinez-Teipel B., *J. Liq. Chromatogr., 18* (1995) 1495.

[5] Berthod A., Liu Y., Bagwill C., Armstrong D. W., *J. Chromatogr. A, 731* (1996) 123.

[6] Gasper M. P., Berthod A., Nair U. B., Armstrong D. W., *Anal. Chem., 68* (1996) 2501.

[7] Nair U. B., Chang S. S.C., Armstrong D. W., Rawjee Y. Y., Eggleston D. S., McArdle J. V., *Chirality, 8* (1996) 590.

[8] Ekborg-Ott K. H., Liu Y., Armstrong D. W., *Chirality, 10* (1998) 434.

[9] Peter A., Torok G., Armstrong D. W., *J. Chromatogr. A, 793* (1998) 283.

[10] Peter A., Torok G., Armstrong D. W., Toth G., Tourwe D., *J. Chromatogr. A, 828* (1998) 177.

[11] Joyce K. B., Jones A. E., Scott R. A., Biddlecombe R. A., Pleasance S., *Rapid Commun. Mass Spec., 12* (1998) 1899.

[12] Fried K. M., Koch P., Wainer I. W., *Chirality, 10* (1998) 484.

[13] Aboul-Enein H. Y., Serignese V., *Chirality, 10* (1998) 358.

[14] Tesarova E., Bosakova A., Pacakov V., *J. Chromatogr. A, 838* (1999) 121.

[15] Sun Q., Olesik S. V., *Anal. Chem., 71* (1999) 2139.

[16] Lehotay J., Hrobonová K., Krupcik J., Cizmárik J., *Pharmazie, 53* (1998) 863.

[17] Ekborg-Ott E. H., Wang X., Armstrong D. W., *Microchem. J., 62* (1999) 26.

[18] Scott R. P.W., Beesley T. E., *Analyst, 124* (1999) 713.

[19] Tesarova E., Zaruba K., Flieger M., *J. Chromatogr. A, 844* (1999) 137.

[20] Ramos L., Bakhtiar R., Majundas T., Hayes M., Tse F. L.S., *Rapid Commun. Mass Spec., 13* (1999) 2054.

[21] Bakhtiar R., Tse F. L.S., *Rapid Commun. Mass Spec., 14* (2000) 1128.

[22] Wang A. X., Lee J. T., Beesley T. E., *LCGC, 18* (2000) 626.

[23] Berthod A., Chen X., Kullman J. P., Armstrong D. W., Gasparrine F., D' Acquarica I., Villani C., Carotti A., *Anal. Chem., 72* (2000) 1767.

[24] Karlsson A., Aspergren A., *Chromatographia, 47* (1998) 189.

[25] Wang T., Chen Y. W., Vailaga A., *J. Chromatogr., 902* (2000) 345.

[26] Armstrong D. W., Lee J. T., Chang L. W., *Tet. Asym., 9* (1998) 2043.

[27] Armstrong D. W., He L., Yu T., Lee J. T., Liu Y.-S., *Tet. Asym., 10* (1999) 37.

CHAPTER 5. ASSIGNMENT OF ABSOLUTE CONFIGURATION OF A CHIRAL PHENYL-SUBSTITUTED DIHYDROFUROANGELICIN

A paper published in Organic and Biomolecular Chemistry[1]

Gennaro Pescitelli and Nina Berova
Dept. of Chemistry, Columbia University, 3000 Broadway, New York, NY 10027

Tom L. Xiao, Roman V. Rozhkov, Richard C. Larock and Daniel W. Armstrong
Department of Chemistry, Iowa State University, Ames, IA 50011

ABSTRACT

A phenyl-substituted chiral dihydrofuroangelicin, 4-methyl-8-(2-*E*-phenylethenyl)-8,9-dihydro-2*H*-furo[2,3-*h*]-1-benzopyran-2-one, synthesized in racemic form, has been resolved by HPLC chiral separation, and its absolute configuration determined by the non-empirical exciton chirality method. The solution conformation has been investigated through NMR and molecular modeling methods: two minima found by molecular mechanics and DFT methods are in keeping with observed ^{1}H–^{1}H ^3J coupling constants and NOE effects. The experimental CD spectrum for the second eluted enantiomer shows a positive couplet between 230 and 350 nm (amplitude A = + 15.7); by application of the exciton chirality method, the absolute configuration of this enantiomer at C8 is determined as (*S*). The experimental spectrum is in very good agreement with the one evaluated by means of DeVoe coupled-oscillator calculations, using the DFT calculated geometries.

---

[1]Reprinted with permission from Organic & Biomolecular Chemistry, 2003, 1, 186-190.
Copyright © the Royal Society of Chemistry 2003

5.1. INTRODUCTION

It is well known that many substituted furocoumarins are pharmacologically active. For example, they have been used for the treatment of skin diseases such as psoriasis and vitiligo.[1] Warfarin is an anticoagulant that depresses formation of prothrombin and also increases the fragility of capillaries which can lead to hemorrhages.[2] Recently, a variety of chiral, substituted dihydrofurocoumarins have been isolated as natural products and shown to have several useful pharmacological properties. For example, marmesin and columbionetin derivatives have been shown to exhibit cytotoxicity against KB cells,[3] to inhibit c-AMP (which affects coronary vasodilation),[4] and to mediate the action of acetylcholinesterase (which plays a role in Alzheimer's disease).[5] A related dihydropsoralen, isolated from *Dorstenia contrajerva*, may moderate the adverse effects of rattlesnake venom.[6]

Because of their importance, numerous syntheses of dihydrofurocoumarins have been published over the last 30 years.[7,8] The earlier methods were characterized by numerous steps (8 to 10) and relatively low yields (2–20%).[7] Later methods have required fewer steps and generally produce higher yields.[8] One of the most recent and more general approaches involves the palladium catalyzed annulation of 1,3-dienes by *o*-iodoumbelliferones.[9] This annulation proceeds in 70–85% yields with a variety of 1,3-dienes.[9] Numerous substituted dihydrofuroangelicins **1** and dihydrofuropsoralens **2** (Chart 1) have been produced *via* this approach.

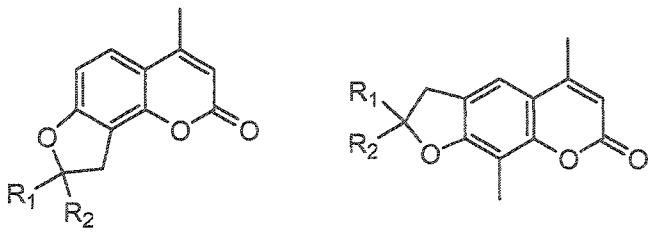

1 2

Chart 1.

Although these compounds are usually chiral (when $R_1 \neq R_2$), no efficient asymmetric synthesis has yet been reported. Also, the absolute configuration of some of the natural products has not been determined. In cases where one of the substituents (R_1 or R_2 above) contains an aromatic moiety, the possibility exists of using the exciton chirality method to determine the absolute configuration of these compounds. To test this possibility, compound **3** (Chart 2) was synthesized, resolved, and its absolute configuration investigated.

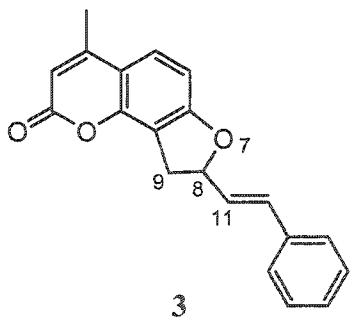

3

Chart 2.

The exciton chirality method is a convenient and versatile approach for the structural investigation of chiral organic molecules when their absorption and circular dichroism

spectra are dominated by intense electric dipole allowed transitions, such as the ones allied to strong aromatic chromophores.[10] Any electric dipole allowed transition may be described in terms of a transition dipole moment. When two transition dipole moments are close in energy, lie near to each other in space and form a chiral array, their through-space interaction gives rise to distinctive spectral features: in the CD spectrum, a bisignate couplet is obtained whose sign is determined by the absolute sense of twist defined by the two dipoles; a positive twist corresponds to a positive couplet (*i.e.*, with a positive long-wavelength branch), and *vice versa*. If the direction of transition dipoles within the molecular geometry is known, the absolute configuration may be derived.[10] The presence of conformational ambiguity, or an unsuitable geometrical arrangement between dipoles, however, may preclude the straightforward application of this method.[11]

Full exciton-coupled CD spectra can be calculated with various methods; DeVoe coupled-oscillator calculations[12,13] have been widely used for small organic molecules and polymers.[14] The parameters necessary for the calculations are: (1) the molecular geometry, determined through experimental techniques and molecular modeling; (2) the spectral parameters (transition frequency, dipolar strength and bandwidth) extracted from the absorption spectra of the isolated chromophores; (3) position and direction of transition moments, usually determined by quantum mechanical calculation methods.

The inspection of the molecular structure of **3** (Chart 2) commends attention to the exciton chirality method as a most suitable approach for the determination of the absolute configuration in this case. This compound is in fact endowed with two strong aromatic chromophores (the coumarin and the styrene) located nearby in space, which give rise to intense electronic absorptions close in energy. Moreover, the spatial arrangement between

the two chromophores, investigated through CD, will largely depend and be sensitive to the absolute configuration at the stereogenic center.

By taking into consideration these characteristic features of **3**, we performed molecular mechanics and DFT modeling, as well as CD and NMR experimental studies, before applying DeVoe calculations of circular dichroic properties.

5.2. Results and discussion

Molecular modeling

The molecular conformation of **3** was investigated through a combination of molecular mechanics and DFT calculations. The whole conformational space was sampled by means of Monte Carlo (MC) simulations[15] with the molecular Merck force field (MMFFs), which is known to be very accurate for small organic molecules.[16] MC/MMFFs calculations, run in $CHCl_3$, reveal the presence of two main degrees of freedom, related to the five-membered ring conformation and the rotation around the C8–C10 bond, described through the H8–C8–C10–H10 dihedral angle d_1 (Scheme 1a). Six minimum energy conformations were found overall by MC/MMFFs, which were further optimized by DFT calculations with B3LYP/6-31G** in $CHCl_3$, resulting in the two structures shown in Scheme 1a as the lowest energy minima. In conformer I, the substituent occupies the pseudo-equatorial, and in conformer II the pseudo-axial position of the five-membered ring. In both structures the C=C styrene double bond is *syn* to the C8–H8 bond, with $d_1 \approx 175°$. The four other minima have energies higher than 6 kJ mol^{-1} with respect to conformer I and negligible Boltzmann populations at room temperature.

Scheme 1.

(a) DFT calculated conformations

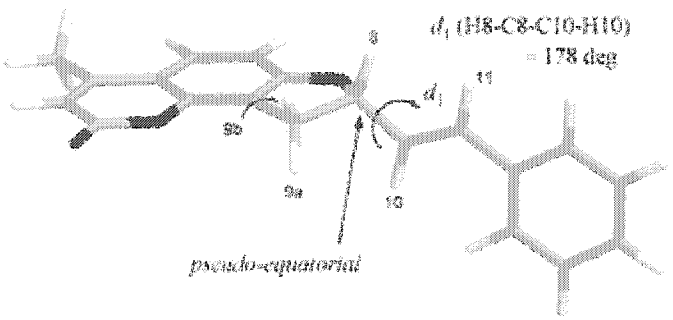

Conformer I
(absolute minimum)

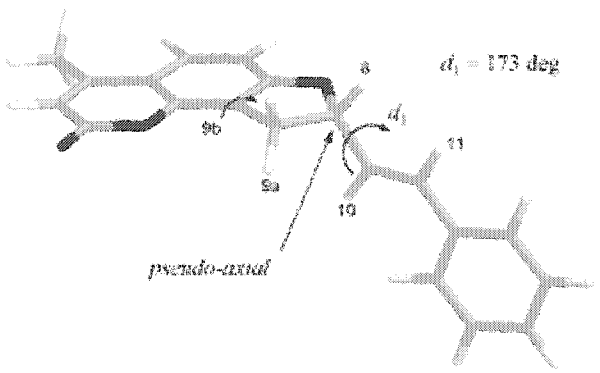

Conformer II
(relative E = + 1.4 kJ/mol)

(b) Relevant NMR data

Relative NOE's:
- 8-9b >> 8-9a
- 9a-10 > 9a-11
- 8-11 >> 8-10

^3J's:
- 8-9a: 7.5 Hz
- 8-9b: 9.4 Hz
- 8-10: 7.4 Hz

NMR spectra

^{1}H NMR spectroscopy and, in particular, the chemical shifts, the ^3J couplings and the relative NOE's between protons H8, H9, H10 and H11 (Chart 2 and Scheme 1), have been used to check the conformational picture arising from molecular modeling.

Only one set of signals is apparent in the ^{1}H NMR spectrum in $CDCl_3$, proving that either only one conformer is present, or the interconversion between conformers is fast on the NMR timescale; this is expected for the five-membered ring flip and the rotamerism around the C8–C10 bond. Proton H9a is upfield shifted with respect to H9b by 0.4 ppm, and may be assigned a pseudo-axial position, considering both that axial protons generally resonate upfield of equatorial ones,[17] and that the equatorial H9b is subjected to the deshielding effect of the phenyl ring current shift. Based on the relative NOE's (Scheme 1b), derived from a NOESY spectrum (not shown), proton H8 is closer and *cis* to H9b, and *trans* to H9a; this is also substantiated by the different values of ^3J ($J_{H8,H9a}$ = 7.5 Hz, $J_{H8,H9b}$ = 9.4 Hz) analyzed through the Karplus equation.[18] Thus, proton H8 lies in a pseudo-axial position, and the substituent at the stereogenic center occupies a preferred pseudo-equatorial position; this is the same situation occurring for the absolute minimum (Scheme 1a, conformer I) found by DFT.

The value of $J_{H8,H10}$ = 7.42 Hz, analyzed through a Karplus-type equation for vinylic/allylic protons,[19] leads to an estimated H8–C8–C10–H10 average dihedral angle $d_1 \approx 140°$; structures with large values of d_1 are therefore dominant in solution, in agreement with the modeling results. This geometry around the C8–C10 bond is further confirmed by the strong NOE's between protons H8/H11 and H9a/H10 (Scheme 1b). It may be concluded that the DFT

results faithfully depict the conformational situation in solution, and can be confidently used for the subsequent CD calculations.

Chromophore electronic structure

The UV absorption spectrum of compound **3** above 230 nm (Fig. 1, bottom) is dominated by the π–π^* transitions of the aromatic chromophores. Two maxima are detected at 321 nm (ϵ = 12700 M^{-1} cm^{-1}) and 252 nm (ϵ = 23000 M^{-1} cm^{-1}) in acetonitrile, allied respectively to the conjugation or K bands of the coumarin and styrene chromophores.[20]

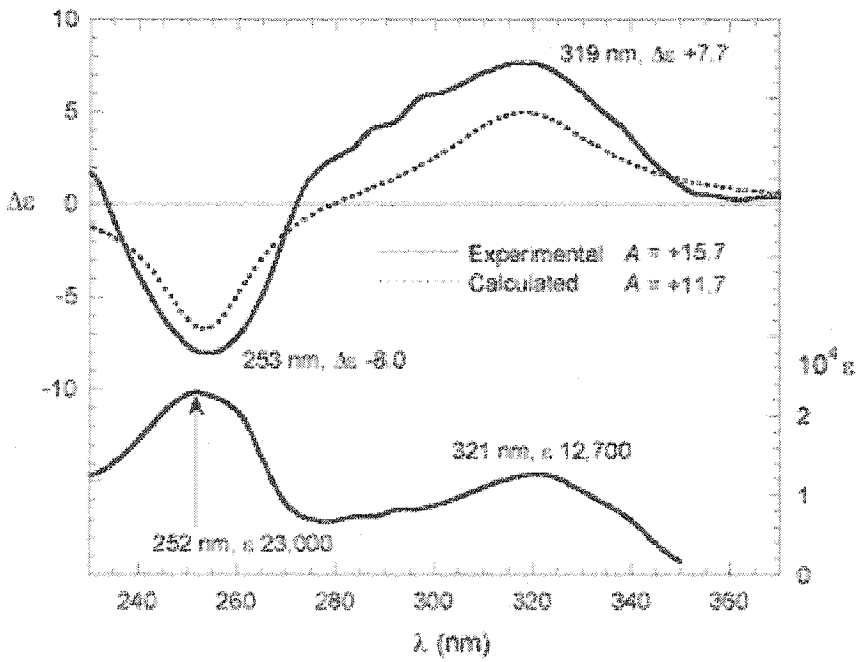

Fig. 1 UV (bottom) and CD (top) spectra of compound **3** in acetonitrile. Top, solid line: experimental CD spectrum for second eluted enatiomer 1.84×10^{-5}M in acetonitrile. Top, dotted line: CD calculated as Boltzmann average of DFT derived structures for the (*S*) configuration, with the DeVoe method and parameters as in Table 1 and Scheme 2.

The relevant parameters for DeVoe calculations have been extracted from the UV spectra of 7-hydroxy-4,8-dimethylcoumarin in acetonitrile and styrene in hexane,[21] and adapted to reproduce better the UV spectrum of **3**, and are reported in Table 1. Both transitions have long-axis polarization in the respective ring systems. Due to the presence of substituents (in particular, the oxygen at position 7, Chart 2), the exact polarization of the coumarin transition needed to be calculated. By a CNDO-S/CI calculation on 7-hydroxy-4,8-dimethylcoumarin (geometry obtained with DFT, B3LYP/6-31G**), we found a small rotation (<5°) between the transition dipole and the coumarin ring long axis (as shown in Scheme 2).

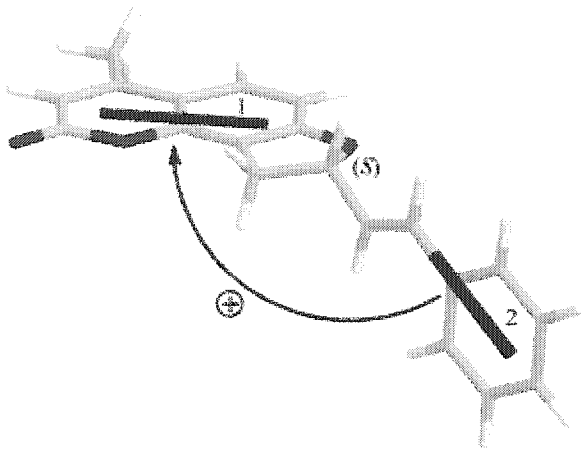

Scheme 2.

Table 1. Spectroscopic parameters[(a)] of electronic transitions of compound RR-210 used for DeVoe's calculations.

#	Type	λ_{max}/nm	D/D^2	ν_{max}/cm^{-1}	$\Delta\nu_{1/2}/cm^{-1}$
1	Coumarin[(b)]	318	20	31,400	4,000
2	Styrene[(c)]	254	30	39,400	3,600

[(a)] λ_{max} wavelength maximum; D dipolar strength; ν_{max} frequency maximum; $\Delta\nu_{1/2}$ half-height width.
[(b)] From UV spectrum of 7-hydroxy-4,8-dimethyl coumarin in acetonitrile.
[(c)] From UV spectrum of styrene in hexane (ref. 21).

CD spectrum, exciton chirality method and DeVoe calculation

The experimental CD spectrum of the second eluted enantiomer (Fig. 2; see Experimental Section for chiral HPLC conditions) of **3** in acetonitrile (Fig. 1, top, solid line) shows a positive couplet between 230 and 350 nm with a peak at 319 nm, $\Delta\varepsilon = +7.7$, a trough at 253 nm, $\Delta\varepsilon = -8.0$, and couplet amplitude $A = +15.7$. The symmetrical appearance of the couplet supports its interpretation as being due to non-degenerate exciton coupling between the two above discussed transitions, with small interference from higher energy ones. Integrated rotational strengths are $+2.5 \times 10^{-39}$ and -1.8×10^{-39} cgs units, respectively; the negative low wavelength branch is partially cancelled by superimposition with the positive Cotton effect appearing at higher energies.

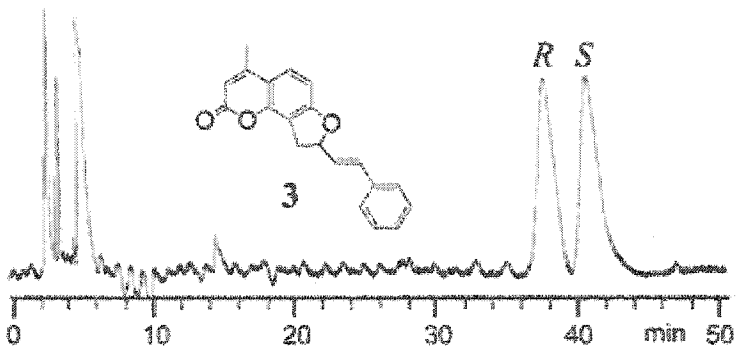

Fig. 2 HPLC chromatogram of the enantiomeric separation of compound **3**. The chromatogram was obtained using a Chirobiotic T column and a hexane plus 2% ethanol (by volume) mobile phase. The flow rate was 1.0 mL min^{-1}. See the Experimental section for further details. The absolute configurations (*S* and *R*) of the first and the second eluted enantiomers for **3** were determined as outlined in the Results and discussion.

Therefore, the absolute configuration of **3** can be assigned by the exciton chirality analysis of the experimental CD. By inspection of the molecular structure of the (*S*) enantiomer in the lowest energy conformation I (Scheme 2), it is apparent that the two above discussed

transition dipoles define a positive chirality (that is, the transition moment 2 in front may be superimposed on the moment 1 in the back after a *clockwise* rotation). The same is true for the (*S*) enantiomer in the conformation II. Thus, the second eluted enantiomer, showing a positive CD couplet between 230 and 350 nm, may be assigned the (*S*) configuration.

Furthermore, this assignment is confirmed by quantitative CD theoretical calculations using the DeVoe method and the spectral and geometrical parameters discussed above, placing the dipoles in the middle of the styrene and coumarin chromophores (Scheme 2). The CD calculated as a Boltzmann-weighted average at room temperature for conformers I and II with an (*S*) configuration, shows a positive couplet with amplitude A = 11.7 (Fig. 1, top, dotted line), in good agreement with the experimental spectrum for the second eluted enantiomer. Other conformations with higher energies have calculated CD with intensities comparable to the ones for the first two, and after weighing with respective Boltzmann factors they give a negligible contribution. Small displacement (within 0.3Å) and/or rotations (within 10°) of dipoles affected the calculated CD intensity only to a minor extent, and in no case was the sign reversed. Thus, DeVoe CD calculations can be reliably applied for the present configurational assignment.

5.3. Conclusion

The absolute configuration of a chiral, phenyl-substituted dihydrofuroangelicin (compound **3**) has been assigned by means of the exciton chirality method and DeVoe CD calculations. The solution structure of **3** has been determined by NMR spectroscopy and molecular modeling with molecular mechanics and DFT methods. The spectroscopic parameters necessary for the CD calculations have been extracted from the UV spectra of isolated

chromophores, and calculated by a CNDO method. The second eluted enantiomer of **3** (Fig. 2), with positive CD at 319 nm and negative CD at 253 nm, has an (*S*) absolute configuration.

5.4. EXPERIMENTAL AND COMPUTATIONAL SECTION

General procedures

HRMS experiments were performed on the Kratos MS50TC double focusing magnetic sector mass spectrometer using EI at 70 eV. IR spectra were performed on the IR-Bomen Michelson MB-102 FT-IR spectrometer.

^{1}H and ^{13}C spectra were recorded at 400 and 100.5 MHz respectively using a Varian 400 MHz instrument, and chemical shifts are reported in ppm relative to TMS (δ), with coupling constants (J) in Hz; proton numbering refers to Chart 2. ^{1}H-NOESY spectrum was recorded at 600 MHz using a Varian Unity INOVA 600 with 1.5 s mixing time.

The UV spectrum for **3** was recorded on a Varian Cary 100 Bio UV-VIS spectrophotometer. The molar absorptivity was determined at three wavelengths (204 nm, 252 nm, and 321 nm). The concentration of all samples was adjusted so that their absorbance was in the range of 0.2 and 1.5 absorbance units. The molar absorptivities of **3** are: 59000, 23000, and 12700 at the aforementioned three wavelengths respectively.

CD spectra were measured in spectroscopy grade acetonitrile with a Jasco J-810 spectropolarimeter, using a 1 cm cell, and the following conditions: SBW 1 nm, 50 nm min^{-1}, response 1 s, 8 scans.

MC/MMFFs and DFT calculations were run respectively with MacroModel 7.1 and Jaguar 4.1 (Schrödinger, Inc., Portland, OR).[22]

CNDO/S–CI calculations were run with a CNDO/M program, according to Del Bene and Jaffé's formulation,[23] with Mataga approximation of two-electron repulsion integrals, including in the CI up to 648 singly excited states, with maximum energy values of 7.0 eV.

DeVoe calculations were run with a Fortran program due to Hug and co-workers.[13]

Synthesis of the dihydrofuroangelicin 4-methyl-8-(2-*E*-phenylethenyl)-8,9-dihydro-2*H*-furo[2,3-*h*]-1-benzopyran-2-one (**3**) was accomplished by annulation of (*E*)-1-phenylbuta-1,3-diene by the corresponding 7-acetoxy-8-iodo-4-methylcoumarin as reported elsewhere (Scheme 3).[9]

Mp 145–148 °C; ^{1}H NMR ($CDCl_3$) δ/ppm 2.32 (3 H, d, $J_{CH3,3}$ = 0.8 Hz, CH_3), 3.16 (1 H, dd, $J_{H9a,H9b}$ = 16.1 Hz, $J_{H9a,H8}$ = 7.5 Hz, H9a), 3.55 (1 H, dd, $J_{H9b,H9a}$ = 16.1 Hz, $J_{H9b,H8}$ = 9.4 Hz, H9b), 5.49 (1 H, m, $J_{H8,H9b}$ = 9.4 Hz, $J_{H8,H9a}$ = 7.5 Hz, $J_{H8,H10}$ = 7.4 Hz, $J_{H8,H11}$ = 1.0 Hz, H8), 6.03 (1 H, d, $J_{3,CH3}$ = 0.8 Hz, H3), 6.28 (1 H, dd, $J_{H10,H11}$ = 15.8 Hz, $J_{H10,H8}$ = 7.4 Hz, H10), 6.67 (1 H, dd, $J_{H11,H10}$ = 15.8 Hz, $J_{H11,H8}$ = 1.0 Hz, H11), 6.72 (1 H, d, $J_{H6,H5}$ = 8.4 Hz, H6), 7.17–7.36 (5 H, m), 7.35 (1 H, d, $J_{H5,H6}$ = 8.4 Hz, H5); ^{13}C NMR ($CDCl_3$) δ19.24, 33.28, 85.90, 106.77, 111.50, 113.69, 114.34, 125.76, 126.97, 127.33, 128.51, 128.85, 133.32, 136.02, 151.10, 153.26, 161.28, 163.44; IR (neat) 3050 (=CH), 1727 (C=O), 1615 (C=C) cm^{-1}; HRMS for $C_{20}H_{16}O_3$ found: 304.1104, calc.: 304.1099.

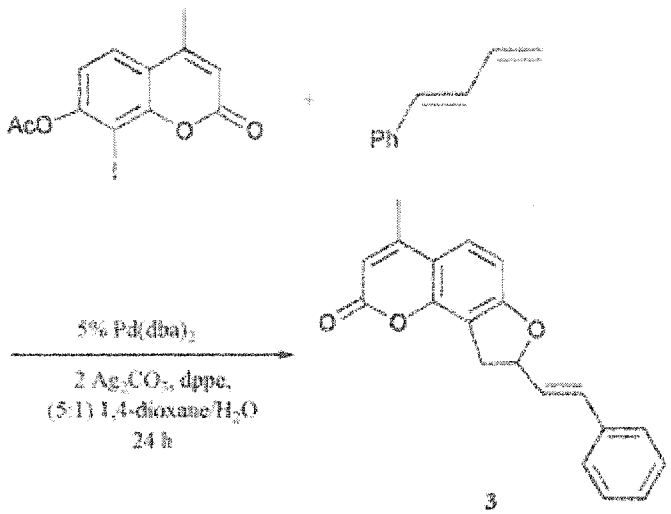

Scheme 3

The enantiomeric separation of racemic **3** was performed on an HP 1050 HPLC system equipped with UV detector, auto-injector, and computer controlled Chem-station data processing software. Both preparative and analytical separations were carried out using a Chirobiotic T, 250 × 4.6 mm id, (Advanced Separation Technologies Inc., Whippany, NJ) column[24] with baseline resolution and very good reproducibility (Fig. 2). The first eluted and second eluted peaks were collected manually. The normal phase mode was used for the enantiomeric separation with a mobile phase of hexane and 2% (by volume) ethanol. The injection volume was 2 μL. Separations were carried out isocratically at a flow rate of 1 mL min^{-1} at room temperature (22 °C). The mobile phase was premixed and degassed under vacuum conditions. All HPLC grade solvents were purchased from Fisher Chemical. Detection wavelengths were monitored at both 254 nm and 220 nm for confirmation that the same peak absorption ratio for the enantiomer pairs occurred.

ACKNOWLEDGEMENTS

Dr Lorenzo Di Bari, University of Pisa, is gratefully thanked for the help in NMR measurements. D.W.A. and T.L.X. acknowledge NIH grant RO1 GM53825–07 for partial support of this work. N.B. acknowledges NIH grants GM 34509 and GM 36564 for financial support. G.P. acknowledges the Italian C.N.R. grant (203.03.26) for financial support. R.V.R. and R.C.L. acknowledge the donors of the Petroleum Research Fund, administered by the American Chemical Society, for partial support of this research, and Kawaken Fine Chemicals Co., Ltd., and Johnson Matthey, Inc. for donations of $Pd(OAc)_2$ and PPh_3.

REFERENCES

1. G. Rodigliero, *J. Photochem. Photobiol., B*, 1992, **14**, 1–22.

2. R. G. Bell, J. A. Sadowski and J. T. Matschiner, *Biochemistry*, 1972, **11**, 1959–1961.

3 D. Guilet, J.-J. Helesbeux, D. Seraphin, T. Sevenet, P. Richomme and J. Bruneton, *J. Nat. Prod.*, 2001, **64**, 563–567.

4. O. Thastrup, B. Fjalland and J. Lemmich, *Acta Pharmacol. Toxicol.*, 1983, **52**, 246–250.

5. S. Y. Kang, K. Y. Lee, S. H. Sung, M. J. Park and Y. C. Kim, *J. Nat. Prod.*, 2001, **64**, 683–685.

6. R. Tovar-Miranda, R. Cortes-Garcia, N. F. Santos-Sanchez and P. Joseph-Nathan, *J. Nat. Prod.*, 1998, **61**, 1216–1220.

7. (*a*) W. Steck, *Can. J. Chem.*, 1971, **49**, 1197–1201; (*b*) S. Yamaguchi, R. Miyakawa, S. Yonezawa and Y. Kawase, *Bull. Chem. Soc. Jpn.*, 1989, **63**, 3593–3597.

8. (*a*) J. T. Trumble and J. G. Millar, *J. Agric. Food. Chem.*, 1996, **44**, 2859–2864; (*b*) V. Stanjek, M. Milksch and W. Boland, *Tetrahedron*, 1997, **53**, 17699–17710.

9. R. V. Rozhkov and R. C. Larock, *Org. Lett.*, 2002, in press.

10. (*a*) N. Harada and K. Nakanishi, *Circular Dichroic Spectroscopy –Exciton Coupling in Organic Stereochemistry*, University Science Books, Mill Valley, CA, 1983; (*b*) N. Berova, K. Nakanishi, in *Principles and Applications of Exciton Chirality Method*, ed. N. Berova, K. Nakanishi, and R. Woody, Wiley-VCH, New York, 2000.

11. R. Person, K. Monde, H.-U. Humpf, N. Berova and K. Nakanishi, *Chirality*, 1995, **7**, 128–135.

12. (*a*) H. DeVoe, *J. Chem. Phys.*, 1964, **41**, 393–400; (*b*) H. DeVoe, *J. Chem. Phys.*, 1965, **43**, 3199–3208; (*c*) C. Rosini, M. Zandomeneghi and P. Salvadori, *Tetrahedron: Asymmetry*, 1993, **4**, 545–554.

13. C. L. Cech, W. Hug and I. Tinoco, Jr., *Biopolymers*, 1976, **15**, 131–152.

14. (*a*) F. Castronovo, M. Clericuzio, L. Toma and G. Vidari, *Tetrahedron*, 2001, **57**, 2791–2798; (*b*) L. Di Bari, G. Pescitelli, G. Reginato and P. Salvadori, *Chirality*, 2001, **13**, 548–555; (*c*) C. Rosini, M. I. Donnoli and S. Superchi, *Chem. Eur. J.*, 2001, **7**, 72–79; (*d*) L. Di Bari, S. Mannucci, G. Pescitelli and P. Salvadori, *Chirality*, 2002, **14**, 611–617; (*e*) A. olladié-Cavallo, C. Marsol, G. Pescitelli, L. Di Bari, P. Salvadori, X. Huang, N. Fujioka, N. Berova, X. Cao, T. B. Freedman and L. A. Na.e, *Eur. J. Org. Chem.*, 2002, 1788–1796.

15. G. Chang, W. C. Guida and W. C. Still, *J. Am. Chem. Soc.*, 1989, **111**, 4379–4386.

16. T. A. Halgren, *J. Comput. Chem.*, 1996, **17**, 490–519.

17. E. L. Eliel and S. H. Wilen, *Stereochemistry of Organic Compounds*, Wiley-Interscience, New York, 1994.

18. From the Karplus equation $3J = 7 - \cos\phi + 5\cos 2\phi$, where ϕ is either the H8–C8–C9a–H9a (ϕ **8–9a**) or the H8–C8–C9b–H9b (ϕ **8–9b**) dihedral angle, two possible sets of values

are obtained: (1) ϕ **8–9a** = 23 and ϕ **8–9b** = 134°, or (2) ϕ **8–9a** = 144 and ϕ **8–9b** = 37°. Only the first set is consistent with the DFT molecular models.

19. E. W. Garbisch, Jr., *J. Am. Chem. Soc.*, 1964, **86**, 5561–5564.

20. (*a*) R. A. Friedel and M. Orchin, *Ultraviolet Spectra of Aromatic Compounds*, Wiley, New York, 1951; (*b*) H. H. Ja.é and M. Orchin, *Theory and Applications of Ultraviolet Spectroscopy*, Wiley, New York, 1962; (*c*) L. Salem, *The Molecular Orbital Theory of Conjugated Systems*, Benjamin, New York, 1966.

21. A. Kaito, A. Tajiri and M. Hatano, *J. Am. Chem. Soc.*, 1976, **98**, 384–388.

22. F. Mohamadi, N. G. J. Richards, W. C. Guida, R. Liskamp, M. Lipton, C. Cau.eld, G. Chang, T. Hendrickson and W. C. Still, *J. Comput. Chem.*, 1990, **11**, 440–467.

23. J. Del Bene and H. H. Ja.e, *J. Chem. Phys.*, 1968, **49**, 1221–1229.

24. D. W. Armstrong, Y. Liu and H. K. Ekborg-Ott, *Chirality*, 1995, **7**, 474–497.

CHAPTER 6.
ABSOLUTE STEREOCHEMISTRY OF DIHYDROFUROANGELICINS BEARING C-8 SUBSTITUTED DOUBLE BONDS: A COMBINED CHEMICAL/EXCITON CHIRALITY PROTOCOL

A Paper published in Organic & Biomolecular Chemistry[1]

Katsunori Tanaka, Gennaro Pescitelli, Lorenzo Di Bari, Koji Nakanishi, and Nina Berova
Department of Chemistry, Columbia University, New York, New York 10027, USA;

Tom L. Xiao and Daniel W. Armstrong
Department of Chemistry, Iowa State University, Ames, IA 50011, USA

ABSTRACT

Coumarins are associated with a variety of pharmacological activities which have led to the synthesis of numerous derivatives. However, no general method for determination of the absolute configuration of chiral coumarins is known. This has now been achieved for a series of dihydrofuroangelicins bearing a variety of C-8 substituted double bonds, synthesized in the racemic form and resolved through enantioselective chromatography. A combined chemical/chiroptical protocol has been developed in which the C=C double bonds are replaced with a styrenoid chromophore through either (i) cross metathesis, (ii) Heck reaction, or (iii) a combined method of cross metathesis and Heck reaction with about 1 mg sample under mild conditions. The coupling between the styrenoid and coumarin chromophores

---

[1]Reprinted with permission from Organic & Biomolecular Chemistry, 2004, 2, 48-58.
Copyright © the Royal Society of Chemistry 2004

gives rise to clear-cut exciton coupled CD curves, suitable for assignments of absolute configurations. The solution conformation of the styrenoid derivatives is determined by NMR and DFT molecular modeling; the electronic structure of the 7-hydroxy coumarin chromophore is also clarified by semi-empirical and TDDFT methods. The conformation thus derived, in conjunction with quantitative DeVoe's coupled-oscillator CD calculation, establishes the absolute configurations of the coumarins. The theoretical study described herein justifies the straightforward approach of the current chemical/exciton chirality protocol to this type of dihydrofuroangelicins.

6.1. INTRODUCTION

Coumarins exhibit various pharmacological activities.[1] Marmesin and columbianetin derivatives are cytotoxic against KB cells,[2] inhibit cAMP[3] and mediate the action of acetylcholinesterase involved in Alzheimer's disease, while a related dihydropsoralen, from *Borstenia contrajerva*, is reported to moderate the toxicity of rattlesnake venom.[4] Warfarin is an anticoagulant (the *S* isomer is more potent) that depresses the formation of prothrombin,[5] while synthetic coumarins have been used for treating skin diseases such as psoriasis and vitiligo.[6] Such conspicuous pharmacological activities have led to numerous syntheses of chiral coumarins over the past 30 years, including the recent preparations of substituted dihydrofuroangelicins **A** and dihydrofuropsoralens **B** (Chart 1).[7] This method relies on the palladium catalyzed annulation of 1,3-dienes by *o*-iodoumbelliferones, proceeding in 70–85% yields with a variety of 1,3-dienes; many substituted furocoumarins **A** and **B** have been synthesized using this route. Although efficient enantiomeric separations of these compounds have been reported,[8] no efficient method to determine their absolute configurations (when

$R_1 \neq R_2$) is known. In general, the assignment of the absolute configuration of chiral coumarin and isocoumarin derivatives has relied on chemical correlations with compounds of known configuration,[9] empirical comparisons of optical rotations and CD curves,[10] or other empirical approaches such as Horeau's or modified NMR Mosher's method.[11]

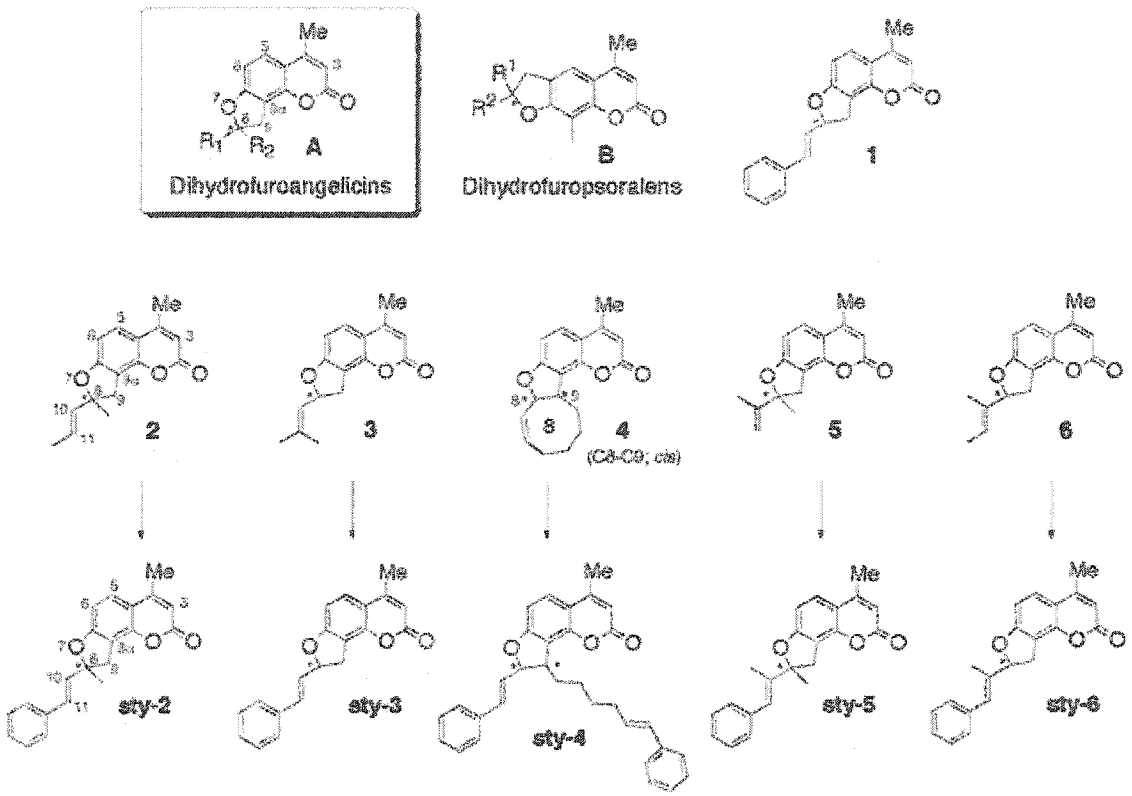

Chart 1 The structures of various C-8 alkenyl substituted dihydrofuroangelicins and their corresponding styrene derivatives.

The circular dichroic (CD) exciton chirality method is a reliable non-empirical approach based on the coupled-oscillator theory, which has been widely employed for determining the absolute configuration of various organic compounds, including many natural products.[12] In the context of coumarin chemistry, the application of the exciton method has so far been

limited to rigid dimers;[13] on the other hand, it is noteworthy that a coumarin-based chromophore, 7-diethylaminocoumarin-3-carboxylic acid, has been recently proposed as an exciton CD-reporter group.[14] In view of the potentiality offered by the presence of the coumarin chromophore in compounds **A** and **B** (Chart 1), it was considered that if a suitable chromophore were present at C-8, it might lead to diagnostic exciton coupling with the coumarin moiety and allow determination of the absolute configuration.

This strategy was tested with one of the synthetic chiral dihydrofuroangelicins, 4-methyl-8-(2-*E*-phenylethenyl)-8,9-dihydro-2*H*-furo[2,3-*h*]-1-benzopyran-2-one **1**.[15] This compound was already endowed with a styrenoid chromophore which coupled favorably with the coumarin moiety due to the proximity of their UV bands. In fact, the CD spectrum of **1** showed a moderately intense CD couplet in the 240–330 nm region, in correspondence with the two more intense red-shifted electronic absorptions of the styrene and coumarin chromophores. The solution conformation of **1** was elucidated by NMR and molecular modeling, and the interchromophoric arrangement turned out to be sensitive to the absolute configuration at the stereogenic center. Application of the exciton chirality approach, substantiated by quantitative CD calculations by means of DeVoe's method, afforded assignment of the absolute configuration of **1** in a non-empirical manner.[15]

On the basis of these results, we report herein a general protocol for the determination of absolute configurations of dihydrofuroangelicins **2–6** linked at C-8 to variously substituted double bonds (R_1 or R_2, Chart 1). As shown in Fig. 1 for chiral furocoumarins **2**, **5**, and **6**, these compounds have weak CD spectra above 200 nm; in particular, the intense red-shifted coumarin π–π^* transition (band I at λ_{max} *ca.* 320 nm, ϵ= 13000) gives rise to only modest Cotton effects. It is conceivable that some contributions to the observed CD arise from the

exciton coupling between the coumarin and the lowest energy π—π * transition of the C=C double bond (*ca.* 195 nm, ϵ12000); however, the latter is clearly obscured by overlap with other transitions around 200 nm. In conclusion, the weakness of these bands and absence of a clear-cut exciton feature hampers direct application of the exciton chirality.

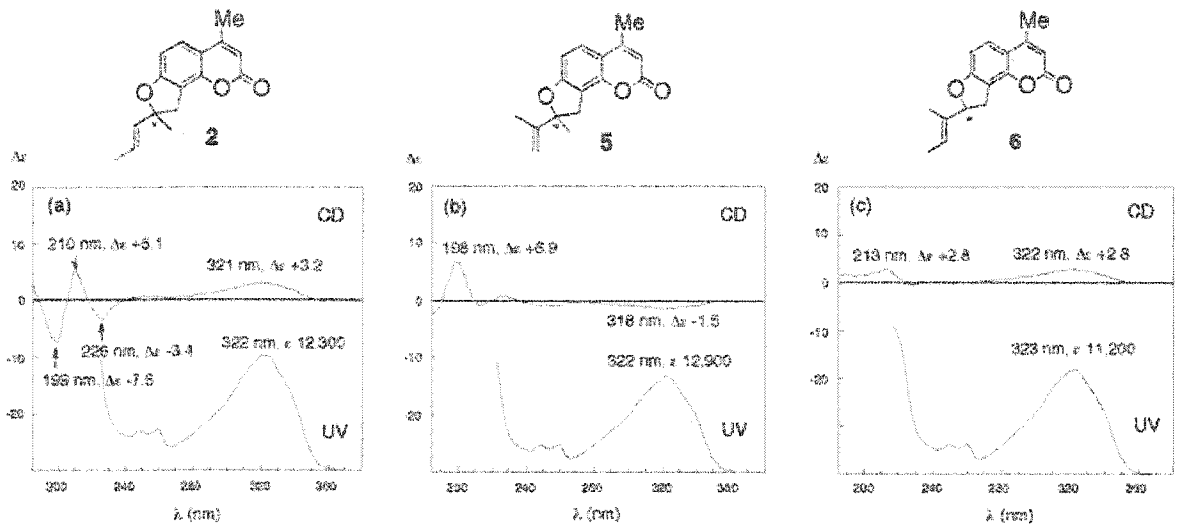

Fig. 1 UV (bottom) and CD (top) spectra of dihydrofurocoumarins **2**, **5**, and **6** in acetonitrile. Spectrum (a), first eluted enantiomer of **2** separated by chiral HPLC, 4.16×10^{-4} M; spectrum (b), first eluted enantiomer of **5** separated by chiral HPLC, 6.46×10^{-4} M; spectrum (c), first eluted enantiomer of **6** separated by chiral HPLC, 4.34×10^{-4} M. HPLC methodologies are given in reference 8.

Therefore, it was desirable to devise a scheme that converts the side chain double bond of dihydrofuroangelicins **2**–**6** into other suitable chromophores, for example, a styrenoid (K band at λ_{max} 248 nm, ϵ= 15000),[16] that would couple more effectively with the coumarin. Moreover, considering the scarcity of such chiral coumarins either from natural sources or upon enantioselective separation of racemates, it was important to have an efficient micro-scale method to convert the variously substituted double bonds into aromatic chromophores

under mild conditions, leaving the coumarin moiety intact. Once the derivatization into suitable styrenoid chromophores was achieved, the corresponding CD spectra were found to be suitable for a straightforward exciton analysis. Prior to this, the solution conformations were extensively studied by means of NMR and DFT molecular modeling. Moreover, the qualitative exciton chirality assignment was substantiated by means of quantitative CD calculations run with DeVoe's method;[17] to provide better parameters for DeVoe calculations, the electronic structure of 7-hydroxy coumarin chromophore was also investigated with semi-empirical and time-dependent DFT techniques. The agreement between experimental and calculated CD (Boltzmann-weighted average for DFT-computed structures) allowed the absolute configuration of these furocoumarins to be established. Furthermore, the results from theoretical studies provide a sound basis for application of the combined chemical/chiroptical approach described in this paper to new C-8 alkenyl dihydrofuroangelicin analogs in a straightforward manner without extensive conformational analysis and CD calculations.

6.2. RESULTS AND DISCUSSION

Derivatization of dihydrofuroangelicins (2–6) into the styrenoid derivatives

The initial strategy for the conversion of dihydrofuroangelicins **2–6** (Chart 1) into styrene derivatives is shown in Scheme 1. The dihydrofuroangelicins would be converted to the corresponding carbonyl compounds *via* the oxidative cleavage of the double bonds directly by ozonolysis or by the two-step procedure of dihydroxylation with osmium tetroxide (OsO_4) followed by treatment with sodium periodate ($NaIO_4$). Then, these carbonyl compounds were thought to react with Wittig reagents to provide the styrenoid derivatives. This strategy was

first tested on racemic **2** and **5**, which were prepared in a large quantity according to the established method of palladium catalyzed annulation of 1,3-dienes by *o*-iodoumbelliferones.[7] Thus racemic **2** was reacted with a catalytic amount of OsO_4 in the presence of two equivalents of $NaIO_4$ for three hours at room temperature to give the corresponding aldehyde **7** in 44% yield. The employment of $OsO_4/NaIO_4$ oxidant was preferable to ozonolysis, because the exact amount of the reagent could be measured, thus avoiding over-oxidation of the coumarin double bond. When aldehyde **7** was reacted with Horner–Emmons reagent, diethyl benzylphosphonate, at 100 °C in THF, the corresponding (*E*)-styrene derivative of **2** was obtained with very low yield (less than 5% yield) and most of the starting material **7** was recovered. Presumably this was due to the sterically hindered quaternary carbon atom next to the aldehyde group in **7**.

Furthermore, the treatment of racemic **5** with $OsO_4/NaIO_4$ oxidant unexpectedly provided the diols **8a** and **8b** in 1 : 1 diastereomeric ratio in 48% yield, without any trace of the carbonyl derivative even at elevated temperatures. The resistance of these diols toward $NaIO_4$ oxidation might be related again to the steric hindrance around the two consecutive quaternary carbon centers in **8a** and **8b**. Namely, the oxidant $NaIO_4$ would fail to access the diols to form the corresponding cyclic iodoester that provides the ketone derivative. Therefore, it was concluded that conventional oxidative cleavage of the double bonds followed by Wittig chemistry is not applicable for derivatization of these sterically hindered furocoumarins such as **2** and **5**.

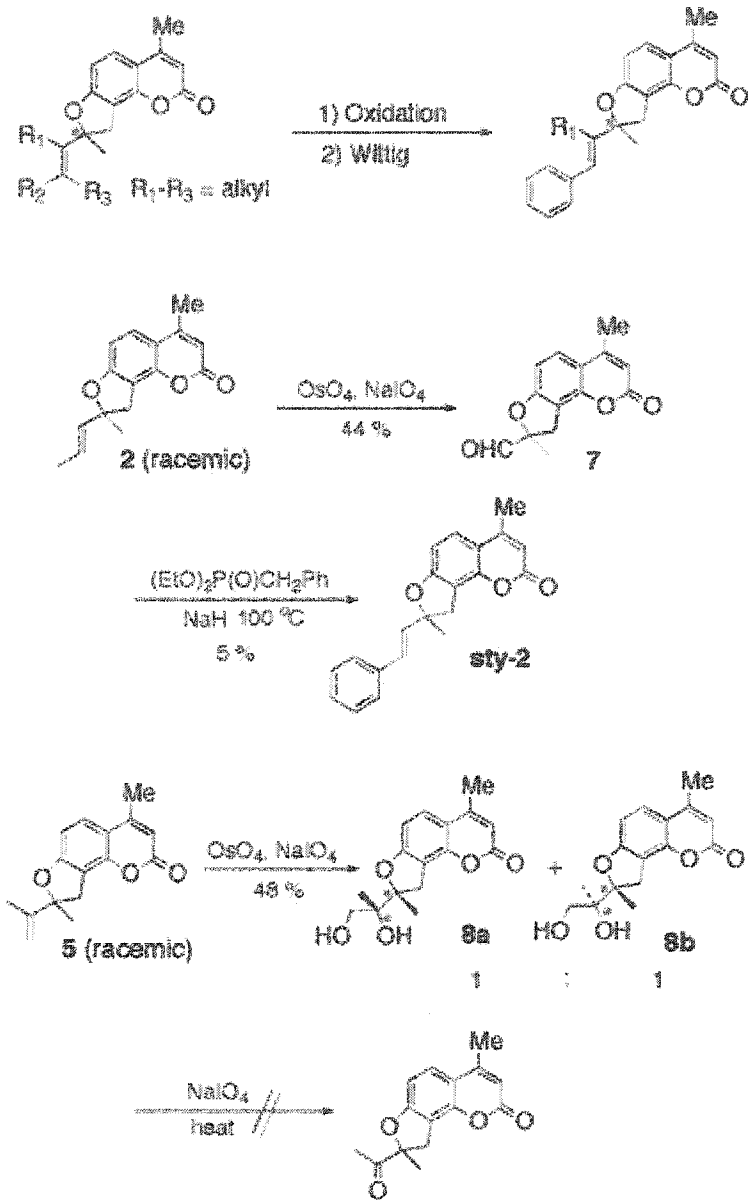

Scheme 1 Initial trials for conversion of **2** and **5** into styrenoids *via* an oxidation–Wittig strategy.

On the other hand, during our recent study on developing a new chemical/chiroptical method for configurational assignment of allylic alcohols and amines,[16] we found out that cross olefin metathesis[18,19] is suited for introducing the styrene chromophore as a CD reporter

group. By using the recently developed Grubbs' second generation ruthenium catalyst **9**[20] (structure shown in Scheme 2), the linear allylic mono- and 1,2-disubstituted C=C double bonds can be replaced with the styrene group in high yields under mild conditions without epimerization of the substrates.[21] The styrenoid chromophore introduced then couples with the allylic acylate to yield a distinct couplet. The method overcomes the restriction of the conventional allylic benzoate method that gives rise to weak CD couplets, for which in many cases only one wing of the couplet is observable.[16] Therefore, we considered cross metathesis as an attractive alternative in the present case; it was interesting to examine how this chemistry would work in the conversion of a variety of the sterically hindered C=C double bonds, namely, 1,2-disubstituted (**2**), 1,2,2-trisubstituted (**3**), endocyclic double bond (**4**), 1,1-disubstituted (**5**), and 1,1,2-trisubstituted (**6**) double bonds into the corresponding styrenoids. If the cross metathesis did not work, combined methods with other chemical transformations, *i.e.* Heck reaction, would be utilized.

After examination of a variety of reaction conditions, it was found that the adaptation of either cross metathesis,[18,19] Heck reaction, or combined cross metathesis and Heck reaction, satisfied the criteria of mild micro-scale reactions; all double bond substitution patterns in the dihydrofuroangelicins **2**–**6** (Chart 1) could be replaced with the styrenoid chromophore, yielding the styrene derivatives **sty-2**–**sty-6**. The final optimized results on the derivatization of the enantiopure coumarins, all of which were the first eluted enantiomers resolved by HPLC, are shown in Schemes 2–4 . The coumarins **3**–**5** were resolved by using a Chirobiotic TAG column, eluent heptane/ethanol and as first eluted enantiomers they are of (*R*)-configuration. The coumarins **2** and **6** were resolved on Chirobiotic T on the reversed phase, therefore these first eluted enantiomers **2** and **6** are of (*S*)-configuration (*cf.* Table 1). The

detailed enantioselective separation of these dihydrofuroangelicins **2**–**6** is described in the Experimental section.

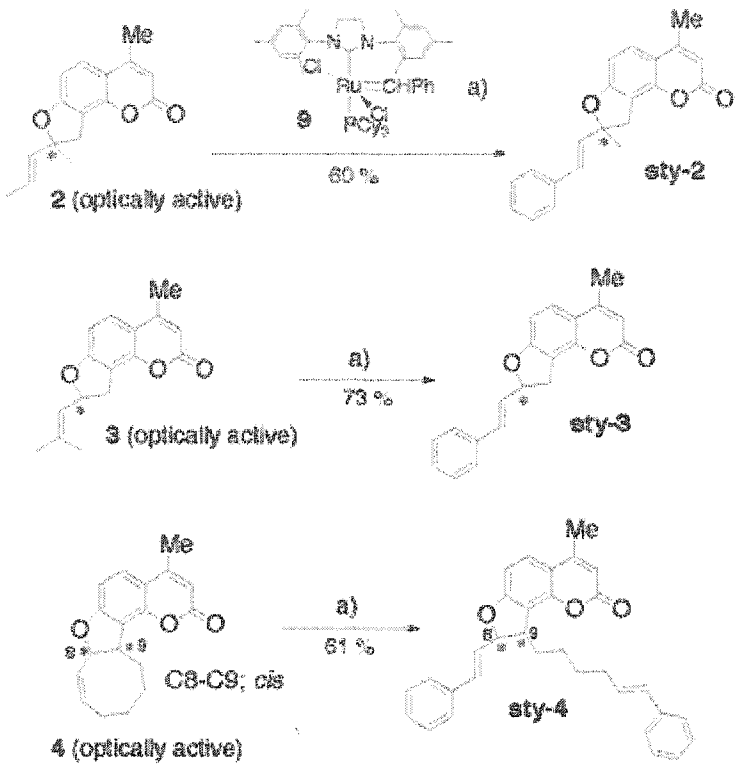

Scheme 2 Conversion of **2**, **3**, and **4** into styrenoids *via* cross metathesis with styrene. *Reagents and conditions*: (a) 10 equiv. styrene, 10 mol% of Grubbs' catalyst **9**, CH_2Cl_2, 40 °C.

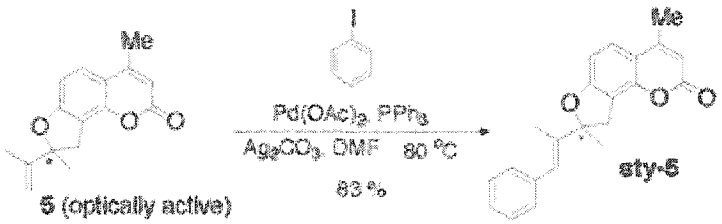

Scheme 3 Conversion of **5** into styrenoid *via* Heck reaction with iodobenzene.

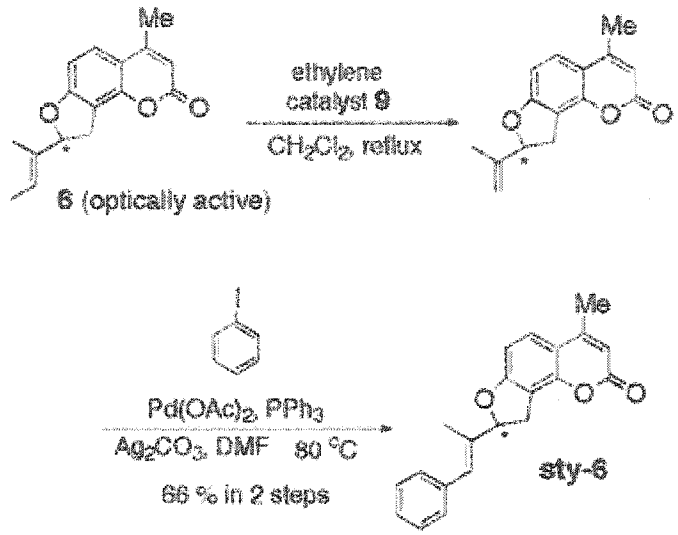

Scheme 4 Transformation of **6** into styrenoid *via* combined cross metathesis and Heck reaction.

The chemical transformations employed for the conversion of dihydrofuroangelicins **2–6** into the corresponding styrenoids, depending on the substitution patterns of the C=C double bonds, are summarized as follows.

(i) *Conversion by cross metathesis with styrene* (Scheme 2): The olefin cross metathesis is successful with 1,2-disubstituted, 1,2,2-trisubstituted, and endocyclic double bonds such as **2**, **3**, and **4**, respectively. Thus the reaction of 1,2-disubstituted derivative **2** with an excess amount of styrene, using 10 mol% of Grubbs' ruthenium catalyst **9** in CH_2Cl_2 at 40 °C for 10 h, cleanly provided the corresponding (*E*)-styrenoid derivative **sty-2** in 60% yield. Similarly, the 1,2,2-trisubstituted derivative **3** was transformed into the corresponding styrenoid, **sty-3**, in 73% yield. Furthermore, the endocyclic double bond in the eight-membered ring of **4** also gave the corresponding styrenoid derivative **sty-4** in 61% yield. As Grubbs and co-workers reported,[18] the thermodynamically more stable (*E*)-isomers could be obtained exclusively by the cross metathesis reaction with styrene and no (*Z*)-stereoisomers were observed. Furthermore, enantioselective HPLC analysis demonstrated that no epimerization occurs

during the cross metathesis reaction: starting from an enantiopure sample of **3**, the corresponding enantiopure **sty-3** was obtained in >99% enantiomeric excess.

Table 1 UV and CD[a] spectra of **sty-2** - **sty-6** in acetonitrile.

substrate	UV λ / ε	CD λ / Δε	A_{CD} amplitude observed	abs. config. at C8
sty-2	321 nm (14,000) 251 nm (20,000)	320 nm +14.7 250 nm -16.9	+31.5	*S*
sty-3	322 nm (11,200) 251 nm (17,400)	318 nm -12.5 254 nm +16.6	-29.2	*R*
sty-4	320 nm (13,200) 251 nm (35,100)	320 nm -10.9 251 nm +12.1	-23.0	*R*
sty-5	322 nm (13,500) 247 nm (16,900)	320 nm -14.3 243 nm +14.0	-28.3	*R*
sty-6	321 nm (14,200) 249 nm (19,900)	320 nm +14.6 247 nm -10.2	+24.8	*S*

[a] $\Delta\varepsilon$ [L · mol^{-1} · cm^{-1}]

(ii) *Conversion by Heck reaction with iodobenzene* (Scheme 3): The 1,1-disubstituted *exo*-methylene double bond in **5** (first eluted enantiomer) was unexpectedly inactive to the cross metathesis with styrene, and starting material was recovered. We therefore utilized Heck reaction by reaction of **5** with iodobenzene in the presence of $Pd(OAc)_2$, triphenylphosphine, and silver carbonate in DMF at 80 °C for 5 h, to give the corresponding **sty-5** in 83% yield (Scheme 3).

(iii) *Transformation by the combined method of cross metathesis and Heck reaction* (Scheme 4): In the case of 1,1,2-trisubstituted derivative **6**, the direct transformation into the styrene derivative by use of either cross metathesis with styrene or Heck reaction was unsuccessful. Therefore, we utilized the combined method of cross metathesis with ethylene and Heck reaction as shown in Scheme 4. Thus the trisubstituted double bond in **6** was first converted into an exomethylene double bond by reaction with ethylene in the presence of Grubbs catalyst **9** in almost quantitative yield. Subsequently, the obtained exomethylene intermediate was subjected to Heck reaction, by reaction with iodobenzene, $Pd(OAc)_2$, triphenylphosphine, and silver carbonate in DMF, to provide the desired styrenoid derivative of **6** in 66% yield for two steps. It is noteworthy that the intermolecular metathesis, Heck reaction, and combined chemical transformations converted all the substitution pattern of the C=C double bonds in **2**–**6** (Chart 1) into the styrenoids **sty-2**–**sty-6** with about 1 mg sample under mild conditions.[16]

Conformational analysis of styrenoid derivatives sty-2–sty-6

Inspection of molecular models of **1** and **sty-2**–**sty-6** (Chart 1) suggests strong similarity between the conformational spaces for all the styrenoid compounds. In particular, two main degrees of conformational freedom may be recognized in all cases (Fig. 2): (a) the rotamerism around the C8–C10 bond, described by the dihedral angle O7–C8–C10–C11 ($d_{8,10}$); and (b) the dihydrofuranyl ring flip, which may be described by the O7–C8–C9–C9α torsion ($d_{8,9}$). These two are especially relevant to the application of exciton chirality method because, in principle, the variation of both $d_{8,10}$ and $d_{8,9}$ may affect the relative arrangement of

the coumarin and styrene chromophores. Our previous experience on compound **1** (which coincides with **sty-3**) confirmed that both torsional modes are effective;[15] the presence of further methyl groups at C-8 and C-10 position in **sty-2** and **sty-4**–**sty-6**, however, is likely to affect these torsions in an unpredictable way and cause some difference with respect to **1**.

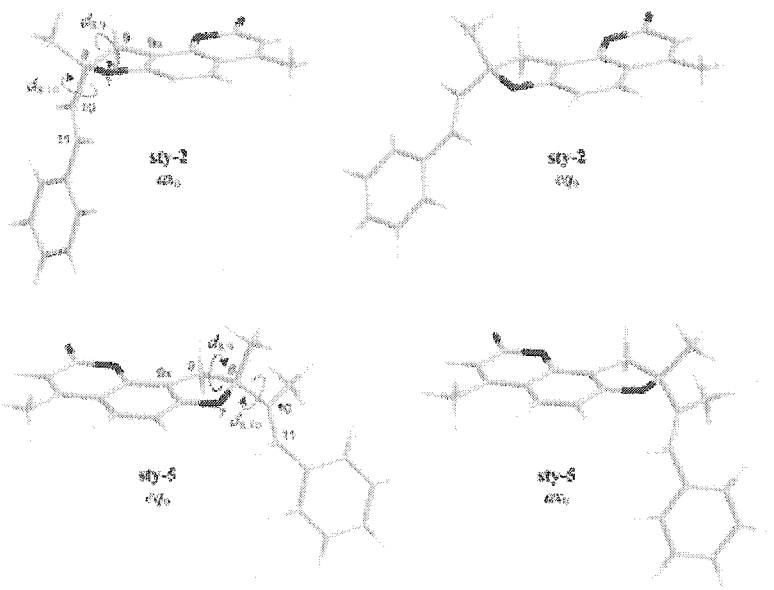

Fig. 2 The two lowest energy DFT (B3LYP/6-31G**, $CHCl_3$) optimized structures of (*S*)-**sty-2** and (*R*)-**sty-5**.

Knowledge of the molecular conformation in solution is essential for applying the exciton chirality approach. It is well-known that application of the exciton chirality CD method for elucidation of absolute configuration is straightforward only in those cases where no conformational ambiguity exists.[22] In the current case, however, the solution conformations of styrenoid derivatives **sty-2** to **sty-6** are not necessarily clear since the styrene moieties are attached to five-membered rings that can adopt variable conformations depending on the substitution pattern. Therefore a completely novel conformational analysis for the

compounds described in this paper, concentrating especially on **sty-2** and **sty-5**, was performed. The results for these two models may be easily transferred to the other derivatives **sty-4** and **sty-6**; as for the former, the conformational freedom of the chain at C-9 may be disregarded due to its negligible contribution to the CD (*vide infra*).

Molecular modeling of sty-2 and sty-5. The molecular conformations of **sty-2** and **sty-5** were investigated by means of DFT calculations (see Computational section for details). The dihydrofuranyl five-membered ring is capable of assuming two main conformations where the styrenyl substituent occupies a pseudo-equatorial (*eq*) or pseudo-axial (*ax*) position. For each *eq* and *ax* conformer, three energy minima (indicated with subscripts 0–2) were isolated relative to the variation around the $d_{8,10}$ dihedral, resulting in overall six conformers within 1.3–1.5 kcal mol^{-1} (that is, with non-negligible population at room temperature). The two lowest energy conformers (ax_0 and eq_0) for each compound are shown in Fig. 2; the relative energies and main geometrical parameters for all computed minima are listed in ESI† (Table ESI1). For both compounds, DFT calculations predict that *eq* and *ax* conformers are almost equally probable. The preferred value of the $d_{8,10}$ angle is around 0°, corresponding to a *syn* orientation between the C10–C11 double bond and the C8–O7 bond (Fig. 2); on the other hand, the energy barrier between the various C8–C10 rotamers is quite low (below 4–5 kcal mol^{-1}). Interestingly, such a preferred conformation is at odds with the results of DFT calculations for **1**, which favor a strongly preferred *eq* conformation with $d_{8,10} \approx \pm 120°$ (C10–C11 double bond *syn* to C8–H8).

NMR experiments on sty-2 and sty-5. Modeling results predict that compounds **sty-2** and **sty-5** may assume multiple conformations that presumably are fast exchanging in solution, due to the low energy barriers relative to the $d_{8,10}$ and $d_{8,9}$ torsional modes. Therefore, NMR

spectra represent the average conformational situation in which all conformers with significant population contribute. In fact, the ^{1}H-NMR spectra of **sty-2** and **sty-5** show a single set of signals at room temperature in $CDCl_3$.

The conformational situation about the dihydrofuranyl ring was investigated by means of NOE (Fig. 3) and long-range heteronuclear $^3J_{C,H}$ measurements (the numbering of protons (H_x) and methyl (Me_y) groups is according to Fig. 3). For both compounds **sty-2** and **sty-5**, proton H_{9a} which resonates at higher field than H_{9b} (3.27 *vs.* 3.43 ppm for **sty-2**, and 3.25 *vs.* 3.46 ppm for **sty-5**), shows an almost twofold stronger NOE with methyl Me_8 with respect to H_{9b}. On the contrary, H_{9b} shows stronger NOEs with the protons of the styrenyl group (H_{10} or Me_{10}, and H_{11}) with respect to H_{9a} (Fig. 3). It may be easily concluded that the styrenyl group is *cis* to H_{9b} and *trans* to H_{9a}. It is generally observed that axial protons are upfield shifted with respect to equatorial protons in cyclic systems.[23] This would lead to the conclusion that, in the average situation detected by NMR, proton H_{9a} and the styrenyl substituents are both pseudo-axial, while proton H_{9b} and Me_8 are both pseudo-equatorial. However, such generalization may hardly be extended to the dihydrofuranyl rings in **sty-2** and **sty-5**; effects other than the axial/equatorial position are likely to determine the chemical shifts of protons H_{9a}/H_{9b}, in particular the coumarin and styrene ring anisotropies.

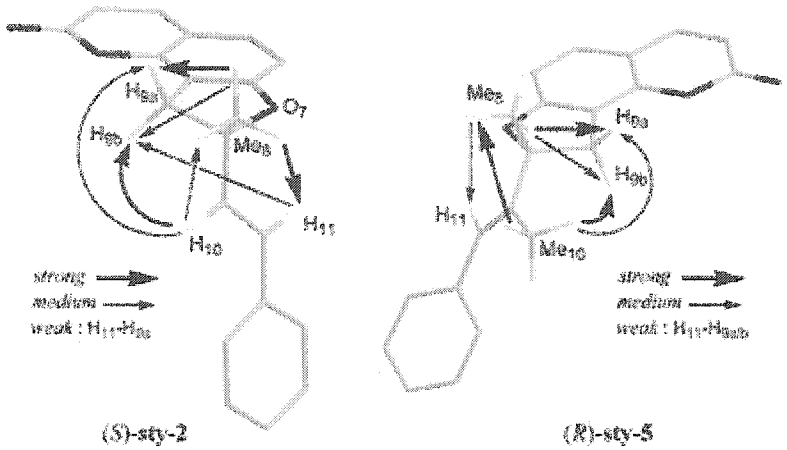

Fig. 3 Relevant ^{1}H NMR NOEs measured for (*S*)-**sty-2** and (*R*)-**sty-5**(ROESY spectra, mixing time 200 ms).

The *J*-couplings between protons H_{9a}/H_{9b} and methyl carbon at C-8 ($^3J_{Me8,H9a}$ and $^3J_{Me8,H9b}$) were expected to be informative of the respective dihedral angles, and ultimately of the $d_{8,9}$ torsion, through a specific Karplus-type relation (see Computational section).[24] We found that the experimental pairs of $^3J_{C,H}$ values fit reasonably well with those calculated as the average of all the DFT-computed minima (Boltzmann-weighted at 300 K), although experimental values are especially closer to the estimates for the *eq* conformers (see ESI,† Table ESI2).

The rotamerism around the C8–C10 bond may be depicted by means of relative NOEs (Fig. 3). For compound **sty-5**, methyl protons Me_{10} show similar NOE with Me_8 and H_{9b} protons, while proton H_{11} has twofold stronger NOE with Me_8 than H_{9b} and almost negligible with H_{9a}. The same is true for compound **sty-2**, where proton H_{10} shows relative NOEs in the order $H_{9b} > Me_8 \approx H_{9a}$ and proton H_{11} in the order $Me_8 > H_{9b} > H_{9a}$. The average situation detected is in accord with modeling results, which predict a favored conformation with *syn*-oriented C10–C11 double bond and C8–O7 bond.

In conclusion, the combination of computational and experimental techniques discloses the existence of multiple and fast-exchanging conformations for compounds **sty-2** and **sty-5**. However, this conformational heterogeneity does not affect the following exciton chirality analysis, because molecular models suggest that the relative arrangement between the coumarin and styrene chromophores is not dramatically influenced by the possible molecular motions.

Experimental CD spectra and application of exciton chirality method

The absorption and CD spectra of the non-styrenoid compounds **2–6** (Fig. 1) are dominated by a strong broad band with a maximum at 322–323 nm, $\epsilon \approx 1000$–13000. It is due to the electric dipole allowed HOMO–LUMO transition (band I) delocalized over the entire 7-hydroxy coumarin chromophore.[25] Instead only very weak bands are present in the 230–260 region, where the styrene chromophore undergoes a strong π–π^* transition centered around 250 nm (substituted benzene K band), which may couple favorably with the above coumarin one.

In fact, in the CD spectra in acetonitrile of compounds **sty-2**–**sty-6** (Table 1, Fig. 4a,b, and 5b,d), distinctive exciton couplets appear in the 230–350 nm region, with short wavelength maximum at 243–254 nm, crossover around 270 nm, and long wavelength maximum at 318–320 nm. These couplets mainly arise from the exciton coupling between the above styrene K and coumarin transition I; both transitions are polarized along the long axes of the respective aromatic systems[15] (see also next section). In keeping with our expectations, all compounds exhibit a split CD pattern typical for exciton chirality, namely, two opposite Cotton effects of moderate intensity (absolute amplitudes between 23–31 M^{-1} cm^{-1}) and rather symmetrical

appearance (in terms of integrated areas of the two components). In particular, the exciton-coupled CD spectra of styrene derivatives are far more intense than the inherent CD of the parent coumarins above 240 nm (absolute $\Delta\varepsilon$ less than 3 M^{-1} cm^{-1} around 320 nm, Fig. 1); therefore, the contribution of optical activity mechanisms other than the coupled-oscillator one is minor. Although **sty-4** is endowed with a further styrene substituent, its CD spectrum is perfectly comparable to those of other mono-styrenoid derivatives; it is likely that, due to the long and flexible aliphatic chain attached at C-9, the second styrene makes only a small contribution to the overall CD spectrum.

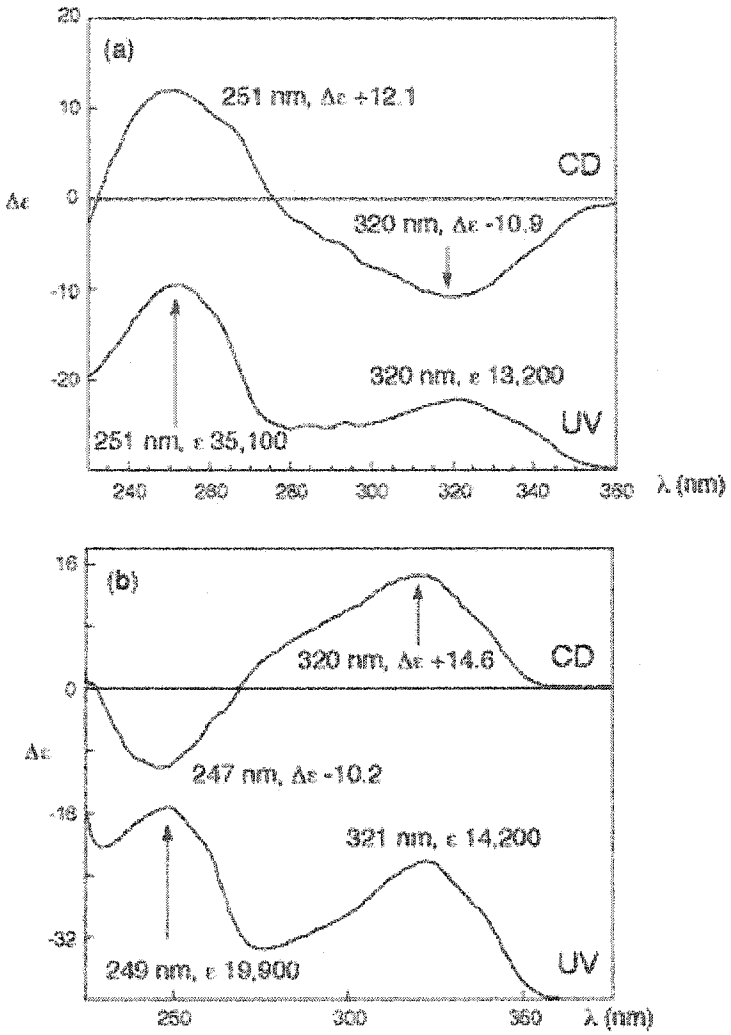

Fig. 4 UV (bottom) and CD (top) spectra of **sty-4** and **sty-6** in acetonitrile. Spectrum (a), (8*R*,9*R*)-**sty-4**, 1.17×10^{-5} M; spectrum (b), (8*S*)-**sty-6**, 3.02×10^{-5} M.

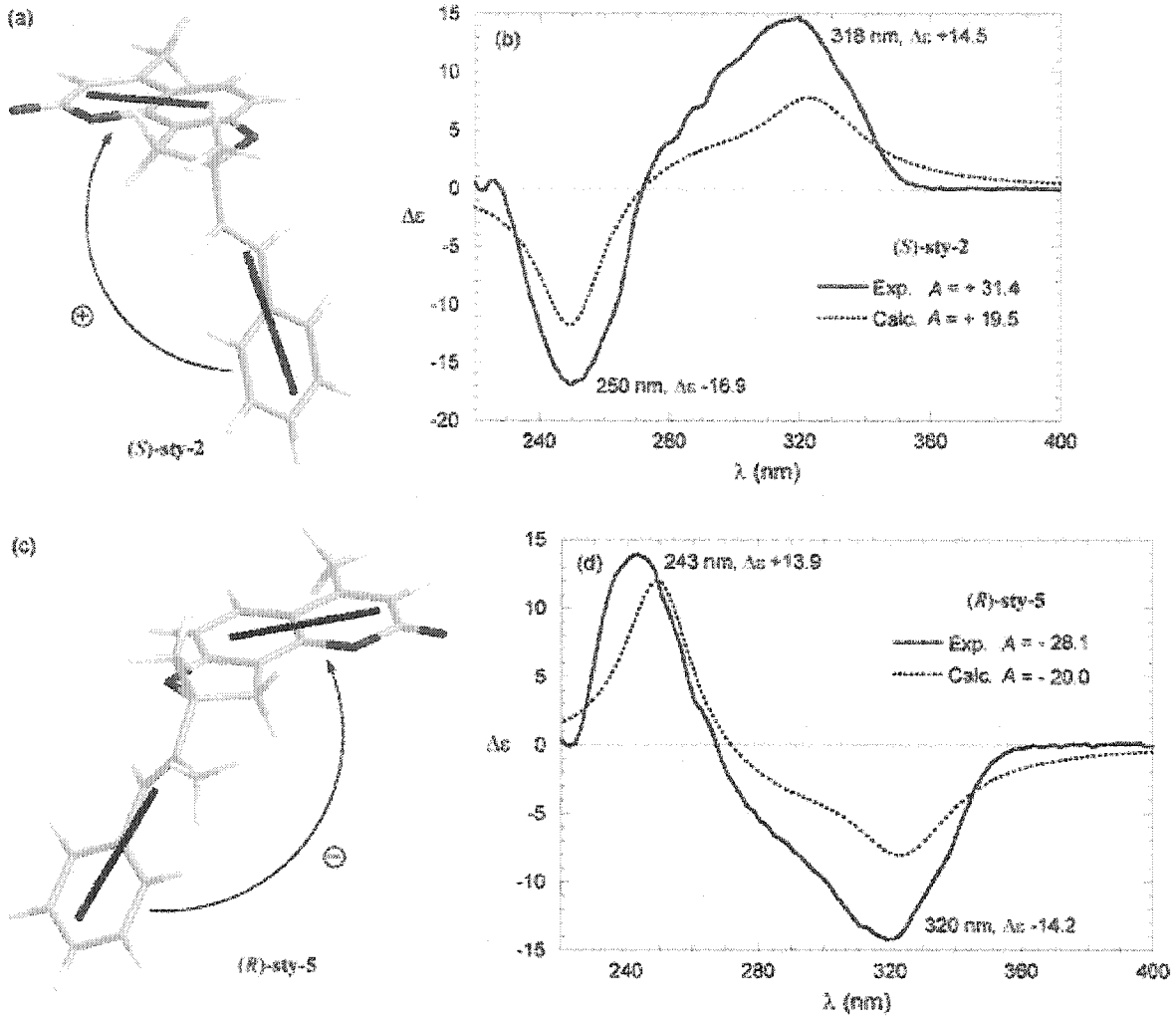

Fig. 5 (a,c) Absolute sense of twist defined by styrene K (in the front) and coumarin I transition (in the back) for the lowest energy conformers of (*S*)-**sty-2**(a) and (*R*)-**sty-5**(c). (b,d) Experimental (in acetonitrile, solid lines, $c = 4.94 \times 10^{-5}$ M (**sty-2**) and $c = 1.40 \times 10^{-5}$ M (**sty-5**)) and calculated (dotted lines) CD spectra of compounds (*S*)-**sty-2**(b) and (*R*)-**sty-5**(d). Calculated spectra were obtained with the DeVoe method as the Boltzmann-weighted average at room temperature for the six lowest energy minima computed by DFT (see text).

Simple inspection of the molecular models leads to the conclusion that all the styrene derivatives showing a positive exciton couplet in the 230–350 nm region, namely **sty-2** and

sty-6, have the (8*S*) absolute configuration, while those showing a negative couplet, namely **sty-3**, **sty-4**, and **sty-5**, have the (8*R*) absolute configuration; compound **sty-4** is therefore (8*R*,9*R*). For example, in **sty-2** (Fig. 5a), in the lowest energy DFT conformer with an (8*S*) absolute configuration, a positive chirality is clearly defined by the long axes of the two aromatic chromophores; in other words, a clockwise twist is necessary to bring the transition dipole in the front in Fig. 5a (styrene K transition) onto the one in the back (coumarin transition I). For the second model compound **sty-5**, the (8*R*) absolute configuration for the lowest energy DFT conformer corresponds to a negative chirality defined by the two chromophores (Fig. 5c).

Importantly, for **sty-2** all six minimum energy conformations computed by DFT with (8*S*) absolute configuration, define similar positive chirality; this is quantitatively confirmed by DeVoe calculations (see following section). Similarly, all six DFT-computed conformations for (8*R*)-**sty-5** define a negative chirality. The same behavior has been observed for compound **sty-3** (which coincides with that previously reported for **1**),[15] and may be safely considered for the remaining derivatives **sty-4** and **sty-6**. It is apparent that, due to a favorable characteristic for this type of chiral coumarin and geometrical arrangement, *the chirality defined by the two transition dipoles responsible for the CD spectrum above 230 nm is completely dictated by the absolute configuration at C-8, independent of conformational rearrangements*. We believe that the underlying reason for this is the relative rigidity of the dihydrofurocoumarin skeleton which determines a definite orientation of the styrene substituent at the C-8 position with respect to the coumarin ring; the sense of twist between the two long-axis directions is thus unambiguous for all populated conformers.

In conclusion, the current combined chemical/chiroptical protocol based on styrene as the CD reporter group is an efficient and versatile method of assigning the absolute configuration of C-8 alkenyl substituted dihydrofuroangelicins. In particular, in the absence of substituents at C8–C10 which may revert the formal chirality, *a positive CD couplet in the 230–350 nm region is a proof of the (8S) configuration, and vice versa.*

Quantitative coupled-oscillator CD calculations

In order to test the scope and limitation of the previous qualitative application of the exciton chirality approach to coumarin derivatives **sty-2**–**sty-6**, we undertook a quantitative chiroptical analysis by means of coupled-oscillator DeVoe calculations for the two model compounds **sty-2** and **sty-5**. The DeVoe method[17] offers a means for calculating full CD spectra[26] in the approximation that the coupled-dipole mechanism makes the dominant contribution to the CD spectrum, in common with the exciton chirality method. In the current case it was especially interesting to compare calculated spectra for various possible conformations of **sty-2** and **sty-5**, given the difficulty of obtaining experimental data concerning conformer populations.

It is a necessary prerequisite for any exciton chirality application to clarify, in addition to the molecular conformation, the polarization directions of the coupled transition moments. In a previous paper,[15] we obtained such information with semi-empirical CNDO/S-CI calculations. As a matter of fact, higher level theoretical treatments seem to be lacking for 7-hydroxy coumarin,[25,27] while available for the parent coumarin chromophore and some of its derivatives.[28] It is noteworthy that in some special cases, a critical geometrical situation also renders the knowledge of the exact position of the transition dipoles within the chromophore

framework indispensable for application of exciton chirality.[29] While this parameter is not experimentally accessible, it can be calculated if accurate molecular orbitals are available.[30] For these reasons, the electronic properties of 7-hydroxy coumarin chromophore were newly investigated prior to DeVoe calculations.

Chromophore electronic structures. The absorption spectrum of 7-hydroxy coumarin chromophore exhibits, in addition to the above discussed band I (λ_{max} = 319 nm, ε_{max} = 13,500 for 7-hydroxy-4-methyl coumarin in acetonitrile; see Figure ESI1), a distinctive shoulder around 290 nm, allied to a second π-π^* transition (band II).[25] Weaker bands are also present in the 240-250 nm region (band III). Below 220 nm strong bands appear due to higher energy transitions.

The results of our electronic structure calculations (see Computational section), with both semi-empirical ZINDO/S-CI and TDDFT (PBE0/6-311+G(d,p) level) methods, are summarized in Table 2. ZINDO/S-CI predicts well the position and intensity of the observed bands I-III above 230 nm; however, a fourth intense band is found at 232 nm which has no experimental correspondence. TDDFT calculations, on the other hand, underestimate the intensity of band II. A switch of the functional to B3LYP or changes in the basis size and inclusion of diffuse functions did not appreciably affect the calculated intensities, and the vertical excitation energies shifted only modestly.

Interestingly, transition dipole directions and positions are calculated in a very similar way by both methods used (see structures in Table 2), which is relevant to the chiroptical analysis. In particular, transitions I and II are polarized almost parallel to the coumarin long axis (tilt angles are less than 5° for transition I). The center of transition dipole I is almost in the middle of the coumarin chromophore, slightly displaced toward the pyranone ring (see

ESI† for details on the transition dipole position calculations). It may be concluded that in the case of the red-shifted transition I of 7-hydroxy coumarin, using the semi-empirical transition moment direction and naively placing the dipole in the center of the chromophore, would not introduce any sizeable error in coupled-oscillator calculations.

Table 2.

Experimental and calculated electronic transitions in the 240-330 nm region for 7-hydroxycoumarin and styrene chromophores.[a]

7-Hydroxy coumarin												
Trans.	Experimental[b]					ZINDO[c]			TDDFT[d]			
	λ_{max}	ν_{max}	$\Delta\nu_{max}$	D	f	λ_{max}	f	α	λ_{max}	f	α	
I	323	31.0	3.0	14.0	0.20	315	0.38	+1	293	0.32	+2	
II	292	34.2	4.0	8.5	0.14	290	0.19	+5	271	0.03	–6	
III	254	39.3	nc	0.3	0.01	237[e]	0.03	–44	238	0.05	–63	

Styrene								
Trans.	Experimental[f]					ZINDO[c]		
	λ_{max}	ν_{max}	$\Delta\nu_{max}$	D	f	λ_{max}	f	β
K	250	40.0	4.0	30.0	0.56	243	0.65	+12

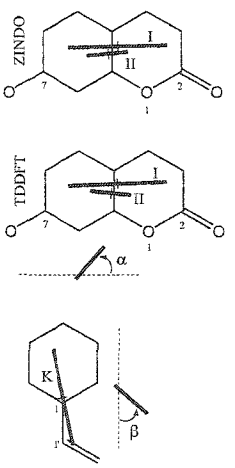

[a] λ_{max} wavelength maximum, nm; ν_{max} frequency maximum, $10^3 cm^{-1}$; $\Delta\nu_{1/2}$ half-height width, $10^3 cm^{-1}$; D dipolar strength, square Debye; f, oscillator strength; α and β, tilt angles between transition polarization and chromophore long axes (see structures).

[b] From the UV spectrum of 7-hydroxy-4-methylcoumarin in acetonitrile.

[c] ZINDO/S-CI calculations with 16×16 (7-hydroxycoumarin) and 8×8 (styrene) single CI.

[d] TDDFT calculations with PBE0/6-311+G(d,p).

[e] A further band calculated at 232 nm, $f = 0.49$, $\alpha = -61$.

[f] From the UV spectrum of styrene in hexane.

As for the styrene chromophore, a recent theoretical CASPT2 study afforded reliable transition dipole polarization for the K band.[31] This is in excellent agreement with our

ZINDO/S-CI calculation, which also placed the center of K transition dipole very close to phenyl C-1 carbon (Table 2).

DeVoe coupled oscillator calculations. Fig. 5b and d show the comparison between experimental CD spectra for compounds (*R*)-**sty-5** and (*S*)-**sty-2**, and those calculated with the DeVoe method as a Boltzmann-weighted average at 300 K of DFT-computed structures (see Computational section for details on calculation parameters). The agreement between calculated and experimental CD is very good, which confirms the exciton chirality assignment above. The weaker CD amplitude (by about 30–35%) might be due to various factors, in particular, to other mechanisms of optical activity: first, the inherent CD of C-8 alkenyl dihydrofuroangelicins **2–6**, contributing to around 10–20% of the experimental 320 nm CD band of **sty-2**–**sty-6**; second, a coupling with some high energy transitions. However, it must be stressed that in general the agreement between experimental and DeVoe-calculated intensities is expected not to be perfect, especially for such extended π-chromophoric systems at relatively short interchromophoric distances (around 7Å between the effective point-dipole positions, and only 2.5 Å between the closest points).

The most important result from DeVoe calculations is that *all the six DFT minimum energy conformations for (S)-**sty-2** give a positive CD couplet with comparable intensity*; similarly, *all six (R)-**sty-5** conformers give a negative CD couplet with comparable intensities*. This is a final proof that the configurational assignment made on the basis of the straightforward exciton chirality approach is trustworthy. In conclusion, the theoretical findings above justify *the application of the current chemical/exciton chirality methodology to new C-8 alkenyl dihydrofuroangelicin homologues without the need for extensive*

conformational analysis or quantitative CD calculations, unless there is reason to suspect some conformational ambiguity.

6.3. CONCLUSION

The absolute configurations of the chiral dihydrofuroangelicins **2–6** bearing a variety of C-8 substituted double bonds have been assigned based on a new combined chemical/chiroptical protocol. The method consists of the conversion of C=C double bonds into a styrenoid chromophore through either (i) cross metathesis, (ii) Heck reaction, or (iii) a combined method of cross metathesis and Heck reaction. The styrenoid derivatives **sty-2–sty-6** are obtained in good yields and mild conditions with about 1 mg samples. They exhibit moderately intense and clear-cut CD couplets in the 230–350 nm region, arising from the exciton coupling between the coumarin chromophore (band I around 320 nm) and the introduced styrene chromophore (K band around 250 nm). A straightforward exciton analysis of the CD spectra leads to the assignment of the absolute configurations of the styrenoid derivatives, and therefore of the parent compounds.

In order to test the scope and limitation of the current exciton chirality approach, quantitative CD calculations on **sty-2** and **sty-5** (as model compounds) were performed with the DeVoe coupled-oscillator method. The necessary geometrical and spectroscopic parameters were extracted from: (a) a thorough confomational analysis in solution, with NMR and DFT molecular modeling; (b) semi-empirical and TDDFT electronic structure calculations of 7-hydroxy coumarin chromophore. Excellent agreement was seen between the calculated and experimental CD spectra.

6.4. EXPERIMENTAL

Materials and general procedures

Anhydrous dichloromethane and dimethylformamide were dried and distilled from CaH_2. Acetonitrile used for CD and UV-vis measurements was Optima grade. Unless otherwise noted, materials were obtained from a commercial supplier and were used without further purification. Grubbs' second generation ruthenium catalyst, tricyclohexylphosphine[1,3-bis(2,4,6-trimethylphenyl)-4,5-dihydroimidazol-2-ylidene][benzylidine]ruthenium(IV) dichloride **9**, is commercially available from Strem Chemicals. All reactions were performed in pre-dried glassware under Ar. Purification was performed either by column chromatography using ICN silica gel (32–63 mesh) or by preparative TLC using silica gel plates, 60 F-254, 0.25 mm, E. Merck.

^{1}H NMR spectra were obtained on Bruker DMX 300 or 400 MHz spectrometers and are reported in parts per million (ppm) relative to TMS (δ), with coupling constants (J) in Hertz (Hz). 2D NMR spectra were obtained on a Varian INOVA 600 spectrometer. 2D ROESY spectra were recorded by the hypercomplex method, using cw irradiation (3 kHz rf field), with the following parameters: mixing time 200 ms, 8 scans, 196 time increments, 2048 data points zero-filled to 1K–4K. $^3J_{C,H}$ couplings were measured by means of pulsed field gradient HMBC spectra, recorded by varying J-refocusing time τ between 0.04–0.15 s (10 ms interval), corresponding to $J = ½\ \tau = 3.3–12.5$ Hz. $^3J_{C,H}$ values were estimated with least-squares sinusoidal fit of the experimental cross-peaks intensities as a function of J.[32]

Low- and high-resolution FAB mass spectra were measured on a JEOL JMS-DX303 HF mass spectrometer using a glycerol matrix and Xe ionizing gas.

UV-vis spectra were recorded on a Perkin-Elmer Lambda 40 spectrophotometer, and reported as λ_{max}/nm (ϵ_{max}/L mol^{-1} cm^{-1}). The CD spectra were recorded on a JASCO-810 spectrophotometer, using a 1 cm cell, and the following conditions: SBW 1 nm, 50 nm min^{-1}, response 1 s, and 16 scans. The CD spectra were measured in millidegrees and normalized into $\Delta\varepsilon_{max}$/L mol^{-1} cm^{-1}.

Enantiomeric separation conditions

Separations and collections of dihydrofurocoumarin enantiomers **2–6** were achieved using a HP 1050 HPLC system with UV detector, auto injector, using computer controlled Chem-station data processing software. Two chiral stationary phases, trade named Chirobiotic T and Chirobiotic TAG columns (250 × 4.6 mm i.d.), were obtained from Advanced Separation Technologies, Inc. (Astec, Whippany, NJ, USA). The chiral stationary phases were prepared by bonding the chiral selectors to a 5 μm spherical porous silica gel through a linkage chain.[8] Detection wavelengths were varied between 220 nm and 327 nm, which correspond to the two molecular absorption maxima of the dihydrofurocoumarins. Analytical separations were reported previously.[8] The preparative separation conditions used to isolate mg quantities of the pure enantiomers of compounds **2–6** are as follows. Racemates **3–5** were dissolved in neat ethanol to a concentration of 10 mg ml^{-1}. Up to 100 microliters of each sample were injected onto a Chirobiotic TAG column and eluted with heptane/ethanol, 90/10 (v/v). The individual enantiomers were collected manually and concentrated by evaporation at room temperature (21 °C). Racemates **2** and **6** were dissolved in neat methanol to a concentration of 5 mg ml^{-1}. Up to 20 μl of each sample were injected onto a Chirobiotic T column and eluted in the reversed mode with H_2O/methanol, 65/35 (v/v). Fractions of the individual

enantiomers (from successive injections) were added together after manual collection. They were concentrated under vacuum at room temperature (21 °C). All mobile phases were premixed and degassed before use. The flow rate was 1.0 ml min^{-1}.

Styrenoid derivative of 2(sty-2)

To a solution of **2** (first eluted enantiomer, 1.0 mg, 3.9 μmol) in dichloromethane (2.0 mL) was added Grubbs' second generation ruthenium catalyst **9** (760 μg, 890 nmol) and styrene (890 nL, 7.8 μmol) at room temperature, and the mixture was stirred at 40 °C for 5.5 h. The reaction mixture was concentrated *in vacuo* to give the crude products which were purified by preparative thin layer chromatography on silica gel (17% ethyl acetate in hexane) twice to afford the corresponding styryl derivative (750 μg, 60%) as a white solid: IR ($CHCl_3$, cm^{-1}) 1717, 1616, 1385, 1046; ^1H NMR (400 MHz, $CDCl_3$) δ1.72 (s, 3H), 2.39 (d, 3H, J = 0.8 Hz), 3.29 (d, 1H, J = 16.0 Hz), 3.46 (d, 1H, J = 16.0 Hz), 6.09 (d, 1H, J = 0.8 Hz), 6.40 (d, 1H, J = 16.4 Hz), 6.67 (d, 1H, J = 16.0 Hz), 6.80 (d, 1H, J = 8.4 Hz), 7.24 (d, 1H, J = 7.6 Hz), 7.31 (dd, 2H, J = 7.6, 7.6 Hz), 7.38 (d, 2H, J = 7.2 Hz), 7.43 (d, 1H, J = 8.8 Hz); HRFABMS calcd for $C_{21}H_{19}O_3$ $[M + H]^+$ 319.1334, found 319.1343.

Styrenoid derivative of 3(sty-3)

To a solution of **3** (first eluted enantiomer, 2.3 mg, 9.0 μmol) in dichloromethane (2.0 mL) was added Grubbs' second generation ruthenium catalyst **9** (1.7 mg, 2.0 μmol) and styrene (2.1 μL, 18 μmol) at room temperature, and the mixture was stirred at 40 °C for 3.5 h. The reaction mixture was concentrated *in vacuo* to give the crude products which were purified by preparative thin layer chromatography on silica gel (25% ethyl acetate in hexane) to

afford the corresponding styryl derivative (2.0 mg, 73%) as a white solid. The spectral data were in good agreement with those reported previously.

Styrenoid derivative of 4(sty-4)

To a solution of **4** (first eluted enantiomer, 1.5 mg, 5.3 μmol) in dichloromethane (1.0 mL) was added Grubbs' second generation ruthenium catalyst **9** (1.0 mg, 1.2 μmol) and styrene (6.1 μL, 53 μmol) at room temperature, and the mixture was stirred at 40 °C for 2.0 h. The reaction mixture was concentrated *in vacuo* to give the crude products which were purified by preparative thin layer chromatography on silica gel (17% ethyl acetate in hexane) twice to afford the corresponding styryl derivative (1.5 mg, 61%) as a white solid: ^{1}H NMR (400 MHz, $CDCl_3$) δ1.38–1.46 (m, 2H), 1.60–1.68 (m, 1H), 1.84–1.89 (m, 2H), 2.14–2.17 (m, 2H), 2.31–2.40 (m, 1H), 2.38 (d, 3H, J = 0.8 Hz), 3.77 (dd, 1H, J = 13.6, 7.6 Hz), 5.42 (dd, 1H, J = 8.0, 8.0 Hz), 6.09 (d, 1H, J = 1.2 Hz), 6.11 (ddd, 1H, J = 16.0, 7.2, 7.2 Hz), 6.29 (d, 1H, J = 16.0 Hz), 6.44 (dd, 1H, J = 16.0, 8.0 Hz), 6.80 (d, 1H, J = 8.4 Hz), 6.82 (d, 1H, J = 16.4 Hz), 7.15–7.19 (m, 1H), 7.25–7.38 (m, 7H), 7.41–7.44 (m, 3H).

Styrenoid derivative of 5(sty-5)

To a solution of **5** (25.0 mg, 97.5 μmol, an entry of the best yield obtained was shown here during optimization of the reaction conditions using the racemic sample) in dimethylformamide (2.0 mL) was added iodobenzene (21.8 μL, 195 μmol), palladium(II) acetate (1.31 mg, 5.85 μmol), triphenylphosphine (3.07 mg, 11.7 μmol), and silver carbonate (53.8 mg, 195 μmol) at room temperature. After the reaction mixture was stirred for 2.5 h at 80 °C, H_2O was added, and the resulting mixture was extracted with ethyl acetate. The organic layers were combined, washed with H_2O, brine, dried over Na_2SO_4, filtered and

concentrated *in vacuo* to give the crude products, which were purified by column chromatography on silica gel (from 9% to 25% ethyl acetate in hexane) and then by preparative thin layer chromatography on silica gel (9% ethyl acetate in hexane) five times to afford the corresponding styryl derivative as its 2.7 : 1 mixture of **sty-5** and the minor isomer with an internal double bond (27 mg, 83%). These isomers were separated by HPLC using a YMC-Pack ODS-AM column (S- 5 μm, 120 A, 25 cm × 10 mm) eluted with ethyl acetate/hexane (1 : 9) at 1 mL min^{-1}, while monitoring at 254, 280, and 318 nm. The retention times are 87 (major isomer **sty-5** as a white solid) and 82 (minor isomer with internal double bond) min: IR ($CHCl_3$, cm^{-1}) 1724, 1616, 1385, 1051; ^1H NMR (400 MHz, $CDCl_3$) δ1.69 (s, 3H), 1.93 (d, 3H, J = 1.6 Hz), 2.40 (d, 3H, J = 1.2 Hz), 3.27 (d, 1H, J = 16.0 Hz), 3.48 (d, 1H, J = 16.0 Hz), 6.08 (d, 1H, J = 1.2 Hz), 6.68 (s, 1H), 6.80 (d, 1H, J = 11.6 Hz), 7.20–7.26 (m, 3H), 7.33 (dd, 2H, J = 7.4, 7.4 Hz), 7.44 (d, 1H, J = 8.5 Hz); ^{13}C NMR (100 MHz, $CDCl_3$) δ14.6, 19.2, 26.6, 38.5, 93.6, 106.6, 111.0, 113.2, 113.8, 123.9, 125.4, 126.4, 127.9, 128.9, 137.2, 139.1, 150.8, 152.9, 160.9, 162.4; HRFABMS calcd for $C_{22}H_{21}O_3$ $[M + H]^+$ 333.1490, found 333.1486.

Styrenoid derivative of 6(sty-6)

To a solution of **6** (first eluted enantiomer, 2.2 mg, 8.6 μmol) in dichloromethane (2.0 mL) was added Grubbs' second generation ruthenium catalyst **9** (1.7 mg, 2.0 μmol) and styrene (2.0 μL, 17 μmol) at room temperature, and the mixture was stirred at 40 °C for 7.0 h. The reaction mixture was concentrated *in vacuo* to give the crude products which were roughly purified by column chromatography on silica gel (from 9% to 17% ethyl acetate in hexane) to afford the corresponding *exo*-methylene derivative (2.5 mg, quant.) as a white solid. The

obtained compound was used for the next Heck reaction without further purification: ^{1}H NMR (400 MHz, $CDCl_3$) δ1.78 (s, 3H), 2.39 (s, 3H), 3.19 (dd, 1H, J = 16.4, 8.0 Hz), 3.52 (dd, 1H, J = 16.0, 9.6 Hz), 4.96 (s, 1H), 5.11 (s, 1H), 5.35 (dd, 1H, J = 8.8, 8.8 Hz), 6.10 (s, 1H), 6.78 (d, 1H, J = 8.4 Hz), 7.41 (d, 1H, J = 8.4 Hz).

To a solution of the *exo*-methylene derivative obtained above (2.5 mg, 10 μmol) in dimethylformamide (1.0 mL) was added iodobenzene (2.3 μL, 21 μmol), palladium(II) acetate (0.14 mg, 620 nmol), triphenylphosphine (0.32 mg, 1.2 μmol), and silver carbonate (5.7 mg, 21 μmol) at room temperature. After the reaction mixture was stirred for 3.5 h at 80 °C, H_2O was added, and the resulting mixture was extracted with ethyl acetate. The organic layers were combined, washed with H_2O, brine, dried over Na_2SO_4, filtered and concentrated *in vacuo* to give the crude products, which were purified by column chromatography on silica gel (25% ethyl acetate in hexane) twice to afford the corresponding styryl derivative as its 5 : 1 mixture of **sty-6** and the minor isomer with an internal double bond (1.8 mg, 66% in two steps). These isomers were separated by HPLC using a YMC-Pack ODS-AM column (S-5 μm, 120 A, 25 cm × 10 mm) eluted with ethyl acetate/hexane (1 : 9) at 1 mL min^{-1}, while monitoring at 254, 280, and 319 nm. The retention time of the major isomer **sty-6** is 111 min: ^{1}H NMR (400 MHz, $CDCl_3$) δ1.89 (d, 3H, J = 1.0 Hz), 2.40 (s, 3H), 3.29 (dd, 1H, J = 16.4, 7.9 Hz), 3.60 (dd, 1H, J = 16.4, 9.9 Hz), 5.49 (dd, 1H, J = 9.5, 9.5 Hz), 6.11 (s, 1H), 6.65 (s, 1H), 6.81 (d, 1H, J = 8.5 Hz), 7.18–7.35 (m, 5H), 7.43 (d, 1H, J = 8.6 Hz); HRFABMS calcd for $C_{21}H_{19}O_3$ $[M + H]^+$ 319.1334, found 319.1326.

COMPUTATIONAL SECTION

Molecular modeling

All DFT calculations were run with Jaguar 4.2 (Schrödinger, Inc., Portland OR) with B3LYP functional, and 6-31G* or 6-31G** basis sets, either *in vacuo* or in $CHCl_3$ (GB/SA solvation model), with default parameters and convergence criteria. Initial *eq* and *ax* geometries for **sty-2** and **sty-5** were built starting from previously DFT optimized structures of **1**,[15] and pre-optimized with DFT at the B3LYP/6-31G* level. Angle $d_{8,10}$ was then scanned by 15° steps followed by geometry relaxation at the B3LYP/6-31G* level *in vacuo*. For each *eq* and *ax* conformer, three energy minima were isolated, which were finally optimized at the B3LYP/6-31G** level in $CHCl_3$. The resulting relative energies for all minima are reported in ESI† (Table ESI1); the two lowest energy conformers for each compound are showed in Fig. 2.

Electronic structure calculations

TDDFT calculations[33] were run with Gaussian 03 (Gaussian, Inc., Pittsburgh PA) with either B3LYP[34] or PBE0[35] functionals, and various basis sets (6-31G(d,p), 6-311G(d,p), 6-311+G(d,p), aug-cc-pVDZ), solving for up to 12 excited states, *in vacuo*; a selected result is showed in Table 1. ZINDO-S/CI calculations[36] were run with Hyperchem 7.1 (Hypercube, Inc., Canada) with default parameters and convergence criteria, including the highest 16 (8 for styrene) occupied and the lowest 16 (8 for styrene) virtual orbitals in the CI. Input structures for all calculations, having C_s symmetry, were optimized with DFT at the 6-31G** level *in vacuo*.

Coupled-oscillator calculations

DeVoe calculations were run with a Fortran program developed by Hug.[37] DFT-optimized structures (B3LYP/6-31G**) were used as input geometries; average CD spectra were

calculated as Boltzmann-weighted at 300 K, using DFT energies. Spectroscopic parameters (transition frequency, dipole strength and half-height bandwidth) were extracted from the UV spectrum of 7-hydroxy-4-methyl coumarin in acetonitrile and styrene in hexane, and are summarized in Table 2. Transition moments directions were obtained with TDDFT and ZINDO-S/CI calculations for 7-hydroxy coumarin, and with ZINDO-S/CI calculations for styrene, and are shown in Table 2. Transition moment positions were estimated using the molecular orbitals resulting from ZINDO/S-CI and TDDFT methods (PBE0/6-311+G(d,p)), using the procedure described by Mason,[30] with both dipole-length (DL) and dipole-velocity (DV) formulations. In the latter case, average expectation values of the dipole-velocity elements for C–C and C–O bonds, $\langle\nabla_{C-C}\rangle$ and $\langle\nabla_{C-O}\rangle$, were taken from Inskeep *et al.*;[38] further details about the DL and DV calculations may be found in the ESI†. The results for the positions of transition I and II dipole moments of 7-hydroxy coumarin, using ZINDO/S-CI and TDDFT with PBE0/6-311G+(d,p) methods, are displayed in Table 2 as the center of the corresponding dipoles. Using TDDFT instead of ZINDO-derived parameters for the dipole positions and polarizations affected the DeVoe calculations to a very small extent. Moving the dipole positions within 0.5Å from the calculated centers affected the calculated CD intensities without reverting the couplet sign for all structures.

Both coumarin transitions I and II were included in the DeVoe calculations; transition II did not dramatically affect the computed spectra in terms of intensity, but slightly improved their general appearance. The very small coumarin transition III did not affect the result at all. Only the styrene K band was considered in the final calculations, with the view that higher energy bands did couple with coumarin I–II to a much lesser extent. Higher energy coumarin bands were also neglected. It must be noted that, regardless of the presence of further bands

at higher energies, the sign of at least the first Cotton effect allied to the coumarin transition I will be mainly dictated by the coupling with the styrene K band, therefore the couplet sign is safely predicted.

Quantitative NMR analysis

Experimental $^3J_{Me8,H9a}$ and $^3J_{Me8,H9b}$ values were compared with those estimated for the DFT calculated structures on the basis of the Karplus-type relation: $^3J_{C,H} = 3.6 \cos 2\phi - \cos\phi + 4.3$, where ϕ is one of the dihedrals $\phi_{Me8-C8-C9-H9a}$ or $\phi_{Me8-C8-C9-H9b}$. This equation had been purposely developed for $^3J_{Cexo-C(-O)-C-H}$ systems with a methyl or methylene carbon C_{exo} attached to a tetrahydrofuranyl ring.[24] In Table ESI2 of the ESI†, experimental values (estimated error +0.1 Hz) are compared with those evaluated on DFT-computed structures, both for the lowest energy eq_0 and ax_0 conformers as well as the Boltzmann's average at 300 K for all the minima.

ACKNOWLEDGEMENTS

This research is supported by the National Institutes of Health, NIH Grant GM 34509 (K.N. and N.B.). K.T. is grateful to the JSPS Postdoctoral Fellowships for Research Abroad. L.D.B. and G.P. acknowledge Italian Prin-MIUR, project "Fitoterapici: ottimizzazione delle caratteristiche tecnologiche e biofarmaceutiche". D.W.A. and T.L.X. acknowledge the National Institutes of Health, NIH RO1 GM53825-06 for partial support of this work.

REFERENCES

1. (*a*)D. Egan, R. O'Kennedy, E. Moran, D. Cox, E. Prosser and R. D. Thornes, *Drug Metab. Rev.*, 1990, **22**, 503–529. (*b*) J. R. S. Hoult and M. Paya, *Gen. Pharmacol.*, 1996, **27**, 713–722.
2. D. Guilet, J.-J. Helesbeux, D. Seraphin, T. Sevenet, P. Richomme and J. Bruneton, *J. Nat. Prod.*, 2001, **64**, 563–567
3. O. Thastrup, B. Fjalland and J. Lemmich, *Acta Pharmacol. Toxicol.*, 1983, **52**, 246–250.
4. R. Tovar-Miranda, R. Cortes-Garcia, N. F. Santos-Sanchez and P. Joseph-Nathan, *J. Nat. Prod.*, 1998, **61**, 1216–1220.
5. R. G. Bell, J. A. Sadowski and J. T. Matschiner, *Biochemistry*, 1972, **11**, 1959–1961.
6. G. Rodigliero, *J. Photochem. Photobiol., B*, 1992, **14**, 1–22.
7. (*a*) R. V. Rozhkov and R. C. Larock, *Org. Lett.*, 2003, **5**, 797–800; (*b*) R. V. Rozhkov and R. C. Larock, *J. Org. Chem.*, 2003, **68**, 6314–6320.
8. T. L. Xiao, R. V. Rozhkov, R. C. Larock and D. W. Armstrong, *Anal. Bioanal. Chem.*, 2003, **377**, 639–654.
9. (*a*) H. Arakawa, *Bull. Chem. Soc. Jpn.*, 1960, **33**, 200–202; (*b*) B. D. West, S. Preis, C. H. Schroeder and K. P. Link, *J. Am. Chem. Soc.*, 1961, **83**, 2676–2679; (*c*) P. P. Mehta and W. B. Whalley, *J. Chem. Soc.*, 1963, 3777–3779; (*d*) M. F. Grundon and I. S. McColl, *Phytochemistry*, 1975, **14**, 143–150; (*e*) N. Choukchou-Braham, Y. Asakawa and J.-P. Lepoittevin, *Tetrahedron Lett.*, 1994, **35**, 3949–3952; (*f*) T. Kinoshita, J.-B. Wu and F.-C. Ho, *Chem. Pharm. Bull.*, 1996, **44**, 1208–1211; (*g*) M. Murakata, Y. Mizuno, H. Yamaguchi and O. Hoshino, *Chem. Pharm. Bull.*, 1999, **47**, 1380–1383; (*h*) L.-Y. Kong, N.-H. Yao and M. Niwa, *Heterocycles*, 2000, **53**, 2019–2025; (*i*) D. R. Boyd, N. D. Sharma, P. L. Loke, J. F. Malone, W. C. McRoberts and J. T. G. Hamilton, *Chem. Commun.*, 2002, 3070–3071.
10. (*a*) H. Arakawa, *Bull. Chem. Soc. Jpn.*, 1968, **41**, 2541; (*b*) K. Hata and M. Kozawa, *Yakugaku Zasshi*, 1968, **88**, 293–298; (*c*) H. Arakawa, N. Torimoto and Y. Masui, *Liebigs Ann. Chem.*, 1969, **728**, 152–157; (*d*) J. F. Grove and M. Pople, *J. Chem.*

Soc., Perkin Trans. 1, 1979, 2048–2051; (*e*) T. Hashimoto, M. Tori and Y. Asakawa, *Phytochemistry*, 1987, **26**, 3323–3330; (*f*) P. Salvadori, S. Superchi and F. Minutolo, *J. Org. Chem.*, 1996, **61**, 4190–4191; (*g*) K. Krohn, R. Bahramsari, U. Florke, K. Ludewig, C. Kliche-Spory, A. Michel, H.-J. Aust, S. Draeger, B. Schulz and S. Antus, *Phytochemistry*, 1997, **45**, 313–320; (*h*) J. Latip, T. G. Hartley and P. G. Waterman, *Phytochemistry*, 1999, **51**, 107–110; (*i*) M. Yoshikawa, T. Murakami, T. Ueda, H. Shimoda, J. Yamahara and H. Matsuda, *Heterocycles*, 1999, **50**, 411–418; (*j*) S. Paraschos, P. Magiatis, E. Kalpoutzakis, C. Harvala and A.-L. Skaltsounis, *J. Nat. Prod.*, 2001, **64**, 1585–1587.

11. (*a*) B. R. Barik, A. K. Dey, P. C. Das, A. Chatterjee and J. N. Shoolery, *Phytochemistry*, 1983, **22**, 792–794; (*b*) Y. Shikishima, Y. Takaishi, G. Honda, M. Ito, Y. Takeda, O. K. Kodzhimatov, O. Ashurmetov and K.-H. Lee, *Chem. Pharm. Bull.*, 2001, **49**, 877–880.
12. N. Berova and K. Nakanishi, in *Circular Dichroism. Principles and Applications*, 2nd edn., ed. N. Berova, K. Nakanishi and R. W. Woody, Wiley-VCH, New York, 2000, pp. 337–395.
13. (*a*) K. Saigo, K. Sekimoto, N. Yonezawa and M. Hasegawa, *Tetrahedron Lett.*, 1983, **24**, 5381–5384; (*b*) K. Saigo, N. Yonezawa, K. Sekimoto, M. Hasegawa, K. Ueno and H. Nakanishi, *Bull. Chem. Soc. Jpn.*, 1985, **58**, 1000–1005.
14. L.-C. Lo, Y.-C. Liao, C.-H. Kuo and C.-T. Chen, *Org. Lett.*, 2000, **2**, 683–685.
15. G. Pescitelli, N. Berova, T. L. Xiao, R. V. Rozhkov, R. C. Larock and D. W. Armstrong, *Org. Biomol. Chem.*, 2003, **1**, 186–190.
16. K. Tanaka, K. Nakanishi and N. Berova, *J. Am. Chem. Soc.*, 2003, **125**, 10802–10803.
17. (*a*) H. DeVoe, *J. Chem. Phys.*, 1964, **41**, 393–400; (*b*) H. DeVoe, *J. Chem. Phys.*, 1965, **43**, 3199–3208; (*c*) C. Rosini, M. Zandomeneghi and P. Salvadori, *Tetrahedron: Asymmetry*, 1993, **4**, 545–554.
18. A. K. Chatterjee, F. D. Toste, T.-L. Choi and R. H. Grubbs, *Adv. Synth. Catal.*, 2002, **344**, 634–637.
19. S. J. Connon and S. Blechert, *Angew. Chem., Int. Ed.*, 2003, **42**, 1900–1923.

20. M. Scholl, S. Ding, C. W. Lee and R. Grubbs, *Org. Lett.*, 1999, **1**, 953–956.

21. A. S. Ratnayake and T. Hemscheidt, *Org. Lett.*, 2002, **4**, 4667–4669.

22. For some recent discussions see: (*a*) S. Matile, N. Berova, K. Nakanishi, J. Fleischhauer and R. W. Woody, *J. Am. Chem. Soc.*, 1996, **118**, 5198–5206; (*b*) L. Alcaraz, G. Macdonald, J. P. Ragot and R. J. K. Taylor, *J. Org. Chem.*, 1998, **63**, 3526–3527; (*c*) J. D. Chisholm, J. Golik, B. Krishnan, J. A. Matson and D. L. Van Vranken, *J. Am. Chem. Soc.*, 1999, **121**, 3801–3802; (*d*) X. Huang, N. Fujioka, G. Pescitelli, F. E. Koehn, T. R. Williamson, K. Nakanishi and N. Berova, *J. Am. Chem. Soc.*, 2002, **124**, 10320–10335.

23. E. L. Eliel and S. H. Wilen, *Stereochemistry of Organic Compounds*, Wiley-Interscience, New York, 1994.

24. (*a*) J. A. Schwarcz and A. S. Perlin, *Can. J. Chem.*, 1972, **50**, 3667–3676; (*b*) R. Wasylishen and T. Schaefer, *Can. J. Chem.*, 1973, **51**, 961–973; (*c*) A. Nagatsu, R. Tanaka, H. Mizukami, Y. Ogihara and J. Sakakibara, *Tetrahedron*, 2001, **57**, 3369–3372.

25. R. H. Abu-Eittah and B. A. H. El-Tawil, *Can. J. Chem.*, 1985, **63**, 1173–1179.

26. For some recent examples see: (*a*) F. Castronovo, M. Clericuzio, L. Toma and G. Vidari, *Tetrahedron*, 2001, **57**, 2791–2798; (*b*) L. Di Bari, G. Pescitelli, G. Reginato and P. Salvadori, *Chirality*, 2001, **13**, 548–555; (*c*) C. Rosini, M. I. Donnoli and S. Superchi, *Chem. Eur. J.*, 2001, **7**, 72–79; (*d*) L. Di Bari, S. Mannucci, G. Pescitelli and P. Salvadori, *Chirality*, 2002, **14**, 611–617; (*e*) A. Solladié-Cavallo, C. Marsol, G. Pescitelli, L. Di Bari, P. Salvadori, X. Huang, N. Fujioka, N. Berova, X. Cao, T. B. Freedman and L. A. Nafie, *Eur. J. Org. Chem.*, 2002, 1788–1796; (*f*) L. Di Bari, M. Lelli, G. Pintacuda, G. Pescitelli, F. Marchetti and P. Salvadori, *J. Am. Chem. Soc.*, 2003, **125**, 5549–5558; (*g*) G. Pescitelli, S. Gabriel, Y. Wang, J. Fleischhauer, R. W. Woody and N. Berova, *J. Am. Chem. Soc.*, 2003, **125**, 7613–7628.

27. (*a*) H. Nakazumi, T. Ueyama, T. Kitaguchi and T. Kitao, *Phosphorus, Sulfur Silicon Relat. Elem.*, 1983, **16**, 59–66; (*b*) O. A. Ponomarev, E. R. Vasina, V. G. Mitina and A. A. Sukhorukov, *Zh. Fiz. Khim.*, 1990, **64**, 974–981.

28. (*a*) R. J. Cave and E. W. Castner Jr., *J. Phys. Chem. A*, 2002, **106**, 12117–12123; (*b*) R. J. Cave, K. Burke and E. W. Castner Jr., *J. Phys. Chem. A*, 2002, **106**, 9294–9305; (*c*) J. Llano, J. Raber and L. A. Eriksson, *J. Photochem. Photobiol., A*, 2003, **154**, 235–243.

29. (*a*) J. Tanaka, F. Ogura, M. Kuritani and M. Nakagawa, *Chimia*, 1972, **26**, 471–473; (*b*) S. F. Mason, *J. Chem. Soc., Chem. Commun.*, 1973, 239–241; (*c*) G. Gottarelli, G. Proni, G. P. Spada, D. Fabbri, S. Gladiali and C. Rosini, *J. Org. Chem.*, 1996, **61**, 2013–2019.

30. S. F. Mason, *Molecular Optical Activity and the Chiral Discrimination*, Cambridge University Press, Cambridge, 1982, pp. 66–69.

31. V. Molina, B. R. Smith and M. Mercha, *Chem. Phys. Lett.*, 1999, **309**, 486–494.

32. (*a*) W. Willker and D. Leibfritz, *Magn. Reson. Chem.*, 1995, **33**, 632–638; (*b*) K. Furihata and H. Seto, *Tetrahedron Lett.*, 1999, **40**, 6271–6275; (*c*) K. H. Sze, X. Z. Yan, X. M. Kong, C. T. Che and G. Zhu, *Tetrahedron Lett.*, 1999, **40**, 5587–5591; (*d*) H. Seki, T. Tokunaga, H. Utsumi and K. Yamaguchi, *Tetrahedron*, 2000, **56**, 2935–2939; (*e*) B. L. Marquez, W. H. Gerwick and R. T. Williamson, *Magn. Reson. Chem.*, 2001, **39**, 499–530.

33. (*a*) R. E. Stratmann, G. E. Scuseria and M. J. Frisch, *J. Chem. Phys.*, 1998, **109**, 8218–8224; (*b*) M. Parac and S. Grimme, *Chem. Phys.*, 2003, **292**, 11–21.

34. A. D. Becke, *J. Chem. Phys.*, 1993, **98**, 5648–5652.

35. (*a*) J. P. Perdew, M. Ernzerhof and K. Burke, *J. Chem. Phys.*, 1996, **105**, 9982–9985; (*b*) C. Adamo and V. Barone, *J. Chem. Phys.*, 1999, **110**, 6158–6170.

36. (*a*) J. Ridley and M. Zerner, *Theor. Chim. Acta*, 1973, **32**, 111–134; (*b*) J. E. Ridley and M. C. Zerner, *J. Mol. Spectrosc.*, 1974, **50**, 457–473.

37. C. L. Cech, W. Hug and I. Tinoco Jr., *Biopolymers*, 1976, **15**, 131–152.

38. W. H. Inskeep, D. W. Miles and H. Eyring, *J. Am. Chem. Soc.*, 1970, **92**, 3866–3872.

Footnote

†Electronic supplementary information (ESI) available: Relative energies and relevant geometrical parameters of DFT-optimized structures of **sty-2** and **sty-5** (Table ESI1). Calculated and experimental $^{3}J_{Me8,H9a}$ and $^{3}J_{Me8,H9b}$ values (in Hz) for **sty-2** and **sty-5** (Table ESI2). UV absorption spectrum of 7-hydroxy-4-methylcoumarin in CH_3CN (Fig. ESI1). Description of the procedure for estimating transition dipole moment positions from excited-states calculations.

CHAPTER 7

GENERAL CONCLUSIONS

The research outlined in part one of this dissertation demonstrates a series of unique analytical applications of macrocyclic antibiotic-based CSPs in the separation of enantiomers of racemic compounds. It was found that the observation of the elution order reversal within this class of CSPs is very difficult due to the complex structure of the macrocyclic glycopeptides and the unavailability of their enantiomers. After a thorough study with over a thousand separations using these CSPs, a few cases were found in which the enantioselectivity of a separation could be reversed either by using a related glycopeptide CSP or, in one case, by altering the mobile phase composition. These compounds are oxazolidinones, dansyl amino acids, and sulfoxides. This behavior has not been reported previously for this class of CSPs.

The method development of enantiomeric separation of chiral sulfoxide compounds extended the use of this class of chiral selectors to compounds with sulfur stereogenic centers. The teicoplanin and TAG CSPs with the normal phase mode and the reversed phase mode are the most effective CSP-mobile phase associations for the enantioseparation of these compounds. An important feature involving the chiral recognition mechanism of sulfoxide compounds seems to be steric repulsion. Also it appears that intramolecular stacking of some of the larger chiral sulfoxides can greatly affect its enantiorecognition. The enantiomeric retention order of the enantiomer showed a great deal of consistency for any single CSP and mobile phase. However, reversing the enantiomeric retention order is

possible by changing the CSP. The sugar moieties of teicoplanin and vancomycin were found to play a negative role in chiral separation of sulfoxides possiblely due to the steric hinderance effect of the sugar moieties. Sterically bulky groups attached to the carbon next to the chiral center of the analyte were found to play a positive role in enantiomeric separation for this class of compounds.

One of the most successful applications using macrocyclic glycopeptide CSPs are the separations of chiral furocoumarin derivatives by HPLC. Furocoumarin derivative are important pharmacologically active compounds. Effective, high efficiency enantiomeric separation methods were developed using these two classes of CSPs. The whole set of over 30 compounds were baseline separated with high efficiency. It was found that a mobile phase with hydrogen bonding ability (methanol, ethanol or isopropanol) is essential in the polar organic mode for the separation of this class of compounds. A hydroxyl group on the analyte near the stereogenic center greatly enhanced its enantioselectivity with all CSPs in all mobile phase modes. Hydrophobic interactions are important in the RP mode. Steric repulsive effects are very important for achieving chiral recognition on all three CSPs, and in both the NP and RP modes. However, the steric bulk near the chiral center of the dihydroangelicin tends to enhance the NP enantiomer separations and inhibit the corresponding RP separations. The exact opposite trend is seen for dihydropsoralens. The absolute configuration of selected, collected enantiomers has been determined and therefore the enantiomer elution orders for these particular compounds on a particular CSP under specific mobile phase conditions have been determined.

The absolution configuration determinations of the dihydrofurocoumarins provide the possibility of assessing the biological activity of single enantiomers. This work expands the application of the exciton chirality method to the determination of the absolute configuration of dihydrofurocoumarins for the first time. Since this method requires two chromophores (one on different substituents off the stereogenic center) appropriate derivatization methods followed by chiral separation were used. The absolute configurations of most of the dihydrofuroangelicin enantiomers were determined using this newly developed approach.

For future efforts, the selective permethylation of the teicoplanin aglycon will be very useful in helping to elucidate the chiral recognition mechanism by comparing the separations of enantiomers using native teicoplanin, teicoplanin aglycon and the methylated form as CSPs. Preliminary results of this effort confirmed that the amine group on teicoplanin aglycon is believed to be a chiral recognition site for the separation of amino acids.

A linear free energy solvation model developed by Abraham can also be a very useful tool to characterize the different interactions that occur between solutes and the CSPs with a fixed mobile phase in HPLC. Our preliminary results showed that chiral recognition responsible interactions between the analytes and the CSP could be recognized by the application of this linear free energy salvation model.

Some molecular modeling programs can also be used to understand the chiral recognition process. It is my hope that the mechanism by which the macrocyclic antibiotics are able to separate and resolve enantiomers will be completely understood in the future.

ACKNOWLEDGEMENT

As I finished my dissertation, I felt compelled to express my sincere thanks to those who have paved the path toward the pursuit of my Ph.D degree.

First of all, it has been an honor to have done my Ph.D work under the guidance and supervison of my major advisor, Professor Daniel W. Armstrong, a brilliant scientist and a great mentor. His scientific intelligence and attitude toward science greately influenced me and stimulated my interest in science and technology. It is his inspiration and encouragement that made my life of my graduate study here at Iowa State unforgettable and full of fun.

Secondly, my sincere thanks go to my current POS committee members, Prof. Robert S. Houk, Prof. Patricia Thiel, Prof. Qijing Zhang and Prof. Yan Zhao, as well as my previous committee members Prof. V. Shears and Prof. Taochou Chang for their time and support. It has been my great honour to have you serve as my committee members.

Thirdly, my appreciation go to all of our collaborators during my research, including Prof. Nina Berova and Prof. Koji Nakanishi's research team at Columbia Univerisity, Prof. Larock's research group and Prof. Jenks' groups at Iowa State University for their work and collaboration. I would also thank all of Professor Armstrong's group members who provided helps and enlightening discussions involving my research. I really enjoyed working as a part of this great team.

Finally, I would especially like to thank my wife, Michelle Wang, for her hard work and support and in giving me such an enjoyable and happy family. Without her helps, it would not have been possible for me to effectively and efficiently complete my research.

The financial support from Iowa State Univeristy for this work is greatly appreciated.